

UNIVERSITY OF CANTERBURY, WORLEYPARSONS, CONTACT ENERGY

# **Investigating Retrofitting an Existing Geothermal Power Plant with a Biomass Gasifier for Additional Power Generation**

A Thesis Submitted in Fulfilment of the Requirements for the  
Degree of Master of Engineering in Chemical and Process  
Engineering

**Steven Chester**

**9/10/2016**

## Abstract

Hybridization of geothermal and biomass resources for power generation is a potential step in the increased commercial utilization of biomass gasifiers in New Zealand. There is generally an increase in the power generation efficiency by hybridizing two power generation technologies. Hybrid power generation also reduces the capital costs for power plants, due to shared equipment. The Taupo Volcanic Zone is home to a large geothermal reservoir, is proximate to the largest area for commercial forestry in New Zealand, and is therefore a promising location for hybridizing geothermal and biomass resources. The Wairakei Power Plant has been used to generate power for over 50 years, but declining reservoir enthalpy and the preferential use of geothermal steam at other geothermal power plants causes there to be unused power generation capacity.

This study examines the potential for integration of biomass gasification as an additional fuel source in the Wairakei Power Plant so as to increase power generation. Possible approaches to integrating syngas firing into the steam system were investigated and the derived hybrid configurations modelled using the heat and material balance software UniSim to estimate the additional power generation possible. Experimental work was limited to measurements on steam condensate in the existing geothermal systems so as to establish steam purity and required clean-up approaches to utilize steam condensate as a source of boiler feed water. This study addresses some of the practical problems related to silica carryover and plant integration so to allow the utilization of biomass synthesis gas to directly heat geothermal steam.

Four hybrid configurations were investigated in order to generate additional power by integrating a biomass gasifier and syngas fired heating to the Wairakei Geothermal System:

- Superheating of geothermal steam for more efficient power generation
- Syngas fired heating used to boil condensate available on site for additional steam generation
- Boiling separated geothermal water immediately after the first separation stage
- Heating of separated geothermal water available at Wairakei to increase power generation at an existing binary power plant

The performance of the dual fluidized bed gasifier was seen to achieve cold gas efficiencies as high as 84% based on the lower heating value of the landing residue feed and the generated syngas. However, this does not include the thermal input of steam used as the gasification agent, as geothermal steam generated on the Wairakei Geothermal Field was used to satisfy this steam requirement. Flue gas from the biomass gasifier and the combustion of syngas on site was used as the drying agent to dry the wet wood chips prior to these wood chips being introduced to the gasifier.

It was found that the geothermal steam supply to Wairakei greatly impacts the power generation that is possible the hybrid configurations. Three scenarios for the potential steam supply conditions were created in order to represent the changes in the additional hybrid power generation that is expected to occur with changing reservoir enthalpy:

- Scenario 1: Steam supply consistent with that for January 2015 – July 2016. Sporadic bypassing of turbines by intermediate pressure steam occurs, all steam turbines at Wairakei are fully loaded.
- Scenario 2: Reduced steam supply to Wairakei. No steam bypassing occurs, all steam turbines at Wairakei are fully loaded.
- Scenario 3: Further reduced steam supply to Wairakei. No steam bypassing occurs, but not all steam turbines are fully loaded. Additional generated steam may be used in partially loaded steam turbines to increase power generation.

Capital cost estimation and an economic evaluation was performed for the proposed hybrid plants in order to quantify the financial implications of implementing the hybrid configurations for each of the steam flow scenarios investigated.

In order to modify the 30 MWe mixed pressure geothermal steam turbines to utilize superheated steam, it was found that there would be an estimated 2.6 MWe decrease in the power generation of the turbines when fully loaded. However, as the modified turbines will use less steam compared to the unmodified turbines, there is a net increase in power generation possible, due to the power generation that may be performed using the saved geothermal steam. This configuration was seen to be the most efficient in Scenario 3, where an average additional power generation of 11.9 MWe is possible from a 15 t/h input of wet landing residues. This resulted in a fuel to electricity efficiency of 29.7% based on the lower heating value of the landing residues. The project was, however, expected to lose \$27 million over a 30 year hybrid plant life, and required an estimated capital investment of \$48 million.

Water testing was performed on several sources of water available on the Wairakei Geothermal System, in order to evaluate suitability as boiler feed water. It was found that the most appropriate source of water was condensate from the Poihipi Rd Power Plant, which has an estimated average of 54 t/h of condensate available for use. A water cleaning process was then designed based on the contaminants present in the water, in order to ensure safe and reliable operation of the boiler. The process modelling revealed that this configuration generated electricity most efficiently in the conditions of Scenario 3, with an average of 6.2 MWe additional power being generated from a 15 t/h input of wet landing residues. The resulting fuel-electricity was calculated at 14.8% based on the lower heating value of the forest residues. There was a projected loss of \$32 million from the implementation of this project over a 30 year hybrid plant life, requiring a \$9.6 million investment.

It was found that boiling separated geothermal water after the first separation stage resulted in a decrease in the metals being discharged into the Waikato River due to an increased proportion of the metals being reinjected into the geothermal reservoir. It was found that power could be generated most efficiently in the conditions of Scenario 3, using the additional steam created from boiling the separated geothermal water. An estimated 6.8 MWe of additional electricity could be generated using an input of 15 t/h of wet landing residues, resulting in a fuel to electricity efficiency of 16.2% based on the lower heating value of the landing residues. The project was expected to lose \$27 million for a 30 year plant life, and required a capital investment of \$8.3 million.

The Wairakei Binary Plant is designed to generate an average of 15 MWe, however an average generation of approximately 13 MWe has been observed for the plant, this is attributed to the flowrate of separated geothermal water being lower than the plant was designed for. In order to supplement the separated geothermal water flow to the Wairakei Binary Plant, the additional

geothermal water was expected to require heating in order to avoid increasing silica scaling in the Binary Plant. The heating of additional separated geothermal water for use in the Wairakei Binary Plant was seen to have the highest efficiency in Scenario 1. An increase of 1.4 MWe was expected using a 3.4 t/h average wet wood input, resulting in a fuel to electricity efficiency of 15.5%, based on the lower heating value of the wet landing residues. This project was expected to lose \$17 million over the 30 year life of the hybrid plant, and require a capital investment of \$7.8 million.

The poor economics associated with implementing any of the hybrid configurations are attributed both to the design constraints of retrofitting the hybrid configurations, and the relatively high cost of the landing residues. It was initially thought that the close proximity and availability of forestry landing residues would result in viable options for boosting geothermal power generation using syngas fired heating. However, due to the inefficiencies associated with retrofitting the hybrid configurations to an existing geothermal plant, and the relatively low sale price of power; the delivered cost of the forest residues was seen to exceed the value of the additional power generation in most cases. It is therefore recommended that the integration of a gasifier into a new geothermal plant from the design stage, and alternative, cheaper, feedstocks for gasification be investigated. It is also believed that the generation and sale of liquid biofuels using geothermal steam as an input to a gasifier may prove to be profitable.

## Acknowledgements

I would first like to acknowledge Callaghan Innovation NZ for its funding support of this project.

Thanks to my supervisors, Chris Williamson, George Hooper, and Mike Dunstall, for their help and advice throughout the course of this project, without them, this project never would have happened.

The Staff and Management at Contact Energy's Wairakei Plant, where I spent several months researching, were beyond helpful, and very welcoming. The commercial perspective was invaluable in ensuring this project took practical considerations for retrofitting the Wairakei Plant with biomass gasification into account.

Thanks also to the staff at the WorleyParsons Christchurch office for all of their expertise and helping with my professional development as an engineer.

# Table of Contents

Abstract .....	iii
Acknowledgements .....	vi
Table of Contents .....	vii
Abbreviations .....	xi
List of Figures .....	xii
List of Tables .....	xvi
1.0 Introduction.....	1
1.1 Geothermal Energy .....	2
1.1.1 The Relative Cost of Geothermal Power Production.....	4
1.2 Gasification .....	5
1.2.1 University of Canterbury's Gasifier.....	6
1.3 Wairakei Geothermal Field .....	7
1.3.1 Wairakei A and B Power Stations .....	10
1.3.2 The Te Mihi Power Station.....	11
1.3.3 The Poihipi Rd Power Station.....	12
1.3.4 The Wairakei Binary Plant.....	13
1.4 Hybrid Power Generation.....	14
1.5 Reason for Investigation.....	15
2.0 Potential Hybrid Plant Configurations.....	18
2.1 Factors for Consideration .....	18
2.1.1 Dissolved Minerals .....	18
2.1.2 Dissolved Gasses .....	19
2.1.3 Design Limitations of the Existing Plant.....	19
2.1.4 Syngas Purity .....	19
2.2 Superheating of Geothermal Steam.....	20
2.3 Vaporization of Steam Turbine Condensate .....	23
2.4 Heating Separated Geothermal Water after the First Separation Stage .....	25
2.5 Heating Additional Separated Geothermal Water for Use in a Binary Plant.....	28
3.0 Process Modelling of the Wairakei Geothermal System and Hybrid Configurations .....	30
3.1 Modelling Biomass Gasification.....	30
3.1.1 Biomass Drying .....	30

3.1.2	Dual Fluidized Bed Gasifier .....	31
3.1.3	Modifications Made to the Biomass Gasification Model .....	33
3.2	Modelling Steam Flow at the Wairakei A and B Stations .....	35
3.2.1	Modelling Geothermal Steam Flow to the Wairakei Turbines .....	35
3.2.2	Estimating IP Steam Bypassing .....	36
3.2.3	Modelling Power Generation from Additional Steam Supply .....	40
3.2.4	Decreasing Steam Supply to the Wairakei A and B Stations .....	42
3.3	Modelling the Hybrid Configurations .....	44
3.3.1	Superheating of Geothermal Steam .....	44
3.3.2	Vaporization of Steam Turbine Condensate .....	47
3.3.3	Heating the Separated Geothermal Water after the First Separation Stage .....	48
3.3.4	Heating Additional Separated Geothermal Water for use in a Binary Plant .....	49
3.4	Energy Efficiency .....	56
4.0	Determining the Suitability of Geothermal Waters to be used as Boiler Feed Water .....	57
4.1	Boiler Feed Water Tolerances .....	57
4.2	Water Available on Site .....	59
4.3	Factors Affecting Water Purity .....	60
4.4	Sampling and Testing Procedure .....	61
4.5	Water Sample Results .....	63
4.6	Techniques for Condensate Cleaning .....	65
4.6.1	pH Dosing .....	66
4.6.2	Deaeration .....	67
4.6.3	Blowdown Control of Boiler Water .....	68
4.6.4	Boiler Water Monitoring .....	69
4.6.5	Reliability of Results .....	70
4.7	Poihipi Rd Condensate Availability .....	71
5.0	Plant Design and Cost Estimation .....	72
5.1	Economic Environment .....	72
5.1.1	Forest Residue Availability and cost .....	72
5.1.2	Sale Price of Power .....	76
5.2	Additional Process Equipment and Modifications Required .....	77
5.2.1	Gasification and Landing Residue Pre-treatment .....	77
5.2.2	Superheating Geothermal Steam .....	78
5.2.3	Boiling Poihipi Rd Condensate .....	78

5.2.4	Boiling IP SGW .....	79
5.2.5	Heating Additional SGW to use in the Binary Plant .....	79
5.3	Equipment Design and Capital Cost Estimation .....	79
5.3.1	Landing Residue Pre-treatment and Handling.....	79
5.3.2	Gasification .....	87
5.3.3	Returning Steam Turbines to Service .....	89
5.3.4	Furnaces and Fans.....	90
5.3.5	Modifying Existing MP Steam Turbines to use Superheated Steam .....	92
5.3.6	Boiling Poihipi Rd Condensate.....	94
5.3.7	Boiling IP SGW .....	97
5.3.8	Total Installed Costs .....	98
5.4	Operating costs .....	99
5.4.1	Ongoing Costs from Bringing Turbines Back into Service .....	99
5.4.2	Parasitic Load.....	99
5.4.3	Silica Scale Removal .....	101
5.4.4	Silica Inhibition at the Binary Plant.....	103
5.4.5	Wages.....	103
5.5	Economic Evaluation .....	103
5.6	Economic Optimization.....	104
5.7	Different Scenarios for the Steam Flow to Wairakei .....	105
6.0	Results.....	107
6.1	Gasification Model.....	107
6.2	Superheating Geothermal Steam.....	107
6.2.1	Scenario 1.....	108
6.2.2	Scenario 2.....	111
6.2.3	Scenario 3.....	113
6.3	Creating Additional IP Steam by Boiling Poihipi Rd Condensate.....	116
6.3.1	Scenario 1.....	116
6.3.2	Scenario 2.....	118
6.3.3	Scenario 3.....	121
6.4	Creating Additional IP Steam by Boiling IP SGW .....	123
6.4.1	Scenario 1.....	123
6.4.2	Scenario 2.....	126
6.4.3	Scenario 3.....	129



6.5	Heating Additional SGW to Utilize in the Binary Plant .....	131
6.5.1	Scenario 1.....	131
6.5.2	Scenario 2 & Scenario 3 .....	133
6.6	Discussion .....	136
6.6.1	Biomass Gasification .....	136
6.6.2	Hybrid Power Plant Energy Efficiency.....	136
6.6.3	Hybrid Power Plant Economic Assessment.....	138
6.6.4	Using Natural Gas Instead of Biomass Gasification.....	140
6.6.5	Remaining Life of the Wairakei A and B Stations .....	141
7.0	Conclusions and Recommendations .....	142
7.1	Recommendations .....	143
7.1.1	Power and Fuel Cogeneration .....	143
7.1.2	Further Research into Gasification Feedstocks Prices.....	144
7.1.3	Designing a New Geothermal/Gasification Power Plant.....	144
8.0	References.....	146
9.0	Appendices.....	151
9.1	Water testing results .....	151
9.1.1	Boiler water testing .....	151
9.1.2	Previous Testing Performed on the Poihipi Rd Condensate .....	154
9.2	Process Equipment Capital Costs.....	156
9.3	Cash Flow Analysis for the Implementation of the Hybrid Configurations .....	158

## Abbreviations

ABMA	American Boiler Manufacturers Association
APHA	American Public Health Association
BFB	Bubbling Fluidized Bed
CFB	Entrained Flow Fluidized Bed
DFB	Dual Fluidized Bed
FACT	First Approximation Costing Technique
FP	Flash Plant
ILP	Intermediate Low Pressure
IP	Intermediate Pressure
IP SGW	Separated Geothermal Water from IP Steam
LP	Low Pressure
LPG	Liquefied Petroleum Gas
LP SGW	Separated Geothermal Water from LP Steam
MP	Mixed Pressure (a mixture of Intermediate Pressure and Low Pressure)
NZD	New Zealand Dollar
ORC	Organic Rankine Cycle
SGW	Separated Geothermal Water
WB	Wet Basis

## List of Figures

Figure 1. The annual electricity generation in New Zealand from 1976 to 2014 by fuel type[5].	1
Figure 2. A simplified schematic of a two flash geothermal power plant.	3
Figure 3. A typical temperature-entropy state diagram for a two flash geothermal power plant, modified from [11].	4
Figure 4. The relative power generation costs for different energy sources in New Zealand [14]	5
Figure 5. The range of applicability of different gasifier types [19].	6
Figure 6. The Dual Fluidized Bed used at the University of Canterbury[20].	7
Figure 7. The schematic for the steam extraction manifold of the Wairakei Geothermal System [21].	8
Figure 8. Schematic of the separated geothermal water manifold at the Wairakei Geothermal System [21]	9
Figure 9. Schematic of the Wairakei Power Plant A and B Stations[22].	11
Figure 10. A diagram of one of the two identical turbine cycles at the Te Mihi Power Station ..	12
Figure 11. Diagram of the Poihipi Rd Power Plant	13
Figure 12. Diagram of one of the twin pair of binary plant cycles within the Wairakei Binary Plant (Dotted lines represent pentane flow) [24]	14
Figure 13. The pressure drop at several steam extraction wells at the Wairakei Geothermal Field [29].	16
Figure 14. A simplified diagram of syngas fired superheating of geothermal steam prior to utilization in a steam turbine.	21
Figure 15. A temperature entropy diagram for the superheating of geothermal steam modified from [11].	22
Figure 16. A diagram of using geothermal steam turbine condensate as feed water to a syngas fired boiler	24
Figure 17. Mollier Diagram illustrating the effect heating separated geothermal water has on increasing the amount of water in the vapour phase, modified from [11].	25
Figure 18. Diagram of the current steam and water flows at Flash Plant 14	26
Figure 19. A diagram of performing fired heating on IP SGW for additional IP steam generation	27
Figure 20. The Power Generation of the Wairakei Binary Plant for 2015	28
Figure 21. Diagram of heating additional SGW for use in the Wairakei Binary Plant	29
Figure 22. Overview of the dual fluidized bed gasifier UniSim model, taken from Puladian's Thesis [43]	31
Figure 23. The daily average valve positions for two bypass valves, PRV1 and PRV4	37
Figure 24. The estimated flowrates of IP steam bypassing through PRV1 and PRV4	38
Figure 25. The estimated bypassing steam calculated using IP steam flow estimates within and measured IP steam input to the Wairakei A and B Stations	39
Figure 26. The estimated bypassing steam based on both the estimated unused IP steam, and the pressure relief valve positions	40
Figure 27. The power generation from the three LP turbines at Wairakei	41
Figure 28. The total steam input to the Wairakei A and B Stations, and the estimated bypassing steam	44

Figure 29. Entropy-Enthalpy diagram for steam in a MP turbine, for saturated IP steam (blue), and steam superheated to 350°C (red) .....	46
Figure 30. Numbered streams of steam and SGW around the modified FP14.....	48
Figure 31. Power Output Correction Factors for the Wairakei Binary Plant with Separated Geothermal Water inlet temperature.....	51
Figure 32. The mass flowrate of SGW feed to the Wairakei Binary Plant, and the estimated amount of SGW bypassing the Binary Plant. ....	52
Figure 33. Power output correction factors for the Wairakei Binary Plant with separated geothermal water flowrate to the Binary Plant. ....	53
Figure 34. The additional SGW from T-Line that may be added to the feed of the Binary Plant and the resultant total SGW flowrate.....	54
Figure 35. The Power Generation of the Wairakei Binary Plant for 2015 and the estimated power generation by heating and adding additional SGW from T-Line .....	55
Figure 36. The heat requirement and associated biomass input in order to heat additional SGW in T-line.....	55
Figure 37. The permissible amount of silica in the boiler water in order to produce steam with a silica content of 10 and 20 ppb [40].....	58
Figure 38. Diagram of apparatus used to minimize oxygen contamination during dissolved oxygen sampling .....	61
Figure 39. The solubility of oxygen in water under different temperatures and pressures [40] ...	68
Figure 40. The daily average of Poihipi Rd condensate flow to Te Mihi.....	71
Figure 41. The delivered costs for landing residues for different delivery distances, assuming 8 GJ/m <sup>3</sup> [66] .....	72
Figure 42. Yearly average prices for radiata pine pulp logs in New Zealand [68].....	73
Figure 43. The distribution of planted forests in the North Island as of 2008, modified from [69]. .....	74
Figure 44. The wholesale prices of power used for the economic evaluations of the hybrid configurations .....	77
Figure 45. Diagram of a disc chipper [73].....	80
Figure 46. A diagram of a drum chipper [73].....	81
Figure 47. A diagram of a hammer mill hog [73].....	81
Figure 48. Diagram of a cascade co-current rotary drum dryer [79] .....	83
Figure 49. A cross section of a cascade rotary drum dryer [79] .....	83
Figure 50. The biomass feed preparation and storage equipment .....	84
Figure 51. The estimated cost (December 2004 NZD) for belt and bucket conveyors based on the FACT Method .....	85
Figure 52. The estimated cost (December 2004 NZD) for auger and apron conveyors based on the FACT Method .....	86
Figure 53. The estimated cost (December 2004 NZD) for electric motors based on the FACT Method .....	87
Figure 54. The estimated cost (1st Quarter 1998 USD) for furnaces based on the heat duty of the furnace [90].....	91
Figure 55. The estimated cost (1 <sup>st</sup> Quarter 1998 USD) for packaged steam boilers based on the steam production capacity [90] .....	96
Figure 56. The estimated cost (December 2004 NZD) for steam boilers based on the heating duty [71]......	97

Figure 57. The installed capital cost breakdown for modifying two MP turbines to utilize superheated steam in Scenario 1 and Scenario 2 .....	109
Figure 58. The cumulative discounted cash flow for modifying two MP turbines to utilize superheated steam in Scenario 1 .....	109
Figure 59. Sensitivity analysis for modifying two MP turbines to utilize superheated steam in Scenario 1.....	110
Figure 60. The cumulative discounted cash flow for modifying two MP turbines to utilize superheated steam in Scenario 2 .....	112
Figure 61. Sensitivity analysis for modifying two MP turbines to utilize superheated steam in Scenario 2.....	113
Figure 62. The installed cost breakdown for modifying two MP turbines to utilize superheated steam in Scenario 3 .....	114
Figure 63. The cumulative discounted cash flow for modifying two MP turbines to utilize superheated steam in Scenario 3 .....	114
Figure 64. Sensitivity analysis for modifying two MP turbines to utilize superheated steam in Scenario 2.....	115
Figure 65. The installed cost breakdown for using Poihipi Rd condensate as boiler feed water in Scenario 1.....	117
Figure 66. The cumulative discounted cash flow for using Poihipi Rd condensate as boiler feed water in Scenario 1.....	117
Figure 67. Sensitivity analysis for using Poihipi Rd condensate as boiler feed water in Scenario 1 .....	118
Figure 68. The installed capital cost breakdown for using Poihipi Rd condensate as boiler feed water in Scenario 2.....	119
Figure 69. The cumulative discounted cash flow for using Poihipi Rd condensate as boiler feed water in Scenario 2.....	120
Figure 70. Sensitivity analysis for using Poihipi Rd condensate as boiler feed water in Scenario 2 .....	121
Figure 71. The cumulative discounted cash flow for using Poihipi Rd condensate as boiler feed water in Scenario 3.....	122
Figure 72. Sensitivity analysis for using Poihipi Rd condensate as boiler feed water in Scenario 1 .....	123
Figure 73. The breakdown of the installed capital costs for using IP SGW from FP14 to generate additional steam in Scenario 1 .....	124
Figure 74. The cumulative discounted cash flows for generating additional steam by boiling IP SGW from FP14 in Scenario 1 .....	125
Figure 75. Sensitivity analysis for generating additional steam fusing IP SGW from FP14 as feed water in Scenario 1.....	126
Figure 76. The breakdown of the installed capital costs for using IP SGW from FP14 to generate additional steam in Scenario 2 and Scenario 3 .....	127
Figure 77. The cumulative discounted cash flows for generating additional steam by boiling IP SGW from FP14 in Scenario 2 .....	127
Figure 78. Sensitivity analysis for using Poihipi Rd condensate as boiler feed water in Scenario 2 .....	128
Figure 79. The cumulative discounted cash flows for generating additional steam by boiling IP SGW from FP14 in Scenario 3 .....	129

Figure 80. Sensitivity analysis for using Poihipi Rd condensate as boiler feed water in Scenario 3 .....	130
Figure 81. The breakdown of the installed capital costs for generating additional power by heating makeup SGW for the Binary Plant.....	132
Figure 82. The cumulative discounted cash flows for generating additional power by heating makeup SGW for the Binary Plant for Scenario 1 .....	132
Figure 83. Sensitivity analysis for generating additional power by heating makeup SGW for the Binary Plant for Scenario 1 .....	133
Figure 84. The cumulative discounted cash flows for generating additional power by heating makeup SGW for the Binary Plant for Scenario 2.....	134
Figure 85. Sensitivity analysis for generating additional power by heating makeup SGW for the Binary Plant for Scenario 2.....	135
Figure 86. The industrial natural gas prices in New Zealand from 1999-2015 [101] .....	140

## List of Tables

Table 1. The tolerances of internal combustion engines and gas turbines to various contaminants present in syngas [34].	20
Table 2. The steam flows for the steam turbines at the Wairakei Power Plant operating at full load.	36
Table 3. The no load steam flows and power generation rates for the steam turbines at the Wairakei A and B Stations.	36
Table 4. The assumed flow coefficients for 20" butterfly valves [50]	37
Table 5. The predicted mass flowrates of steam through each stage in a MP turbine, and the resulting power generation for saturated steam at 150°C and 4.5 bara and superheated steam at 350°C and 4.5 bara.	46
Table 6. ASME guidelines for feed water quality in modern industrial water tube boilers for reliable continuous operation [40]	57
Table 7. ASME guidelines for boiler water quality in modern industrial water tube boilers for reliable continuous operation [40]	58
Table 8. The contaminant testing method and detection limits for the tests performed on the geothermal waters	62
Table 9. The results for the sample impurities for the Poihipi Rd condensate, Te Mihi blowdown, and Ohaaki blowdown performed by Hill Laboratories	63
Table 10. The measured dissolved oxygen for the geothermal waters	63
Table 11. The hardness of the different sources of water.	64
Table 12. Boiler feed water impurities, their effects and removal [40].	66
Table 13. The calculated blowdown required to mitigate problems that may be caused by silica, TDS, and alkalinity in order to ensure safe boiler operation.	69
Table 14. Testing results for the species of interest in Poihipi Rd condensate to assess the variability of the condensate	70
Table 15. Manufacturer's data for wood chip transfer screw conveyers [86]	86
Table 16. The assumed superficial gas velocities for the University of Canterbury's dual fluidized bed gasifier.	88
Table 17. The estimated costs of recertifying turbines at the Wairakei Power Plant	89
Table 18. The cost correction factors for centrifugal fans [71].	92
Table 19. The cost of pumps and motors for single stage pumps [71].	94
Table 20. Heat flux typical for different types of heat exchange in tubular heat exchangers [71]	95
Table 21. The prices for heat exchangers based on their design pressures [71].	95
Table 22. Costs associated with purchasing and installing process equipment based on the equipment cost [71].	98
Table 23. Pressure ratios and associated compressibility factors for centrifugal air fans [40].	100
Table 24. Results for modifying two MP turbines to utilize superheated steam in Scenario 1 ..	108
Table 25. The cash flow summary for superheating geothermal steam in Scenario 1, all values given in \$1000's.	110
Table 26. Results for modifying two MP turbines to utilize superheated steam in Scenario 2 ..	111
Table 27. The cash flow summary for superheating geothermal steam in Scenario 2, all values given in \$1000's.	112

Table 28. Results for modifying two MP turbines to utilize superheated steam in Scenario 23	113
Table 29. The cash flow summary for superheating geothermal steam in Scenario 1, all values given in \$1000's.....	115
Table 30. Results for generating steam from Poihipi Rd condensate in Scenario 1 .....	116
Table 31. The cash flow summary for using Poihipi Rd condensate as boiler feed water n Scenario 1, all values given in \$1000's .....	118
Table 32. Results for generating steam from Poihipi Rd condensate in Scenario 2 .....	119
Table 33. The cash flow summary for using Poihipi Rd condensate as boiler feed water n Scenario 2, all values given in \$1000's .....	120
Table 34. Results for generating steam from Poihipi Rd condensate in Scenario 1 .....	121
Table 35. The cash flow summary for using Poihipi Rd condensate as boiler feed water n Scenario 3, all values given in \$1000's .....	122
Table 36. Results for generating steam using IP SGW from FP14 in Scenario 1 .....	123
Table 37. The cash flow summary for boiling IP SGW from FP14 in Scenario 1, all values given in \$1000's.....	125
Table 38. Results for generating steam using IP SGW from FP14 in Scenario 2 .....	126
Table 39. The cash flow summary for boiling IP SGW from FP14 in Scenario 2, all cash values given in \$1000's.....	128
Table 40. Results for generating steam using IP SGW from FP14 in Scenario 3 .....	129
Table 41. The cash flow summary for boiling IP SGW from FP14 in Scenario 3, all values given in \$1000's.....	130
Table 42. Results for generating additional power by heating makeup SGW for the Binary Plant for Scenario 1 .....	131
Table 43. Cash flow analysis for generating additional power by heating makeup SGW for the Binary Plant in Scenario 1, all values given in \$1000's .....	133
Table 44. Results for generating additional power by heating makeup SGW for the Binary Plant for Scenario 2.....	134
Table 45. Cash flow analysis for generating additional power by heating makeup SGW for the Binary Plant in Scenario 2 and Scenario 3, all cash values given in \$1000's .....	135
Table 46. The breakeven prices of landing residues for the hybrid configurations.....	139



## 1.0 Introduction

Due to declining fossil fuel reserves and the evidence of environmental damage and global warming caused by fossil fuel use; renewable energy technologies are being increasingly utilized to supply the growing demand for power [1]. Countries are committing to reducing climate warming emissions, with recently two of the largest emitting countries, the USA and China, ratifying the Paris agreement to curb climate warming emissions [2]. This will certainly increase the demand for renewable energy sources.

New Zealand has historically generated a large proportion of its electricity from renewable energy sources; with approximately 80% of the electricity generation in New Zealand coming from renewable sources in 2014. This is due mainly to the utilization of hydro and geothermal resources as can be seen in Figure 1.

The consumption of electricity in New Zealand has more than doubled since 1975 [3], though the electricity demand has been seen to stagnate in recent years. This flattening of demand is attributed to plant closures in the high energy use area such as pulp and paper, better insulation and more efficient electrical appliances [4].

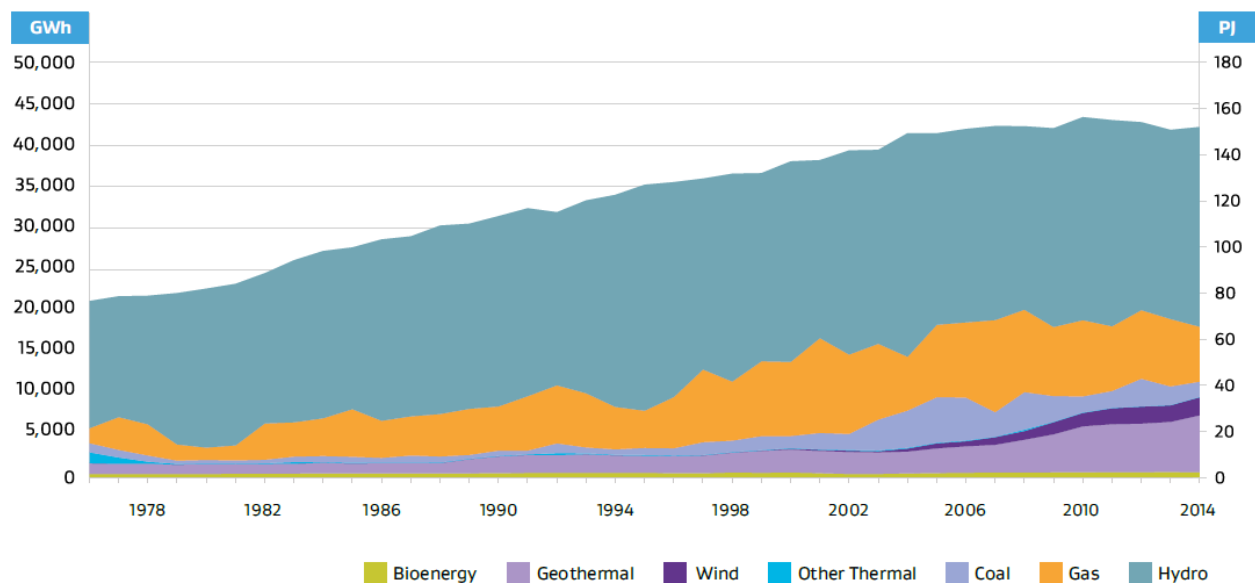


**Figure 1. The annual electricity generation in New Zealand from 1976 to 2014 by fuel type[5].**

Flat demand and a competitive electricity market has resulted in some displacement of less efficient energy sources with more efficient and renewable sources, such as wind and Geothermal [4]. This trend can be expected to continue with increased awareness of climate change and the gradual depletion of fossil fuels.

Although electricity demand has been flat over the last few years there is the potential for demand to grow significantly over the next decade or so. This demand would be driven by the transport industry converting from a non-renewable fuel base to electric vehicles. It would be desirable to

meet this increased electricity demand with renewable power generation. There may be a need to implement this additional renewable generating capacity relatively quickly, depending on the rate of electric vehicle uptake.

The following sections aim to introduce:

- Technical and economic aspects of both geothermal energy and gasification
- The relevant features of existing geothermal power stations in the Wairakei geothermal field
- Technical and economic features of hybrid power generation
- The rationale for this investigation

## 1.1 Geothermal Energy

Geothermal energy has been utilized for thousands of years in the form of hot springs, while geothermal power generation has been performed since the early 1900s. Geothermal energy is the heat of the earth and is present around the world, though high temperature geothermal resources can only be found in places where the geology permits the transference of heat from the Earth's mantle to the crust. This generally only occurs when seismic activity causes distortions or fractures in the Earth's crust [6]. Where high temperature geothermal resources meet water reservoirs in the ground, hot water and steam are produced. Geothermal power generation is most commonly achieved by using geothermal steam to drive turbines which generate electricity.

Geothermal resources are defined as being dry or wet, depending on if there is liquid present in the geothermal reservoir. If the geothermal resource is dry, then the geothermal steam extracted may be directly passed through steam turbines for power generation. Dry steam plants are generally simpler and less expensive than two-phase steam plants, and account for 26% of global geothermal power production as of 2007 [7]. Two-phase steam plants utilize wet geothermal resources that have both liquid and gas in the geothermal fluid; generally this fluid is separated so the steam may be used with a steam turbine. Fluid separation usually occurs in a single or two steps of flash separation, two-phase steam plants account for the majority of global geothermal power generation, with 42% of geothermal power generation coming from single flash plants, and 23% of power generation coming from double-flash plants.

A simplified schematic of a two flash plant producing energy from extracting two-phase geothermal fluid, separating the liquid and vapour components, and using the steam to drive a turbine is displayed in Figure 2. As can be seen, intermediate pressure (IP) steam is separated from the two-phase geothermal fluid, the resulting separated geothermal water (SGW) is then reduced in pressure, and additional low pressure (LP) steam is generated in a second separator.

Two-flash separation allows for more complete utilization of the steam, however it does require additional process equipment in the form of a second turbine and separator. The remaining SGW and the condensate formed from condensing the steam at the back end of the LP turbine may then be reinjected into the reservoir, or otherwise disposed of.

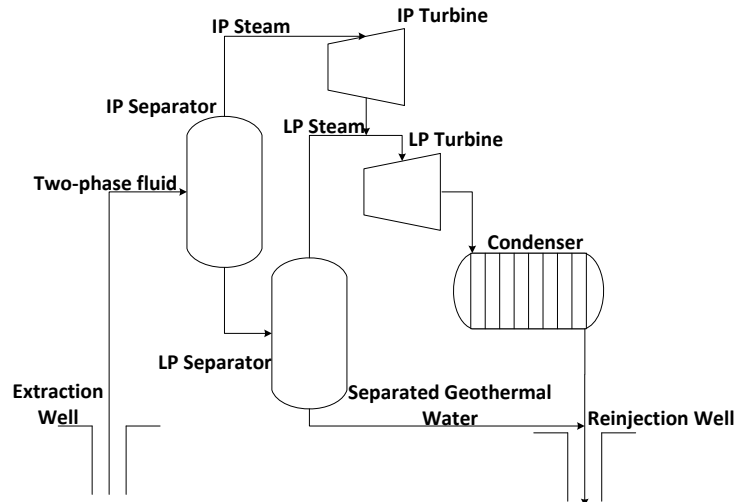


**Figure 2. A simplified schematic of a two flash geothermal power plant.**

Geothermal energy has been used for electricity production on an industrial scale for over 50 years, and has been developed into an important form of power generation, especially in New Zealand. As of May 2007 there were 23 countries utilizing geothermal power generation over 504 sites to produce over 9500 MW [8]. New Zealand has historically been a world leader in geothermal power generation; with the first industrial scale developments to utilize liquid dominated geothermal resources being implemented at Wairakei in the Taupo Volcanic Zone. The installed capacity at Wairakei was initially 47 MW, however due to expansions and redesigning certain parts of the plant, the installed capacity at Wairakei has varied throughout the plants operation, peaking at 172 MW [9]. Several power plants operate utilizing steam from the Wairakei Geothermal Field, which currently provides geothermal steam to several power stations: Wairakei A, Wairakei B, Te Mihi, and Poihipi Rd. There are also two binary plants operating on the Wairakei Geothermal Field, the Wairakei and Te Huka Binary Plants, which generate power using organic Rankine cycles (ORC).

The thermodynamic process of a two flash geothermal power plant is displayed on a Mollier diagram in Figure 3. The numbered labels on Figure 3 represent the different states of the geothermal fluid throughout the process of generating power from the geothermal fluid. Power is generated from the two-phase fluid by the following steps:

- The two-phase geothermal fluid is extracted from the wellhead at State 1
- The fluid is flashed as it enters the first stage separator, decreasing its pressure to State 2
- The geothermal fluid is then separated in the separator into the liquid and vapour components at State 3 and State 6 respectively
- The separated liquid is then passed to the second stage separator, and again flashed to a lower pressure at State 4
- The lower pressure geothermal fluid is then separated into its liquid and vapour components at State 5 and State 7 respectively
- The SGW at State 5 can then be used in an organic Rankine cycle plant to generate additional power, reinjected to the geothermal reservoir, or otherwise disposed of
- The high pressure steam is expanded from State 6 to State 7 using a turbine
- The low pressure steam at State 7 is then expanded across a second turbine to State 8

- The resulting low quality steam at State 8 is condensed to State 9, where the condensate may be disposed of or otherwise used on the plant [10].

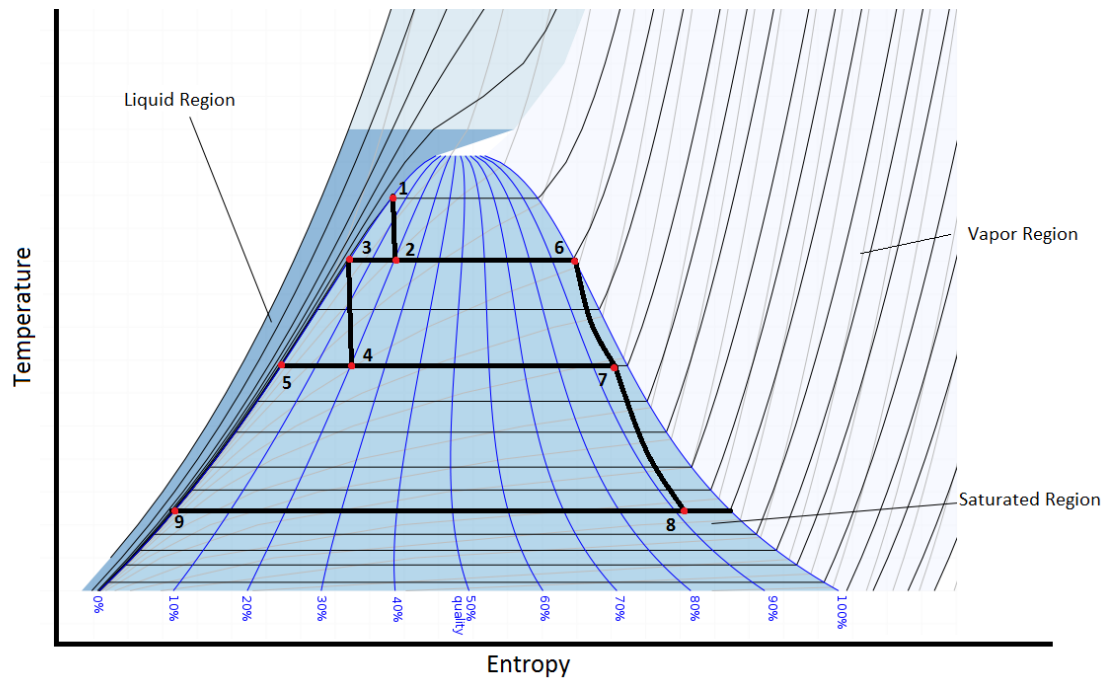


Figure 3. A typical temperature-entropy state diagram for a two flash geothermal power plant, modified from [11].

Geothermal energy is considered to be renewable as the heat extracted from the Earth is small compared to the Earth's large heat content. Geothermal energy does however usually produce emissions of greenhouse gasses due to non-condensable gasses being desorbed from the geothermal fluid. Though, these emissions are generally much lower than most alternatives for energy production. Geothermal power plants have been seen to have a median of 38 gCO<sub>2</sub>eq/kWh, in comparison; coal and gas power plants have been seen to have median emissions of 820 gCO<sub>2</sub>eq/kWh and 490 gCO<sub>2</sub>eq/kWh respectively [12]. Geothermal resources can also be utilized in a binary power plant, which can theoretically have zero direct greenhouse gas emissions, though in reality venting of CO<sub>2</sub> is generally performed [13].

### 1.1.1 The Relative Cost of Geothermal Power Production

A further point to put the attractiveness of geothermal electricity generation into perspective is the relative cost of new generating capacity compared to other renewable and non-renewable sources, as displayed in Figure 4 [14]. It is clear that geothermal is one of the cheapest electricity generation sources.

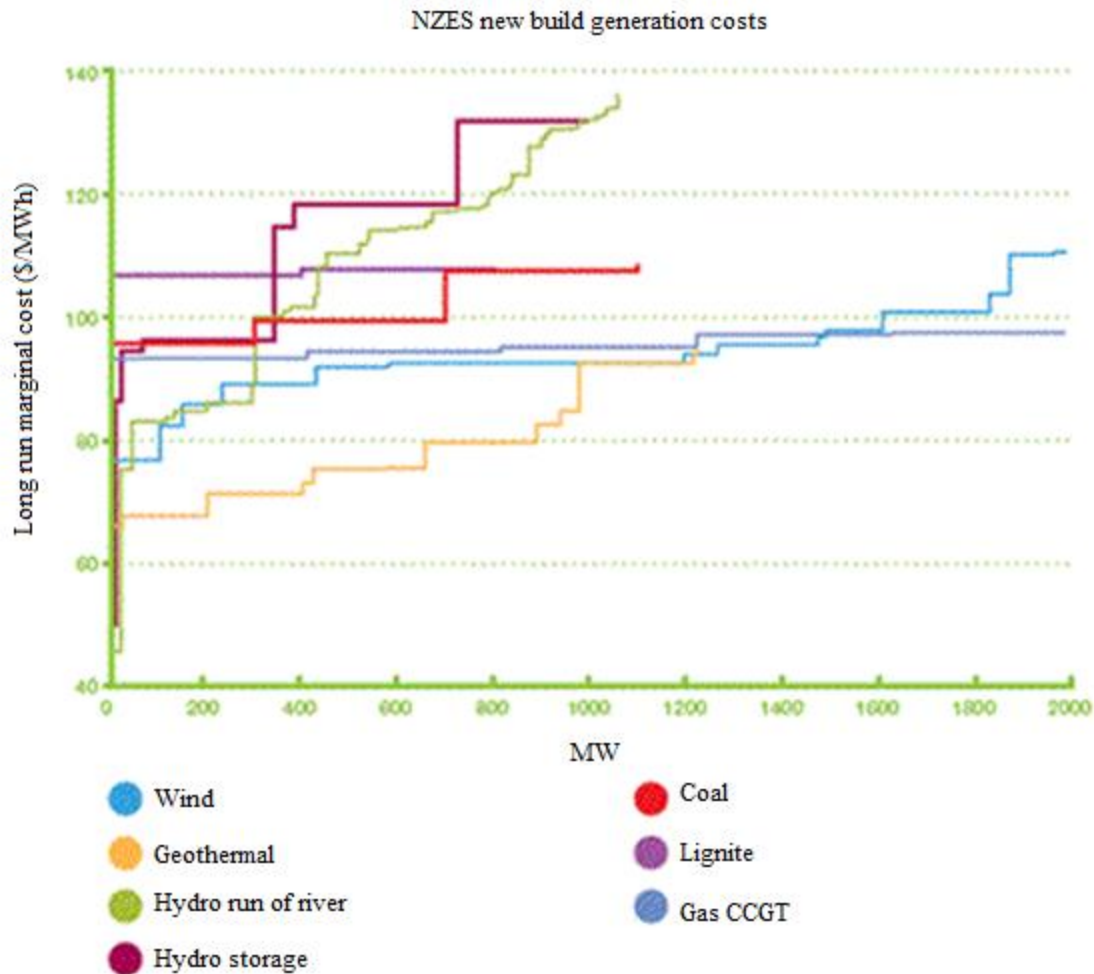


Figure 4. The relative power generation costs for different energy sources in New Zealand [14]

## 1.2 Gasification

Gasification is the process of converting a carbonaceous fuel to a gas with a usable heating value; this gas is called: synthesis gas, syngas, or producer gas. In this study the gas produced from gasification will be called syngas. During gasification, partial oxidation generally occurs to the gasification feedstock creating  $H_2$  and  $CO$ , of varying ratios within the syngas. The produced syngas can be burned directly to produce heat, used to produce work by using a gas engine or a gas turbine, or refined into liquid fuels. Coal was the first feedstock used for industrial gasification, though gasifiers have been developed so that they may produce syngas from biomass and waste products. If biomass is used as the feedstock for gasification then the process is considered to be renewable, and can have minimal emissions. Provided there is regrowth or replanting of the feedstock biomass, then any  $CO_2$  emitted from the burning of syngas will be balanced by a corresponding amount of absorbed  $CO_2$  by the biomass during its growth. Therefore, biomass gasification is considered to be at worst, a carbon neutral form of energy production [15],[16].

Biomass gasification can exist in conjunction with other industrial activities, such as forestry, as there are often large quantities of biomass that are by-products or waste products [17].

Within gasifiers, a range of different reactions occur in order to convert biomass feed into combustible gasses. The reactions can be split into four steps within the gasification process; drying, pyrolysis, combustion, and gasification. Drying is the process of vaporizing water within the biomass. The moisture content of woody biomass can be as large as 50% by weight on a wet basis (WB), while most gasifiers require moisture content within the range of 10-20% (WB). Therefore, the majority of biomass drying required to be performed prior to feeding the biomass into the gasifier. The remainder of the moisture content of the biomass is removed in the gasifier as the biomass is heated to approximately 200°C. As the dried biomass is heated to above 230°C, pyrolysis occurs which decomposes the biomass into volatile gasses, char, and tars. If the gasifier is operated with air or oxygen as the gasification agent, then combustion of carbon and hydrogen will occur, providing heat for gasification. The gasification step has several different reactions occurring; the rates of these reactions are determined by the reaction conditions and type of feed to the gasifier. The reaction rates of the different reactions in the gasification step can serve to determine the composition of the syngas [18].

Gasification can occur in several different types of gasifiers, with fixed or fluidized bed material, and with updraft or downdraft flow configurations. The range of applicability for different gasifier types is represented in Figure 5, based on the thermal input of the feedstock to the gasifier. The type bed material used within the gasifier can also be selected in order to aid in gasification, with some bed materials acting as catalysts to the reactions being carried out within the gasifier.

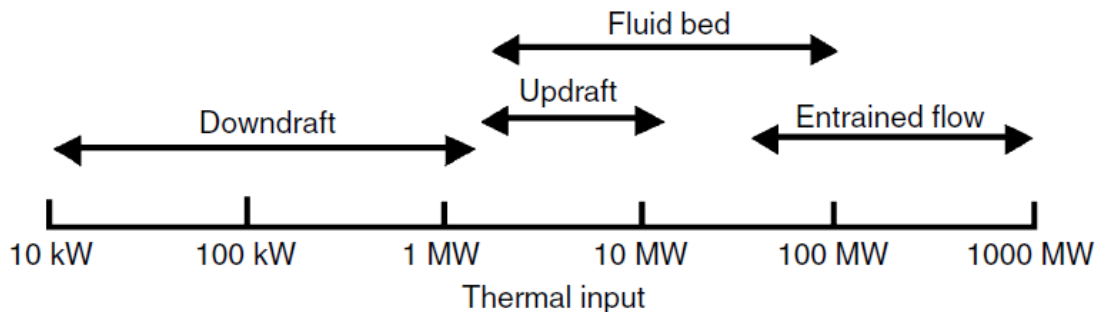


Figure 5. The range of applicability of different gasifier types [19].

### 1.2.1 University of Canterbury's Gasifier

At the University of Canterbury research into gasification is being performed on a promising type of gasifier called a dual fluidized bed (DFB) gasifier, which consists of two fluidized beds. The combustion of char and makeup fuel occurs in the first fluidized bed which is an entrained flow fluidized bed (CFB), which then passes heated bed material to the second fluidized bed; a bubbling fluidized bed (BFB), which uses the high temperature bed material to provide the necessary heat for the gasification reactions. Figure 6 illustrates the flow paths of the biomass, air, steam, flue gas, and syngas within the gasification system.

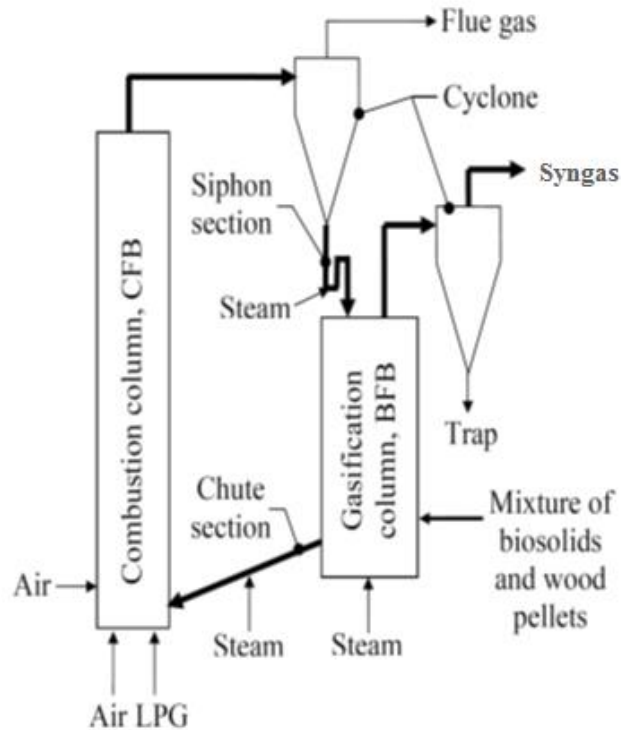


Figure 6. The Dual Fluidized Bed used at the University of Canterbury[20].

The majority of the heat required by the DFB gasifier is provided by the combustion of the char content of the biomass in the CFB, though some additional fuel is required. LPG is used as the makeup fuel for the University of Canterbury's DFB gasifier, recycled syngas could also be used to provide the additional heat for gasification.

### 1.3 Wairakei Geothermal Field

The existing electricity generation plant at Wairakei utilizes a liquid dominated geothermal reservoir, and predominantly two-stage flash separation is used prior to piping the steam to the steam turbines. The Wairakei Steam Field Schematic is displayed in Figure 7, showing the steam manifold joining the Wairakei A, Wairakei B, Te Mihi, and Poihipi Rd Power Stations. There is also the nearby Ohaaki Geothermal Power Station, which is also owned by Contact Energy, but does not utilize the Wairakei Geothermal Field

A large amount of separated geothermal water (SGW) is produced by separating steam from the two-phase fluid extracted from the reservoir. As the SGW is still at high temperatures some SGW is used to provide heating to other companies such as a prawn farm and local hot pools. SGW is also used to provide the heat for the Wairakei Binary Plant. The SGW is disposed of either by reinjection or by draining into the Waikato River. The schematic for SGW use and disposal on the Wairakei Geothermal Field is displayed in Figure 8.

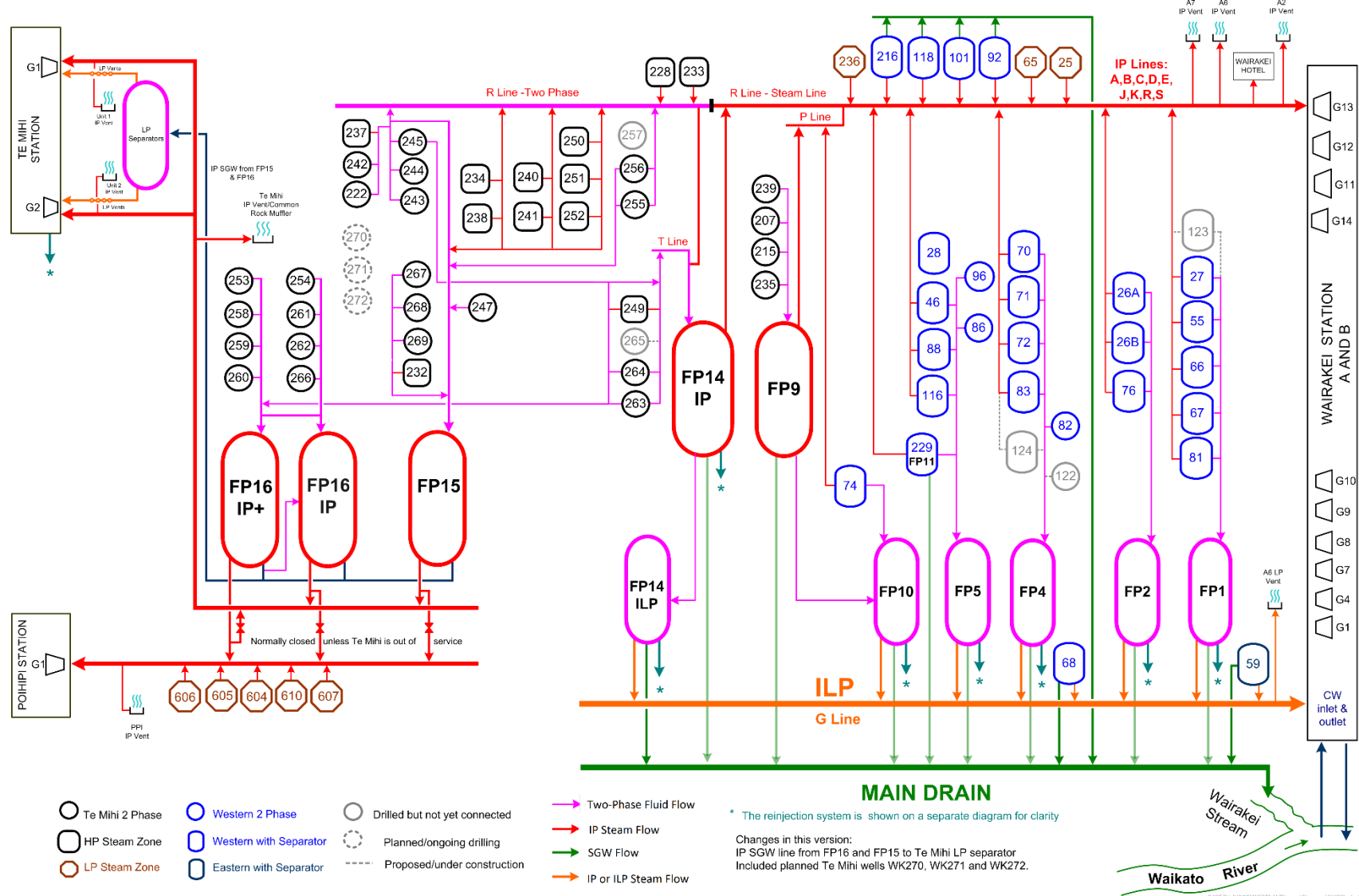


Figure 7. The schematic for the steam extraction manifold of the Wairakei Geothermal System [21]



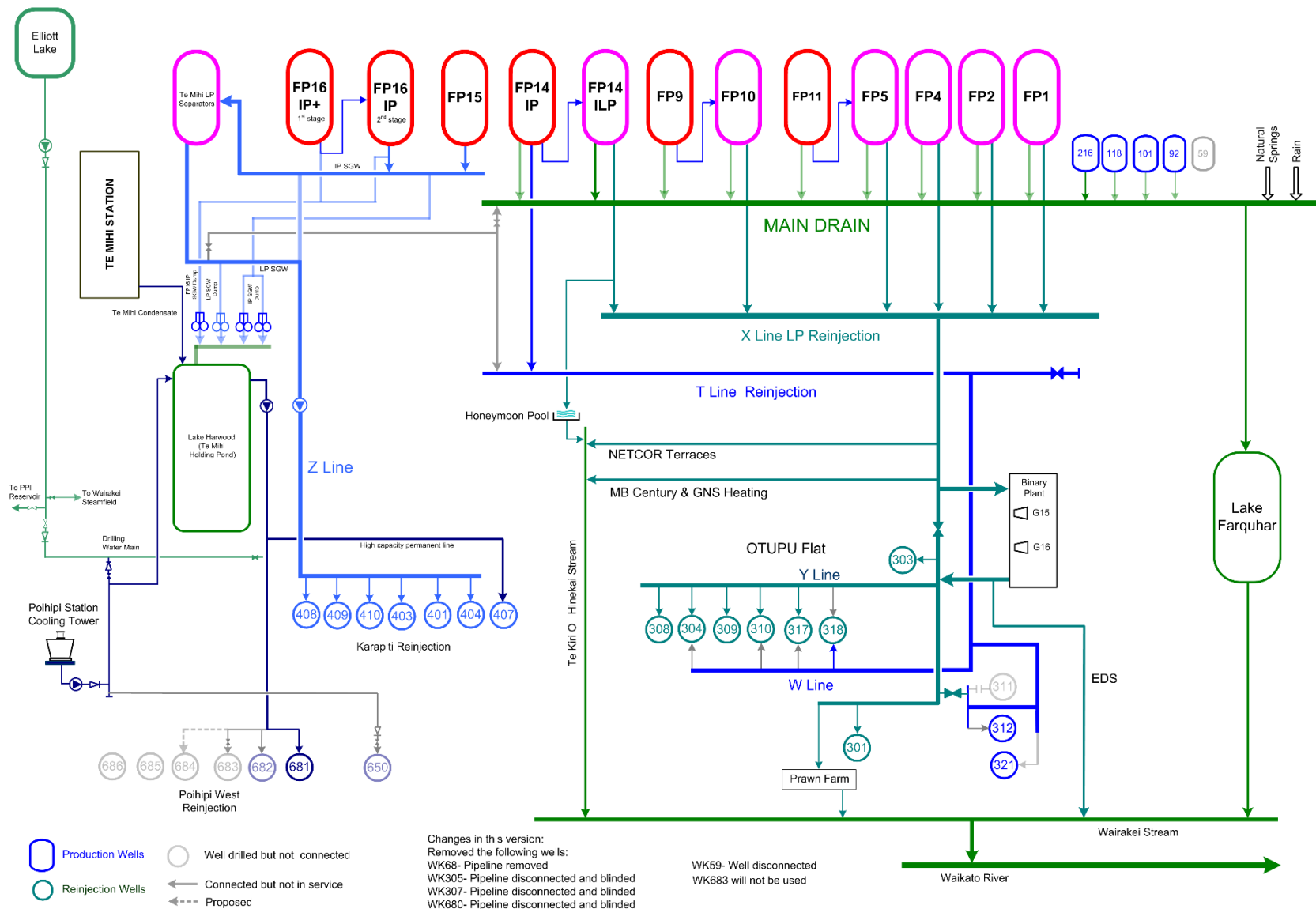


Figure 8. Schematic of the separated geothermal water manifold at the Wairakei Geothermal System [21]

### **1.3.1 Wairakei A and B Power Stations**

The oldest Power Station on the Wairakei Geothermal Field, the Wairakei A and B Stations were commissioned in 1958. Currently, there are 8 steam turbines in operation at the Wairakei A and B Stations. The current designed output for the Wairakei A and B Stations is 134.8 MWe. There are four types of turbines at the Wairakei A and B Stations:

- One intermediate pressure (IP) turbine, which generates 11.2 MWe at full load using IP steam at 4.5 bara and exhausting LP steam at approximately 1.1 bara into the LP turbine manifold
- Three low pressure (LP) condensing turbines, which generate 11.2 MWe each at full load, use LP steam at 1.1 bara, and produce condensate under vacuum conditions using water from the Waikato River
- Three mixed pressure (MP) condensing turbines which generate 30 MWe each at full load, utilize steam at 4.5 bara and then 1.1 bara through different passes, and produce condensate under vacuum conditions using Waikato River water
- One Intermediate Low Pressure (ILP) turbine, which generate 4 MWe at full load, uses steam at approximately 2.1 bara, and creates LP steam at its exhaust

The Wairakei A and B Stations, are displayed in Figure 9 [9]. The A and B Stations have previously had a designed generation of 161.2 MWe, but the removal of an 11.2 MWe IP turbine, G1 and an 11.2 MWe LP turbine, G8, has reduced the installed capacity.

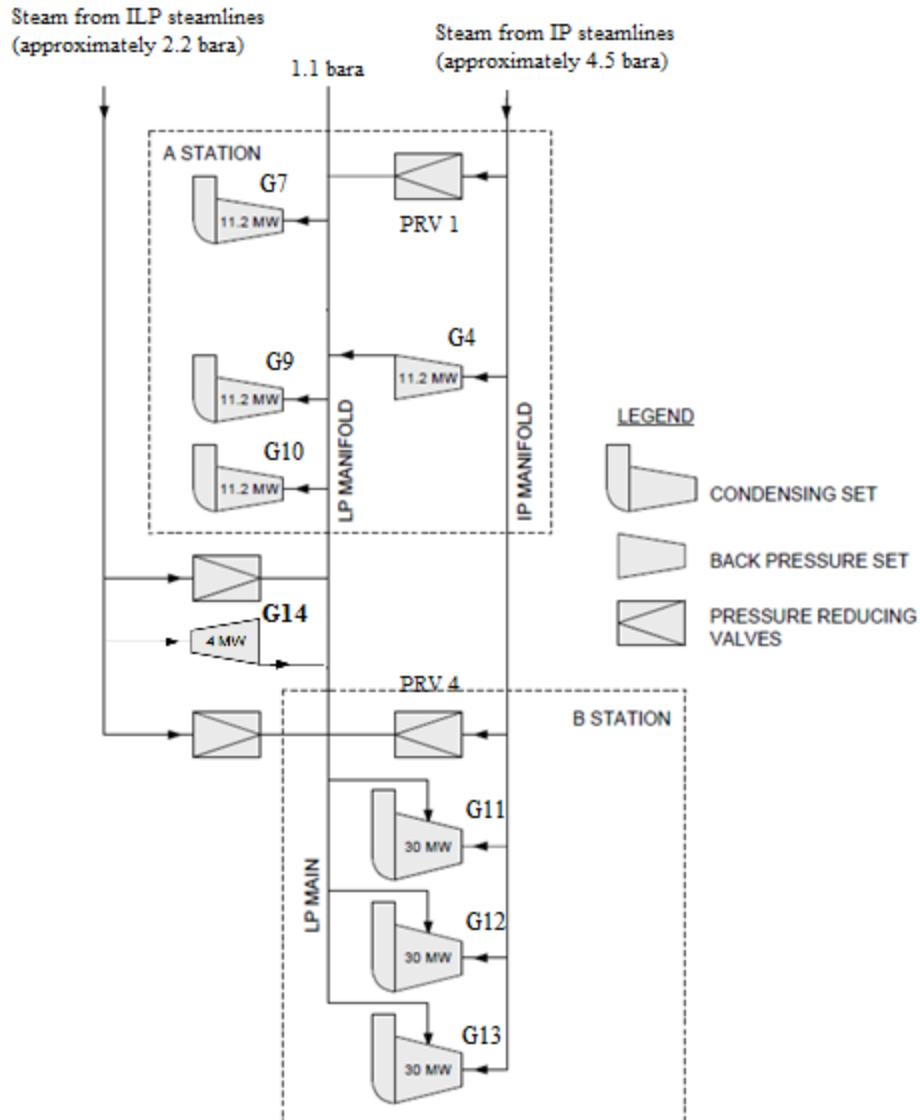


Figure 9. Schematic of the Wairakei Power Plant A and B Stations[22].

### 1.3.2 The Te Mihi Power Station

The Te Mihi Power Station is the most recent addition to the Wairakei Geothermal Field, it was opened in 2014 and is rated to produce a total of 166 MWe [23]. It uses two mixed pressure 83 MWe MP steam turbines that operate using a mixture of IP and LP steam. Direct contact condensers are used in order to condense the steam at the back end of the turbines. The condensers utilize water from cooling towers in order to perform condensation, which is predominantly composed of Te Mihi condensate, though Poihipi Rd condensate is also added to the cooling tower blowdown in order to regulate the water chemistry. A diagram of one of the two turbine cycles at the Te Mihi Power Station is displayed in Figure 10.

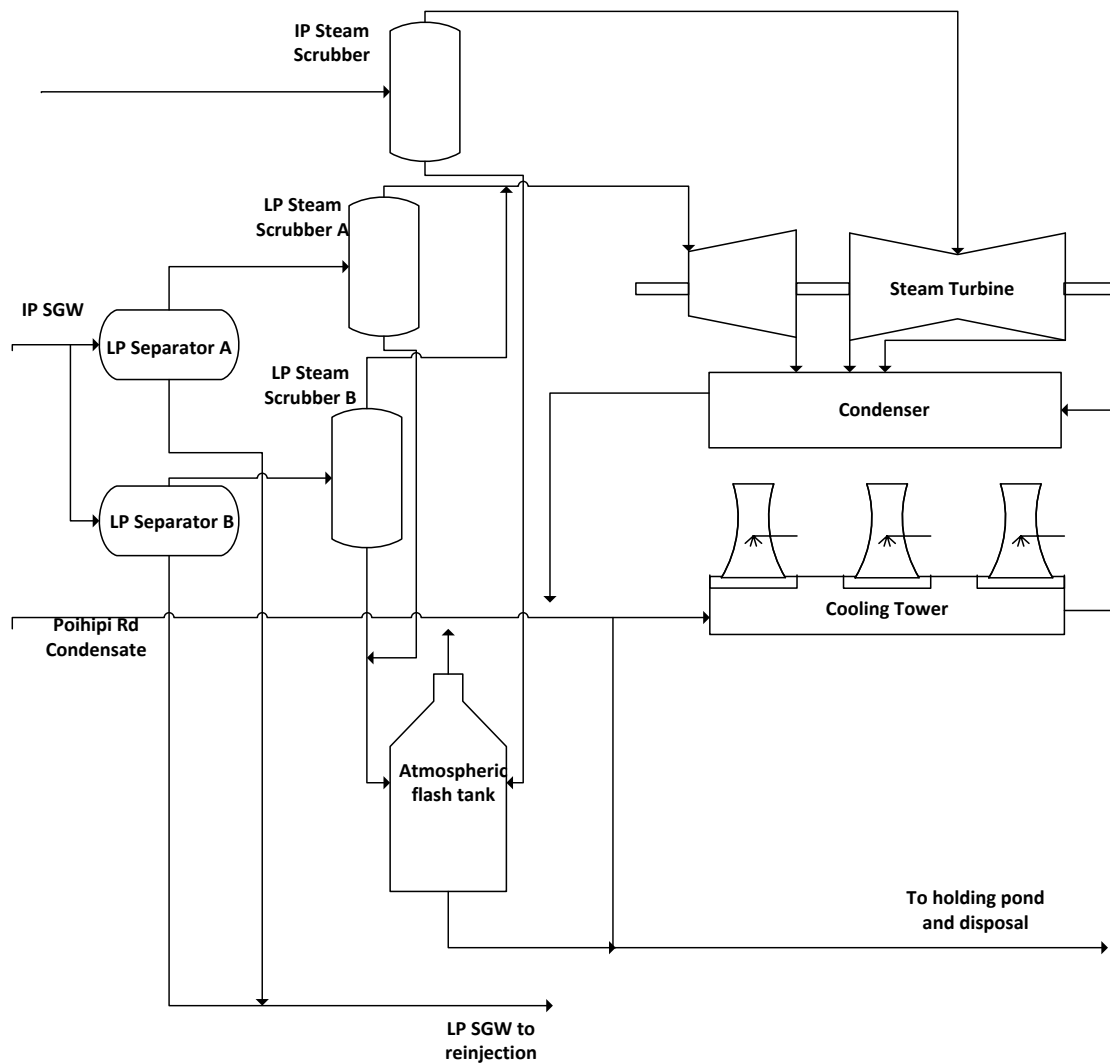
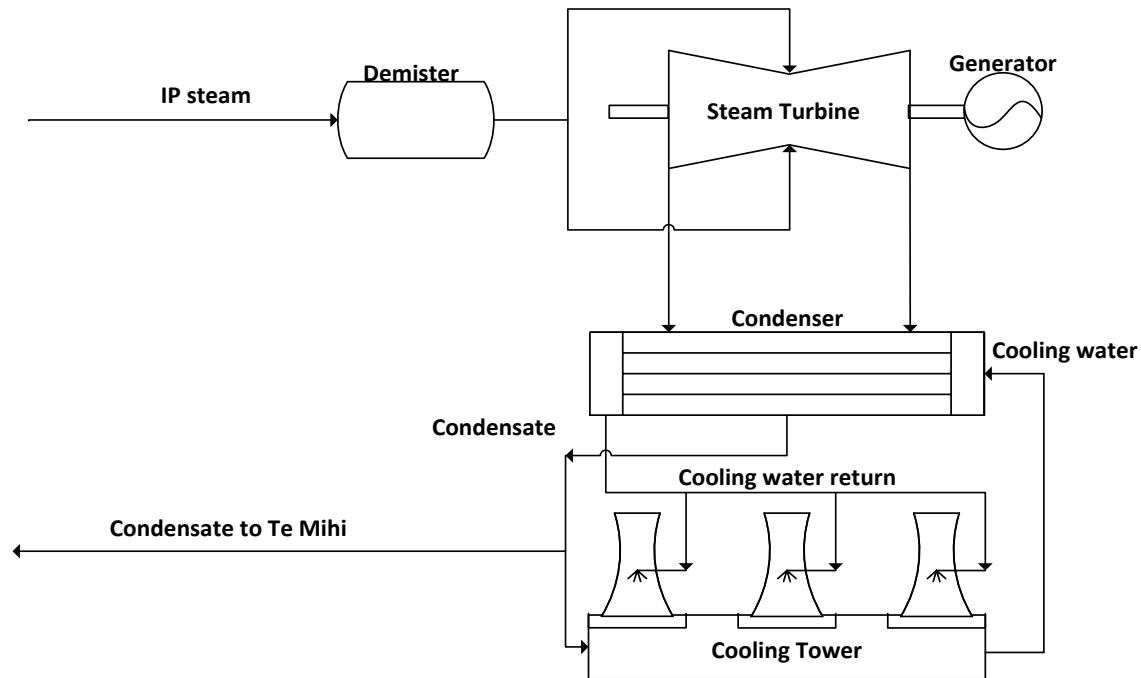


Figure 10. A diagram of one of the two identical turbine cycles at the Te Mihi Power Station

### 1.3.3 The Poihipi Rd Power Station

The Poihipi Rd Power Station was constructed in the mid-1990s as a joint venture between Mercury Energy and Geotherm Energy, however it was acquired by Contact energy in 2000 [9]. Poihipi Rd has a single 55 MWe steam turbine that operates using IP steam from the Wairakei Geothermal Field. Poihipi Rd is unique in the Wairakei Geothermal Field, as it uses a shell and tube condenser to condense the geothermal steam at the back end of the turbine, as opposed to the direct contact condensers used at the Wairakei A and B, and the Te Mihi Power Stations. As no water from the Waikato River is mixed with the Poihipi Rd steam condensate and there is no contact with the atmosphere, Poihipi Rd condensate is considered to be cleaner than that from the direct contact condensers. A diagram of the Poihipi Rd Power Plant is displayed in Figure 11.



**Figure 11. Diagram of the Poihipi Rd Power Plant**

### **1.3.4 The Wairakei Binary Plant**

The Wairakei Binary Plant was constructed in 2005 in order to generate additional power by utilizing some of the high temperature SGW available in T-Line prior to its reinjection. The Binary Plant consists of two twin power generating units, G15 and G16, which generate power using pentane as the working fluid in organic Rankine cycles as displayed in Figure 12. G15 and G16 are designed to produce an average combined power output of 15 MWe, though this fluctuates with changing ambient temperature, SGW flowrate, and SGW temperature, and has been as high as 20 MWe. Currently silica scaling is observed within the plant, which serves to increase pressure losses within the plant, and results in a reduction in the power generation of the Binary Plant, thus silica removal is currently performed biannually.

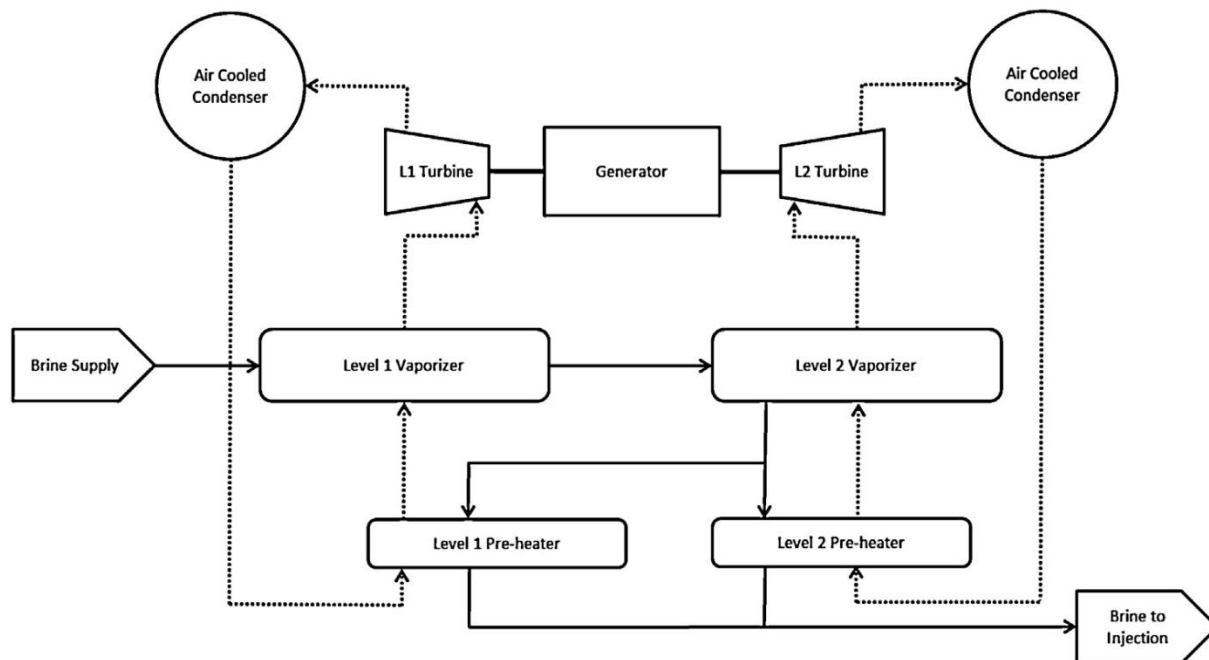


**Figure 12. Diagram of one of the twin pair of binary plant cycles within the Wairakei Binary Plant (Dotted lines represent pentane flow) [24]**

## 1.4 Hybrid Power Generation

Hybrid power generation is the generation of power using two or more sources integrated together that may serve to increase the stability of power generation and increase plant efficiency[25]. Currently many sources of energy are utilized to perform power generation; this is due in part to both capacity limitations of power generation sources and the desire to spread the risk of source specific outages that drastically effect power generation. This use is of particular import to renewable power generation, as fossil fuels are seen to provide relatively reliable power generation. Sources such as wind, solar, and hydroelectric power generation however, are affected by weather events, and can produce highly variable amounts of power depending on the weather conditions.

Geothermal power is currently being utilized in conjunction with biomass and solar resources for hybrid power generation. A biomass/geothermal power plant has been in operation since 1989 in Honey Lake, California. Geothermal resources are used to preheat boiler feed water, and biomass in the form of forest trimmings, urban wood waste, and sawmill by-products, is used to generate steam for use in a turbine[26]. An integrated solar/geothermal plant is also currently in operation in Nevada; the Stillwater plant combines solar photovoltaics, and an organic Rankine cycle (ORC) plant using geothermal brine for power generation. Originally the plant was an ORC plant utilizing a geothermal reservoir, though due to the pressure decrease that is often associated with geothermal reservoirs, the power output of the plant was seen to decrease. Solar photovoltaics were then introduced to the plant instead of drilling additional wells in order to supplement the power generation from the ORC. Though there was not direct hybridization of these two power sources, some electrical equipment was shared, serving to reduce capital investments. However, in 2014 an array or parabolic troughs were installed at the Stillwater plant in order to concentrate solar energy

to increase the temperature of the geothermal brine before entering the ORC plant. This addition of solar thermal power generation adds 2 MWe to the power generation of the plant, and is expected to slow the depletion of the geothermal reservoir. It has similarly been suggested that concentrated solar thermal energy could be used in conjunction with biomass gasification in order to provide the heat for gasification [27]. These hybrid power plants illustrate that different renewable sources of power generation may be combined in order to attain a greater efficiency than if each were utilized separately.

## **1.5 Reason for Investigation**

Though gasification is a promising renewable technology which could serve to produce sustainable combustible gas or liquid fuels if the syngas is further refined; there are very few commercial biomass gasification plants globally. This is generally attributed to the relatively high cost of biomass derived fuels compared to the fossil fuel alternatives. Biomass gasification is also not a mature technology, and government support and clean energy incentives are generally required for a biomass gasification plant to be considered commercially viable. However if the capital costs of a biomass gasification plant can be reduced by hybridization with an existing plant, this may serve to make the gasification plant viable. It is also possible that power generation using a hybrid gasification/geothermal plant would have a higher efficiency than a standalone biomass electricity generation plant, as this is commonly the case with hybrid power plants[28].

Contact Energy owns and operates several geothermal power plants in the Taupo Volcanic Zone in the Central North Island of New Zealand. During the utilization of the Wairakei field, there has been a significant decrease in the pressure of the reservoir as displayed in Figure 13. Though, the reservoir pressure has been increasing since 1997 with part of this attributed to the in-field injection of the geothermal brine occurring [29]. In order to maintain the Wairakei Geothermal Field, steam extraction limits are in place in order to regulate the amount of steam that can be utilized, to maintain the pressure of the field and ensure subsidence does not occur [30].

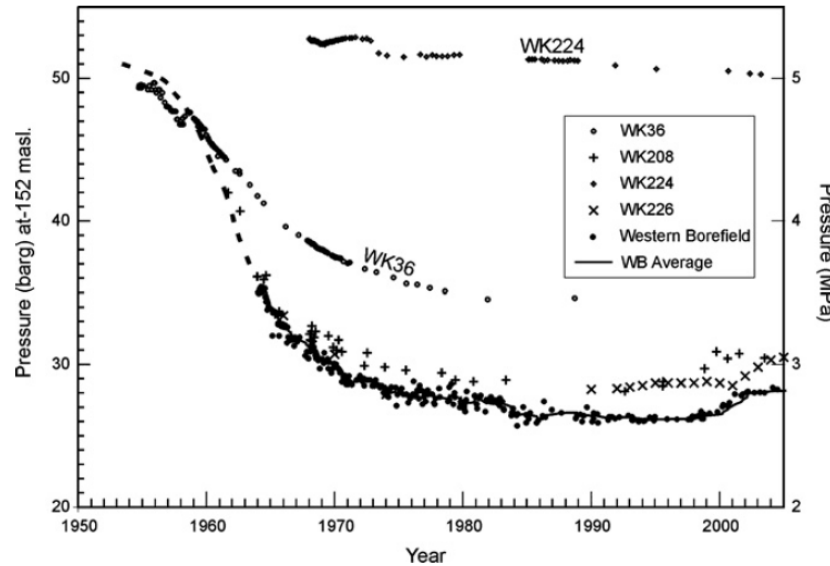


**Figure 13. The pressure drop at several steam extraction wells at the Wairakei Geothermal Field [29]**

There are currently multiple power plants operating on the Wairakei Geothermal field, the Wairakei A Station, the Wairakei B station, the Te Mihi Station, and the Poihipi Rd Station, all of which are connected by a steam manifold. The Te Mihi and Poihipi Rd Stations are more recent additions to the Wairakei Geothermal Field, and can more efficiently generate power from the geothermal steam than the Wairakei A and B Stations. Because of this, the steam is generally used preferentially at the Te Mihi and Poihipi Rd Stations to ensure maximum power generation. The combination of the steam extraction limits imposed on the Wairakei Geothermal Field, and the preferential utilization of steam at Te Mihi and Poihipi Rd, has caused there to be some unused capacity for power generation at the Wairakei A and B Stations.

Due to the unused capacity at Wairakei, and the proximity of Wairakei to the largest area for forestry in New Zealand; there may be a case for the retrofitting of the Wairakei plant or other geothermal plants in this area with biomass gasifiers. This hybridization could serve to augment the power generation at the geothermal plant, or used to reduce steam extracted from the geothermal reservoir if the steam extraction becomes further limited.

In short, the salient factors relating to this study are as follows:

- It is desirable to increase the proportion of electricity generated from renewable energy sources
- Geothermal electricity production is relatively cheap, renewable, and a proven technology
- Geothermal steam fields often decrease in enthalpy over time, decreasing the electricity generation possible utilizing the field
- New Zealand has a large amount of currently unused biomass in the form of landing residues in close proximity to geothermal power plants in the Central North Island
- Hybrid Power Plants are generally more efficient than single fuel plants, as there is sharing of infrastructure and opportunities to optimize efficiency



- There are very few commercial gasification plants, and hybridization of biomass gasification with a proven technology could act as an intermediate step in the implementation of biomass gasification
- Biomass gasification could be retrofitted to a geothermal power plant to; boost electricity production, mitigate reservoir deterioration by reducing the steam extraction to achieve the same power production, or a combination of these.
- This investigation focuses on retrofitting the underutilised Wairakei Geothermal Stations with biomass gasification facilities. Various design options are considered and an initial economic analysis is performed.

## **2.0 Potential Hybrid Plant Configurations**

There are a variety of ways of retrofitting an existing geothermal power plant to utilize syngas generated in a biomass gasifier. Several different configurations for a hybrid geothermal/natural gas power plant were discussed in a report by the Kingston, Reynolds, Thom, and Allardice Consulting Company for the New Zealand Energy Research and Development Committee [31], which may also be applicable for a geothermal/gasification hybrid plant. The majority of these configurations were designed to superheat the geothermal steam after the vapour/liquid separation step, and some involved the addition of a gas turbine to generate additional electricity in a combined cycle. There has also been a study performed by Thain and DiPippo into the hybridization of geothermal power generation, using a biomass boiler to provide additional heat to the process [32]. However, these configurations proposed in these studies were related to potential new hybrid plants, and therefore were unconstrained by the limitations associated with retrofitting an existing geothermal plant.

### **2.1 Factors for Consideration**

There are several sources of potential problems from hybridization that are common amongst the different hybrid configurations. These factors are briefly explained in this Section, and expanded on as required for the different configurations.

#### **2.1.1 Dissolved Minerals**

The deposition of mineral scale can occur in wells, separators, pipes, turbines, and heat exchangers in a geothermal power plant. There are many types of minerals that are present in geothermal waters that have the potential to form scale. However at the Wairakei Power Plant, silica is the mineral that is seen to cause the most operational problems at the plant. This scaling can be an obstacle for fluid flow, as it can cause pressure losses in pipes by reducing the diameter of flow paths. The scale can often have a rough texture, increasing the pressure losses caused by the friction of the fluids in the pipe contacting the walls of the pipes. The deposition or precipitation of solids on heat exchanger surfaces is known as fouling. Fouling increases the thermal resistance of the heat exchanger, as the mineral scale has a lower thermal conductivity than the heat exchanger tubes. The removal of silica scale often necessitates plant shut down in order to clean the process equipment of silica scale [24]. The problems encountered with silica and scaling geothermal power plant may be exacerbated with the introduction of a gasifier to augment power generation to the plant, due either to evaporative precipitation or decreasing solubility of the minerals in water occurring with decreasing geothermal water temperature.

### **2.1.2 Dissolved Gasses**

Geothermal fluids usually contain gases such as carbon dioxide, hydrogen sulphide, ammonia, and methane with the concentration generally increasing with reservoir temperature, though it is highly variable between geothermal fields. These gases can prove to be an environmental pollutant if they are released directly, and can also affect the chemistry of the geothermal fluids that must be taken into account with plant design. The hydrogen sulphide and carbon dioxide present in the geothermal fluid are both known causes of plant corrosion [33]. Non-condensable gas removal generally occurs during the condensation of the geothermal steam, in order to maintain the vacuum conditions in the condenser. If hybridization is to occur, care must be taken to ensure the dissolved gases in the geothermal fluids do not cause damage to the new and existing process equipment due to changes in the plants operation.

### **2.1.3 Design Limitations of the Existing Plant**

The fact that this study is concerned with the retrofitting of an existing geothermal power plant with a biomass gasifier must be considered throughout the design process. Due to the plant design and material selection of the existing plant, configurations that may be possible for a new hybrid geothermal-gasification plant may not be practical to retrofit.

### **2.1.4 Syngas Purity**

Syngas created in biomass gasifiers contains contaminants such as; particulates, tars, hydrogen sulphide, carbon dioxide, nitrogen compounds, alkali compounds and chlorine compounds [34]. In order for syngas to be utilized in gas turbines or gas engines, cleaning will be required. With removal of alkali, and sulphur compounds, particulates, tars, and chloride compounds from the syngas needing to be performed [35].

According to Brown, the syngas produced from a dual fluidized bed gasifier will have approximately  $10 \text{ g/m}^3$  of tars, and “high” particulate content from the gasifier [36]. The amount of sulphur, nitrogen, and chloride contaminants in the syngas are dependent on the feed to the gasifier. As it is most likely that any gasifier retrofitted at the Wairakei Power Station will have a feed of landing residues due to the large amount of forestry in the Central North Island; woody biomass is used as the basis for calculating the contaminants of the gasification syngas. It was found that woody crops have a range of concentrations for nitrogen, sulphur, and chlorine of 0.06 – 0.6 wt. %, 0.01 – 0.02 wt. %, and 0.01 – 0.10 wt. % respectively [36].

The tolerance of fired boilers to the contaminants present in syngas is not known, though it is expected that fired boilers will have a higher tolerance to the expected contaminants than internal combustion engines and gas turbines. Some general contaminant tolerances for internal combustion engines and gas turbines are displayed in Table 1.

**Table 1. The tolerances of internal combustion engines and gas turbines to various contaminants present in syngas [34].**

Contaminant	Unit	IC Engine	Gas Turbine
Particulate	$mg/m^3$	< 50	< 30
Tars	$mg/m^3$	< 100	< 8
Sulphur	$ppm$	-	<20
Nitrogen	$ppm$	-	<50
Alkali	$ppb$	-	<24
Chloride	$ppm$	-	<1

It is believed that using cyclones to remove the particulates from the syngas will be sufficient cleaning if the syngas is to be utilized in a boiler or furnace, as direct combustion technologies are much more resilient to contaminants compared to gas engines and gas turbines. Also, tars that are present in the syngas will be able to be burnt by direct combustion, and provide some additional heat for combustion. The precipitation of tars is not expected to occur, if the hot syngas is combusted, however if this syngas stored or otherwise allowed to cool, tar precipitation may occur. As it is assumed that syngas combustion will occur directly after syngas formation, this is not expected to be an issue, but may need to be taken into account with shutdowns for plant maintenance.

## 2.2 Superheating of Geothermal Steam

The superheating of the geothermal steam using gasification syngas is perhaps the simplest concept of the different hybrid configurations. By superheating the geothermal steam, more electricity may be generated with the same amount of steam, or alternatively less steam may be extracted from the geothermal field to generate the same amount of electricity. The concept of superheating geothermal steam is by no means a new one; it has been proposed from as early as 1924 by Coufourier [37]. Originally geothermal hybrid configurations were generally concerned with using fossil fuels to superheat geothermal steam; however in more recent years hybrid configurations utilizing renewable energy sources have been investigated. An investigation into the superheating of geothermal steam using natural gas at the Ohaaki (previously known as the Broadlands) Geothermal Field was performed for the New Zealand Energy Research and Development Committee by the Kingston, Reynolds, Thom and Allardice Consultancy [31]. More recently, the idea of using a biomass boiler to superheat geothermal steam was investigated by Thain and DiPippo [32].

As power generated from a steam turbine can be given by Equation 1 it can be seen that, as the enthalpy of the input steam increases, the amount of work generated by the steam also increases, provided the exit conditions of the steam turbine are not overly altered.

$$\dot{W}_{ST} = \dot{m}_S(h_{in} - h_{out}) \quad (1)$$

Where:

$\dot{W}_{ST}$  = the work performed by the steam turbine (kW)

$\dot{m}_s$  = the mass flowrate of steam to the turbine ( $\text{kg s}^{-1}$ )

$h_{in}$  = the enthalpy of the steam at the inlet of the turbine ( $\text{kJ kg}^{-1}$ )

$h_{out}$  = the enthalpy of the steam at the outlet of the turbine ( $\text{kJ kg}^{-1}$ )

Because of the increase in enthalpy of the steam due to superheating; the power generated by the steam turbine will be increased by superheating the input steam. A simplified representation of the superheating of geothermal steam using a syngas fired heat exchanger is shown in Figure 14. The steam and gas requirements for the gasification section of the process will likely be sourced from the geothermal steam, and a recycle stream on the syngas respectively.

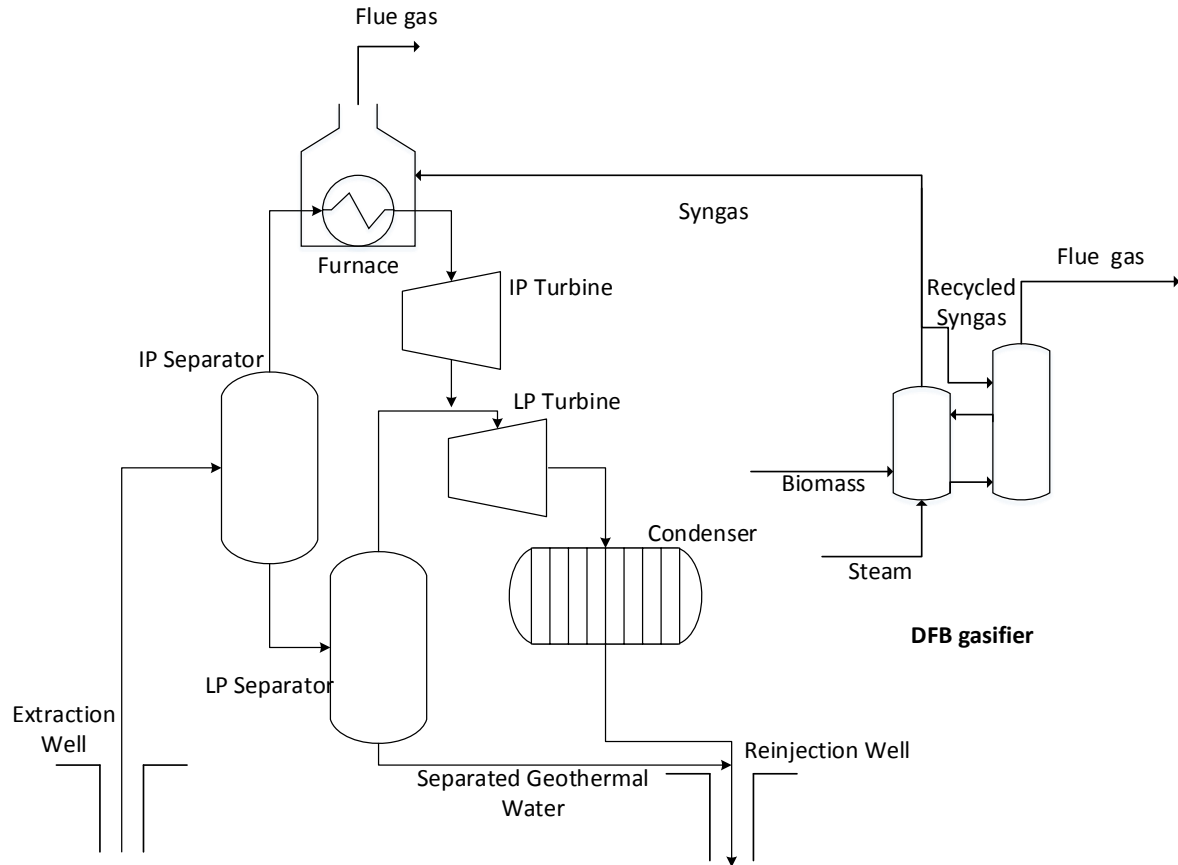


**Figure 14. A simplified diagram of syngas fired superheating of geothermal steam prior to utilization in a steam turbine.**

The process of superheating geothermal IP steam for use in an IP steam turbine may be represented on a temperature entropy diagram as shown in Figure 15. The superheated process is modified from the current steam turbine cycle displayed in Figure 3 by the addition of the superheating from State 6 to State 7 in Figure 15. The steam expansion from State 7 to State 8 is represented as the ideal isentropic expansion, though this will not be the case in reality. The greater temperature drop attained from turbine expansion in the superheated case compared to the base case will have a correspondingly greater enthalpy drop; and consequently more power may be generated from the steam turbine for the same mass flowrate of steam.

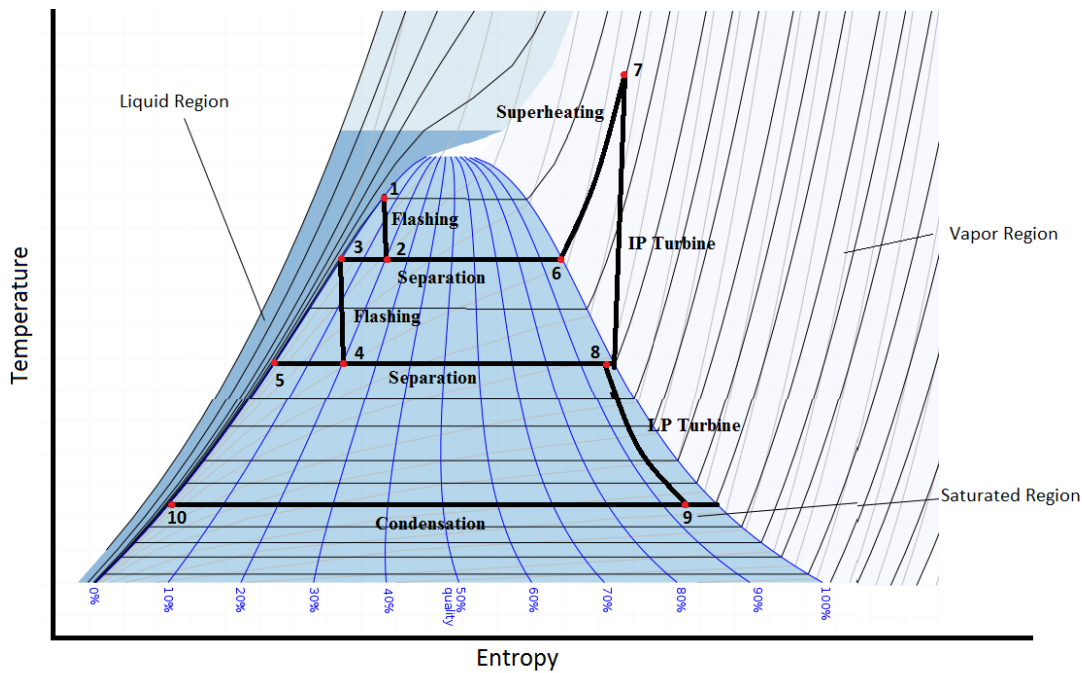


**Figure 15. A temperature entropy diagram for the superheating of geothermal steam modified from [11].**

It was decided that modifying the MP steam turbines at Wairakei to operate using superheated steam would likely be the best option. As the LP turbines are designed for LP steam, there would be limited benefits in superheating the LP steam and retaining it at the LP steam pressure of 1.15 bara. Also, the outlet conditions of an LP turbine would likely be above the saturation line, which could cause problems for condensing the steam after the LP turbine. The IP turbines exhaust the steam into LP manifold, and if superheated steam was fed into the IP turbines, the resultant exhaust would be at a higher temperature, and therefore have a lower density than LP steam. This would cause the LP turbines to require modifications in order to ensure they are utilizing the higher temperature LP steam efficiently. It may be possible to modify both IP and LP turbines and disconnect some LP turbines from the LP manifold to operate using the higher temperature IP steam exhaust. However, as the IP turbine exhaust flowrate is significantly higher than the LP turbine flowrate, multiple LP turbines would be required to be modified. By using the MP turbines, it is believed that superheated IP steam may be introduced to the turbine, and LP steam injected to the second stage of the turbine. This may ensure that the exhaust of the turbine is below the saturation line.

As Waikato River cooling water is used to create the vacuum conditions in the condensers, there is the possibility that by superheating the steam prior to it entering the turbine, there may be difficulty in condensing the steam at the back end of the turbine. The wetness of the outlet of the MP turbines could be as high as 9% during normal operation. However it is expected that the wetness of the outlet of the MP turbine would be lower than this if superheated steam is used as the inlet to the turbine. As the outlet steam becomes drier, more cooling water will be required in order to achieve the necessary condensation. However, provided the steam turbine outlet is below the saturation line condensation will likely be possible, as the outlet steam is already at its saturation temperature. It is also noted that the steam after the first stage generally has some level of condensation occurring within the turbine when saturated steam is used to feed the turbine.

However, if superheated steam is used, this condensation will likely not occur within the first stage of the turbine. As there is an allowance for drainage to occur between stages in the geothermal steam turbines, if no liquid is forming in the turbine, steam may start passing through these drainage holes and causing erosion. This problem is addressed by Morris in his report on using superheated steam in a saturated steam turbine, and he believes that filling these holes will not be an issue, but will limit the ability to operate the turbines using the saturated steam [38].

It may be possible that by superheating the IP steam, evaporation of any liquid carryover present in the geothermal steam will produce small flecks of precipitated minerals. These evaporate particles will be extremely abrasive to the process equipment, and will likely cut into metal, as these particles will be travelling at the same speed as the geothermal steam [38]. The evaporate particles may be able to be eliminated from the feed by utilizing high efficiency separators, and scrubbers to maintain good steam condition. However, currently the relatively large distances between separators and turbines at Wairakei cause the majority of liquid carryover from the separators to form on the walls of the steam lines, and are subsequently removed in drain pots.

## **2.3 Vaporization of Steam Turbine Condensate**

In order to generate additional power from the Wairakei turbines, a boiler creating additional IP steam could be used to supplement the existing geothermal steam supply. In order to reduce the operating costs for the boiler, it would be advantageous to utilize water available on site as the feed water. The majority of the water available at the Wairakei site is in the form of separated geothermal water (SGW), and the high dissolved mineral content of the SGW would likely prove to make the SGW unsuitable to be used as boiler feed water. This is due to the fact that silica scale may form due to both evaporative precipitation, or by precipitation as the geothermal liquid cools, thereby decreasing the solubility of silica in the water [39]. As the solubility of minerals in water is generally much higher in the liquid phase than the gas phase; it may be possible to utilize the steam condensate from the geothermal steam turbines as a source of boiler feed water, as the silica and other minerals have been distilled from the condensate.

Even though the Wairakei A Station is currently the only station with capacity to utilize additional steam on the Wairakei Geothermal Field, it is possible to position the boiler elsewhere on the steam manifold and still utilize this unused capacity. Provided that the IP steam generated is fed into the IP steam lines on the Wairakei Geothermal Field, any additional steam added to the system could result in additional power generation at the Wairakei A Station. This is due to the fact that steam is preferentially used at the Te Mihi and Poihipi Rd Power Stations; any additional steam input into the steam manifold would simply result in less steam being diverted to be utilized at Te Mihi or Poihipi Rd. This is of importance, as it allows sources of condensate other than that formed at Wairakei to be used as boiler feed water in order to generate additional power at Wairakei. The most suitable source of boiler feed water at the Wairakei Geothermal Field was therefore be investigated in Section 4.0 to ensure that the costs associated with cleaning boiler feed water are minimized.

A diagram of the plant configuration utilizing a syngas fired boiler to generate additional steam from the steam turbine condensate is displayed in Figure 16. In order to maximize the steam generation from the boiler, preheating of the geothermal condensate will be performed using SGW.

Though this configuration is expected to have a lower efficiency than other configurations, the fact that it does not obstruct normal operation of the plant, or become integral to the operation of the plant make this configuration more flexible than other configurations.

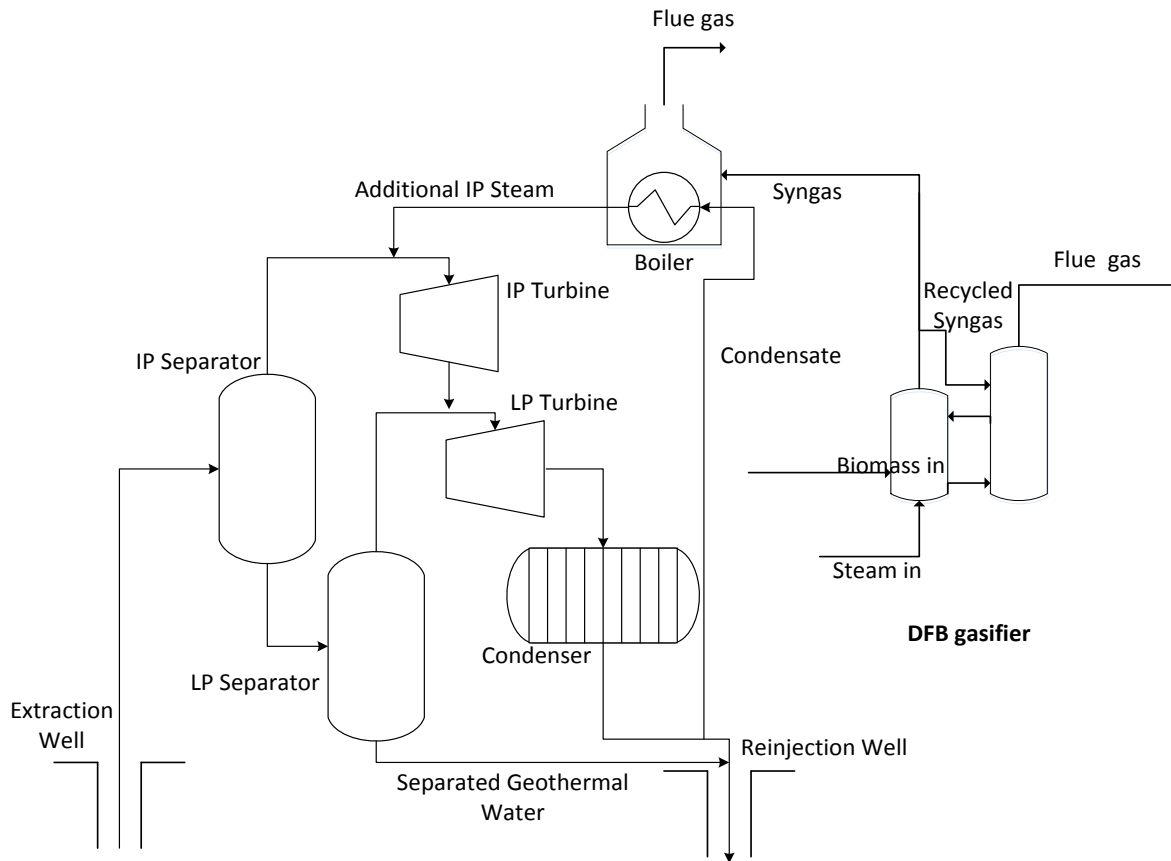


**Figure 16. A diagram of using geothermal steam turbine condensate as feed water to a syngas fired boiler**

It is not only likely that the utilization of condensate for boiler feed water will serve to reduce the risk of mineral scaling compared to utilizing the separated geothermal water; it may even reduce the scaling that already occurs in the geothermal plant. The additional steam generated by vaporizing the geothermal condensate will have a lower concentration of minerals than the IP geothermal steam it is supplementing. This is due to the fact that the blowdown on the boiler will serve to remove the majority of the influent minerals from the boiler [40]. Therefore, implementation of the boiler will reduce the risk of mineral scaling downstream of the boiler. The idea of avoiding silica deposition by dilution has been explored for silica saturated liquids [41], however steam dilution to mitigate silica deposition has not been investigated, to this Author's knowledge. Mineral deposits are known to occur in geothermal steam turbines and are caused by either liquid carry over or evaporated mineral [42]. Therefore, with the addition of supplementary steam that has a lower mineral concentration than the geothermal steam would likely serve to reduce mineral deposition in the geothermal steam turbines.

As it is planned to utilize separated geothermal water in order to preheat the steam turbine condensate, the potential for mineral scaling in the preheater must be taken into account. As the



SGW contains dissolved minerals such as silica, precipitation of these chemicals may occur as the SGW cools, due to the temperature dependence on the solubility of these minerals in water.

There are also strict requirements on the tolerance of boiler feed water to different impurities. Though it is expected that the steam turbine condensate will be significantly cleaner than the SGW, there may still be impurities in the condensate. Investigation of boiler water tolerances, and condensate sampling was therefore performed, to evaluate the suitability of the different water sources at Wairakei for use in a boiler, as discussed in Section 4.0.

There is the potential to vaporize liquid carryover in the geothermal IP steam manifold when the supplementary steam is added to the manifold. If the steam generated in the boiler is at a higher temperature than the IP steam, vaporization of any liquid in the manifold is likely to occur. As this may result in small flecks of precipitated minerals; this drying of the steam could prove damaging to the plant equipment. However, it is believed that control systems on the temperature and pressure of the steam generated in the boiler should ensure that the produced steam is at the same quality as that in the IP steam manifold, and therefore avoid vaporization of liquid carryover.

## 2.4 Heating Separated Geothermal Water after the First Separation Stage

The majority of wells at Wairakei are two-phase, or “wet” wells, and produce a mixture of saturated steam and geothermal liquid. Once the first separation stage has been completed, the separated liquid will still be close to its boiling point, and any heat added to the liquid would result in additional steam being produced, as displayed on the Mollier diagram in Figure 17. Therefore by installing a syngas fired boiler after the first separation stage, additional IP steam could be created to be utilized by the Wairakei Power Plant.

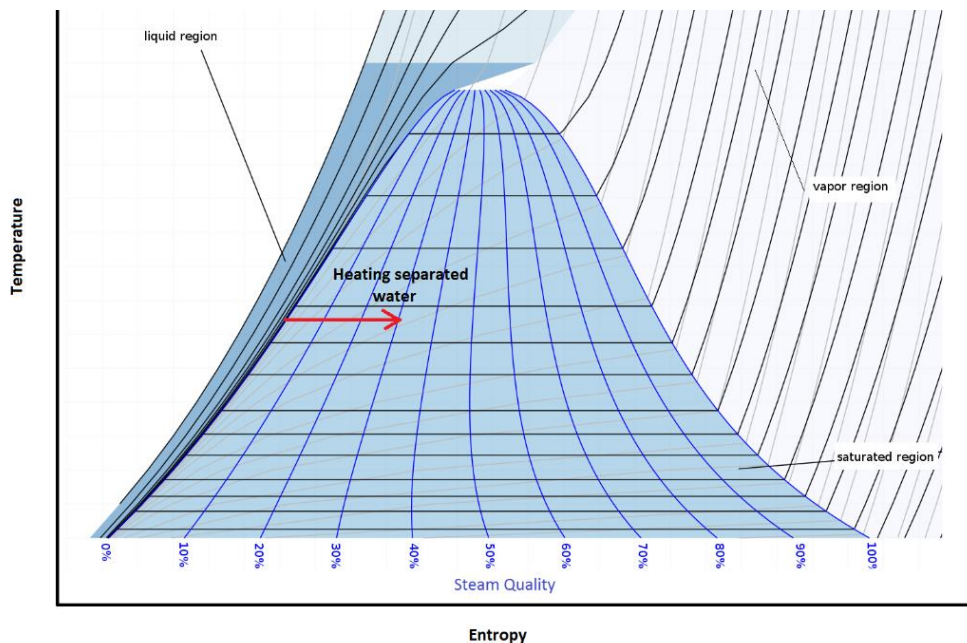


**Figure 17. Mollier Diagram illustrating the effect heating separated geothermal water has on increasing the amount of water in the vapour phase, modified from [11].**

The Wairakei Geothermal Field uses two-stage separation to produce IP and LP steam, and by generating additional steam using the intermediate pressure separated geothermal water (IP SGW) as a boiler feed the amount of LP steam generated would be decreased. This is due to the fact that the overall mass of IP SGW is reduced if heat is added and IP steam produced, therefore reducing the feed to the LP separators. However, there is a second stage separator at Wairakei that is limited by the amount of LP steam it may produce, at Flash Plant 14 (FP14), which feeds to the Wairakei A and B stations. The current configuration of FP14 is displayed in Figure 18.

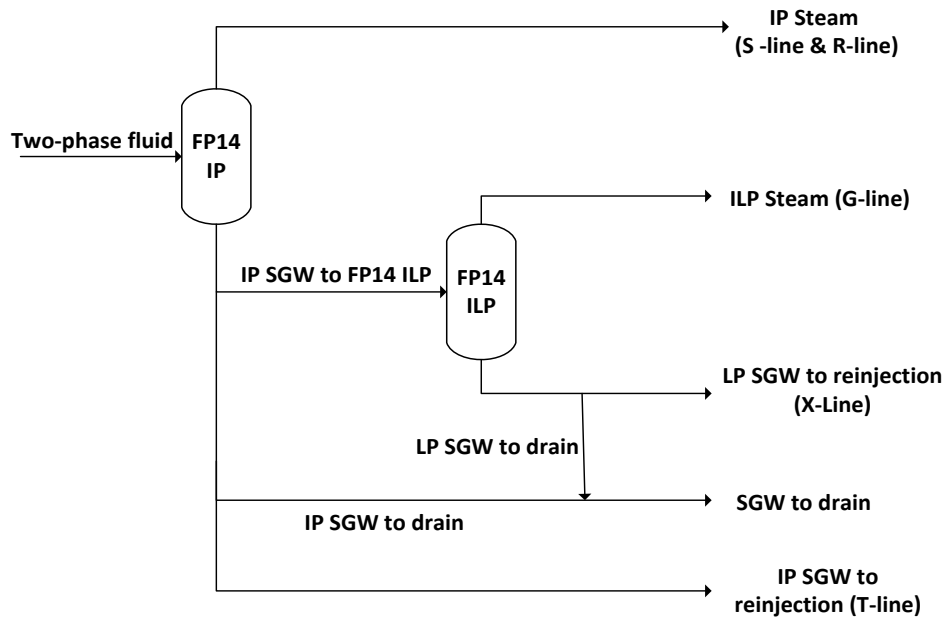


**Figure 18. Diagram of the current steam and water flows at Flash Plant 14**

By heating the separated fluid generated from the first stage separator, more IP steam may be produced without necessarily reducing the amount of LP steam produced in the second separation stage. The amount of additional IP steam that may be produced by heating the two-phase fluid is relatively independent of the flowrate of two-phase fluid unless all of the liquid in the two-phase fluid is being vaporized. Flash Plant 14 has a relatively large flowrate of two phase fluid entering it, at approximately 2000 t/h, and the LP steam produced in the second stage of separation is limited to 40 t/h, the hybridized flash plant 14 and IP SGW boiler configuration is displayed in Figure 19

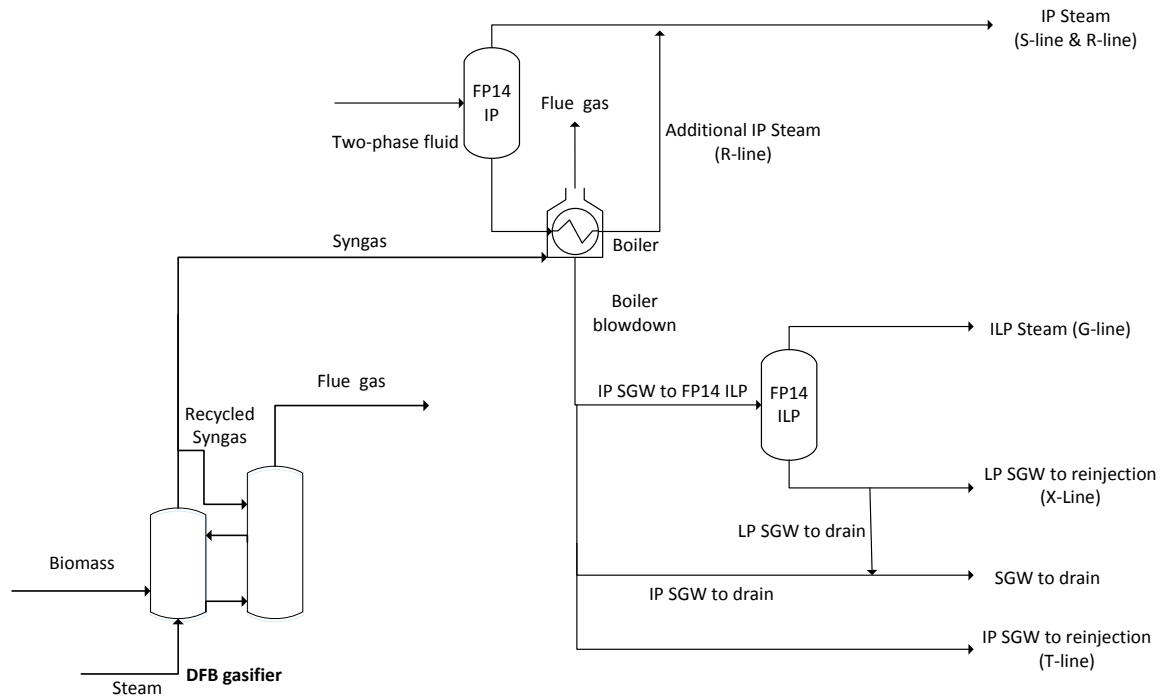


**Figure 19. A diagram of performing fired heating on IP SGW for additional IP steam generation**

The possibility of heating the two-phase fluid prior to the IP separators was also investigated, as this would simply increase the dryness of the two-phase fluid prior to the first stage of separation. However, this would require a boiler using the two-phase fluid as the feed, which would decrease the heat transfer efficiency of the boiler compared to a liquid feed to the boiler.

As the SGW after first stage separation has not been observed to exhibit silica scaling, even though it has a silica content as high as 622 mg/kg, the boiler may be able to operate using the SGW as a feed water. If a continuous blowdown is used, then it is believed that the silica concentration will remain low enough to prevent scaling in the boiler, however it may cause increased scaling downstream of the separation stage. Generally the blowdown of boilers is desired to be minimized in order to prevent the loss of heated boiler water [40]. However, provided there is minimal heat loss after the first separation stage, the SGW is already at its boiling point, a large continuous blowdown may be used without excessive loss of heat, as the heat input should only produce additional steam.

There may also be environmental benefits of implementing this configuration, as the amount of arsenic and other metals entering the Waikato River will be reduced, due to an increased proportion of the metals being reinjected. Currently the resource consent for discharging water to the Waikato from Wairakei is based on the amount of arsenic entering the river. As the flowrates to the T-line and X-line for reinjection are relatively constant, the amount of SGW entering the Waikato River will be reduced by the overall decrease in SGW flowrate caused by the steam generation. As the solubility of arsenic and other metals in the IP steam is negligible, the concentration of these metals in the SGW will be increased due to the evaporation of water in the boiler. This increased concentration will cause a greater proportion of the metals to be reinjected.

## 2.5 Heating Additional Separated Geothermal Water for Use in a Binary Plant

There is the potential for syngas fired heating to be implemented within an existing binary plant at Contact Energy's Wairakei Power Plant. The binary plant currently uses SGW available at approximately 130°C in the X-line prior to its reinjection. The Binary Plant was designed for an average power generation of 15 MWe, however the actual observed average generation is approximately 13MW, as is shown by the red line in Figure 20.

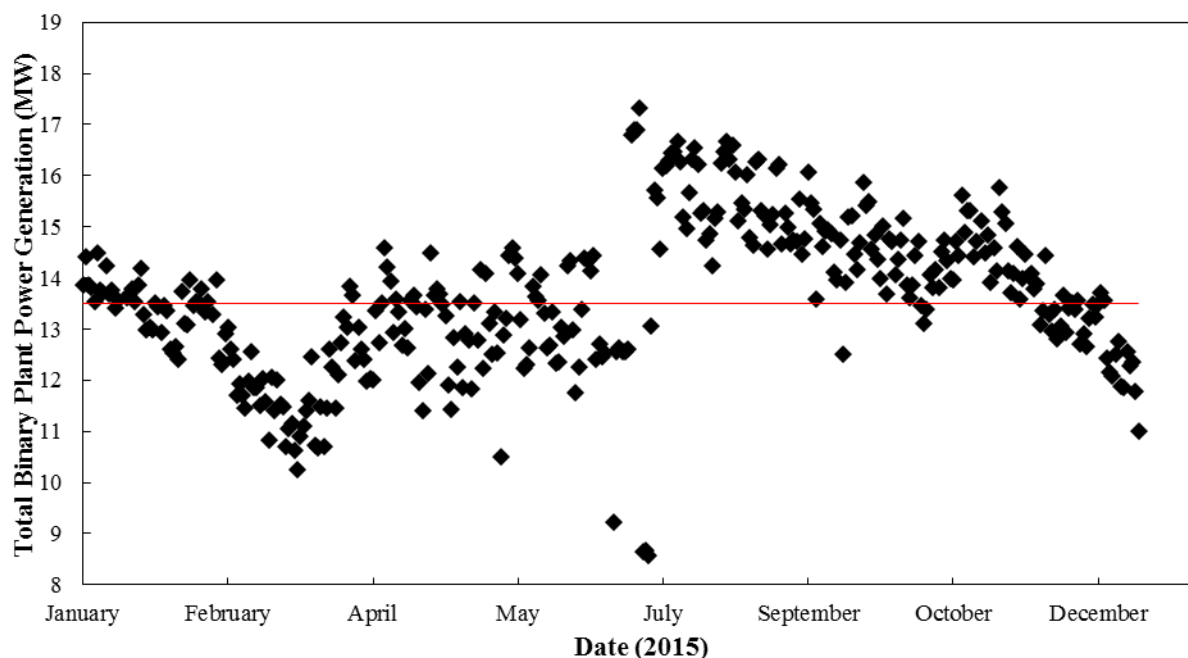


**Figure 20. The Power Generation of the Wairakei Binary Plant for 2015**

The temperature of the SGW directly affects the amount of heating that may be performed on the pentane, though this is limited by the design of the binary plant. As the binary plant is designed to utilize SGW at 127 °C, there is limited benefit to further heating the SGW above this design temperature. Similarly the flowrate of the SGW directly affects the amount of heating that can be performed on the pentane, and limited benefits if the flowrate is raised above the design flowrate of 2800 t/h.

Due to the fact that cooling is being performed on the silica laden SGW, and silica solubility decreases with temperature; silica scaling is observed within the plant. The flowrate of SGW into the binary plant is reduced as scaling increases due to an increase in frictional pressure losses. Silica scaling also decreases the performance of heat exchangers within the plant, and therefore reduces the power generation of the Binary Plant. Therefore silica removal using hydrofluoric acid is currently performed biannually, in order to increase the power generation of the Binary Plant [24].

As can be seen in Figure 20, the actual average power generation of the Wairakei Binary Plant is approximately 2 MWe lower than the designed power generation of 15 MWe. This is attributed to the average mass flow of SGW entering the binary plant being approximately 2300 t/h, significantly lower than the designed flowrate of 2800 t/h. However, it is noted that even though

it appears that there is capacity for additional SGW being fed to the Binary Plant, SGW was observed to bypass the binary plant for much of 2015. This bypassing is attributed to silica scaling within the Binary Plant limiting the flowrate of SGW through the binary plant. It is assumed that more frequent silica removal within the Binary Plant would solve this issue, though this will incur additional costs.

The power output of the Binary Plant is seen to be dependent on several factors, the temperature of the SGW, the flowrate of SGW, and the ambient air temperature. From this, the power output of the binary plant may be increased by increasing the flow of SGW or by increasing the temperature of the SGW. By performing heating on the SGW, more heat can be transferred to the pentane working fluid. However as the designed entrance temperature of SGW to the stage 1 vaporizer is 127°C, and the current average temperature of SGW is 130°C, additional heating would serve to further deviate the temperature of the SGW from the designed entrance temperature. Increasing the flowrate of SGW to the binary plant would also serve to increase the heat transfer to the pentane and result in increased power generation from the binary plant. The only source of SGW available at 130°C is the X-line, and is already allocated to the binary plant, however there is the option to utilize some lower temperature SGW available at approximately 105°C in the T-line. Even though it may be possible to generate additional power from the binary plant without performing any additional heating, it is believed that mixing the two sources of silica laden SGW may result in increased silica deposition within the binary plant. This is based on observations made by Generation Engineers at Wairakei on silica scaling increasing in cases of SGW mixing. Therefore, mixing the X-line SGW at 130°C with the T-line SGW at 105°C could cause a greater amount of silica precipitation and exacerbate silica scaling in the binary plant. However, by heating the SGW in the T-line from approximately 105°C to the same temperature as the SGW in X-line at approximately 130°C; it is believed that this would likely avoid the issue of increased silica precipitation, due to the increased solubility of silica in the higher temperature water. The configuration of heating the SGW in T-line to provide additional SGW flowrate to the Binary Plant is displayed in Figure 21.

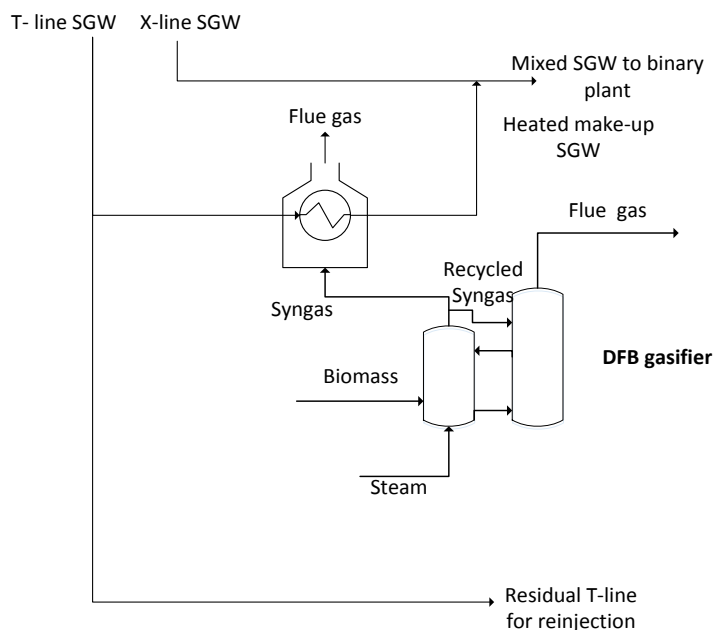


**Figure 21. Diagram of heating additional SGW for use in the Wairakei Binary Plant**

### **3.0 Process Modelling of the Wairakei Geothermal System and Hybrid Configurations**

In order to evaluate the efficacy of the hybrid plant configurations, models were developed to simulate some of the hybrid plants proposed in Section 2.2. A model for biomass gasification had been created by Nargess Puladian during the course of her PhD at the University of Canterbury using the heat and material balance software, UniSim [43]. This model could then be modified in order to better suit the use of syngas for power generation instead of liquid fuel synthesis. Models for the current Wairakei Geothermal Power Plant, and the additional process equipment required to retrofit the Geothermal Power Plant with additional syngas fired heating were created using UniSim.

#### **3.1 Modelling Biomass Gasification**

The gasification portion of the modelling encompasses the drying of the biomass, the combustion of char and syngas in a combustion reactor, and the gasification reactor where pyrolysis and char-gas reactions take place. As the models for gasification and biomass drying created by Puladian during her PhD were originally designed to provide a syngas feed for Fischer-Tropsch synthesis of liquid fuels, some modifications were performed to make these models suitable for power generation using syngas.

##### **3.1.1 Biomass Drying**

In order to estimate the heat requirement for the biomass dryer, a modified version of Puladian's model for biomass drying was employed [43]. The biomass drying mechanism used by Puladian was modelled in three steps using a macro module in UniSim: feed preheating, constant rate drying, and falling rate drying. During feed preheating, the sensible heat of the flue gas drying medium is transferred to the wet biomass raising the temperature of the biomass towards the wet bulb temperature. Moisture in the wet biomass is rapidly evaporated during the constant rate drying, as the drying rate is dominated by the heat transfer to the surface of the biomass. As the biomass dries the drying rate falls due to the movement of moisture within the biomass towards the biomass surface before evaporation occurs. However, as the final moisture content of the biomass is still relatively high (15%), the drying rate is still relatively high at the end of the drying. This causes the drying process to be largely controlled by the heat transfer to the biomass, and not the mass transfer of moisture in the biomass.

The UniSim model created by Puladian to simulate the biomass drying was based on the overall heat and mass balance equations of the biomass and the flue gas used as the drying medium, and the following assumptions:

- The temperature of the biomass and the drying medium at the outlet of the dryer is very close. Rigorous modelling results have shown that the temperature difference at the dryer's

outlet in co-current rotary dryer is insignificant when the final moisture content is less than 15 % as shown in Iguaz et al. [44] and Xu and Pang [45].

- The exhaust gas temperature is always higher than the wet-bulb temperature of the flue gas (70 °C).
- The heat of vaporization of water is kept constant during the drying using the average temperature between inlet and outlet temperatures.
- The heat loss of the dryer is assumed to be 15 % based on the experimental results with a semi-industrial rotary dryer reported in Meza et al. (2008). It does not include the heat loss by the exhaust gas.

The amount of flue gas required for use as the drying medium could then be determined in order to achieve the necessary drying. A controller function was implemented in UniSim to vary the recycled syngas to the gasifier's combustion reactor, and therefore the amount of high temperature flue gas being generated in the reactor. This controller ensured that the flue gas and biomass outlet temperature was 107°C from the rotary dryer; this would allow adequate drying of the biomass in the dryer. This outlet temperature was the one used by Puladian in her thesis, and was concordant with information published by NREL that typical dried biomass temperatures from rotary dryers are between 71-110°C, though most exit temperatures are above 104°C in order to avoid condensation of acids and resins[46].

### 3.1.2 Dual Fluidized Bed Gasifier

The dual fluidized bed gasifier was modelled in UniSim by Puladian in several stages: char and syngas combustion, pyrolysis, and char-gas reactions. In Puladian's thesis there was also a steam-gas shift reactor, which was implemented to generate additional hydrogen to ensure the syngas was suitable as an input for Fischer-Tropsch synthesis to a liquid fuel. The overview of Puladian's dual fluidized bed model is displayed in Figure 22.

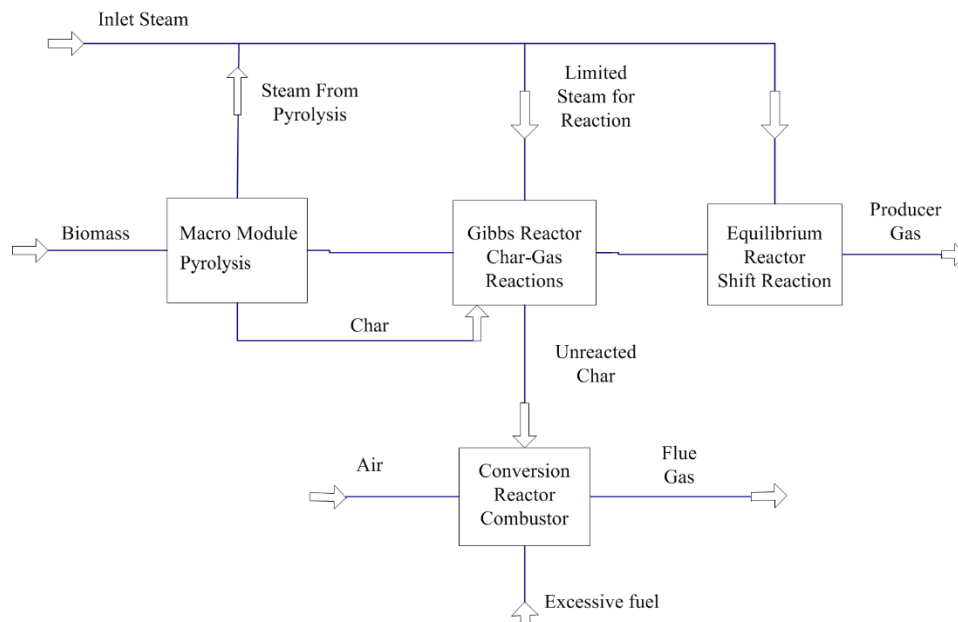
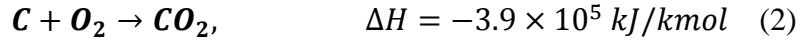


Figure 22. Overview of the dual fluidized bed gasifier UniSim model, taken from Puladian's Thesis [43]

### 3.1.2.1 Char and Syngas Combustion

The heat required for the gasification reactions is supplied by the combustion of char, and often some make up fuel in a combustion reactor. In this case some of the produced syngas would likely be recycled to provide the additional heat for gasification. A conversion reactor was used to model the combustion reactions, char and the components of syngas, hydrogen, carbon monoxide and methane were combusted to generate heat for gasification and the hot flue gas for the drying medium in the rotary dryer, as described by the reactions in Equations 2-5.



### 3.1.2.2 Pyrolysis

During pyrolysis biomass is converted into char and combustible gasses. The major components of the pyrolysis gas were determined by performing elemental balances on C, H, and O, and by introducing two empirical factors,  $\Phi_{CO}$  and  $\Phi_{CH_4}$ . Where  $\Phi_{CO}$  and  $\Phi_{CH_4}$  are the ratios of CO/CO<sub>2</sub> and CH<sub>4</sub>/H<sub>2</sub> respectively. By assuming that C, H, and O were only present in the 5 major components of the pyrolysis gas: H<sub>2</sub>, H<sub>2</sub>O, CO, CO<sub>2</sub>, and CH<sub>4</sub>, the concentration of these components in the pyrolysis gas could be determined. The empirical factors  $\Phi_{CO}$  and  $\Phi_{CH_4}$  were calculated using Equation 6 and Equation 7. These equations were developed by curve fitting of the experimental data reported by Fagbemi et al [47].

$$\Phi_{CO} = A_1 \exp \frac{-B_1}{T_G} \quad (6)$$

$$\Phi_{CH_4} = A_2 \exp \frac{-B_2}{T_G} \quad (7)$$

Where:

$T_G$  = the gasification temperature (K)

$A_1$  = an empirical constant ( $A_1 = 4.7 \times 10^3$ )

$B_1$  = an empirical constant ( $B_1 = 7163.6$ )

$A_2$  = an empirical constant ( $A_2 = 2.28 \times 10^{-3}$ )

$B_2$  = an empirical constant ( $B_2 = 5404.85$ )



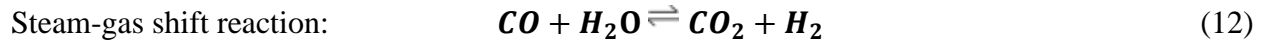
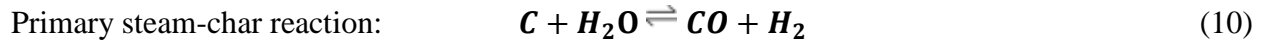
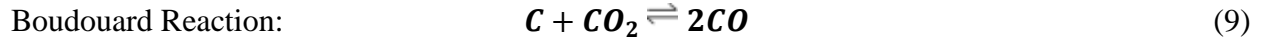
The final tar content (dry basis) of the syngas was assumed to be a function of the gasifier temperature, and the resulting function displayed in Equation 8 was created using the experimental data reported by Koppatz et al [48].

$$Tar(wt\%) = -5.61 \times 10^{-3} \times T_G + 6.95 \quad (8)$$

The concentrations of the remaining species: N<sub>2</sub>, NH<sub>3</sub>, and H<sub>2</sub>S were calculated using elemental balances on the nitrogen and sulphur present in the biomass. The amount of hydrogen in the syngas was also altered by taking into account the hydrogen present in NH<sub>3</sub> and H<sub>2</sub>S.

### 3.1.2.3 Char-Gas Reactions

The char-gas reactions are made up of the Boudouard reaction, the primary steam-char reaction, the secondary steam-char reaction, and the steam-gas shift reaction as displayed in Equations 9-12 respectively.



The steam contribution in the primary and secondary steam-char reactions was calculated using a correlation displayed in Equation 13, taken from Nguyen et al [49].

$$\frac{n_{H_2O,con}}{n_{H_2O}} = 51.4 e^{(-7542.8/T_G)} \quad (13)$$

Where:

$n_{H_2O}$  = the total moles of steam in the system

$n_{H_2O,con}$  = the moles of steam that contributes to the reactions

$T_G$  = the gasification temperature (K)

### 3.1.3 Modifications Made to the Biomass Gasification Model

As Puladian's UniSim model for biomass gasification was created to simulate a syngas feed for a Fischer-Tropsch reactor to create liquid biofuels; modifications had to be made to the model in order for it to better suit the production of syngas for combustion. As the H/CO ratio is very important for creating liquid fuels from syngas, the original gasification model was designed to generate syngas with a H/CO ratio of approximately 2:1. This was done by changing the operating conditions of the gasifier, changing the steam/biomass ratio input to the gasifier, and by

implementing a steam-gas shift reactor. As this investigation was concerned with burning syngas to generate additional power at a geothermal power plant, the H/CO ratio was of less importance than the calorific value of the syngas. Because of this, the steam-gas shift reactor was removed from the model, as it would increase the cost of the gasifier.

As syngas that is to be used for liquid fuel synthesis has a very low tolerance for contaminants and impurities; there were more rigorous syngas cleaning methods employed with Puladian's model than are required for the hybrid configurations described in Section 2.0. The majority of this syngas cleaning was present in separate UniSim models from the gasifier model, and could therefore simply be ignored. However Puladian had used air effluent from an air stripper as part of the cleaning process containing tar as an input for the gasifier's combustion reactor, this was easily modified to suit the new gasifier design by changing the properties of this material stream to those of ambient air. As the combustion using air utilized in the stripper was viewed by Puladian as a disposal method of the air without further treatment, all of the air was introduced to the gasifier combustion chamber. Therefore, further modifications had to be performed to ensure that the optimum flowrate of air was used as an input to the combustion reactor. This was performed by setting a controller to ensure that the input of the ambient air was 130% of the combined stoichiometric requirements for the combustion of char and recycled syngas.

As the syngas being created during gasification would likely be combusted in close proximity to the gasifier for augmenting the power generation at the Wairakei power plant, there would be hot flue gas available from the syngas combustion. This flue gas could be utilized as the drying medium to dry the input biomass in the rotary dryer. This was achieved by using both the flue gas from syngas combustion and from the combustion reactor of the gasifier as the drying medium input to the dryer.

In the unmodified gasification model, LPG was used as the make-up fuel for the combustion reactor in order to supply the heat for gasification. However, it was decided that using a portion of the generated syngas would likely reduce costs. This was performed by removing the LPG input material stream, and replacing it with a partial recycle on the syngas product stream. As Puladian's model calculated the LPG requirement based on a ratio of biomass feed input to the rotary dryer, a new method of determining the required mass flow of recycled syngas was created. As the drying of the biomass would be performed using a combination of the flue gas from the gasifiers combustion reactor and the flue gas from burning the syngas in a boiler or furnace, the amount of syngas recycled to the combustion reactor would alter the drying of the biomass. Therefore, in order to ensure that the biomass input to the gasifier was adequately dried, a controller was placed on the syngas recycle to ensure that an exit temperature of 107°C from the rotary dryer was achieved for the biomass. The temperature of 107°C was chosen based on Puladian's research, as she deemed this temperature sufficient to adequately dry the chipped biomass.

Some of the flue gas generated in the combustion reactor of the gasifier was used to preheat the air inlet to the gasifier in Puladian's model. However, it was decided that this would not be required, as this preheater resulted in efficiency losses as a greater amount of syngas had to be recycled to the gasifier to supply additional heating by the flue gas. This preheater was therefore removed.

## **3.2 Modelling Steam Flow at the Wairakei A and B Stations**

In order to determine the additional power generation that may be possible by implementing the hybrid configurations, the existing steam flows within Wairakei had to be investigated. As the individual steam flows to the geothermal turbines are not directly measured, a model had to be created to estimate any residual steam capacity in the turbines, and the potential power generation possible by filling this capacity.

Steam has also been observed to bypass the IP steam manifold in Wairakei to the LP manifold when there is no additional capacity to utilize the IP steam in IP or MP turbines. This steam would be able to be utilized in any IP steam turbines that are returned to service, along with any additional steam generated by implementing the hybrid configurations. A model was therefore created in order to quantify the amount of bypassing IP steam.

### **3.2.1 Modelling Geothermal Steam Flow to the Wairakei Turbines**

A model for the existing steam turbines, and the IP and LP steam manifolds at the Wairakei A and B Stations was created using UniSim. As described in Section 2.2.1, these Stations consist of one steam turbine using IP steam at 4.5 bara, three steam turbines using LP steam at 1.15 bara, and three MP steam turbines utilizing both IP and LP steam through different passes. The steam turbines were modelled using the expander function in UniSim, where the inlet conditions, outlet conditions, and efficiency of the turbines are used to determine the power generation by the turbines. However, as the expander function in UniSim was not developed with multiple inputs of different pressure; two expanders had to be used to model each of the MP turbines, due to the IP and LP steam inputs to these turbines.

The models of the steam manifolds were created in order to simulate the flow of steam to the different steam turbines. As displayed in Figure 7, IP steam is extracted from the wells and fed to the IP and MP turbines. The inputs to the LP steam manifold are from the exhaust of the IP turbine, G4, any excess IP steam that is not used in the IP or MP turbines is throttled down to LP steam, and all the ILP steam is also throttled down to LP steam at 1.15 bara.

After the model for the steam turbines and steam manifold was created, it then needed to be validated using data from Wairakei on the operating conditions. As flow measurements are not performed on the steam entering the individual turbines, typical steam flows to the individual turbines, and the power output of the turbines were used in order to refine the UniSim model. The steam use by the different turbines used at Wairakei, the steam used by the ejectors to generate the vacuum conditions, and the LP steam flow from the outlet of G4 at full load are displayed in Table 2.

**Table 2. The steam flows for the steam turbines at the Wairakei Power Plant operating at full load**

Estimates for the power generation of the turbines at the Wairakei A and B Stations were based on their no load flow and steam input. The no load flow of the turbines is the amount of steam that is required to be added to the turbines before any power is generated. After the no load flow is met, the efficiency of the turbines is generally constant, with a power generation rate being used to estimate the power output based on the steam flowrate to the turbine. The no load flows and power generation rates for the different types of steam turbines at the Wairakei A and B Stations are displayed in Table 3. As the individual flows of IP and LP steam to the MP turbines are not measured, and as only the total power generation for each of the MP turbines is measured, IP and LP contributions to this total power generation is unknown. Therefore it was assumed that the ratio of IP:LP steam would be essentially constant to the MP turbine, in order to estimate the individual flows of IP and LP steam to the turbine.

**Table 3. The no load steam flows and power generation rates for the steam turbines at the Wairakei A and B Stations.**

Turbine	Maximum power generation	Full load steam input		Ejector steam use	Steam outlet
		IP t/h	LP t/h	IP t/h	LP t/h
MP	30	214	38	14	-
IP	11.2	241	-	-	231
LP	11.2	-	140	6	-

### 3.2.2 Estimating IP Steam Bypassing

There are two pressure relief valves fitted to bypass IP steam from the IP steam manifold to the LP steam manifold, PRV1 and PRV4. The steam bypassing through these valves may not be a large enough flowrate to justify recommissioning of G1, the decommissioned IP turbine. However, if G1 is recommissioned in order to utilize the additional steam generated by retrofitting a gasifier, the bypassing steam will be able to be used in G1 for power generation. Both of the valves are 20” butterfly valves, however there was very limited information on estimating the steam flowrates passing through these valves. The valve opening positions are recorded at Wairakei, and the average daily positions are displayed in Figure 23 for both of the valves.

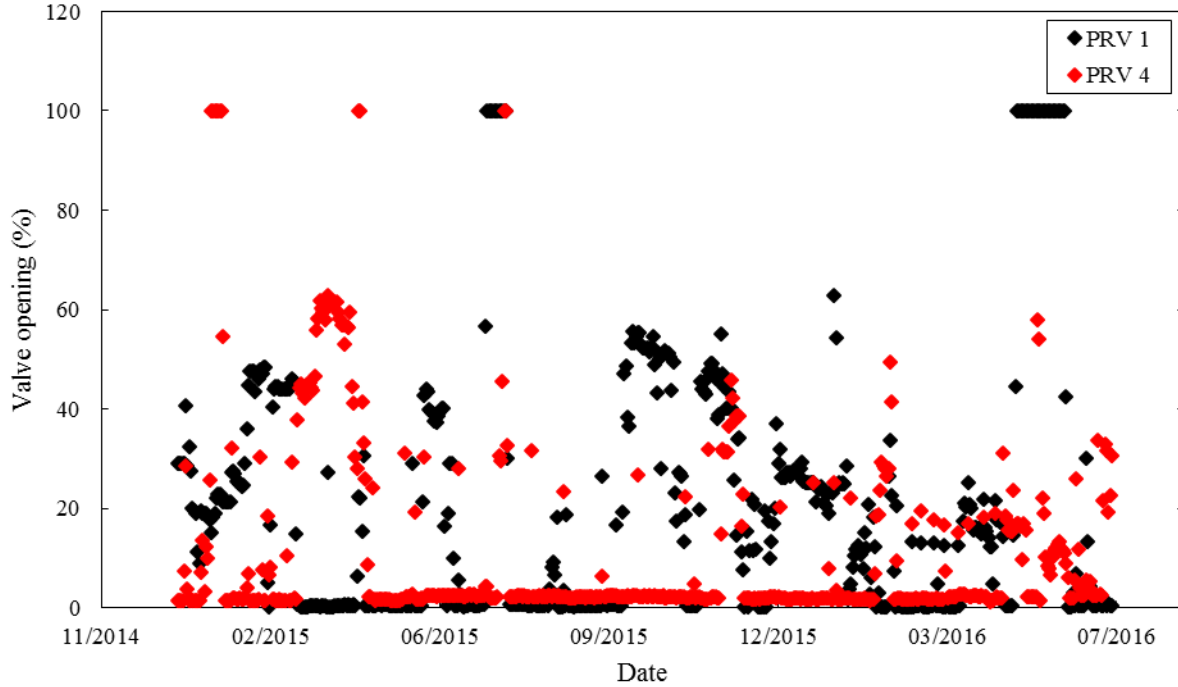


**Figure 23. The daily average valve positions for two bypass valves, PRV1 and PRV4**

In order to estimate the flowrate of steam through the valves, flow coefficients for 20" butterfly valves were investigated from manufacturer's information. It was found that the flow coefficient for butterfly valves changes significantly by manufacturer and for different material specifications. Due to this, there is a relatively large uncertainty attached to any estimations on steam flowrate generated using these values. It was decided to use a conservative estimation for the flow coefficients, in order to not overestimate the bypassing steam flowrate. The flow coefficients used are displayed in Table 4.

**Table 4. The assumed flow coefficients for 20" butterfly valves [50]**

Valve Position (°)	Flow Coefficient (C <sub>v</sub> )
30	2574
50	5720
70	10725
90 (full open)	14300

The flow could then be estimated using Equation 14, [51].

$$W = 2.1 C_v \sqrt{\Delta P (P_1 + P_2)} \quad (14)$$

Where:

$W$  = the flowrate of saturated steam (lbs/h)

$C_v$  = the valve flow coefficient

$\Delta P$  = the pressure drop across the valve (psi)

$P_1$  = the pressure before the valve (psia)

$P_2$  = the pressure after the valve (psia)

By converting the bypassing mass flowrates generated using Equation 14 into t/hr the daily average bypassing flow through the valves could then be estimated, as is displayed in Figure 24.

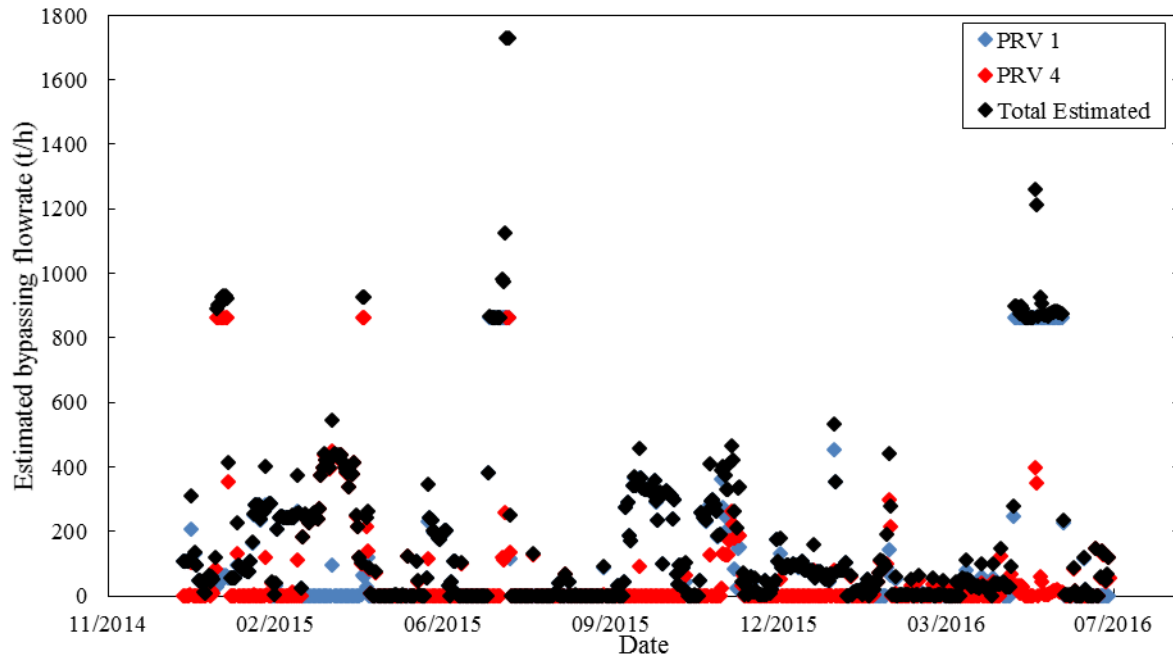


**Figure 24. The estimated flowrates of IP steam bypassing through PRV1 and PRV4**

The estimates for the amount of steam bypassing the IP manifold based on the positions pressure relief valves was then compared to estimates from the expected IP steam use by the IP and MP turbines, and the values for the IP steam input to the Wairakei A and B Stations. The average total steam flow to the Wairakei A and B Stations was approximately 1000 t/h for the same period displayed as in Figure 24. It was therefore considered unlikely that the bypassing flow would be as large as is indicated by the peaks in Figure 24, as this would require all of the IP and MP turbines to be removed from service, which is a very rare occurrence. Therefore, it was assumed that the bypassing flowrate based on the valve opening positions resulted in a significant overestimation of the bypassing flowrate of IP steam. A second method was then employed in order to estimate the bypassing steam using the expected IP steam use of the IP and MP turbines, and the measured mass flowrate of IP steam to the Wairakei A and B Stations. The IP steam use in the IP turbine was based on the no load flow requirement and power generation rate estimations discussed in Section 3.2.1. The resultant calculated bypassing steam based on the expected steam use by the IP and MP turbines, and the measured IP steam input to the Wairakei A and B Stations is displayed in Figure 25.

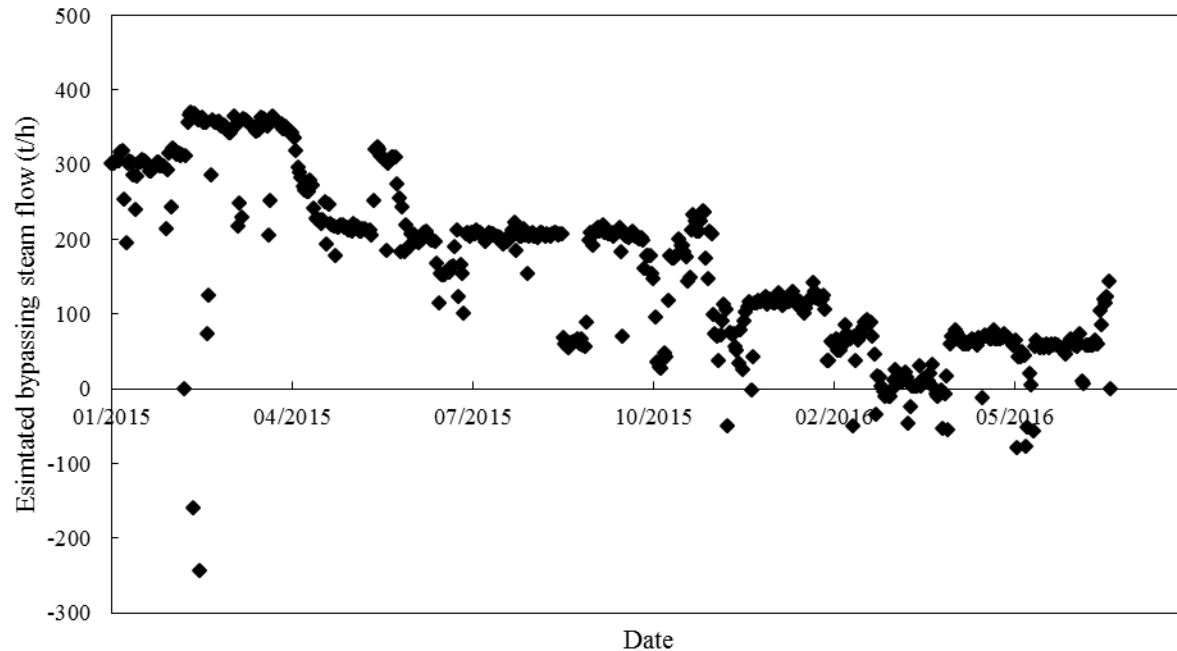


**Figure 25. The estimated bypassing steam calculated using IP steam flow estimates within and measured IP steam input to the Wairakei A and B Stations**

As can be seen in Figure 25, the estimates for the maximum amount of bypassing steam are much more reasonable when based on the expected steam flowrates within the plant, compared to the bypassing valve opening position. The trend of the decreasing amount of steam bypassing was deemed to be sensible, as the flowrate of IP steam to the Wairakei A and B Stations has a corresponding decrease across this period. A decreased amount of IP steam input would have a reduction in the amount of bypassing steam, provided there was no change in the turbines that are in operation. However, as there is an estimated uncertainty of  $\pm 10\%$  on the flow measurements of IP steam to the plant, and the steam use within the plant is based on “rules of thumb” about the steam use of the different turbines, there is significant uncertainty on the estimated bypassing steam. It is also noted, the estimates shown in Figure 25 indicate that bypassing occurs almost constantly throughout the period. It was therefore decided that a technique using both the data for the valve position and the estimates for the steam flow within the plant should be employed.

As the estimates for the amount of steam bypassing based on the valve positions was seen to be an overestimation, it was decided that the estimates generated based on the expected steam use within the plant would be more suitable. However, it was decided that it was likely that the information on when the valves are fully closed could be used to estimate when no bypassing was occurring. As bypassing only occurs sporadically within the plant, the estimates of near consistent bypassing displayed in Figure 25 were deemed unlikely. Therefore, the minimum estimate on the amount of bypassing steam generated by either of the methods was used in order to estimate the bypassing steam. This ensured that the majority of the time there was essentially no steam bypassing, as would be expected based on the positions of the control valves, and there was not the massive estimations for bypassing steam that is observed when estimating bypassing steam based on the valve positions. The amount of steam estimated to be bypassing using this method is displayed in Figure 26.

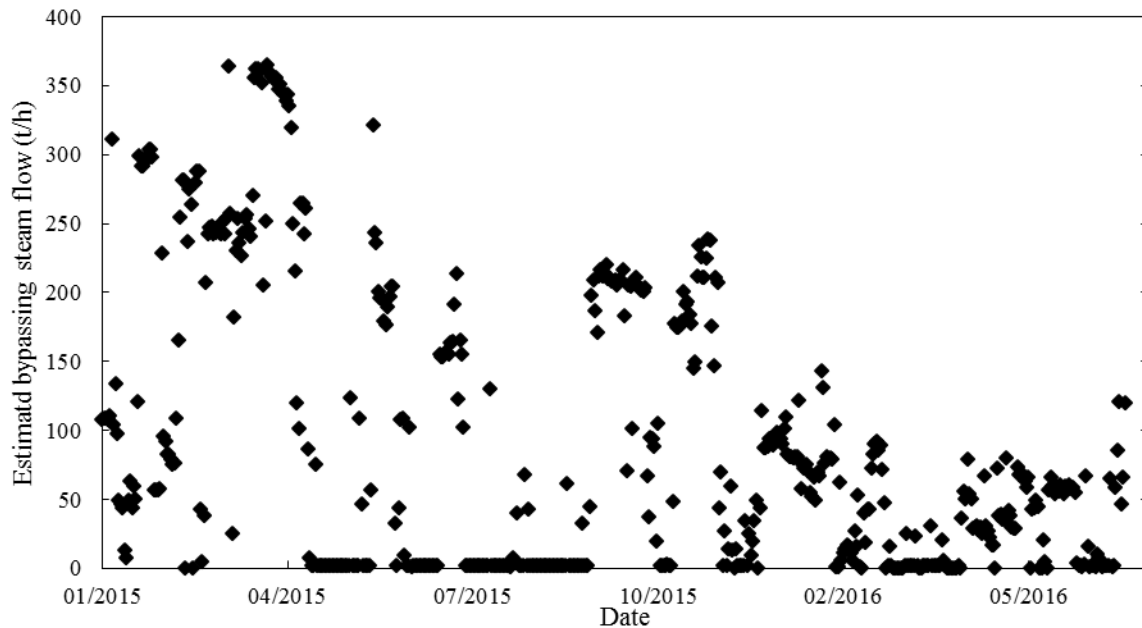


**Figure 26. The estimated bypassing steam based on both the estimated unused IP steam, and the pressure relief valve positions**

The estimated bypassing steam could then be added to any additional IP steam from the hybrid configurations, in order to estimate the potential power generation in the IP turbines. However, as there is some condensation of the steam in the IP turbines, there is consequently a slightly reduced flowrate of the steam added to the LP manifold if it is utilized in the IP turbine instead of bypassing.

Similarly, the fact that there is IP steam bypassing into the LP manifold will reduce the power losses from using IP steam as an input to the gasifier. In most of the potential hybrid configurations, additional steam is being added to the IP manifold, so there is no decrease in power generation by using this steam. However, as heating SGW for use in the binary plant does not produce IP steam, there is a net decrease in the power generation at the Wairakei A and B Stations. If steam is bypassing the IP turbines, the reduction of the IP steam to the Station will not necessarily reduce the power generation from the IP turbines. Therefore, the expected power losses can be more accurately estimated using the data for the expected steam bypassing the IP turbines.

### 3.2.3 Modelling Power Generation from Additional Steam Supply

As several of the hybrid configurations proposed generate additional power by increasing the steam supply to the Wairakei Power Station, a method to estimate the power gains from the steam was created. The gasifier is modelled to utilize geothermal IP steam, the potential power gains must therefore be evaluated based on net steam generation, not the gross steam generation. Any additional steam that may be generated at Wairakei would likely be utilized in IP and LP turbines instead of MP turbines. This is due to the fact that there are unused IP and LP turbines that have been removed from service at Wairakei, and one LP turbine is currently not fully loaded, as displayed in Figure 27. The power generation expected from the turbines from the additional steam



was evaluated using the values for power generation after the no load flow has been met displayed in Table 3.

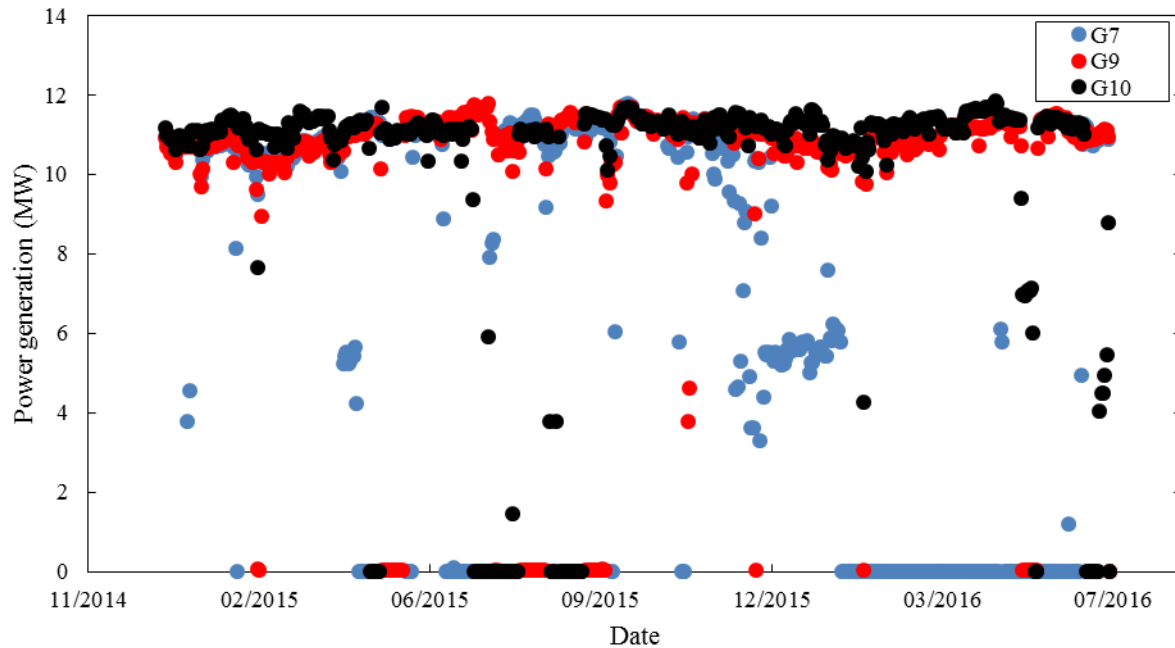


**Figure 27. The power generation from the three LP turbines at Wairakei**

As can be seen in Figure 27, one of the LP turbines is generally unloaded, especially in 2016. It is therefore valid to assume that one LP turbine is available for utilization without the associated costs of bringing a turbine back into service. For simplicity it is assumed that G7 is unloaded, as it can be seen that G7 is the turbine most consistently unutilized. Therefore, there is capacity for approximately 140 t/h of LP steam to be used in G7, however, there is little to no capacity for IP steam generation without bringing turbines back into service. There are currently two turbines that are removed from service that may be returned to service, though this will require a workover and recertification, the IP turbine G1, and the LP turbine G8. As approximately 95% of the steam input to IP turbines is throttled down to LP, it is preferable to utilize the steam first in IP turbines, then in the LP turbines. 6 t/h of IP steam is also required in order to operate the ejectors to operate each LP turbine, and this must be factored in. As there is the no load flow requirement of 100 t/h for IP turbines, if less than 106 t/h of IP steam is generated, there is no benefit in using the IP turbine at all, and all of the steam should be passed through a pressure reducing valve and passed to the LP manifold.

The power that may be generated from the additional steam was evaluated based on the steam that can be generated. If less than 106 t/h of IP steam is available, including any estimated bypassing steam, then there will be insufficient steam to utilize IP turbines. Thus, the steam will be throttled down to LP, and be utilized in the LP turbines. By analysing the performance of the turbines, the equations for power generation may be calculated. Also, as the maximum amount of IP steam that can be utilized in IP turbines is approximately 241 t/h, any IP steam above this amount will be bypassed to the LP manifold. Similarly, there is a maximum flowrate of approximately 140 t/h of LP steam that can be used in each of the LP turbines. Therefore a flowrate of LP steam larger than

280 t/h will not generate any additional power from the LP turbines, as there is one unloaded LP turbine (G7), and one LP turbine that may be returned to service (G8).

If steam available is > 106 t/h Equations 15-17 should be used:

$$P_{IP} = \frac{(\dot{m}_{IP} - (100 + 6n_{LP}))}{14} \quad (15)$$

$$\dot{m}_{LP} = \frac{231}{241} \dot{m}_{IP} \quad (16)$$

$$P_{LP} = \frac{(\dot{m}_{LP} - 19n_{LP})}{11} \quad (17)$$

However, if the IP steam available is not sufficient to meet the no load flow for the IP turbines, then Equations 18-20 should be used:

$$P_{IP} = 0 \quad (18)$$

$$\dot{m}_{LP} = \dot{m}_{IP} \quad (19)$$

$$P_{LP} = \frac{\dot{m}_{LP} - 19n_{LP}}{11} \quad (20)$$

Where:

$P_{IP}$  = the additional power generation from IP turbines (MW)

$\dot{m}_{IP}$  = the net flowrate of IP steam available, maximum of 241, (t/h)

$\dot{m}_{LP}$  = the net flowrate of LP steam available, maximum of 280, (t/h)

$n_{LP}$  = the number of LP turbines that may be operated with the steam generated

$P_{LP}$  = the additional power generation from LP turbines (MW)

The overall additional power generation is the sum of the power generation from the IP and LP turbines. If less than 13 t/h of steam is available for use, no power will be generated in the IP turbines or LP turbines, as the no load flow will not be able to be met for either the IP or the LP turbines.

### 3.2.4 Decreasing Steam Supply to the Wairakei A and B Stations

There are steam extraction limits on the amount of the two-phase fluid that may be extracted at the Wairakei Geothermal Field. The amount of two-phase fluid is therefore expected to remain relatively constant. However the average enthalpy of the extracted two-phase fluid is decreasing, and therefore there is a corresponding decrease in the mass flowrate of the steam generated. While the total mass flowrate decrease is relatively small, the Wairakei A and B Stations observe significant reductions in the mass flowrate of input steam. As IP steam is preferentially used at the Te Mihi and Poihipi Rd Power Stations, the reduction of mass flowrate is compounded for the

Wairakei A and B Stations. The IP steam flowrate to the Wairakei A and B Stations, and the estimated bypassing flowrate is displayed in Figure 28. Due to the decreasing steam flowrate, much of the analysis of the bypassing steam at the Wairakei A and B Stations will likely not be representative of future bypassing steam flowrates. Consequently, analysis performed on the power generation that may be possible using the bypassing steam if utilized in a recertified IP turbine will overestimate the power generation that may be possible. Therefore, three scenarios were created in order to represent different possibilities for the amount of steam passing to Wairakei:

- Bypassing, G4 fully loaded

This is the case for the most of 2015, where there is some bypassing, and G4 is almost continuously fully loaded. In this case, an IP turbine would need to be brought back into service in order to utilize additional IP steam. The bypassing steam would also be able to be used to generate power from the recertified IP turbine.

- No bypassing, G4 fully loaded

As can be seen in Figure 27, the amount of steam bypassing has been decreasing consistently throughout 2015 and into 2016, there is almost no steam bypassing for the majority of 2016. If it is assumed that the amount of steam input to Wairakei is at a point where no bypassing occurs, but the IP and MP turbines are fully loaded, then additional power generation would be hindered. This is due to the fact that any steam generated would need to surpass the no load flow of the IP turbines of approximately 100 t/h in order to generate any power from the IP turbines, and the steam generated is not augmented by any bypassing steam.

- No bypassing, G4 and G9 not fully loaded

If the steam supply to the Wairakei A and B Stations drops even further, then this will cause the IP turbine G4 to not be fully loaded. Due to this, any IP steam generated may be used in G4. This will result in increased power generation, as the no load flow for G4 may be met by the existing IP steam supply. Similarly, the no load flow for G9 is assumed to be met by the existing geothermal LP steam, and therefore additional LP steam may be use to directly generate power.

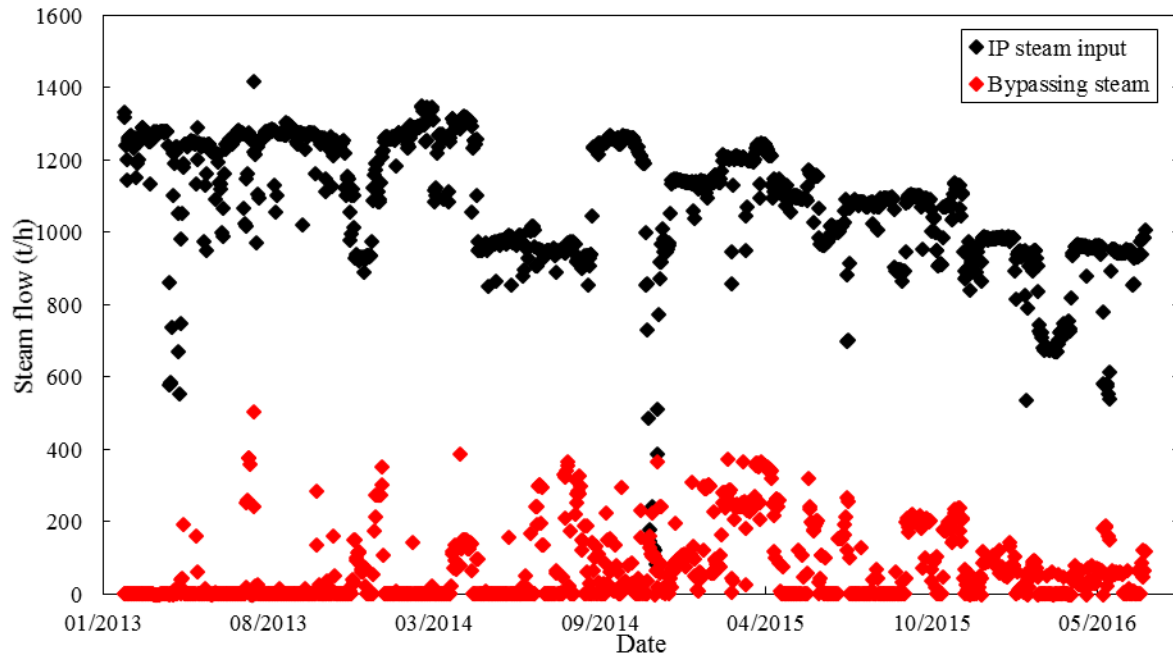


**Figure 28. The total steam input to the Wairakei A and B Stations, and the estimated bypassing steam**

The decision was made to create the three cases for steam input to Wairakei instead of extrapolating steam data to estimate the future steam flowrates, due to the many factors involved with the future steam flowrates. One of the factors of concern was the fact that the Te Mihi Power Plant is limited by the amount of SGW it can reinject. Therefore as the average enthalpy of the two-phase fluid decreases, relatively more SGW will be generated for the same steam flowrate. There is a pipeline that is currently being used to provide the Wairakei A and B Stations with steam which can instead be used as a SGW reinjection line for Te Mihi if need be. Therefore there would be a significant step reduction in the steam supply to Wairakei, if the average enthalpy of the reservoir decreases to the point where the existing SGW reinjection infrastructure for Te Mihi becomes undersized.

### 3.3 Modelling the Hybrid Configurations

Once models for biomass gasification, and the Wairakei steam manifold and steam turbines were created, the modifications required to implement the hybrid configurations could be modelled using UniSim. The syngas created in the gasifier model was then combusted using a conversion reactor function, and the heat generated from this combustion could be used in the different hybrid configurations.

#### 3.3.1 Superheating of Geothermal Steam

In order to evaluate the effect of superheating the geothermal steam would have on the power generation, and steam use in the plant, the gasification and Wairakei Power Station UniSim models

were combined, and a syngas fired steam superheater was added to the combined model. A conversion reactor was used to model the combustion of the syngas, an 80% heat transfer efficiency was used for the energy transferred from the syngas combustor and the steam superheater. It was assumed that this heat transfer efficiency could be calculated in the same manner as for a boiler. This heat transfer efficiency was then estimated using the hydrogen:carbon ratio of the fuel [52] [53]. A 10% oxygen excess was used to calculate the air requirement to the superheater [40]. A flue gas outlet temperature of 200°C from the furnace was assumed in order to estimate the heat transfer to the IP steam, and estimate the amount recycled syngas required in order to adequately dry the wood chips in the rotary dryer. It was also assumed that the adiabatic efficiency of the turbine would remain unchanged after the turbine was modified to operate using superheated steam.

As the superheated steam generated in this case would have to be utilized in the existing Wairakei turbines, the design constraints of this limited how the turbine would likely be able to be used. The design conditions for the modified turbines were largely based on those suggested in a report by Morris investigating superheating geothermal steam for use in existing steam turbines [38]. Due to the fact that the steam turbines would likely not be able to safely use steam that had a much higher pressure than the turbines were designed for, the maximum pressure of the superheated steam was set as the same as the IP steam at 4.5 bara. The amount of superheating that could be performed on the geothermal steam was then limited by the maximum temperature the steam could be heated to. It was decided that this maximum temperature would be limited by the creep range of the low alloy steel used in the plant, at 370°C [54], a safety margin of 20°C was then imposed, changing the maximum operational superheated steam temperature to 350°C. The volumetric flowrate of the superheated steam would also have to be designed to be approximately the same as in the non-superheated case, in order to not damage the turbines. As the volumetric flowrate is to be held constant, the allowable mass flowrate in the superheated case would be lower than in the saturated case, due to the decreased density of superheated steam. The power able to be generated by the steam turbine can be found using Equation 1:

$$\dot{W}_{ST} = \dot{m}_S(h_{in} - h_{out}) \quad (1)$$

The power generated by the superheated steam is reduced due to this decrease in the mass flowrate, and may even be less than in the saturated steam case, depending on the enthalpy drop that can be achieved within the turbine. As the volumetric flowrate is being held constant for both the superheated and saturated steam cases, the mass flowrate can be determined using the ratio of the density of the saturated steam and the superheated steam. The density of the saturated steam at 150°C and 4.5 bara was found to be 2.416 kg/m<sup>3</sup>, and the density of the superheated steam at 350°C and 4.5 bara found at 1.577kg/m<sup>3</sup>, leading to an allowable mass flowrate of superheated steam to be 65.3% of that of the saturated steam. The MP turbines operate in two stages, the first stage brings the IP steam down to LP, and the second stage expands this LP steam and additional LP steam that is injected to the turbine after the first stage to the vacuum conditions. By introducing superheated steam to the MP turbine, the mass flowrate of steam introduced to the first stage is decreased by approximately 35%, but the amount of additional LP steam injected to the MP turbine is increased by 34%. This is due to the relatively lower volumetric flowrate of steam exiting the first stage when superheated steam is used compared to the saturated case, this then requires a larger amount of additional LP steam to be added before the second stage.

In order to ensure a fair comparison between the saturated and superheated steam cases, the same outlet pressure from the turbine was used for both cases, at 6.7 kPa, as this was found to be a typical outlet pressure for G12. The enthalpy changes during the steam expansion for the saturated and superheated cases are displayed in Figure 18. As can be seen, the outlet of the second stage is below the saturation line, due to this, there is not expected to be any issues with the condenser operation. However, it is noted that the exit conditions from the first stage is above the saturation line, due to this the water drainage holes present in the turbine will likely have to be filled in, as is discussed in Section 2.2. The expected power generation from the saturated steam case and the superheated steam case were then calculated using the UniSim model created for the superheated steam case. The comparison of the steam flowrates through each stage in the MP turbines, and the resulting power generation created for the saturated and superheated steam cases are displayed in Table 5.

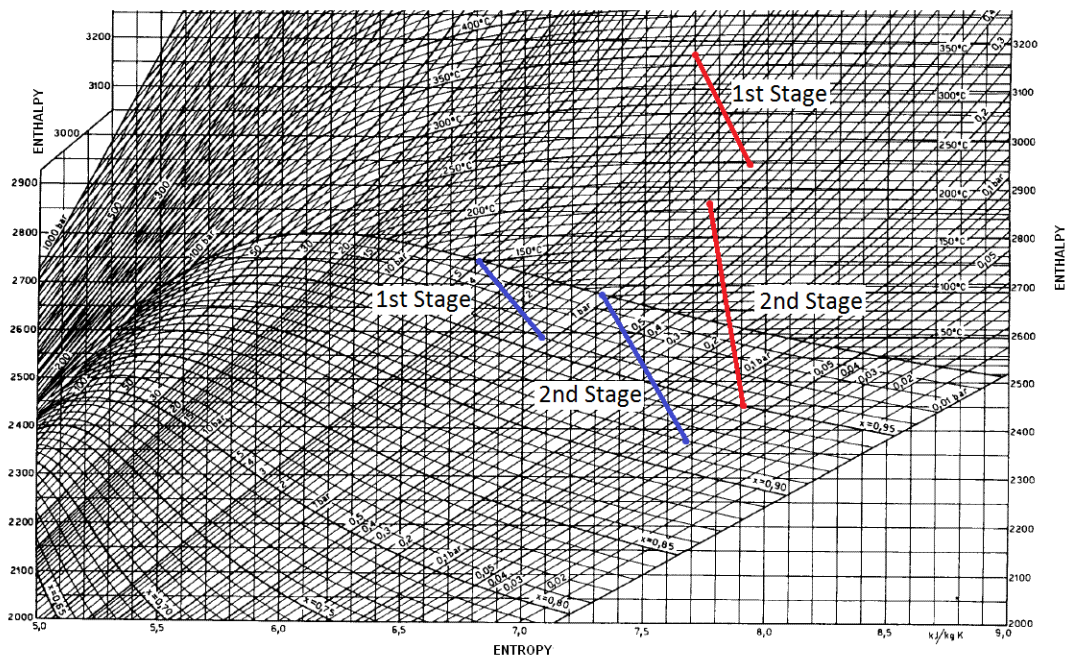


**Figure 29. Entropy-Enthalpy diagram for steam in a MP turbine, for saturated IP steam (blue), and steam superheated to 350°C (red)**

**Table 5. The predicted mass flowrates of steam through each stage in a MP turbine, and the resulting power generation for saturated steam at 150°C and 4.5 bara and superheated steam at 350°C and 4.5 bara**

Case	Mass flow (t/h)		Power generation (MW)		
	1st Stage	2nd Stage	1st Stage	2nd Stage	Total
Saturated steam	214	241.2	10	20	30
Superheated steam	139.7	190.9	9.4	17.6	26.9

As displayed in Figure 29 and Table 5, even though the enthalpy change by using superheated steam is greater than in the saturated steam case, the actual power generation is diminished due to the decreased mass flowrate of the steam. However, as there is a smaller mass requirement of IP

steam for the turbine, there is the potential of utilizing the unused steam in other turbines in order to generate additional power. The method described in Section 3.2.3 could then be used to evaluate the additional power generation that may be possible from the saved steam.

### **3.3.2 Vaporization of Steam Turbine Condensate**

In order to evaluate the additional power that could be generated from the vaporized steam condensate, a model for a boiler was created in UniSim. By investigating the heat transfer efficiencies of boilers, it was found that by using the hydrogen:carbon ratio of the syngas and the flue gas outlet temperature of the syngas as indicators, an 80% heat transfer efficiency could be used for the boiler including the stack losses, and the convection and radiation losses[52] [53]. A 10% air excess was used to calculate the air requirement to the boiler [40]. The flue gas produced by the boiler was used to aid in the drying of the wet biomass to the gasifier, by being used as the drying medium in the rotary drum dryer. A conversion reactor was used in order to model the syngas combustion, and 80% of the heat removed from the reactor was added to the condensate using a heat exchanger. A separator was used in order to model the blowdown of the boiler, the blowdown required by the boiler water chemistry could be input, and the resulting steam generation determined.

In order to increase the amount of additional steam that may be generated, a preheater for the condensate was employed. The temperature of the SGW would depend on the source of the condensate, as the SGW resource would likely be that located in close proximity to condensate to minimize the length of pipelines required. It was assumed that the condensate could be heated to 100°C prior to being introduced into the boiler, as the majority of SGW available is at a higher temperature than this. The outlet temperature of the SGW from the preheater was set as 90°C, as temperatures lower than this may increase the rate of silica precipitation in the heat exchanger [24].

The deaeration of the boiler feed water was then modelled to be performed by further heating the condensate to 103°C using a recycle stream from the steam produced in the boiler. The amount of steam vented in the deaerator was calculated by setting a vent rate of the recycled steam. A controller was used to adjust the amount of recycled steam in order to achieve the desired rate of venting.

The blowdown of the boiler could be set in the UniSim model, to that required based on the boiler water purity. The flowrate of the condensate is then automatically calculated, based on the heat transfer from syngas combustion, the quality of the steam from the boiler, and the boiler blowdown.

As the pressure of the condensate is initially at 7.8 kPaa, pumping needs to be performed before the condensate can be fed to the boiler. As the deaerator operates at approximately 115 kPaa, and the boiler operates at 450 kPaa, two stages of pumping were required for the boiler operation, prior to the preheater, and again after the deaeration stage.

### 3.3.3 Heating the Separated Geothermal Water after the First Separation Stage

In order to estimate the amount of additional steam that may be produced by performing heating on the SGW after the first separation stage, a UniSim model was created. The design of the model was very similar to the model created for the turbine condensate boiler described in Section 2.2.4. An 80% efficiency for the heat transfer to the boiler from syngas combustion was assumed, and a 10% oxygen excess used for the air flowrate to the boiler. It was assumed that heat loss between the first separation stage and the boiler would be negligible, and the temperature of the condensate was found from the saturated steam conditions from the first separation stage.

The reduction of metals being disposed of into the Waikato River was also estimated. As the solubility of metals is much higher in liquid water than in steam, it was assumed that all of the metals in the two-phase fluid are present in the SGW. For simplicity, the water streams have been assigned numbers, as displayed in Figure 30.

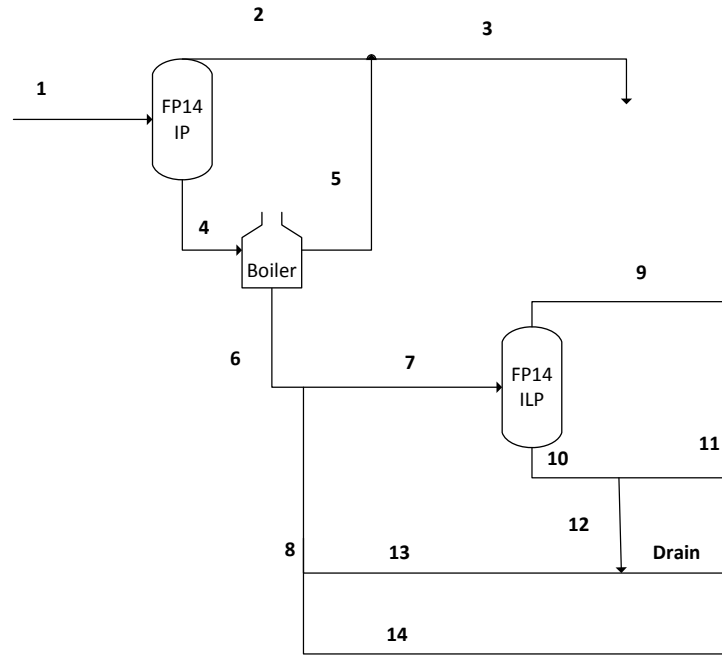


Figure 30. Numbered streams of steam and SGW around the modified FP14

The flowrates for ILP steam (Stream 9), the reinjection in X-line (Stream 11), and the reinjection in T-line (Stream 14) will be relatively constant. Therefore, the flowrate IP SGW to the drain (Stream 13) and the IP steam generated (Stream 3) will be the only exiting streams to have a mass flowrate change with changing IP steam generation in the boiler (Stream 5). The following mass balance was then performed in order estimate the potential decrease in metal flowrate to the Waikato River, where:

$\dot{m}_{m,x}$  = the mass flowrate of the metal of interest in Stream x (g/h)

$\dot{m}_{w,x}$  = the mass flowrate of water (liquid or gas) in Stream x (t/h)



$C_{m,x}$  = the concentration of the metal of interest in Stream x (g/t)

The mass flowrate of metals draining to the Waikato River is the sum of those from Stream 12 and Stream 13, and can be calculated from Equation 21.

$$\dot{m}_{m,Drain} = \dot{m}_{m,12} + \dot{m}_{m,13} = \dot{m}_{w,12}C_{m,12} + \dot{m}_{w,13}C_{m,13} \quad (21)$$

As it is assumed no metals leave in the steam in Streams 2, 5, and 9; Equation 22 can be created.

$$\dot{m}_{m,1} = \dot{m}_{m,4} = \dot{m}_{m,6} \quad (22)$$

The mass flowrate of metals draining into the Waikato from Stream 13 can be found using Equations 23 –26

$$C_{m,6} = C_{m,7} = C_{m,8} = C_{m,13} = C_{m,14} \quad (23)$$

$$\dot{m}_{w,13} = \dot{m}_{w,1} - \dot{m}_{w,2} - \dot{m}_{w,5} - \dot{m}_{w,7} - \dot{m}_{w,14} \quad (24)$$

$$C_{m,6} = \frac{\dot{m}_{w,1}}{\dot{m}_{w,1} - \dot{m}_{w,2} - \dot{m}_{w,5}} C_{m,1} = C_{m,13} \quad (25)$$

$$\dot{m}_{m,13} = \dot{m}_{w,13}C_{m,13} \quad (26)$$

The mass flowrate of metals draining into the Waikato from Stream 12 can be found using Equations 27 –29

$$C_{m,10} = C_{m,11} = C_{m,12} \quad (27)$$

$$C_{m,10} = \left( \frac{\dot{m}_{w,7}}{\dot{m}_{w,7} - \dot{m}_{w,9}} \right) \left( \frac{\dot{m}_{w,1}}{\dot{m}_{w,1} - \dot{m}_{w,2} - \dot{m}_{w,5}} \right) C_{m,1} = C_{m,12} \quad (28)$$

$$\dot{m}_{m,12} = \dot{m}_{w,12}C_{m,12} \quad (29)$$

As the mass flowrate of Stream 12 will remain relatively constant with the amount of additional steam generated in the boiler, the total mass flowrate of metals entering the Waikato may then be calculated. Using the average flowrates for the streams around FP14 for 2015, it was found that the decrease of metal flowrate could be estimated for the amount of additional steam using Equation 30.

$$\dot{m}_{m,\%decrease} = 5.97 \times 10^{-7} \dot{m}_{w,5}^2 + 5.76 \times 10^{-4} \dot{m}_{w,5} \quad (30)$$

Where:

$\dot{m}_{m,\%decrease}$  = the decrease in the flowrate of metals entering the Waikato River from FP14 (%)

### 3.3.4 Heating Additional Separated Geothermal Water for use in a Binary Plant

As the binary plant at Wairakei has been in service since 2009, there are existing correlations used in order to estimate the effect that a change in temperature of the SGW has on the power output of the binary plant. By using a UniSim model to estimate the amount of heating that may be performed on the SGW by a syngas fired heater, the associated power output could be determined. The correction factor for temperature variation of the SGW influent to the binary plant is given by Equation 31 and Equation 32 for different inlet temperatures.

For  $120^{\circ}\text{C} < T < 127^{\circ}\text{C}$  the correction curve the correction curve is linear:

$$F_T = -3.70 + 0.039T \quad (31)$$

For  $127^{\circ}\text{C} < T < 135^{\circ}\text{C}$  the correction curve is a 4<sup>th</sup> order polynomial:

$$F_T = a + bT + cT^2 + dT^3 + eT^4 \quad (32)$$

Where:

$F_T$  = the power output correction factor for changes of inlet SGW temperature

$T$  = the temperature of the SGW entering the binary plant

The values of the constants in Equation 32 are:

$$a = -6231$$

$$b = 192$$

$$c = -2.22$$

$$d = 0.0114$$

$$e = -0.000022$$

By plotting the correction factor against the inlet temperature of the SGW, as displayed in Figure 31, it can be seen that the benefits diminish after heating the SGW above the design temperature of  $127^{\circ}\text{C}$ . As the average temperature of the SGW entering the binary plant is  $130^{\circ}\text{C}$ , there are limited benefits to further heating the inlet SGW away from the designed inlet temperature.

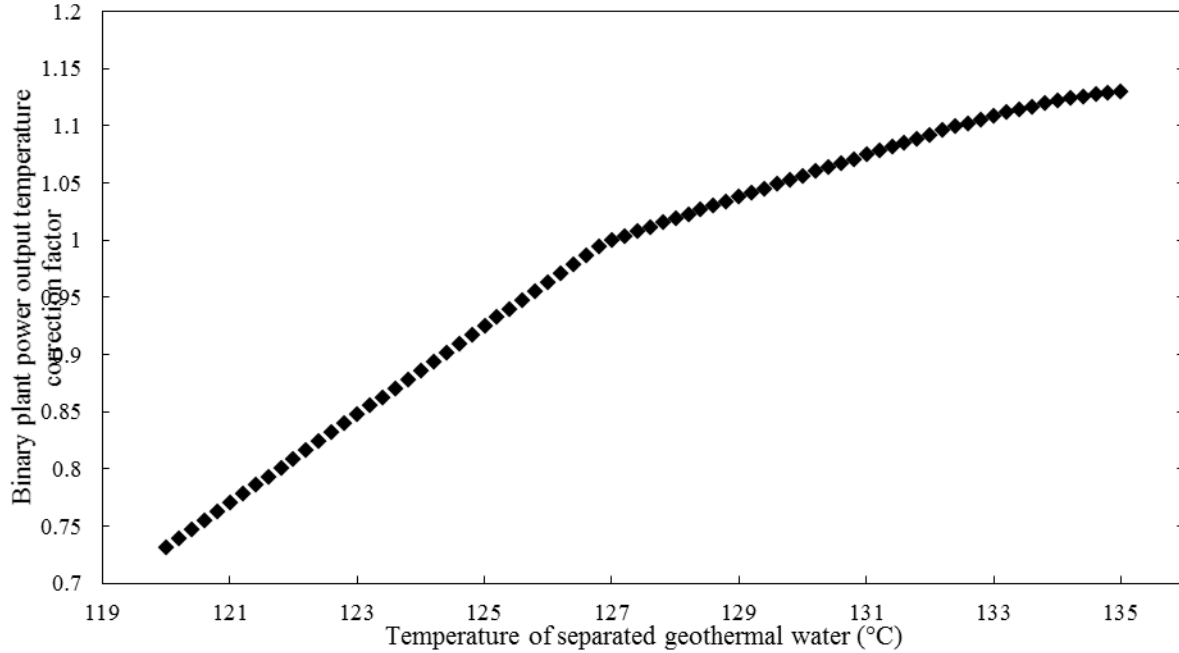


**Figure 31. Power Output Correction Factors for the Wairakei Binary Plant with Separated Geothermal Water inlet temperature.**

Though directly heating the SGW prior to it being utilized in the binary plant has diminishing returns the further the temperature is heated above the designed temperature; there may be capacity to increase the flowrate of SGW to the binary plant. The flow meters on the SGW X-Line that feeds into the binary plant recorded an average of 2811 t/h, however this is believed to be an overestimation of the actual flow. By correcting this value using data from upstream flow meters, the actual amount of SGW in X-Line available to be used by the Binary Plant was estimated to be approximately 2400 t/h. However, this includes the amount of SGW that bypasses the Binary Plant due to flow restrictions attributed to silica scaling. The simple correlations in Equation 33 and Equation 34 were used to estimate the flowrate of bypassing SGW based on data for the valve position for the two bypass valves, PV220 and PV2204.

$$\dot{m}_{V1} = 25B_{2205,\%} \quad (33)$$

$$\dot{m}_{V2} = 8B_{2204,\%} \quad (34)$$

Where:

$\dot{m}_{V1}$  = The mass flowrate of SGW bypassing through the first bypass valve (t/h)

$\dot{m}_{V2}$  = The mass flowrate of SGW bypassing through the second bypass valve (t/h)

$B_{1,\%}$  = The valve position of PV2205 (%)

$B_{2,\%}$  = The valve position of PV2204 (%)

Using Equation 33 and Equation 34, the amount of SGW bypassing the Binary Plant could be estimated and from this the amount of SGW entering the Binary Plant more accurately estimated. It was estimated that the average flowrate of SGW entering the Binary Plant was approximately

2300 t/h for 2015. The flowrate of SGW entering the Binary Plant, bypassing the Binary Plant, and the designed flowrate of SGW for the Binary Plant are displayed in Figure 32.

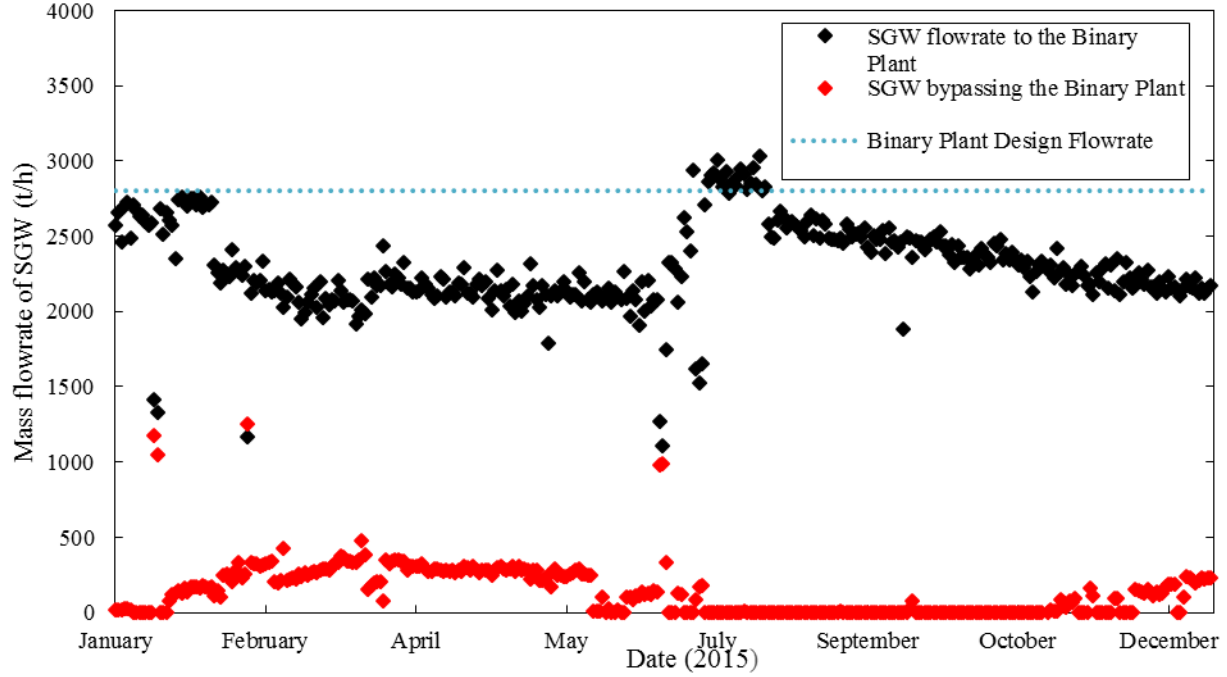


**Figure 32. The mass flowrate of SGW feed to the Wairakei Binary Plant, and the estimated amount of SGW bypassing the Binary Plant.**

The additional power generation that will result from increasing the mass flowrate of SGW to the binary plant is estimated using Equation 35 and Equation 36.

For SGW flow 50% of design  $\leq \dot{m}_{\%OD} \leq 100\%$  of design:

$$F_{\dot{m}} = -0.4288 + 0.014288\dot{m}_{\%OD} \quad (35)$$

For SGW flow 100% of design  $\leq \dot{m}_{\%OD} \leq 114.3\%$  of design:

$$F_{\dot{m}} = 0.83904829 + 0.001609571\dot{m}_{\%OD} \quad (36)$$

Where:

$F_{\dot{m}}$  = The power output correction factor for changes of inlet SGW flowrate

$\dot{m}_{\%OD}$  = The mass flowrate of the SGW entering the binary plant as a % of the designed flowrate

Using Equation 35 and Equation 36, the effect of increasing the flowrate of SGW to the binary plant can be estimated, as is displayed in Figure 33. As can be seen, the benefits of increasing the flowrate of SGW to the binary plant sharply diminish once increased above the design flowrate.

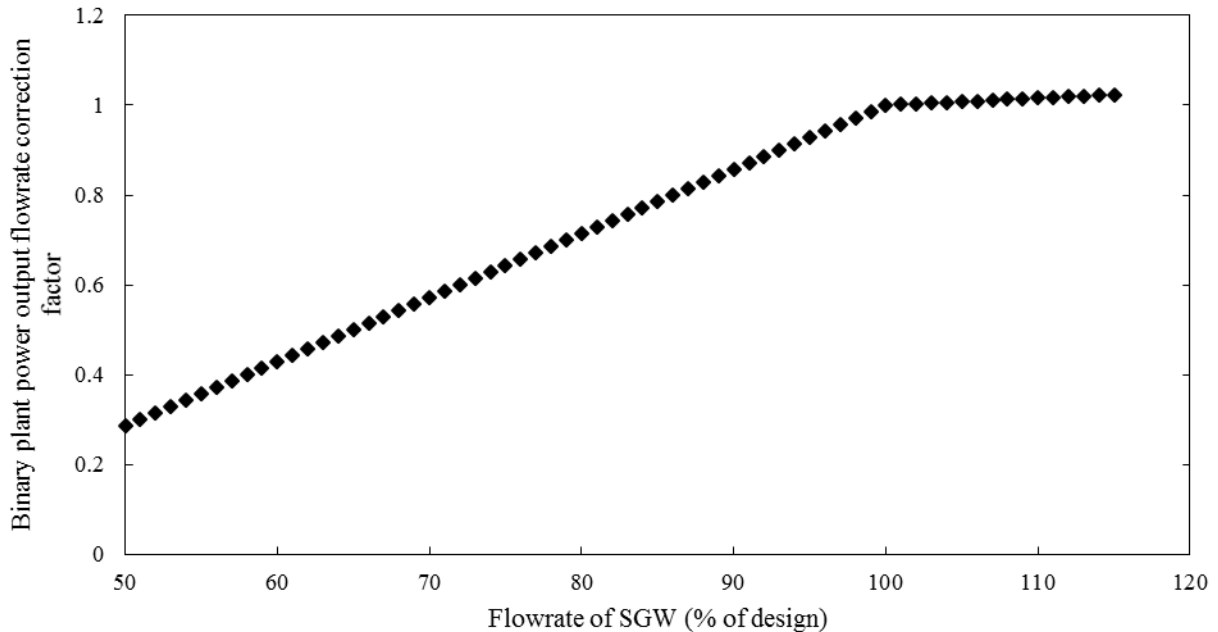


**Figure 33. Power output correction factors for the Wairakei Binary Plant with separated geothermal water flowrate to the Binary Plant.**

Historical data for the flowrate and temperature was used with the correction factors to estimate the amount of additional power that may be generated using a syngas fired heat exchanger to heat T-Line and augment the amount of SGW being fed to the Binary Plant. It was assumed that the maximum flowrate that the Binary Plant could utilize is 3200 t/h, given by the upper bound of Equation 36 at 114.3% of the design flowrate of 2800 t/h. It was found that the most effective use of the syngas fired heating was to heat the SGW in T-Line as little as possible, as the added power generation from increasing the temperature of the SGW did not meet the costs for the landing residues required. The heated temperature of the SGW taken from T-Line was therefore set to be equal to the temperature of the SGW in X-Line. It was also found that the benefits to power generation from increasing the total flowrate to the Binary Plant to higher than the designed flowrate was also offset by the cost of the landing residues required. The amount of T-Line that is to be heated and added to X-Line, and the resulting total mass flowrate of SGW to the Binary Plant are displayed in Figure 34.

As it was determined to heat only the amount of T-Line to satisfy the design flowrate, where possible, and to only heat T-Line to the same temperature as X-Line; there is a relatively small amount of heating required to be performed by the syngas. The amount of heat that was required to be provided by the syngas combustion to achieve the additional power generation displayed in Figure 26 and the corresponding landing residues requirement were calculated and are displayed in Figure 36.

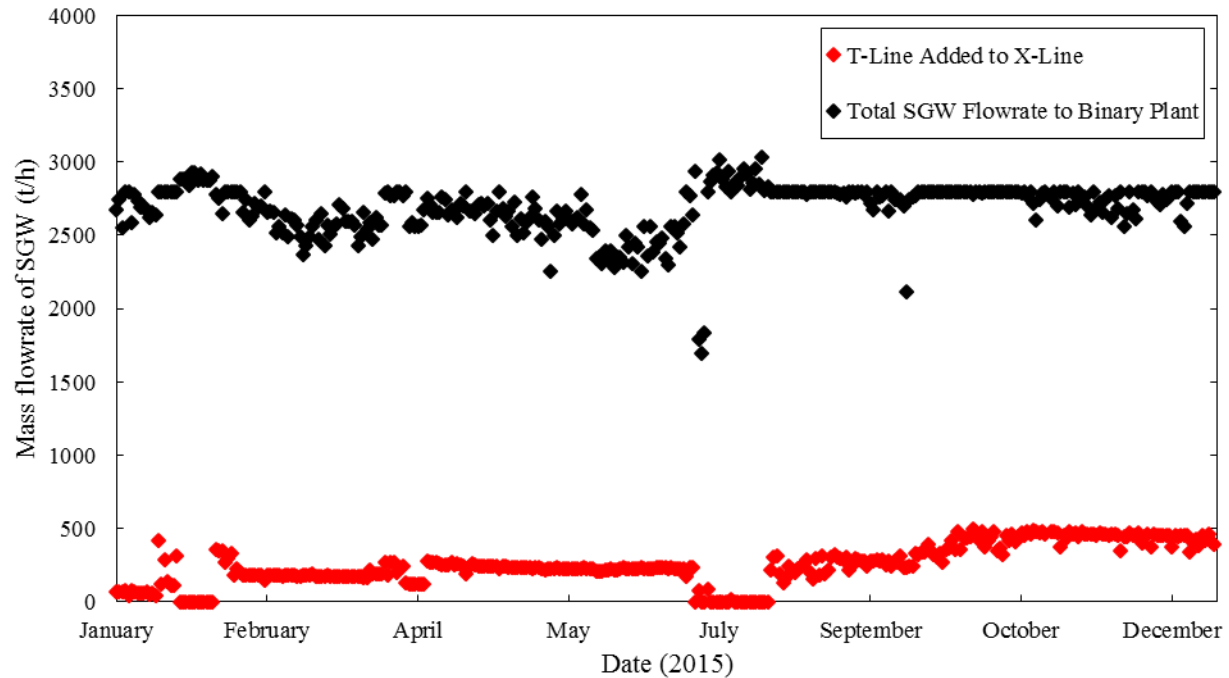


**Figure 34. The additional SGW from T-Line that may be added to the feed of the Binary Plant and the resultant total SGW flowrate**

As can be seen in Figure 34, the SGW in T-Line is only added when the flowrate of X-line is less than the designed flowrate of 2800 t/h. When the combined flow of T-Line and X-Line would be greater than the designed flowrate, only enough of T-Line was added in order to reach the designed flowrate, as exhibited by the plateau in the second half of 2015.

The power generation of the Binary Plant for 2015 and the estimated power generation with the heating and additional SGW from T-Line is displayed in Figure 35. It is estimated that the power generation of the Binary Plant will increase on average from 13.5 MW to 15.3 MW from the additional SGW. However, there will also be a decrease in the power generation at the Wairakei A and B Stations due to the use of IP steam in the gasifier.

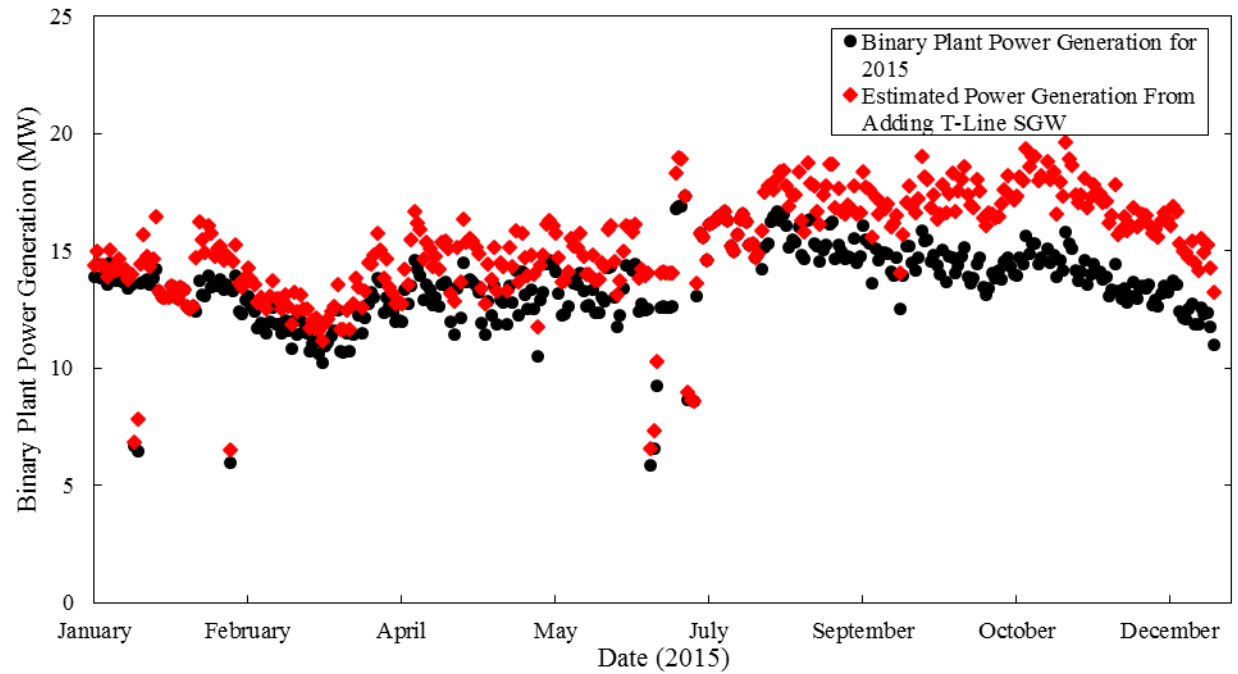


**Figure 35. The Power Generation of the Wairakei Binary Plant for 2015 and the estimated power generation by heating and adding additional SGW from T-Line**

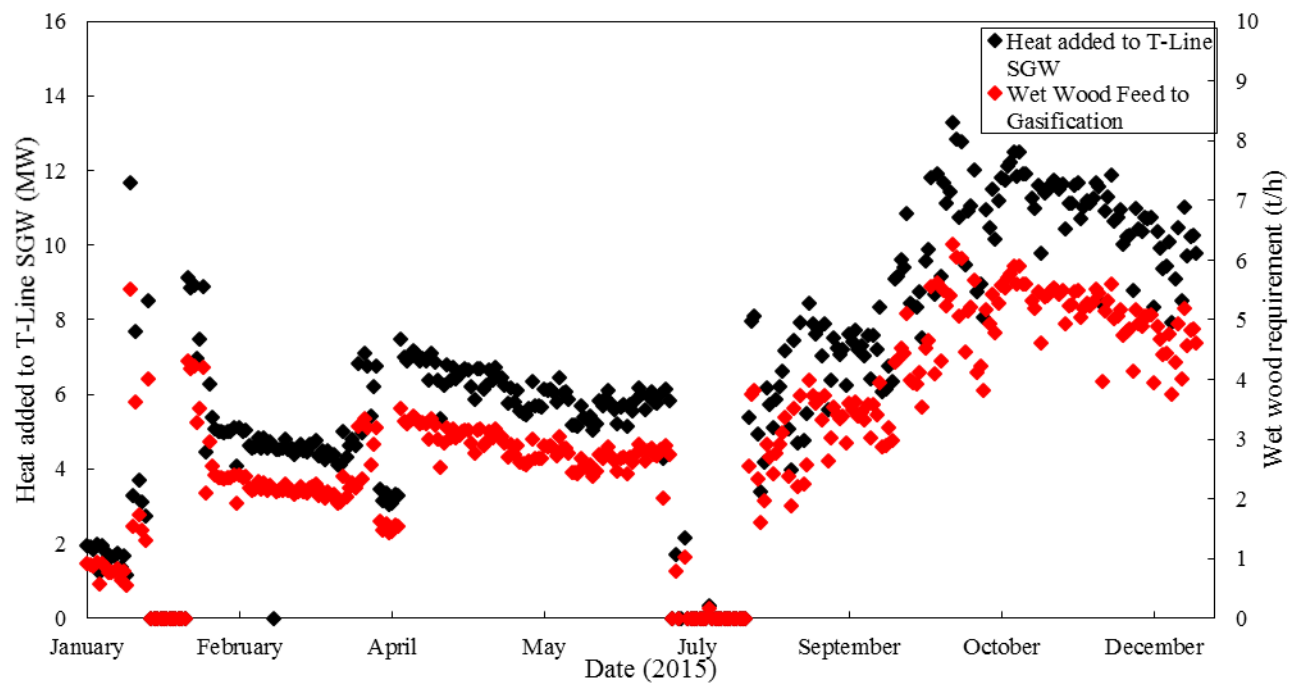


**Figure 36. The heat requirement and associated biomass input in order to heat additional SGW in T-line**

### 3.4 Energy Efficiency

The power generation and the efficiency of power generation from the biomass input were used as a basis, in order to compare the four proposed hybrid geothermal/gasification configurations. The amount of energy present in the biomass feed to the gasifier was calculated using a value for the net calorific value of 19.2 MJ/kg oven dried wood [55]. As a moisture content of 50% (wet basis) was assumed, the net calorific of 9.6 MJ/kg wet wood was used to calculate the energy input from the woody biomass feed. Once the additional power generation was calculated, the electrical energy efficiency could be calculated using Equation 37.

$$\eta = \frac{P_{output}}{P_{input}} \quad (37)$$

Where:

$\eta$	= the electrical energy efficiency
$P_{output}$	= the additional electrical power output from the hybrid configuration (MW)
$P_{input}$	= the power input of the biomass feed based on its calorific value (MW)

The efficiencies of the different configurations are expected to be highly variable with the size of the hybrid configurations, as factors such as the no load flow of the turbines do not scale with the size of the hybrid configurations. As the no load flow of the turbines becomes relatively less influential on the potential power generation from creating additional IP steam, it is expected that in general the larger the hybrid configuration is, the greater the energy efficiency. However, it is also noted, that the most economical sized hybrid configuration will likely not be the most energy efficient, due to the increasing cost of landing residues with increasing residue input. Though the hybridized Binary Plant configuration would not produce additional steam, the average energy efficiency of the plant will still be affected, if a limit is placed on maximum amount of landing residues. The efficiency of the plant will also be highly variable for all of the hybrid configurations, depending on the amount of steam which would otherwise bypass the IP turbines at Wairakei, without these turbines being returned to service, therefore a yearly average for the expected hybrid plant efficiencies will be used for comparison.



## 4.0 Determining the Suitability of Geothermal Waters to be used as Boiler Feed Water

There are strict tolerances on the allowable concentrations of contaminants in boiler feed water, in order to ensure stable and safe operation of the boiler. As the condensate vaporization hybrid configuration described in Section 2.2.4 uses geothermal steam condensate as boiler feed water; it is necessary to perform testing on samples of geothermal condensate in order to determine if the condensate can be used directly as boiler feed water, or failing this a water treatment process stage introduced.

### 4.1 Boiler Feed Water Tolerances

In order to evaluate the relative quality of the geothermal steam condensate, the tolerances for contaminants in boiler feed water were investigated. The tolerances for the boiler feed water were found to be strongly pressure dependent, with the allowable contaminant concentrations decreasing as boiler pressure increases. The American Society of Mechanical Engineers (ASME) has guidelines for boiler feed water and boiler water purity for some contaminants, as displayed in Table 6 and Table 7 respectively[40]. As the condensate boiler would likely be designed to generate steam which may be added directly to the IP steam manifold at the Wairakei Steam Field, the boiler would likely operate at 4.5 bara. As can be seen in Table 6 and Table 7, the relatively low boiler drum pressure required to produce the 4.5 bara steam has less stringent steam purity requirements than for higher pressure boilers.

**Table 6. ASME guidelines for feed water quality in modern industrial water tube boilers for reliable continuous operation [40]**

<b>Drum pressure</b> (bar)	<b>Iron</b> (ppm Fe)	<b>Copper</b> (ppm Cu)	<b>pH</b> pH units	<b>Oxygen</b> (mg/L)	<b>Total hardness</b> (ppm CaCO <sub>3</sub> )
0 - 20.7	0.1	0.05	8-9.5	0.007	0.3
20.7 - 31.0	0.05	0.025	8-9.5	0.007	0.3
31.0 - 41.4	0.03	0.02	8-9.5	0.007	0.2
41.4 - 51.7	0.025	0.02	8-9.5	0.007	0.2
51.7 - 62.0	0.02	0.015	8-9.5	0.007	0.1
62.0 - 69.0	0.02	0.015	8-9.5	0.007	0.05
69.0 - 103.5	0.01	0.01	8.5-9.5	0.007	0
103.5 – 138.0	0.01	0.01	8.5 - 9.2 <sup>1</sup> 9.3 - 9.5 <sup>2</sup>	0.007	0

Note 1: with copper alloys in feed water heaters, Note 2: With carbon steel feed water heaters

**Table 7. ASME guidelines for boiler water quality in modern industrial water tube boilers for reliable continuous operation [40]**

Drum pressure (bar)	Silica (ppm SiO <sub>2</sub> )	Total alkalinity (ppm CaCO <sub>3</sub> )	Total Dissolved Solids (ppm)	Specific conductance (μS/cm) (un-neutralized)
0 - 20.7	150	700	700-3500	7000
20.7 - 31.0	90	600	600-3000	6000
31.0 - 41.4	40	500	500-2500	5000
41.4 - 51.7	30	400	400-2000	4000
51.7 - 62.0	20	300	300-1500	3000
62.0 - 69.0	8	200	250-1250	2000
69.0 - 103.5	2	0	100	150
103.5 - 124.0	1	0	100	100
124.0 - 138.0	1	0	50	100

Generally manufacturers and utility owners recommend that steam should have a silica content between 10 and 20 ppb in order for silica scaling to not occur in steam turbines [40]. A second, more conservative estimate for the permissible amount of silica in the boiler water was found to be between 30-60 ppm, using Figure 37. In order to ensure that damage does not occur to the boiler or to the steam turbines, the conservative estimate of 30 ppm silica in the boiler water was used as the allowable amount of silica in the boiler water.

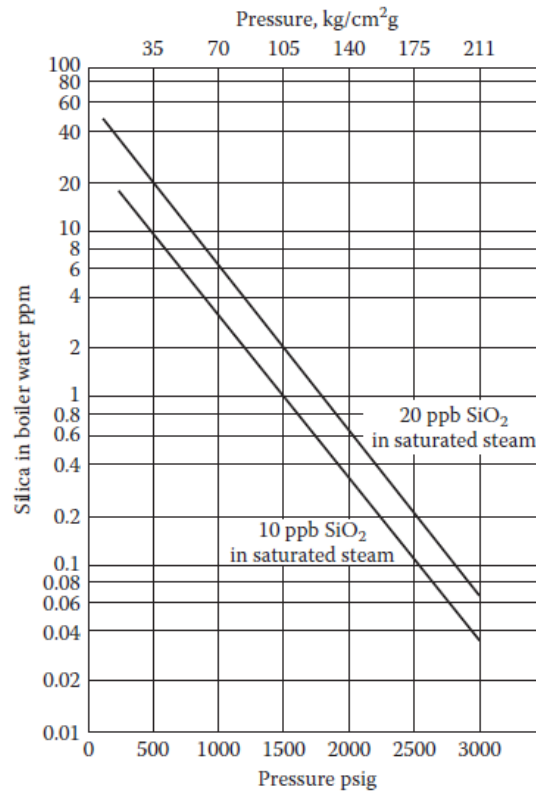


**Figure 37. The permissible amount of silica in the boiler water in order to produce steam with a silica content of 10 and 20 ppb [40].**

After consulting a geothermal water engineer about the contaminants that should be tested for in order for geothermal condensate to be used as boiler feed water, tests on the following were decided to be performed [56]:

- Conductivity
- pH
- SiO<sub>2</sub>
- H<sub>2</sub>S
- CO<sub>2</sub>
- NH<sub>4</sub>
- Chlorides
- Na
- Ca
- Mg
- Sulphates

The concentration of silica, sodium, calcium, and magnesium in the condensate are of interest, as they may cause mineral deposition in a boiler or steam turbine if they are present in high enough concentrations in boiler feed water [57]. Also, the hydrogen sulphide, chlorides, sulphates, and carbon dioxide can cause corrosion within the boiler or turbine if present in the boiler feed water.

## 4.2 Water Available on Site

There are several sources of water available on the Wairakei Steam Field apart from the SGW. These are the blowdown from the Wairakei A and B Power Stations, and Te Mihi Power station, and also the condensate from the Poihipi Rd Power Station. The blowdown at the Wairakei A and B, and the Te Mihi Power Stations is created in direct contact condensers using cooling water to stimulate the condensation of the geothermal steam at the back end of the turbines. The condensate generated in the direct contact condensers is cooled in a cooling tower, then a portion of the cooled blowdown is reused as cooling water in the direct contact condensers. However, the Poihipi Rd Power Station uses a shell and tube condenser and due to this, the condensate does not come into contact with open air, and therefore the chance of contamination or gas absorption reducing the purity of the condensate is removed.

It was decided to perform testing on three sources of water: the condensate from the Poihipi Rd Power Station, the blowdown from Te Mihi, and the Blowdown from Ohaaki. The condensate from the Wairakei A and B stations was not tested, as it was decided due to the fact that the direct contact condensers using the Waikato River water as a cooling fluid would decrease the purity of the resultant condensate, rendering it unsuitable as boiler feed water. The condensate from Poihipi Rd was selected due to the fact that it is the only source of condensate generated in a shell and tube condenser. The blowdown at Ohaaki and Te Mihi were selected in order to evaluate the purity of blowdown generated in direct contact condensers using recycled blowdown as the cooling water.

### 4.3 Factors Affecting Water Purity

There are several factors that can influence the concentration of contaminants in the geothermal condensate. Most of these factors relate to the amount of liquid geothermal water present that is entrained into the steam turbines. This is due to the fact that the dissolved minerals in the geothermal fluid have a much higher solubility in liquid water than in steam. Because of this, the majority of the minerals present in the geothermal condensate are present due to entrained liquid water. It is also known that minerals can be soluble in steam, however, within the range of steam pressures generated at Wairakei, the solubility of minerals in steam is negligible compared to the solubility in liquid water [58],[59]. Because of this, if liquid carryover in the steam increases, more water treatment may be required for the condensate or blowdown to be used as boiler feed water.

Due to the higher mineral solubility in liquid water than in steam, the performance of the flash plants separating the liquid and gasses greatly impacts the condensate and blowdown purity. However, monitoring the performance of the flash plants at Wairakei during operation is difficult, and no continuous monitoring of flash plant performance is conducted. Currently testing of the performance of Flash Plant 15 and Flash Plant 16 are being conducted at Wairakei, in order to address silica scaling problems at the Te Mihi Power Station. Specifically it is of interest to discover the effect that the load on the flash plants and the separation pressure have on liquid carry over. This is performed by injecting tracers into the two-phase fluid prior to the separators and sampling the liquid removed from drain pots downstream. If the results from this flash plant analysis indicate significant variability in flash plant performance, then efforts should be made to evaluate the effect this will have on condensate and blowdown purity.

There are relatively long steam lines at the Wairakei Geothermal Field compared to other geothermal power plants, and consequently there are both relatively high pressure and heat losses from transportation at Wairakei. However, this causes a phenomenon called “passive scrubbing” at Wairakei, where a large portion of the liquid carryover in the steam is deposited on the walls of the pipelines, and subsequently removed in drain pots. This removal of liquid also serves to remove a large amount of the minerals present in the steam.

Currently there are drain pots installed throughout the Wairakei Geothermal Field, in order to remove condensate and liquid carryover in the steam lines. There are also demisters installed at the Te Mihi, and Poihipi Rd Power Plants, in order to scrub any remaining liquid from the steam prior to it being used in the turbines. However, it is believed that the demister at Poihipi Rd is essentially out of operation, due to massive corrosion within it.

The steam wells used to extract the steam are also expected to have a large effect on the resulting condensate and blowdown purity. The pressure and quality of the steam varies depending on the wells used, with some wells at Wairakei even being considered “dry” as they have very low moisture content. The geology at the different steam wells will affect the mineral content in the fluid extracted from the wells, due to the differing mineral compositions of different rock formations.

The oxygen content of the condensate and blowdown will be affected by the exposure of the water to air. Dissolved oxygen must be maintained below a certain concentration in boiler feed water in order to prevent corrosion or pitting in the boiler. The solubility of oxygen in water increases as

pressure increases and as temperature decreases, and the Poihipi Rd condensate is formed from the condensation of geothermal steam under vacuum conditions at approximately 75 mbara and 40°C. Because of this, the Poihipi Rd condensate is expected to have a much lower dissolved oxygen content than the Te Mihi blowdown and Ohaaki blowdown as they are at atmospheric pressure. Provided that there is no exposure of the Poihipi Rd condensate to oxygen, the condensate should retain its low oxygen content even after its pressure is increased by pumping the condensate for use in the boiler.

#### 4.4 Sampling and Testing Procedure

The sampling and testing of the condensate and blowdown sources were designed with reference to the Standard Methods For the Examination of Water and Waste water by the American Public Health Association (APHA) [60]. As the testing for metals required nitric acid preservation on the sample bottle, two separate samples were required to be taken for each source of water. 100 ml of sample was taken in a sample bottle that was treated with nitric acid, along with 2L of raw sample. The testing procedure for each of the contaminants of interest, and the detection limits of each test is displayed in

Table 8.

The dissolved oxygen was tested on site, using a YSI Digital Model 58 Dissolved Oxygen Meter. As the Poihipi Rd sample was the only sample that was not exposed to the open air, and had to be extracted from pipelines, it was desired to minimize the contact with the air, as this would likely result in an inaccurately high oxygen content in the sample. In order to minimize the oxygen contamination, an apparatus was used to minimize contact the sample has with the air, as displayed in Figure 38. A tube was used to inject the condensate directly from the sampling point into the sampling container. The design of the sampling container ensured that the condensate did not come into contact with air, however as there was not a perfect seal between the oxygen meter probe and the sampling container, there may be been some contact with the air.

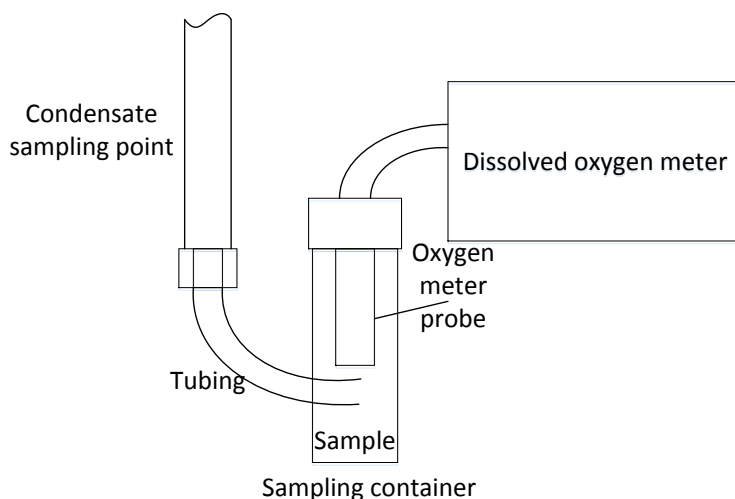


**Figure 38. Diagram of apparatus used to minimize oxygen contamination during dissolved oxygen sampling**

**Table 8. The contaminant testing method and detection limits for the tests performed on the geothermal waters**

Test	Method description	Default detection limits
Filtration, Unpreserved	Sample filtration through 0.45µm membrane filter	-
Total Digestion	Boiling nitric acid digestion. APHA 3030 E 22 <sup>nd</sup> ed. 2012 (modified).	-
pH	pH meter. APHA 4500-H + B 22 <sup>nd</sup> ed. 2012.	0.1 pH Units
Total Alkalinity	Titration to pH 4.5 (M-alkalinity), autotitrator. APHA 2320 B (Modified for alk <20) 22 <sup>nd</sup> ed. 2012.	1.0 g/m <sup>3</sup> as CaCO <sub>3</sub>
Free Carbon Dioxide	Calculation: from alkalinity and pH, valid where TDS is not >500 mg/L and alkalinity is almost entirely due to hydroxides, carbonates or bicarbonates. APHA 4500-CO <sub>2</sub> D 22 <sup>nd</sup> ed. 2012.	1.0 g/m <sup>3</sup> at 25°C
Electrical Conductivity (EC)	Conductivity meter, 25°C. APHA 2510 B 22 <sup>nd</sup> ed. 2012.	0.1 mS/m
Total Dissolved Solids (TDS)	Filtration through GF/C (1.2 µm), gravimetric. APHA 2540 C (modified; drying temperature of 103 - 105°C used rather than 180 ± 2°C) 22 <sup>nd</sup> ed. 2012.	10 g/m <sup>3</sup>
Total Calcium	Nitric acid digestion, ICP-MS, trace level. APHA 3125 B 22 <sup>nd</sup> ed. 2012.	0.053 g/m <sup>3</sup>
Total Copper	Nitric acid digestion, ICP-MS, trace level. APHA 3125 B 22 <sup>nd</sup> ed. 2012 / US EPA 200.8.	0.00053 g/m <sup>3</sup>
Total Iron	Nitric acid digestion, ICP-MS, trace level. APHA 3125 B 22 <sup>nd</sup> ed. 2012.	0.021 g/m <sup>3</sup>
Total Magnesium	Nitric acid digestion, ICP-MS, trace level. APHA 3125 B 22 <sup>nd</sup> ed. 2012.	0.021 g/m <sup>3</sup>
Total Dissolved Silica	Calculation: Silicon x 2.14.	0.005 g/m <sup>3</sup> as SiO <sub>2</sub>
Total Sodium	Nitric acid digestion, ICP-MS, trace level. APHA 3125 B 22 <sup>nd</sup> ed. 2012.	0.021 g/m <sup>3</sup>
Chloride	Filtered sample. Ferric thiocyanate colorimetry. Discrete Analyser. APHA 4500 Cl <sup>-</sup> E (modified from continuous flow analysis) 22 <sup>nd</sup> ed. 2012.	0.5 g/m <sup>3</sup>
Total Ammoniacal-N	Filtered sample. Phenol/hypochlorite colorimetry. Discrete Analyser. (NH <sub>4</sub> -N = NH <sub>4</sub> <sup>+</sup> -N + NH <sub>3</sub> -N). APHA 4500-NH <sub>3</sub> F (modified from manual analysis) 22 <sup>nd</sup> ed. 2012.	0.010 g/m <sup>3</sup>
Silicon	Analysed as received (filtration, if required), ICP-MS, trace level. APHA 3125 B 22 <sup>nd</sup> ed. 2012.	0.005 g/m <sup>3</sup>
Un-ionised hydrogen sulphide	Calculation from Total Sulphide, Electrical Conductivity, pH and Temperature APHA 4500-S <sup>2-</sup> H (modified) 22 <sup>nd</sup> ed. 2012	0.002 g/m <sup>3</sup>
Sulphide Distillation	Acid distillation of sample into alkaline trapping solution using Simple Distillation system. APHA 4500-S <sup>2-</sup> I 22 <sup>nd</sup> ed. 2012.	-
Total Sulphide	Sulphide distillation. Automated methylene blue colorimetry, discrete analyser. APHA 4500-S <sup>2-</sup> I (modified) 22 <sup>nd</sup> ed. 2012.	0.002 g/m <sup>3</sup>
Sulphate	Filtered sample. Ion Chromatography. APHA 4110 B 22 <sup>nd</sup> ed. 2012.	0.5 g/m <sup>3</sup>

## 4.5 Water Sample Results

The results from the tests performed by Hill Laboratories on the condensate and blowdown water samples are displayed in Table 9.

**Table 9. The results for the sample impurities for the Poihipi Rd condensate, Te Mihi blowdown, and Ohaaki blowdown performed by Hill Laboratories**

Tests	Unit	Poihipi Rd condensate	Te Mihi Blowdown	Ohaaki Blowdown
Total alkalinity	<i>ppm as CaCO<sub>3</sub></i>	11 ± 0.80	1.5 ± 0.67	68.8 ± 2.9
Free carbon dioxide	<i>ppm at 25°C</i>	1.21 ± 0.57	81 ± 58	1.98 ± 0.92
Total dissolved solids	<i>ppm</i>	< 10 ± 6.7	26.3 ± 7.3	53.3 ± 9.2
Total Calcium	<i>ppm</i>	< 0.053 ± 0.036	0.060 ± 0.036	1.000 ± 0.054
Total Copper	<i>ppb</i>	<0.053 ± 0.036	<0.053 ± 0.036	<0.053 ± 0.036
Total Iron	<i>ppm</i>	< 0.021 ± 0.014	< 0.021 ± 0.014	< 0.021 ± 0.014
Total Magnesium	<i>ppm</i>	< 0.021 ± 0.014	< 0.021 ± 0.014	< 0.021 ± 0.014
Total dissolved silica	<i>ppm as SiO<sub>2</sub></i>	<0.011 ± 0.0072	0.0458 ± 0.0077	0.640 ± 0.040
Chloride	<i>ppm</i>	0.76 ± 0.35	< 0.5 ± 0.35	< 0.5 ± 0.35
Total Sodium	<i>ppm</i>	0.061 ± 0.015	0.223 ± 0.020	0.270 ± 0.022
Total ammoniacal-N	<i>ppm</i>	2.48 ± 0.20	6.77 ± 0.55	41 ± 3.4
Silicon	<i>ppm</i>	<0.005 ± 0.0034	0.0214 ± 0.0036	0.299 ± 0.019
Sulphate	<i>ppm</i>	< 0.5 ± 0.35	27.5 ± 1.7	71.9 ± 4.4
pH	<i>pH Units</i>	7.3 ± 0.2	4.6 ± 0.2	7.8 ± 0.2
Electrical conductivity	<i>μS/cm</i>	22 ± 1	83 ± 2	371 ± 8
Un-ionised hydrogen sulphide	<i>ppm</i>	0.034	<00.2	0.003
Total sulphide	<i>ppm</i>	0.9 ± 0.33	< 0.002 ± 0.0014	0.0218 ± 0.0080

The results from the dissolved oxygen measurement are displayed in Table 10.

**Table 10. The measured dissolved oxygen for the geothermal waters**

Water Source	Dissolved oxygen (mg/L)
Poihipi Rd Condensate	0.55
Te Mihi Blowdown	6.4
Ohaaki Blowdown	5.16

The hardness of the water is calculated using the amount of calcium and magnesium ions in the water, and represented as the equivalent of calcium carbonate (CaCO<sub>3</sub>). In order to calculate the equivalent total hardness, of the water sources, the measurements for the concentration of magnesium and calcium must be converted to the equivalent of calcium carbonate, this can be performed using Equation 38.

$$[CaCO_3] = \frac{M_{CaCO_3}}{M_{Ca}} [Ca^{2+}] + \frac{M_{CaCO_3}}{M_{Mg}} [Mg^{2+}] \quad (38)$$

Where:

$[CaCO_3]$  = the equivalent concentration of calcium carbonate in the water (ppm)

$[Ca^{2+}]$  = the concentration of calcium ions in the water (ppm)

$[Mg^{2+}]$  = the concentration of magnesium ions in the water (ppm)

$M_{CaCO_3}$  = the molar mass of calcium carbonate (100.1 g/mol)

$M_{Ca}$  = the molar mass of calcium (40.1 g/mol)

$M_{Mg}$  = the molar mass of magnesium (24.3 g/mol)

By applying Equation 38 to the concentrations of calcium and magnesium in the different sources of water, the hardness of the water could be quantified as displayed in Table 11.

**Table 11. The hardness of the different sources of water.**

Source of water	Hardness (ppm as $CaCO_3$ )
Poihipi Rd condensate	$< 0.219 \pm 0.147$
Te Mihi Blowdown	$< 0.236 \pm 0.147$
Ohaaki Blowdown	$2.65 \pm 0.200$

By comparing the three sources of water tested for boiler feed water suitability, it was decided that the Poihipi Rd condensate was the most suitable source of water available. The Poihipi Rd condensate was chosen due to the fact that it was seen to have the lowest mineral content and total dissolved solids (TDS) of the samples tested. Due to this lower TDS, the risk of mineral precipitation on the boiler tubes would be reduced. The Poihipi Rd condensate also had significantly less dissolved oxygen than the other samples, which would ensure less oxygen removal would need to be performed. The low value for the dissolved oxygen in the Poihipi Rd condensate is attributed to the fact that the condensate does not come into contact with the air after the condenser, and the vacuum conditions of the Poihipi Rd condensate. As the blowdown at Te Mihi and Ohaaki is exposed to the air in the cooling tower, oxygen is able to be absorbed by the water. The fact that the gasses are removed from the Poihipi condensate while it is under vacuum conditions at approximately 78 mbara also serves to reduce the dissolved oxygen, as the solubility of oxygen in water increases with pressure.

The purity of the Poihipi Rd condensate was then compared to the purity required for boiler feed water in Table 6. It was noted that the concentration of impurities in the condensate met the requirements for the iron and copper content in the water. The hardness of the water may be suitable as it is below the recommended concentration of 0.3 ppm, however, the uncertainty associated with the testing result could cause the hardness to be as high as 0.366 ppm. The pH, and dissolved oxygen concentration in the condensate however, did not meet the requirements. As the required pH for a boiler operating at 4.5 bara is in the range of 8-9.5, alkali dosing would need to be performed in order to raise the pH from 7.3.



The boiler water purity requirements as displayed in Table 7 are not exceeded by the Poihipi Rd condensate. Due to this demineralization or other water purification techniques may not be required to ensure safe operation of the boiler, as the boiler blowdown may be designed to adequately remove the contaminants. However it may be required to perform additional cleaning in order to reduce the amount of blowdown required.

## **4.6 Techniques for Condensate Cleaning**

In order to achieve the purity required for boiler feed water, the Poihipi Rd condensate must be treated in order to reduce or remove some of its contaminants. Water treatment for boiler feed water is a well-studied field, due to the long use of boilers in industry. The common impurities in boiler feed water, their description, effects, and the method of impurity removal is displayed in Table 12.

Even though the maximum possible hardness of the Poihipi Rd condensate from the samples taken, at 0.366 ppm is slightly above the recommended level of 0.3, water softening will not be designed. This is due to the fact that the actual quantities of calcium and magnesium in the condensate were so small as to not be detectable using the tests performed by Hill Laboratories. It is recommended to perform more comprehensive tests to validate the assumption that the hardness will be in the acceptable range.

The steam generated in the boiler is expected to be relatively more pure than the geothermal IP steam currently being used in the Poihipi Rd steam turbines. This is due to the cleaning performed on the condensate, and the minerals distilled from the condensate into the boiler blowdown. Because of this, the greater the capacity of the boiler, the more IP steam will be displaced by the re-boiled condensate in the Poihipi Rd turbine. This will in turn, purify the condensate further, resulting in steam condensate that is likely purer than that displayed in Table 10. It is therefore likely that the required amount chemical additives used to remove impurities in the condensate will reduce after the condensate has reached its equilibrium purity. The monitoring of the impurities should be performed in order to ensure the correct amount of chemical additives are being administered to purify the condensate to boiler feed water standards.

**Table 12. Boiler feed water impurities, their effects and removal [40]**

Impurity	Description	Effects	Method of Removal
Hardness	Ca, Mg salts as $\text{CaCO}_3$	Scale formation	Softener, demineraliser, internal treatment, surface agents
Alkalinity	$\text{HCO}_3$ , $\text{CO}_3\text{OH}$ as $\text{CaCO}_3$	Foaming, carryover, embrittlement, $\text{CO}_2$ in steam causing corrosion in condensate line	Softener, demineraliser, zeolite softening, dealkalisation by anion exchanger
Free acids	$\text{HCl}$ , $\text{H}_2\text{SO}_4$ , etc as $\text{CaCO}_3$	Corrosion	Neutralisation with alkalis
$\text{CO}_2$		Corrosion in steam and condensate lines	Aeration, deaeration, neutralisation with alkalis
$\text{SO}_4^{2-}$		Forms $\text{CaSO}_4$ scale	Demineralizer
$\text{Cl}^-$		Adds to corrosive nature of water	Demineralizer
$\text{Na}^+$		Corrosion by combining with $\text{OH}$	Demineralizer
$\text{SiO}_2$		Scale in boiler and insoluble deposits in turbine	Adsorption in highly basic anion exchange in demineralizer
Fe and Mn	$\text{Fe}^{2+}$ , $\text{Fe}^{3+}$	Deposits in the boiler and water lines	Aeration, filtration, lime softening, cation exchanger, surface active agents
$\text{O}_2$		Corrosion in boiler, heat exchangers, and water lines	Deaeration, $\text{NaSO}_3$ , Corrosion inhibitors
Dissolved solids		Foaming	Softening, cation exchanger by zeolite, demineraliser
suspended solids		Deposits in boiler, heat exchangers, and water lines	Filtration
Oil		Excessive foaming and hence carryover	Dual media or activated carbon filtration
Turbidity		Imparts unsightly appearance to water; deposits in water lines, process equipment, and so on; interferes with most process uses	Coagulation, settling and filtration

#### 4.6.1 pH Dosing

As free hydrogen ions in boiler water can attack the metal in the boiler, boiler water is generally dosed in order to reduce the amount of free hydrogen ions, increasing the pH of the water. In order to comply with the recommended pH of boiler feed water, the pH of the Poihipi Rd condensate must be increased from approximately 7.3 to 8 - 9.5. Caustic soda ( $\text{NaOH}$ ) is commonly used as dosing chemicals in order to increase the alkalinity of boiler feed water [57]. Though the addition of these chemicals will increase the amount of sodium in the boiler water, sodium generally does not form scale in boilers [61]. A target pH of 9 was assumed for the boiler feed water.

Equation 39 was used in order to calculate the concentration of caustic soda that should be added to the boiler feed water in order to achieve the desired pH.

$$C_{NaOH} = 10^{-(14-pH_2)} - 10^{-(14-pH_1)} \quad (39)$$

Where:

- $pH_1$  = the initial pH of the boiler feed water
- $pH_2$  = the desired pH of the boiler feed water
- $C_{NaOH}$  = concentration of NaOH that should be added to achieve  $pH_2$  (mol/L boiler feed water)

In order to calculate the amount of caustic soda that should be added to the boiler feed water the concentration of caustic soda could be converted to a mass flowrate using Equation 40.

$$\dot{m}_{NaOH} = C_{NaOH} \times M_{NaOH} \times \frac{\dot{m}_{FW}}{\rho_{FW}} \quad (40)$$

Where:

- $\dot{m}_{NaOH}$  = the mass flowrate of NaOH to be added to the boiler feed water (g/h)
- $M_{NaOH}$  = the molar mass of NaOH (39.997 g/mol)
- $\dot{m}_{FW}$  = the mass flowrate of boiler feed water (kg/h)
- $\rho_{FW}$  = the density of the boiler feed water (taken as 0.998 kg/L)

#### 4.6.2 Deaeration

As the dissolved oxygen concentration at 0.55 mg/L in the Poihipi Rd condensate is higher than the recommended boiler feed water limits at 0.07 mg/L, deaeration must be performed on the condensate. As the solubility of oxygen in water increases with pressure and decreases with temperature as shown in Figure 39, by increasing the temperature and/or decreasing the pressure, the oxygen may be desorbed from the water. Deaeration occurs in cylindrical vessels with spray nozzles inside, the feed water is sprayed into very fine droplets to allow for almost complete desorption of the oxygen and other gasses. Deaerators when properly operated may reduce the oxygen concentration of the feed water to below 0.007 ppb [62], orders of magnitude below the required maximum concentration of 0.007 ppm (mg/L).

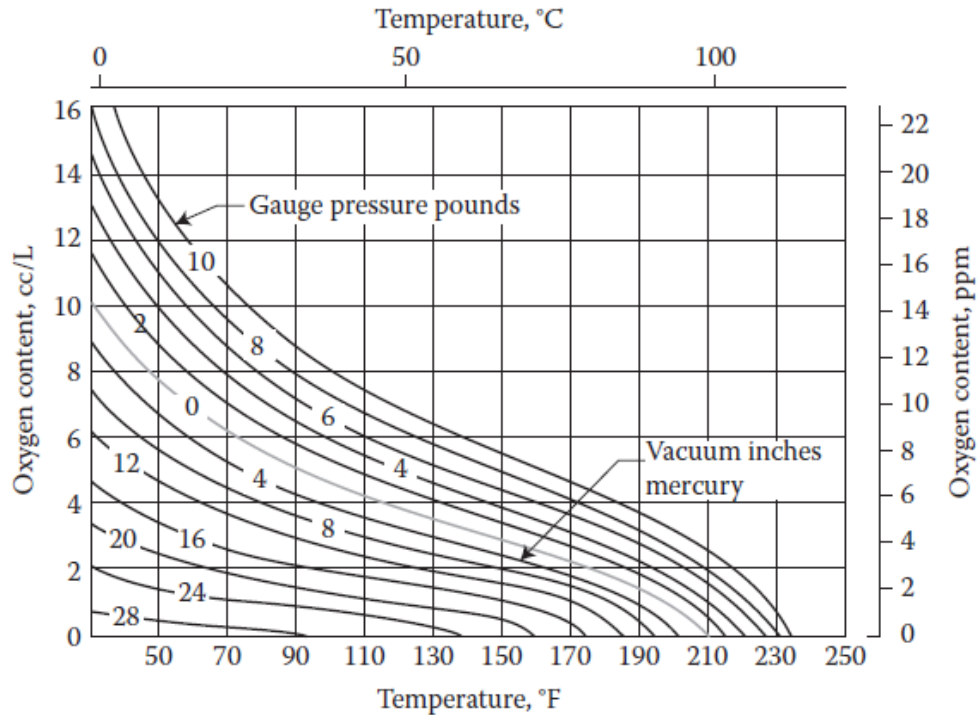


**Figure 39. The solubility of oxygen in water under different temperatures and pressures [40]**

It was decided that in order to simplify the deaerator, it should be operated at slightly above atmospheric pressure, as this will aid in the disposal of oxygen and other gasses from the deaerator. With reference to Figure 39, it can be seen that for a deaerator operating at 2 psig (14 kPag) will require the water to be heated to approximately 103°C. As this is very similar to the boiling point of water at 2 psig, control on the heating will need to be performed in order to ensure minimal loss of steam with the desorbed gasses. The majority of the heating required to be performed on the feed water will be done during the preheating of the feed water using SGW as the heat source, as this is used to heat the water to approximately 100°C. Steam recycled from the boiler will be used to provide the additional heat required for deaeration, the flowrate of this steam may then be altered in order to achieve the necessary heating.

The vent rates of steam from the deaerator are typically between 5% - 14% of the steam introduced to the deaerator [63]. There is a relatively small heating load required to be performed by the steam, as the feed water is only required to be heated approximately 3°C, corresponding to a relatively small mass flowrate of steam required. As one purpose of the recycled steam is to carry away the desorbed gasses, a vent rate of 14% of the recycled steam was chosen to ensure adequate removal of the gasses.

Provided the deaerator is operated correctly, oxygen scavenger additives such as hydrazine are not expected to be required.

#### **4.6.3 Blowdown Control of Boiler Water**

As discussed in Section 4.5, the tolerances for the boiler water may be met with an appropriate blowdown applied to the boiler. The blowdown rate for a boiler may be determined using the contaminant concentration in the boiler feed water and the maximum allowable contaminant concentration in the boiler water using Equation 41.

$$BD_{\%} = \frac{C_{FW}}{C_{BW} - C_{FW}} \quad (41)$$

Where:

$BD_{\%}$  = the blowdown rate as a percentage of the feed rate (%)

$C_{FW}$  = the concentration of the contaminant in the boiler feed water (ppm)

$C_{BW}$  = the maximum concentration of the contaminant in the boiler water (ppm)

The resultant blow down rates in order to ensure the silica, alkalinity, or TDS do not rise above the maximum allowable values are displayed in Table 13. The highest value for the blowdown of the boiler water was 2.4% of the feed water, and typical boiler blowdowns are in the order of 4 - 8% of the boiler feed rate [64], though minimizing this improves energy efficiency. A boiler blowdown rate of 2.5% was considered adequate to reduce the concentration of impurities in the boiler water to allowable levels.

**Table 13. The calculated blowdown required to mitigate problems that may be caused by silica, TDS, and alkalinity in order to ensure safe boiler operation.**

Species	Maximum in Poihipi Rd Condensate <i>ppm</i>	Maximum allowable in boiler water <i>ppm</i>	Required blowdown <i>% of feed rate</i>
Silica	0.0182	30	0.1%
TDS	16.7	700	2.4%
Alkalinity (as CaCO <sub>3</sub> )	11.8	700	1.7%

#### 4.6.4 Boiler Water Monitoring

Monitoring of the solids in the condensate may be achieved using the sodium tracer technique, and a sodium ion analyser. The sodium tracer technique uses the sodium that is present in the boiler feed water to estimate the sodium that will be present in the steam, as the ratio of sodium/solids will be the same in the boiler feed water and steam in all but the highest pressure systems [57]. As sodium may be measured in-situ in order to estimate the amount of solids in the boiler feed water and resulting steam, it may be possible to use sodium concentration to administer the appropriate amount of feed water treatment chemicals. However, as the ratio of minerals in the geothermal steam may vary, regular testing on condensate composition should be performed.

As the dissolved oxygen present in the condensate will be a function of condenser pressure, it is also advised that monitoring of the dissolved oxygen in the boiler feed water be performed. If the dissolved oxygen is measured both upstream and downstream from the deaerator, both the dissolved oxygen content of the boiler feed water and the performance of the deaerator may be

evaluated. If dissolved oxygen concentrations in the boiler feed become too high, it may require the addition of an oxygen scavenger, such as hydrazine in order to reduce the concentration to allowable levels.

#### 4.6.5 Reliability of Results

As the wells used at Poihipi Rd are relatively constant with the operation of the Power Plant, the geometry and length of the steam lines also remained relatively constant. In order to better understand how the purity of the Poihipi Rd condensate will change with time, results from tests performed when different wells were used to supply Poihipi Rd with steam. Results from tests performed on the Poihipi Rd condensate and Poihipi Rd condenser performed from 2007 to 2008 were used to compare with the tests performed for this study. However, as these tests were not performed with focus on utilizing the condensate as boiler feed water, not all of the species of interest were tested for. The tests of the three tests performed from 2007 to 2008, and the test performed for this study are displayed in Table 14. For brevity, not all of the species tested for are displayed in Table 14, the full testing results may be found in the appendices.

**Table 14. Testing results for the species of interest in Poihipi Rd condensate to assess the variability of the condensate**

Species	Units	Poihipi Rd Condensate 17-Jul-07	Poihipi Rd Condensate 30-Apr-08	Poihipi Rd Condenser water 14-May-08	Poihipi Rd Condensate 14-Jun-16
Calcium	ppm	<0.05	<0.053	<0.053	<0.053
Magnesium	ppm	<0.01	<0.021	<0.021	<0.021
Total Hardness (as CaCO <sub>3</sub> )	ppm	<0.166	<0.219	<0.219	<0.219
Silica	ppm	<0.06	-	-	<0.011
Conductivity	µS/cm	24	-	-	22
pH	pH units	6.67	-	-	7.3
Alkalinity (as CaCO <sub>3</sub> )	ppm	-	-	-	11
Iron	ppm	-	0.032	<0.021	<0.021
Copper	ppm	0.002	0.00059	0.00057	<0.000053

It can be seen that the iron and copper concentrations are consistently below the recommended tolerances displayed in Table 6. The hardness of the water was also seen to be relatively constant across the tests performed, and would likely meet the boiler feed water tolerances if the blowdown is designed correctly. The conductivity was only measured in one other test, but was seen to be relatively concordant with the measurement performed for this study. The pH was also only tested for in one other test, and the lower pH of 6.67 would require a larger dosage of NaOH in order to adequately increase the pH. However, as a whole, there was little in the historical testing results that indicates large variability in the purity of the Poihipi Rd condensate. It is therefore considered likely that the feed water cleaning system of deaeration, pH dosing, and boiler blowdown will be sufficient to ensure that the Poihipi Rd condensate is suitable to be used as boiler feed water for a 4.5 bara boiler.

## 4.7 Poihipi Rd Condensate Availability

As the condensate from Poihipi Rd already has several uses on the plant, there are limits on the amount of condensate which may potentially be used as boiler feed water. Currently the majority of the condensate created in the shell and tube condensers at Poihipi Rd is used in the cooling tower at Poihipi Rd. However there is approximately 97 t/h that is available for other plant uses. Of this, condensate is used to dilute acid for acid dosing on SGW reinjection, used for wash water in the Te Mihi cooling towers, and sporadically used to refill the cooling towers following an outage when they have been emptied. The acid dosing requires approximately 18 t/h of the Poihipi Rd condensate, though an allowance of 25 t/h has been made to allow for water leakage without system failure, and any other minor uses. The Te Mihi wash water system uses approximately 18 t/h of the Poihipi Rd condensate, though this is highly variable, and is based off the capacity of 4% of the full steam flow to Te Mihi, as displayed in Figure 40. When refilling of the cooling towers is required to be performed, the vast majority of the Poihipi Rd condensate is used, as this allows the cooling tower to be filled relatively fast, minimizing time delays. The use of the Poihipi Rd condensate to refill the cooling towers is also important, as the clean condensate controls the bacterial growth within the towers.

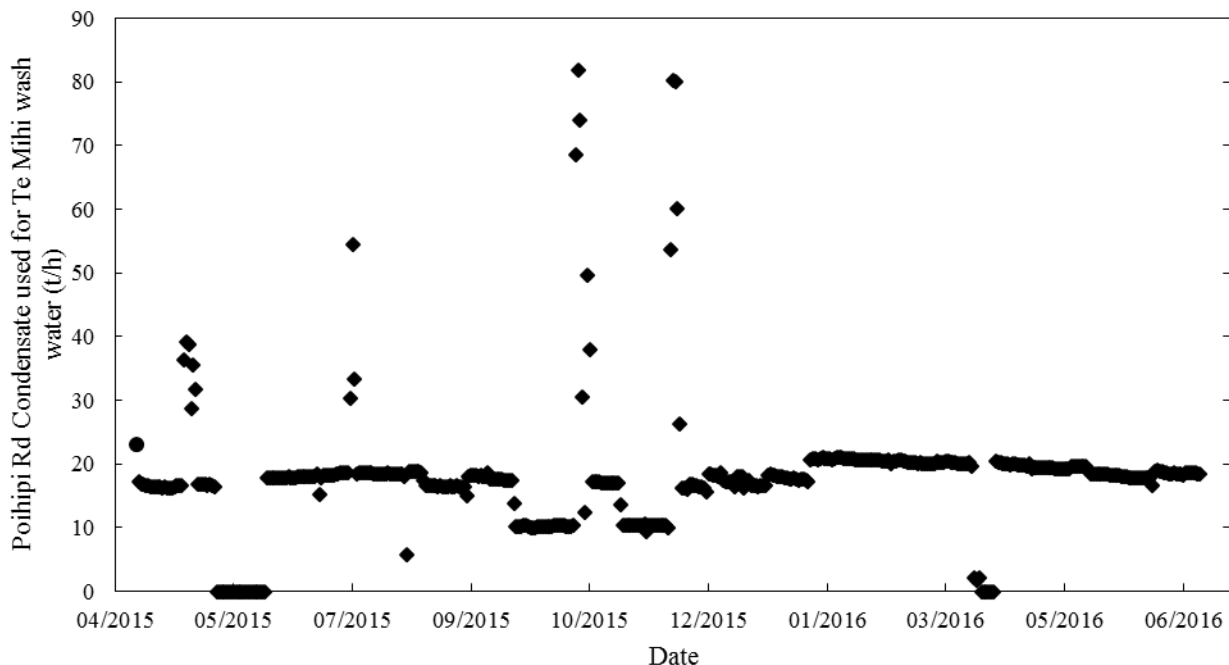


Figure 40. The daily average of Poihipi Rd condensate flow to Te Mihi

Due to this, there is an average of approximately 54 t/h of the clean Poihipi Rd condensate available to be used as boiler feed water during normal operation of the plant. However this flow will likely stop completely whenever refilling of the cooling towers is required to be performed.

## 5.0 Plant Design and Cost Estimation

In order to quantify any potential benefits from implementing the hybrid gasification/geothermal plants proposed in Section 2.0, the costs associated with the additional process equipment must be quantified. New Zealand prices were inflated using the Reserve Bank of New Zealand's inflation calculator [65], which uses data from Statistics New Zealand. United States prices were inflated with reference to the US Government's consumer price index data. When converting between 2016USD and 2016NZD a conversion factor of 1.42 was used.

### 5.1 Economic Environment

The availability and costs for landing residues, and the expected sale price of power were investigated.

#### 5.1.1 Forest Residue Availability and cost

The delivered cost of landing residues increases with increasing delivery distance, the larger the collection area for the landing residues the higher the average cost for the landing residues will be. Thus, the larger the size of the gasifier, the higher the relative costs for the landing residues become, due to the increased feed rate of woody biomass to the gasifier. The delivered costs of landing residues in New Zealand are based on those reported by Hall and Gifford in a report for Scion, as displayed in Figure 41 [66]. The delivered costs are given in 2007 NZD/GJ, and it is assumed in the report that the landing residues have an energy density of  $8 \text{ GJ/m}^3$ . As the calorific value of radiata pine is assumed to be that of softwoods reported in the New Zealand Energy Information Handbook [55] at  $19.2 \text{ GJ/t}$ , the assumed bulk density was calculated to be  $416 \text{ kg/m}^3$ .

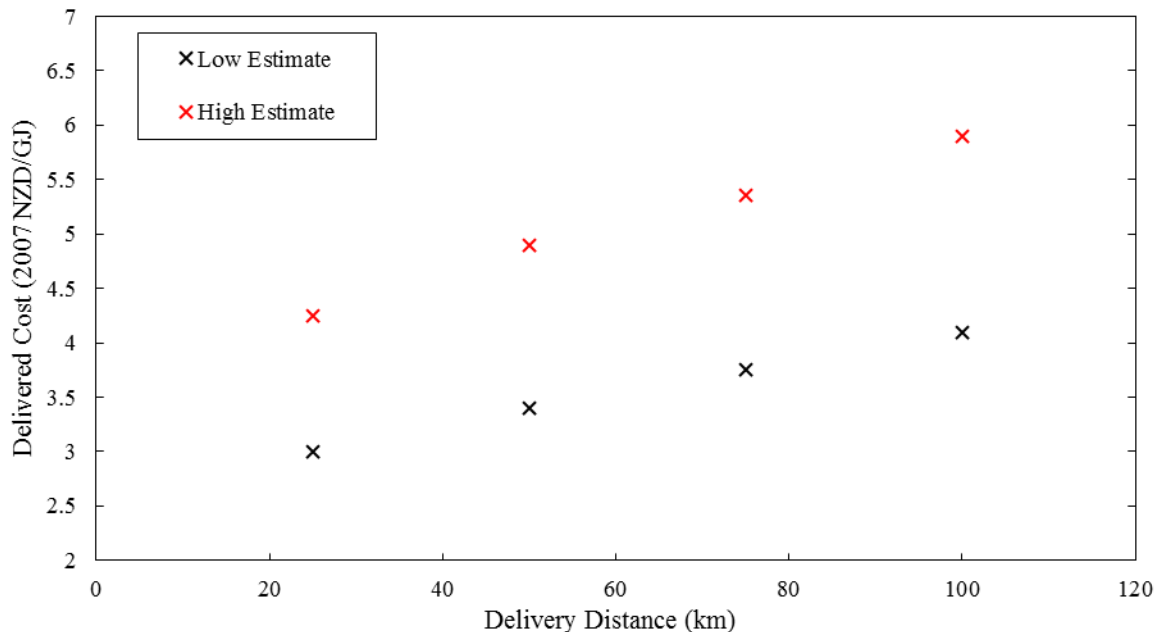
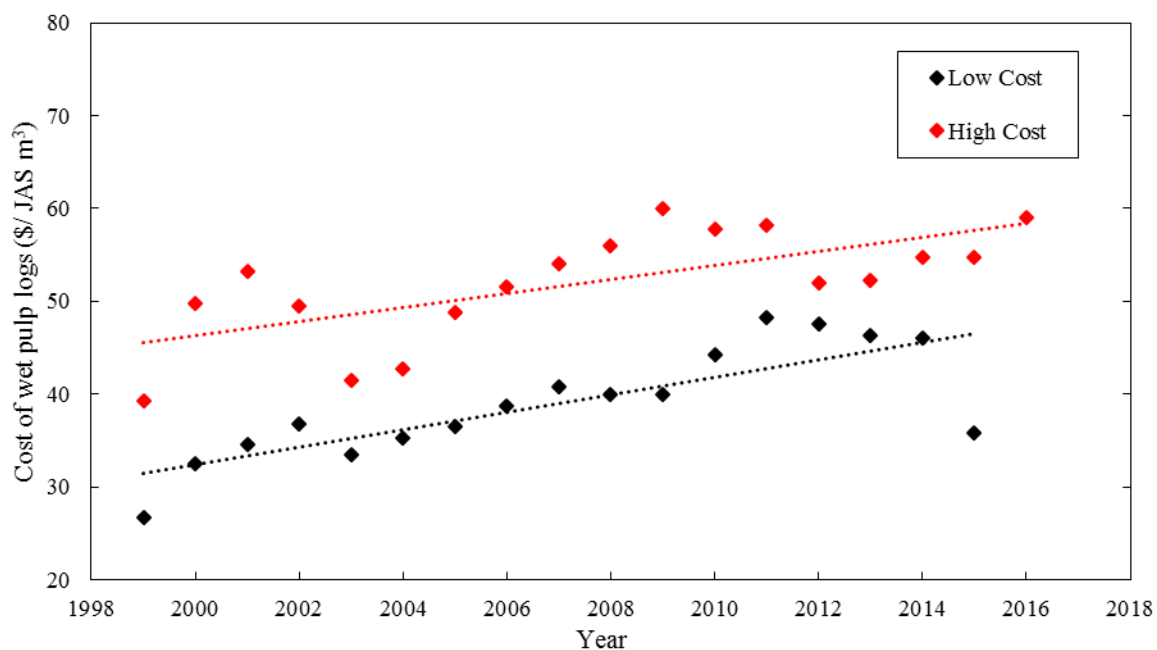


Figure 41. The delivered costs for landing residues for different delivery distances, assuming  $8 \text{ GJ/m}^3$  [66]



In order to estimate the current costs of the landing residues correction factors were created based on the costs of pulp logs. As there is no data available for the changing costs of landing residues, it was assumed that the costs of landing residues would fluctuate with the costs of pulp logs, as displayed in Figure 42. This method is imperfect, as pulp logs are not a direct substitute for landing residues. Landing residues are predominantly used as a bioenergy fuel, whereas pulp log are used to make paper. However, in the absence of information on price fluctuations for landing residues, it is believed that the price for pulp logs and landing residues will be correlated, as they are both low quality wood. The yearly average for the high and low prices of pulp logs are displayed in Figure 42, using data from the Ministry of Primary Industries [67]. From this, the low and high cost estimates for the delivered costs of landing residues purchased in 2016 would be increased by 21% and 13% respectively from the price estimates for 2007. As the inflation from 2007 is approximately 19%, the correction factors of 1.21 and 1.13 were deemed sensible.



**Figure 42. Yearly average prices for radiata pine pulp logs in New Zealand [68]**

The Central North Island is home to the largest forestry sector in New Zealand with approximately 34% of the planted forest estate [69]. As can be seen in Figure 43, there are extensive planted forests located relatively close to the Wairakei geothermal field as of 2008, and the Central North Island still has the largest amount of forestry in New Zealand [66] In order to estimate the delivered cost of the landing residues the following assumptions were made:

- The density of forest plantations is constant within the area of residue collection
- The density of the forest plantations used is that of the Taupo Central District
- The collection area is circular around Wairakei
- That forestry residue distribution (t/ha) is constant for all forestry plantations
- That the difference in forestry plantation area in 2014 and 2016 is negligible for the chosen area of forestry

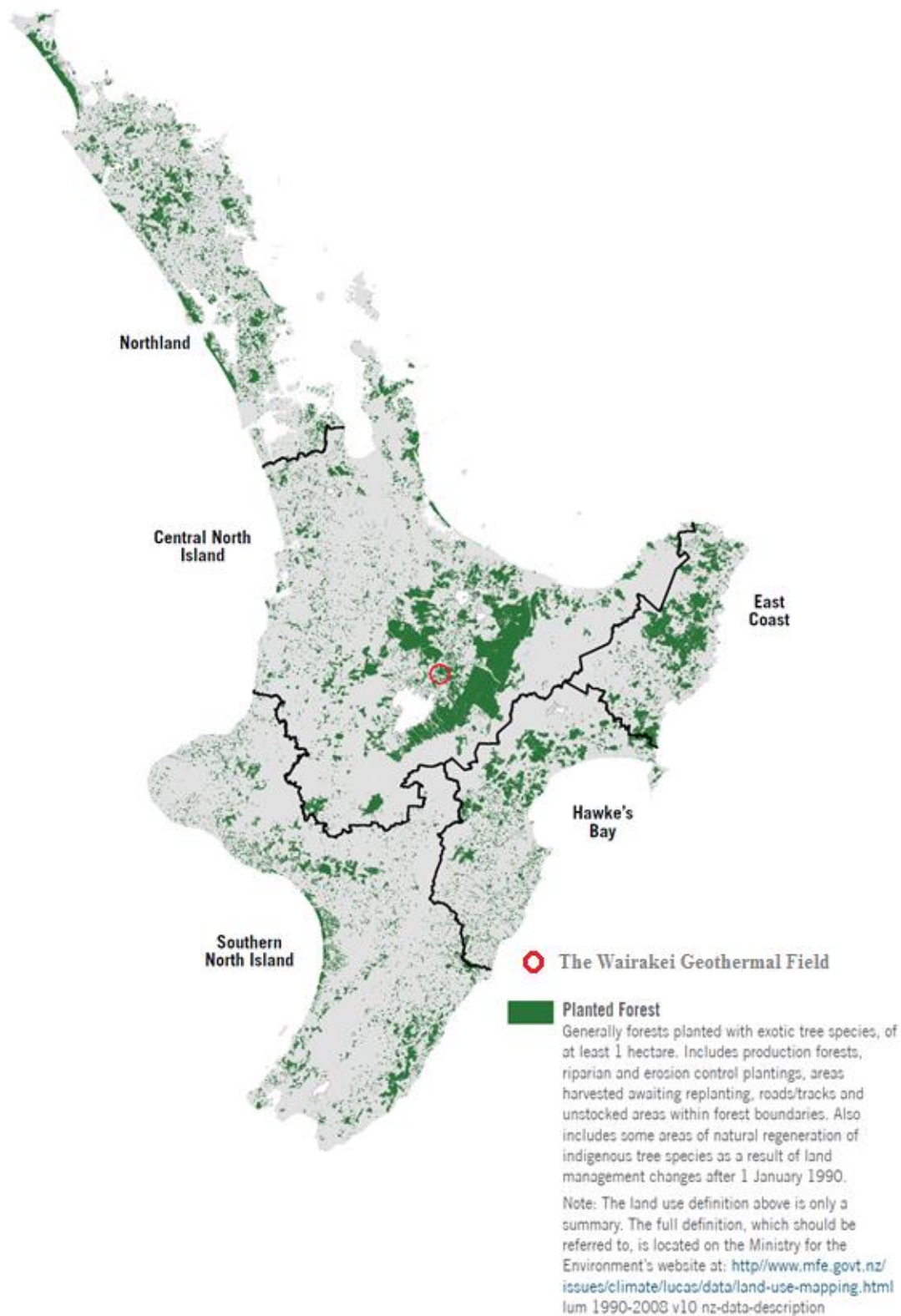


Figure 43. The distribution of planted forests in the North Island as of 2008, modified from [69].

The amount of landing residues available in New Zealand for 2016-2020 has been estimated at 1,223,671 t/year [66]. The total forestry plantation area in New Zealand has been estimated to be 1,746,573 ha in 2014 [69]. From this, it was calculated that each hectare of forest plantation produces an average of 0.7 t/year of landing residues, based on the assumption of negligible change in plantation area between 2014 and 2016.

The Taupo District has a total area of 697,000 ha which encompasses an estimated 172,554 ha of plantation forest area in 2014[69]. From this, it can be calculated that each hectare of land in the Taupo District produces an average of approximately 0.173 t/year of landing residues. The area for landing residue collection could then be estimated using Equation 42.

$$A = \frac{\dot{m}}{W_r} \quad (42)$$

Where:

$A$  = the area required for landing residue collection for use at Wairakei (km<sup>2</sup>)

$\dot{m}$  = the required mass input of landing residues (t/year)

$W_r$  = the landing residue production rate (17.3 t/year/km<sup>2</sup> for Taupo Central District)

From the required landing residue collection area calculated using Equation 42, the average distance for the landing residues to be transported could be estimated. As it is assumed that there is constant landing residue distribution within the area of residue collection, and that this collection area was circular; the average transportation distance would be given by the radius of a circle with half the area required for residue collection, as displayed in Equation 43.

$$D = f_w \sqrt{\frac{A}{2\pi}} \quad (43)$$

Where:

$D$  = the average transportation distance for landing residues (km)

$f_w$  = the wiggle factor

It is noted that the distance calculated is the Euclidean distance to the Wairakei site, and not the actual travel distance. In order to account for this a correction factor is used to convert between straight line distances and actual transport distances, called a “wiggle factor”. Commonly a wiggle factor of 1.2 is used [70], however it is believed that this will underestimate the travel distance, due to the lack of relatively straight roads surrounding Taupo. By comparing the expected travel distances with the Euclidean distances surrounding the Wairakei site, a wiggle factor of 1.35 was deemed appropriate to correct the expected travel distances. However, it is also noted that there is a high density of planted forests in close proximity to the Wairakei site, and therefore distances estimated may be larger than required due to the assumption of constant forest distribution in the Taupo District. A detailed investigation involving transport routes from forest plantations close to Wairakei that could meet the landing residue requirements would need to be performed in order to more accurately estimate landing residue transport distances.

From the average transportation distance calculated using Equation 43, the average transported cost of the landing residues could be calculated using Figure 41 and inflated based on the inflation of pulp logs. The Equations for the high and low estimates for the delivered costs have been modified for the increasing cost of landing residues based on the cost of pulp logs and are displayed in Equation 44 and Equation 45 respectively.

$$C_{LR,High} = 0.0244D + 4.24 \quad (44)$$

$$C_{LR,Low} = 0.0177D + 3.2 \quad (45)$$

Where:

$C_{LR,High}$  = high estimate for the delivered landing residues (2016 NZD/GJ)

$C_{LR,Low}$  = low estimate for the delivered landing residues (2016 NZD/GJ)

When forecasting prices for the cost of landing residues, the inflation rates calculated using the radiate pine pulp logs were again used. The high and low prices for the landing residues were determined using this forecasting, and the average of these two prices was used as the estimated price for the landing residues for the economic evaluations of the hybrid configurations.

### 5.1.2 Sale Price of Power

In order to evaluate the financial benefits from implementing any of the hybrid configurations, the price that the additional power may be sold at was estimated. Price forecasting already performed by Contact Energy staff was used in order to estimate the yearly average wholesale price of power. However, as this price forecasting only extended to 2036, the price of power for years beyond this had to be extrapolated from the price estimates provided by Contact Energy, as displayed in Figure 44. Clearly the price estimates for the years beyond 2036 have a greater uncertainty associated with them than those for 2016-2036.

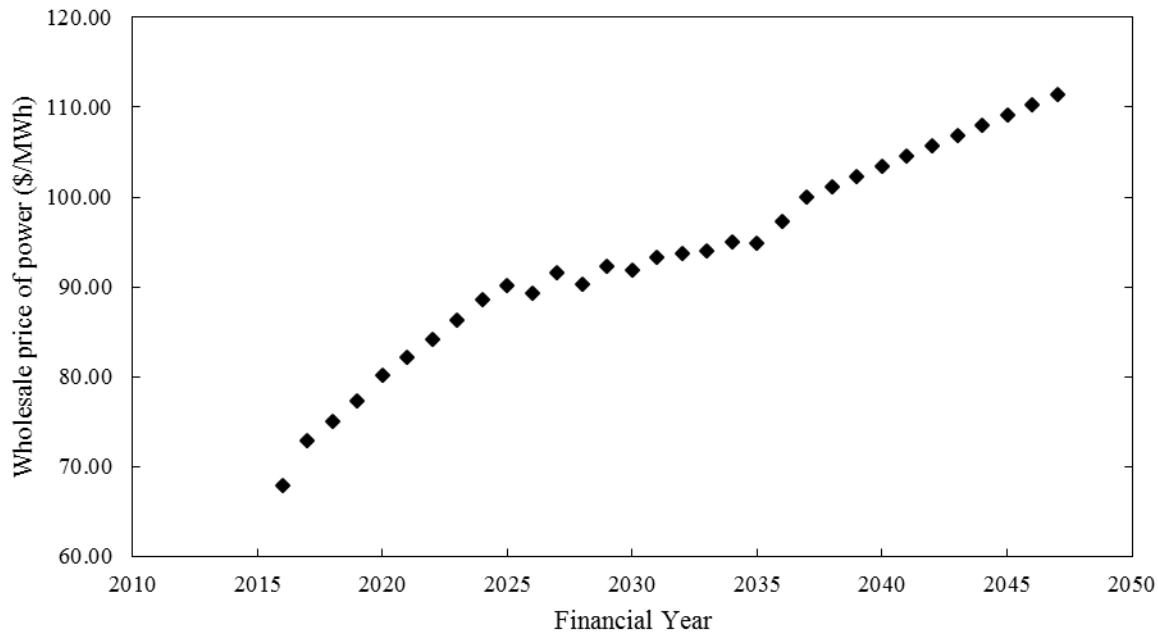


**Figure 44. The wholesale prices of power used for the economic evaluations of the hybrid configurations**

## 5.2 Additional Process Equipment and Modifications Required

As the different hybrid configurations require different process equipment and different modifications to be performed to the existing equipment at the Wairakei Geothermal Field, there will be different capital costs associated with each of the hybrid configurations. However, the gasifier and associated equipment is common to all of the configurations.

### 5.2.1 Gasification and Landing Residue Pre-treatment

The following equipment is required for every hybrid configuration:

- Wood chipper or hog

The landing residues need to be chipped into a form suitable for feeding into the gasifier.

- Wood chip dryer

Drying of the wood chips will be performed in order to reduce the moisture content of the wood to a level appropriate for the gasifier.

- Wood Chip Conveyors

Wood chip conveyors will be required in order to transport the wood chips to the dryer and the gasifier.

- Wood Chip Storage

Wood chip storage will likely be required in order to buffer the syngas production to the periodical landing residue deliveries.

- Gasifier

A gasifier is used in order to convert the chipped and dried landing residues into syngas.

### **5.2.2 Superheating Geothermal Steam**

In order to superheat the IP geothermal steam for use in modified MP turbines, it is expected that the following process equipment and modifications will be required:

- Furnace

The furnace will be used to transfer the heat from syngas combustion to the geothermal IP steam in order to increase its temperature to 350°C. The furnace will also require a fan in order to provide the air required for syngas combustion.

- Modification of MP turbines and associated equipment

As the MP turbines and associated equipment are not designed to operate using superheated steam, modifications will be required in order to utilize superheated steam in these turbines.

- Returning turbines to service

As operating the MP turbines on superheated steam instead of IP steam will reduce the mass flowrate of steam to these turbines, there will be additional unused IP steam to utilize at the Wairakei A and B Stations. This additional steam will require some turbines at Wairakei which have been removed from service to be refurbished and recertified.

### **5.2.3 Boiling Poihipi Rd Condensate**

In order to generate additional IP steam by boiling Poihipi Rd condensate, the following process equipment and plant modifications will be required:

- Water treatment

As described in Section 4.6, it is expected that dereaeration and pH dosing will need to be performed in order to ensure that the Poihipi Rd condensate will meet the water purity requirements to be used as boiler feed water.

- Condensate preheater

A heat exchanger will be required in order to preheat the Poihipi Rd condensate using SGW, in order to increase efficiency and facilitate deaeration.

- Pumping

Pumping of the geothermal condensate will need to be performed in order to achieve the pressure required for both deaeration and the boiler.

- Boiler

A boiler will be required in order to vaporize the Poihipi Rd condensate. Fans will also be required in order to supply the required air for syngas combustion.

- Returning turbines to service

In order to utilize the additional steam generated in the boiler, it is expected that turbines that have been removed from service at Wairakei will need to be refurbished and recertified.

#### **5.2.4 Boiling IP SGW**

In order to use IP SGW at its boiling point as a feed for a boiler, the following process equipment and modifications are expected to be required:

- Boiler

A boiler will be required in order to vaporize some of the IP SGW to produce additional IP steam.

- Returning turbines to service

Turbines which are currently removed from service will need to be refurbished and recertified in order to utilize the additional steam being produced in the boiler.

#### **5.2.5 Heating Additional SGW to use in the Binary Plant**

It was decided that the only process equipment required for this configuration was the furnace used to heat the T-line SGW, and the fan to provide air to the furnace. As two sources of SGW intersect, it was assumed that very little piping would be required, as the heated T-line SGW could potentially be added to the X-line SGW where the two lines intersect.

### **5.3 Equipment Design and Capital Cost Estimation**

Much of the cost estimation performed in this section was performed using the First Approximation Costing Technique or FACT method [71]. This method can be used to estimate the cost of many types of process equipment from the required equipment capacity, based on cost information from vendors.

#### **5.3.1 Landing Residue Pre-treatment and Handling**

All of the different hybrid configurations described in Section 2.0 utilize a dual fluidized bed gasifier to provide syngas. Because of this, the same method for sizing costing this gasifier and feed handling equipment common to all the configurations were used for each configuration, though the actual size of the gasifier and associated equipment will vary. The gasifier and the associated feed equipment were scaled based on the amount of wet wood feed used.

#### 5.3.1.1 Size Reduction of Landing Residues

As the biomass input to the DFB gasifier must be reduced in size to smaller than 35 mm in diameter to be used in the DFB gasifier, size reduction technologies are required [72]. Commonly three types of size reduction machinery are used to produce the wood chips required for gasification: disc chippers, drum chippers, and hammer mill hogs.

Disc chippers reduce the size of the biomass by using straight knives attached to a heavy spinning disk, as displayed in Figure 45. Disc chippers are the most commonly used chippers in the pulp industry, but the size of the wood chips generated is more variable than with other size reduction methods.

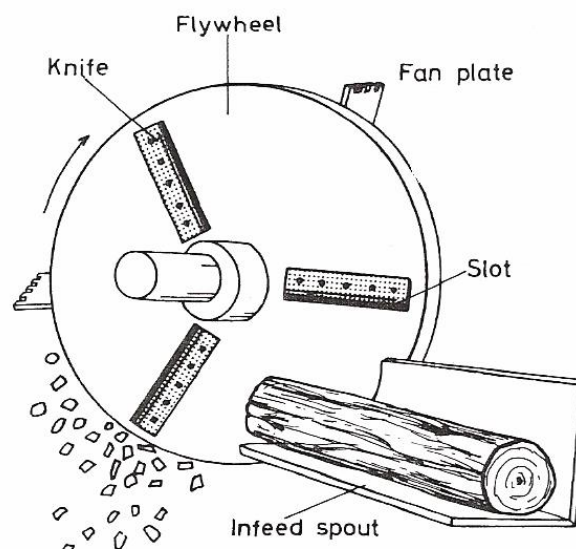


**Figure 45. Diagram of a disc chipper [73]**

Drum chippers utilize a rotating cylinder with radially mounted knives in order to chip wood, a diagram of a drum chipper is displayed in Figure 46. Drum chippers are able to process a wide range of feed materials, and the size of the wood chips produced may be controlled using a screen to stop oversized chips [74].



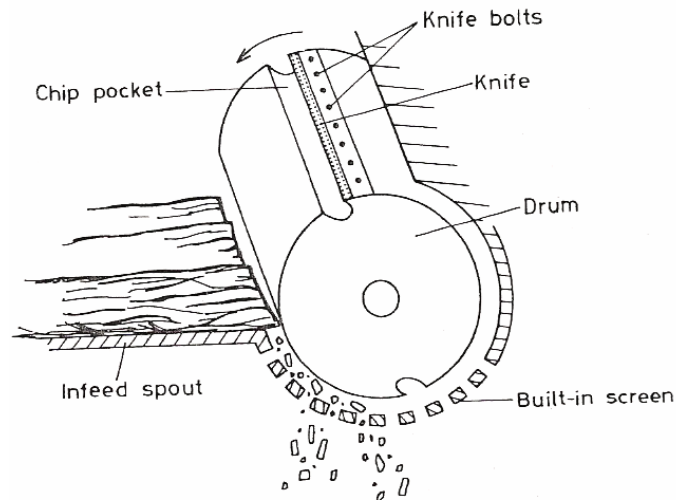


**Figure 46. A diagram of a drum chipper [73]**

Hammer mill hogs reduce the size of biomass by hammering the biomass feed with blunt tools, a diagram of which is displayed in Figure 47. Sand and stones are inevitably present with the biomass feed which can serve to blunt the knives employed in chippers, hogs avoid this problem by using blunt tools such as hammers. Like drum chippers, hammer mill hogs may control the size of the wood grind can be controlled with a built in screen [74].

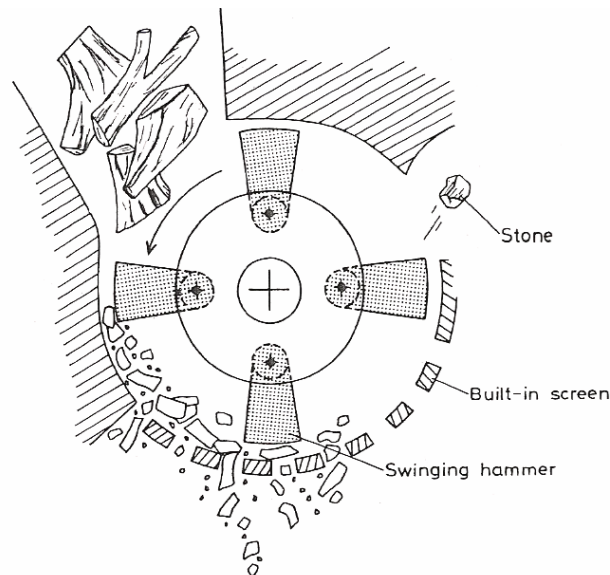


**Figure 47. A diagram of a hammer mill hog [73]**

## Costing of the chipper

The maximum diameter of the landing residues was assumed to be 0.5m, and the maximum length of the landing residues was assumed to be 3m in order to attain a cost estimate for the chipper. These size estimates were based on size distributions of logging residues in Appalachia, West Virginia [75].

After consulting with a New Zealand wood chipper manufacturer, a 75" bottom discharge 4 knife disc chipper was recommended, based on the estimated size of the landing residues [76]. This chipper can process logs with a maximum diameter of 560mm, and produces chips at 19 mm. The life of the chipper was given at approximately 84000 hours, with a maximum flowrate of 50 t/h of wet wood. The budget price for one chipper delivered to the Wairakei site was quoted as \$278,070 GSTinc, which includes:

- Two 150 kW electric motors
- Motor drive base
- Two sets of vee belts
- Vee belt pulleys, one driven from each motor, and one for the chipper shaft
- One knife system
- One babbitting jig

As a large chipper is required in order to handle the diameter of the landing residues, the cost of the chipper is discretized based on the maximum capacity of the chipper. Therefore the costing for the chipper was performed by calculating the amount of identical chippers required based on the mass flowrate of landing residues, and the maximum capacity of the chipper.

As the chippers have an estimated useful life of 84000 hours, it may be required to purchase additional chippers throughout the life of the hybrid plants. The price of additional chippers were calculated to inflate at 3% annually in order to estimate the cost of the additional chippers throughout the life of the hybrid plants.

### 5.3.1.2 Drying

The typical moisture content of woody biomass is between 50% - 60% wet basis (WB) [77], and as biomass gasification requires a moisture content of between 10% - 20% WB [78], drying is required to be performed on the biomass prior to gasification. A moisture content of 15% (WB) was chosen for the biomass feed for the gasifier. As described in Puladian's thesis [43], after comparing three common types of industrial dryers: rotary, pneumatic, and packed moving bed; a co-current rotary cascade dryer was selected, diagrams of which is displayed in Figure 48 and Figure 49. Rotary cascade drum dryers utilize longitudinal flights installed on the inner surface of the dryer to ensure even drying of the wood chips. The rotary drum dryer was selected to perform the biomass drying due to the large capacity of rotary dryers, the fact that rotary dries are relatively insensitive to biomass size, and hot flue gas available from the combustion of char and syngas that can be used as the drying medium. It was decided by Puladian, that the rotary dryer should employ a co-current flow of biomass and flue gas drying medium, as a counter current arrangement may heat the biomass to the auto-ignition temperature of wood (260 - 280°C).

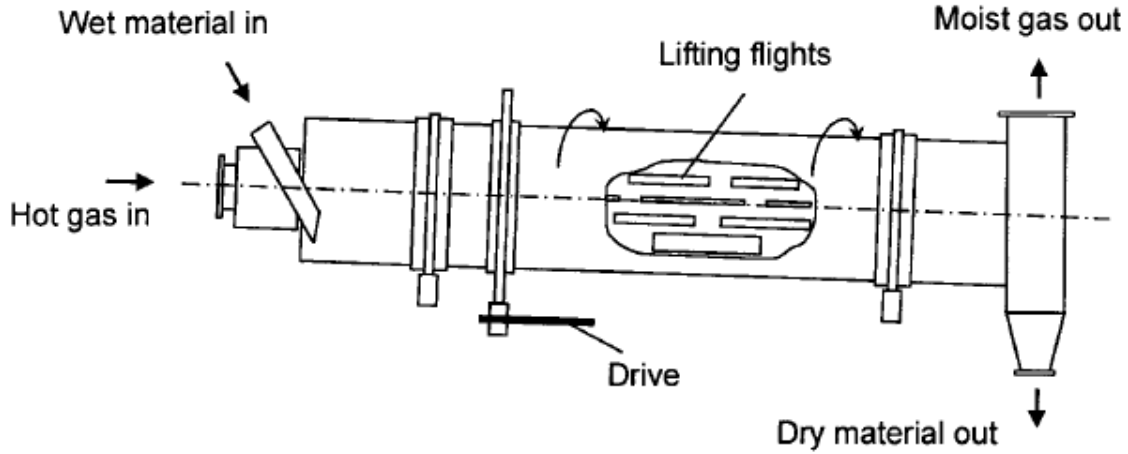


Figure 48. Diagram of a cascade co-current rotary drum dryer [79]



Figure 49. A cross section of a cascade rotary drum dryer [79]

In order to size the rotary drum dryer, the temperature of the wet biomass, and the ambient air were both assumed to be 10°C.

### Costing the rotary drum dryer

The method for estimating the capital cost of a rotary drum dryer was based on that used by Penniall in his Master's Thesis investigating the potential for a gasification plant in the wood process industry [80]. This method was developed due to the extremely high capital costs that were estimated using other methods for rotary drum dryers when the moisture content of the inlet wood is high [81]. Penniall's cost estimate was developed using estimates from New Zealand manufacturers, and has been modified to account for inflation as displayed in Equation 46.

$$C_{Dryer} = 4.2 \times 10^5 m_{moisture} + 4.2 \times 10^5 \quad (46)$$

Where:

$C_{Dryer}$  = the installed capital cost of the dryer (2016 NZD)

$\dot{m}_{moisture}$  = the mass flowrate of moisture removed from the wood (t/h)

### 5.3.1.3 Biomass Storage and Handling Equipment

The feed handling required for a biomass gasification plant is often ignored in the design of woody biomass gasification plants, with the exception of the chipping and drying of the biomass. The biomass storage and metering for this design is loosely based on that designed by Worley and Yale in a gasifier technology assessment commissioned by the National Renewable Energy Laboratory (NREL) [82].

The designed biomass storage and metering system consists of a belt conveyor, a storage bunker, two transfer screw conveyors, and a storage hopper. It is believed that the landing residues should be chipped immediately upon delivery, as wood chips may be more easily stored and moved within the plant than the landing residues. The belt conveyor will feed the landing residues into the biomass chipper. The chipped biomass will then be deposited in a storage bunker, as storage of the biomass will be simpler when it is wet, as dry wood chips are susceptible to moisture contamination. The first transfer screw conveyor be used to transport the wet wood chips to the rotary dryer. The wood chip dryer will discharge into the second hopper, and the electro vibrating feeder will be used to meter the dried wood chips to the gasifier. The second transfer screw conveyor will be used to transport the dried biomass into the gasifier. The biomass storage and preparation system is displayed in Figure 50.

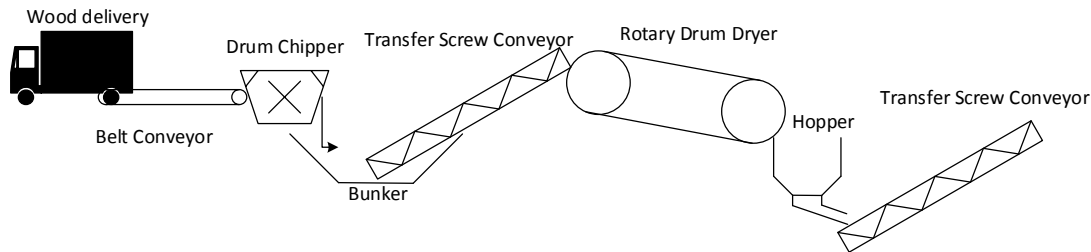


**Figure 50. The biomass feed preparation and storage equipment**

### Costing of hoppers and feeders

The storage bunker for the wet wood chips was designed to store sufficient wood chips for two days of continuous gasifier operation, in order to avoid losses that would be incurred due to irregular wood supply. The dry wood chip storage for the gasifier feed in the hopper was sized to have volume enough for ½ an hour of wood chip feed to the gasifier. The bulk density of the wet wood chips was assumed to be 300 kg/m<sup>3</sup> [83].

The cost of bunker storage has been investigated for grain storage on cattle farms [84], and was altered for wood chip storage. The cost for grain bunkers was given as \$59.72 2006USD/short ton

of grain, the density of wheat grain was taken as  $770 \text{ kg/m}^3$  [85]. This yielded a value of \$168.96 2006USD/t wood chips which converts to 260.83 2016NZD/ton wet wood chips.

The cost of the storage hopper was estimated by assuming the cost would be similar to that for atmospheric storage vessels. The FACT method was then employed in order to estimate this cost [71]. The cost for atmospheric storage vessels may be estimated as 1.25 2010USD/gallon. Using a correction value of 1.102 for inflation, and the currency conversion factor, the cost of the storage hopper may be estimated as 515.8 2016NZD/m<sup>3</sup>.

### Costing of conveyors

The drum chipper has an entry width of 1400 mm based on the design specifications given by a supplier, the belt conveyor will be designed to have a similar width. By using the First Approximation Costing Technique (FACT) Method, costs for belt conveyors may be estimated, as displayed in Figure 51. A conveying distance of 10 m was assumed to be sufficient to feed into the chipper.

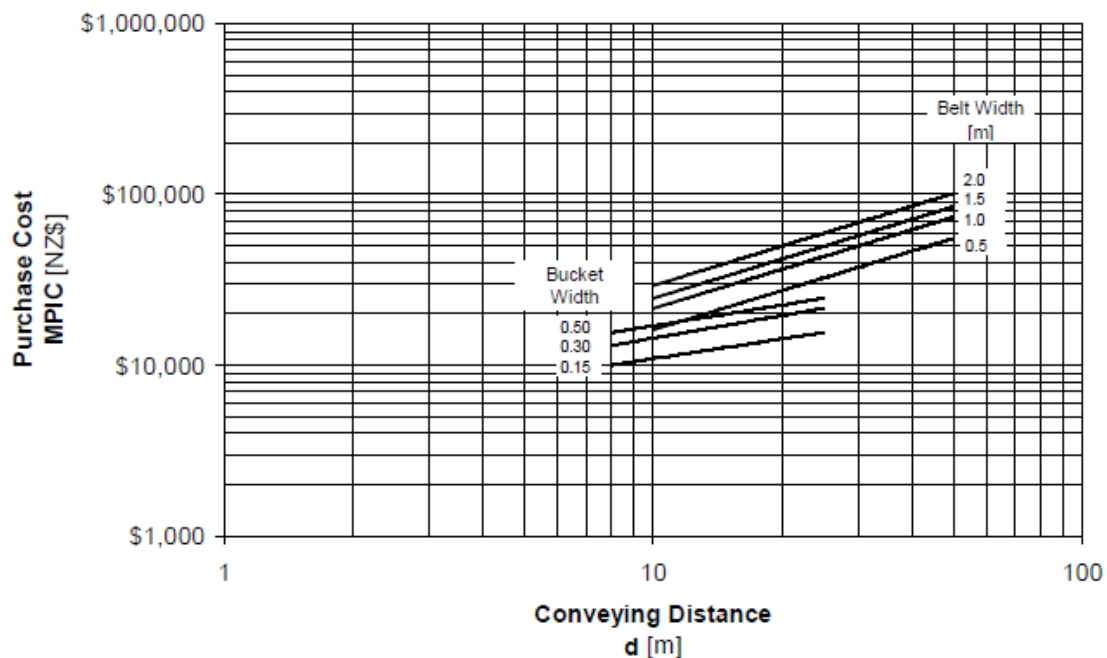


**Figure 51. The estimated cost (December 2004 NZD) for belt and bucket conveyors based on the FACT Method**

The diameter for the transfer screw conveyor was based on manufacturers data found for the expected wood chip transfer capacity for different screw diameters, as displayed Table 15 [86]. A conveyor length of 15 m was estimated for both of the transfer screw conveyors.

**Table 15. Manufacturer's data for wood chip transfer screw conveyers [86]**

Model		WLS150	WLS200	WLS250	WLS300	WLS400	WLS500
<b>Screw Diameter</b>	<i>mm</i>	150	184	237	284	365	470
<b>Casting pipe diameter</b>	<i>mm</i>	180	219	273	351	402	500
<b>Operating angle</b>	<i>°</i>	<30	<30	<30	<30	<30	<30
<b>Maximum delivery length</b>	<i>m</i>	12	13	16	18	22	25
<b>Capacity</b>	<i>t/h</i>	3	7	9	13	18	28
<b>Motor (Length &gt; 7m)</b>	<i>kW</i>	1.5	2.2	3	5.5	11	11
<b>Motor (Length &lt; 7m)</b>	<i>kW</i>	2.2	3	4	7.5	15	15

The FACT method could be used to estimate the cost of the wood chip screw conveyor, also known as a transfer auger, in a similar method to that for the belt conveyor. The estimated costs for auger conveyers are displayed in Figure 52.

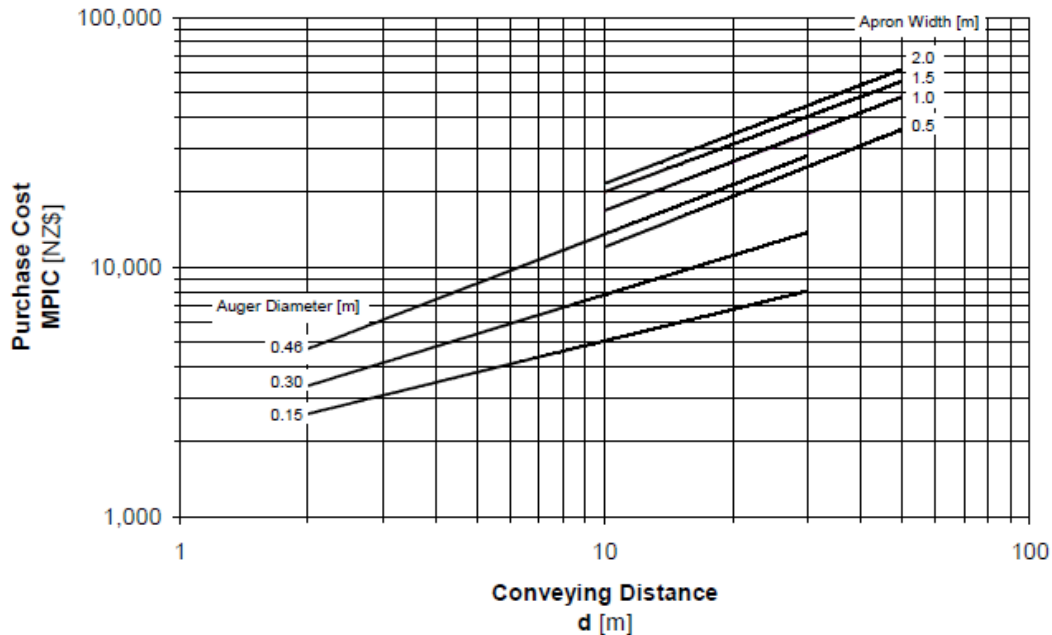


**Figure 52. The estimated cost (December 2004 NZD) for auger and apron conveyors based on the FACT Method**

As the costs for the belt conveyor and the wood chip transfer augers do not include the cost for the motors required, this was calculated separately. Costs for motors can be calculated based on the power requirement of the motor using the FACT Method. Power requirements for the wood chip auger can be estimated from Table 15, provided the required wood chip flowrate, and the length of the auger are known. By researching the expected power requirements for a variety of belt conveyor sizes, it was assumed that the belt conveyor feeding the chipper with a width of 1400 mm would likely have a power requirement of approximately 11 kW [87]. Once the power requirement of the conveyor motors are estimated, the cost for these motors can be calculated using the FACT method shown in Figure 53.

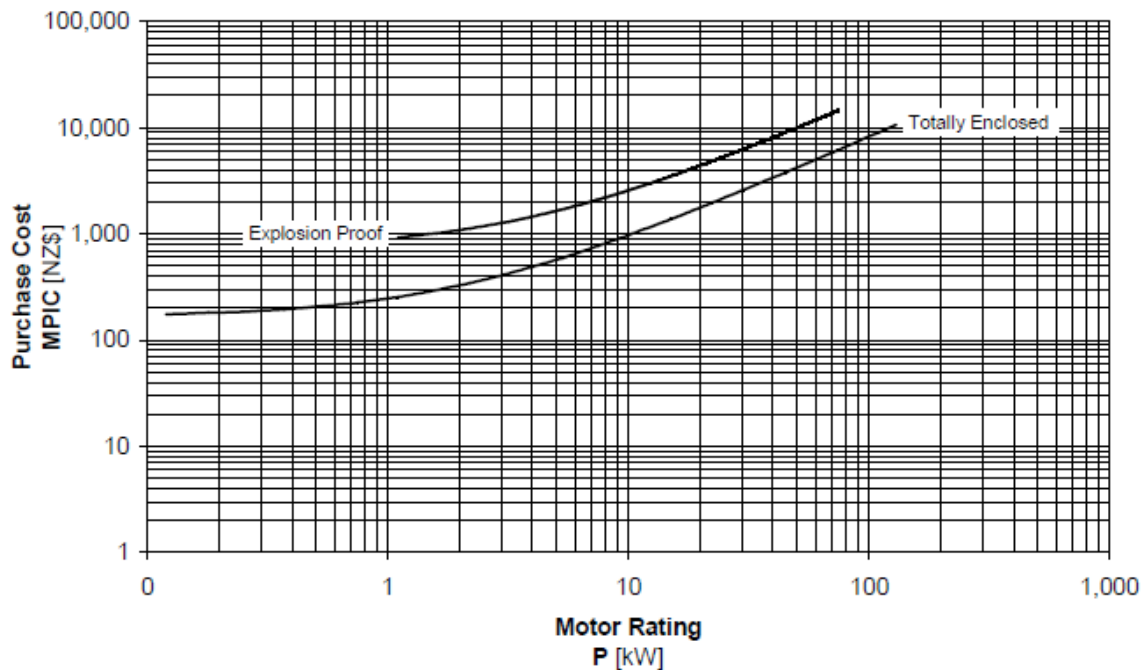


Figure 53. The estimated cost (December 2004 NZD) for electric motors based on the FACT Method

### 5.3.2 Gasification

A dual fluidized bed gasifier was chosen to perform the gasification step as the Chemical and Process Engineering Department at the University of Canterbury has extensive knowledge of this type of gasifier. The gasifier consists of two fluidized beds, two cyclones, two burners, a chute and a siphon to circulate the bed material.

#### Costing of the dual fluidized bed gasifier

A method used at the University of Canterbury to estimate the capital costs associated with a dual fluidized bed gasifier was initially developed by Rutherford for his Masters' Thesis investigating the heat and power applications of biomass gasifiers in New Zealand's wood industry [88]. Due to a lack of information for the cost histories for gasifiers, Rutherford developed a "ground up" approach to estimate the cost based on the individual components of the gasifier and installation factors. As the scaling factors that may be applied to gasification reactors are seen to vary widely, leading to uncertainty in any capital costs generated, this "ground up" method will be used here. As described by Rutherford in his Master's Thesis, the gasifier is broken down into its component pieces, and the superficial velocity of the gas in each of these components used as in the lab scale DFB reactor at the University of Canterbury displayed in Table 16. The components that make up the gasifier are: the bubbling fluidized bed (BFB) reactor, the entrained flow fluidized bed (CFB) reactor, a chute, a siphon, two cyclones, two gas burners, and a blower. The BFB reactor, CFB reactor, chute, and the siphon are all to be lined with 100mm of hot refractory and a further 150mm of cold refractory lining. It was assumed that the geometries of all the vessels involved was to be

cylindrical, and ratios for the dimensions of the vessels are also taken from Rutherford [88]. The BFB reactor was designed to have a height 2.4 times its diameter, and the CFB reactor was designed to be 2m longer than the BFB reactor to allow space for the chute, siphon, and cyclone.

**Table 16. The assumed superficial gas velocities for the University of Canterbury's dual fluidized bed gasifier**

Vessel	Gas Velocity
Entrained flow Fluidized Bed	7 m/s
Bubbling Fluidized Bed	1.5 m/s
Chute	0.15 m/s
Siphon	0.15 m/s

The cost of the blower for the gasifier was found using Equation 47.

$$C_{blower} = 771Q_{air} + 2400 \quad (47)$$

Where:

$C_{blower}$  = the cost for the blowers installed in the gasifier (2006 NZD)

$Q_{air}$  = the volumetric flowrate of air through the CFB (m<sup>3</sup>/s)

The cost of the steel casings for the vessels of the gasifier was found using Equation 48

$$C_{casing} = (3952D_v + 965)H_v^{(0.9749-0.0518D_r)} \quad (48)$$

Where:

$C_{casing}$  = the cost for the steel casing on the vessels of the gasifier (2006 NZD)

$D_v$  = the diameter of the vessel (m)

$H_v$  = the height of the vessel (m)

The cost for the cyclones used in the gasifier was found using Equation 49

$$C_{cyclone} = 2330Q_{cyclone}^{0.912} \quad (49)$$

Where:

$C_{cyclone}$  = the cost for the cyclone in the gasifier (2006 NZD)

$Q_{cyclone}$  = the flowrate of gas through the cyclone (m<sup>3</sup>/s)



The cost for the refractory lining on the vessels in the gasifier is found using Equation 50.

$$C_{refractory} = \frac{45}{28}m_{hf} + \frac{28}{15}m_{cf} \quad (50)$$

Where:

$C_{refractory}$  = the capital cost for the refractory lining on the gasifier (2006 NZD)

$m_{hf}$  = the mass of hot refractory lining required (kg)

$m_{cf}$  = the mass of cold refractory lining required (kg)

The density of the hot and cold face refractory linings were taken to be 960 kg/m<sup>3</sup> and 480 kg/m<sup>3</sup> respectively [89].

The cost for the burners required in the gasifier was based on the cost estimate used by Penniall for his Master's Thesis [80] where burners were costed at 12,000 2006 NZD each.

In order to account for the inflation from 2006 an inflation factor of 1.22 were used to convert the estimates to 2016 NZD.

### 5.3.3 Returning Steam Turbines to Service

In order to utilize steam that is generated in a boiler, or the steam that is saved by the lower mass flowrate required for superheated steam in a modified geothermal turbine, steam turbines at the Wairakei Power Plant will likely need to be brought back into service. Currently there are two turbines that have been removed from service at Wairakei, G1 and G8. G1 is an IP steam turbine, which uses 241 t/h of IP steam to produce 11.2 MWe at full load. G8 is an LP steam turbine, which uses 140 t/h of LP steam to produce 11.2 MWe at full load. As there is not sufficient LP steam to completely load the LP steam turbines currently in service, the LP turbine, G7, is almost continuously unloaded. Due to this, it is assumed that LP steam may be used in G7 without requiring additional LP turbines to be returned to service. Estimates for the cost of recertifying some of the turbines at Wairakei have been performed by Contact Energy employees, and are displayed in Table 17.

**Table 17. The estimated costs of recertifying turbines at the Wairakei Power Plant**

Turbine	Type of Turbine	Estimated cost (2016 NZD)	Current Status
G1	IP	\$760,000	Removed from service 2014
G4	IP	\$659,000	In service
G7	LP	\$520,000	In service
G10	LP	\$599,000	In service
G11	MP	\$1,245,000	In service
G13	MP	\$1,120,000	In service

In order to bring G8, back into service the two oil separators that are used on the LP turbines would need to be replaced, as these have been removed. A rough estimate of \$100,000 has been provided by staff at Wairakei to replace each of these separators. The base cost of refurbishing and recertifying G8 was based on the cost of recertifying G7, at \$520,000 as they are both the same type of turbine. Therefore, the estimate for the total cost of bringing G8 back into service is estimated as \$720,000.

Currently, the turbines in the Wairakei A Station, need recertification every 5 years, due to this, any additional turbines brought back into service will incur the cost of this recertification. The base cost of recertifying G1 and G8 were assumed at \$760,000 and \$520,000 respectively. These costs were then inflated using an assumed annual inflation of 3%, for the 5 yearly recertification.

### **5.3.4 Furnaces and Fans**

Furnaces are designed to be used to superheat the geothermal steam, and to heat the SGW in T-line for use in the Wairakei Binary Plant. The design of the furnaces was based on that given in a report on Process Equipment Cost Estimation by Loh, Lyons, and White for the National Energy Technology Laboratory [90]. Price estimation is performed on furnaces of differing duties, where it is assumed that the design temperature is approximately 400°C and a design pressure is approximately 35 bara. As the pressure of the geothermal steam and SGW is lower than 35 bara, at 4.5 bara and 9 bara respectively, the high design pressure may lead to an oversized furnace with an inflated estimate for the capital cost. The tube material is designed to be constructed using A214 carbon steel that is electro-resistance welded.

The furnace will also require fans in order to supply the necessary air to combust the syngas. The fans were assumed to be centrifugal, and a pressure ratio of 0.95 was designed for the ambient air and the air supply to the furnace, with a resulted in an assumed pressure increase of 5.3 kPa.

#### **Costing the furnace**

The cost estimation of the furnace was performed with reference to the report by Loh, Lyons, and White, where the cost may be estimated from the heating duty required to be performed by the furnace. The cost of the furnace in 1<sup>st</sup> Quarter 1998 USD can be found using Figure 54.

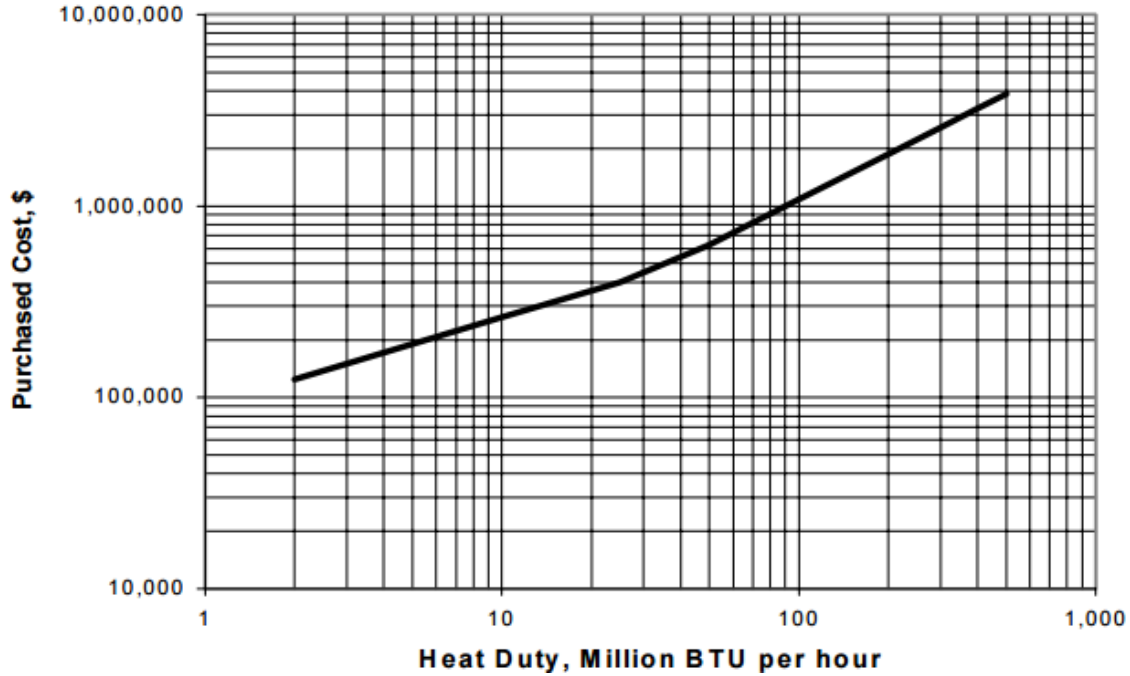


**Figure 54.** The estimated cost (1st Quarter 1998 USD) for furnaces based on the heat duty of the furnace [90]

The estimated purchase cost for the furnace found in Figure 54 was then inflated and converted into 2016 NZD.

### Costing of the Furnace Fans

The cost estimation was performed under the assumption that centrifugal fans would be used in supply the required air flow to the furnace. The method of costing the furnace fans was performed using the FACT method, where the pressure increase and volumetric flowrate of air are used to estimate the capital cost of the fans [71]. The cost of the fans could then be estimated using Equation 51.

$$C_{fan} = F_P(979\dot{V}_{air} + 3048) \quad (51)$$

Where:

$F_P$  = the centrifugal fan cost correction factor

$C_{fan}$  = the cost of the fan (2016NZD)

$\dot{V}_{air}$  = the volumetric flowrate of the air ( $m^3/s$ )

The cost correction factors for the pressure increase delivered by the fans is displayed in Table 18.

**Table 18. The cost correction factors for centrifugal fans [71].**

<b>Pressure increase (kPa)</b>	<b>Centrifugal fan cost correction factor (<math>F_p</math>)</b>
1	1
2	1.15
4	1.3
8	1.45
16	1.6

By interpolating the values for the correction factors, it was found that a correction factor of 1.36 should be applied for a pressure increase of 5.3kPa.

### **5.3.5 Modifying Existing MP Steam Turbines to use Superheated Steam**

In order for superheated steam to be utilized in the MP steam turbines currently at Wairakei, significant modifications would need to be performed to the turbines to allow for the increased temperature and velocity of the steam. The modifications that are expected to be required are as follows:

- **Changing the turbine blades**

The velocity of the steam passing through the MP turbine will be increased, due to the fact that there is a reduction of the amount of steam condensation occurring in the turbine. Due to this, the blade incidence angles will no longer be optimized for the higher steam velocity. Therefore it is expected that new turbine blades will have to be purchased for the modified turbines.

- **New diaphragms and nozzles**

Similar to the requirement for new turbine blades, new diaphragms and nozzles are expected to be required for the steam turbines, in order to optimize the design of the nozzles.

- **Steam turbine casings**

The design of the maximum temperature of the superheated steam was made with reference to the suggestions made by Morris in his investigation into superheating geothermal steam for use in existing steam turbines [38]. However, this temperature was chosen based on the creep range of low alloy steel, and many the casings of the steam turbines are grade 10 grey cast iron, these casing will prove to be incompatible with the higher temperature steam. At temperatures approaching 350°C, grey iron is expected to be an unsuitable material for the steam turbine casings [91]. Due to this, new casing will need to be created, requiring moulds to be created to cast the casings.

- **Valves**

The valves used at Wairakei have valves and seals constructed from PTFE. The operating limit of this material is approximately 200°C, with an absolute limit of 250°C [38]. Due to this new valves and hydraulics would be required in order to utilize superheated steam at 350°C.

- **Insulation and oil cooling**

Due to the higher temperatures of the steam entering the MP turbine, added insulation will be required to avoid exposure dangerously high temperature equipment and pipelines. It is believed that the fiberglass and calcium silicate currently used as insulation at Wairakei will remain suitable for use as insulation at the elevated temperatures, though the thickness of the insulation will have to be increased. The cooling oil flow across the hot end of the turbine is also expected to increase in order to dissipate the higher heat flow.

- **Installation**

It was assumed that once the parts required to perform the modifications to the MP turbines had been fabricated and delivered, there would be a three week installation period. There would therefore be an associated loss of revenue from removing the MP turbines from service to perform these modifications.

## **Costing MP turbine modifications**

As there is very little information on the costs associated with modifying geothermal steam turbines to operate using superheated steam, the costs for these modifications are rough estimates with a large associated uncertainty.

### Turbine blades

It was assumed that the new turbine blades could be costed based on the cost of the current set of turbine blades, as the materials and method of construction would likely be the same. The current MP turbines have 15 rows of blades, 8 in the IP section of the turbine and 7 in the LP section. The first 10 rows have 250 blades each, and the remaining rows have 140 blades each. The blades on the IP rows are estimated at \$1000 each, and the blades on the LP rows are estimated at \$5000 each. The cost of the new blades are therefore estimated at 8,000,000 2016NZD for each turbine.

### Diaphragms and nozzles

The cost of the diaphragms nozzles are estimated at \$1,000,000 for a set, which includes the cost of the nozzles. The diaphragms will likely be fabricated from welded steel components, which would prove to be costly.

### Steam turbine casings

The steam turbine casings are estimated at \$4,000,000 each, these are expected to be very expensive, due to the necessity to create moulds in order to cast the casings.

### Valves, insulation, and oil cooling

It was assumed that the costs associated with the valves, insulation and oil cooling would be included in the costs associated with the minor material of the furnace.

### Installation

It was assumed that staff at Wairakei would be able to perform the modifications to the turbine(s), and therefore there would be no labour cost associated with the installation. However, as it was assumed that there would be a three week installation period for the turbines, there is a maximum loss of 15120 MWh for each turbine removed from service.

### 5.3.6 Boiling Poihipi Rd Condensate

In order to generate additional IP steam using the Poihipi Rd condensate as a boiler feed water, it is expected that two pumps, a preheater, a boiler, a deaerator, and chemical injection apparatus will be required. There are also limits on the amount of the Poihipi Rd condensate that may be used, which must be taken into account when designing the size of the process equipment.

#### 5.3.6.1 Condensate Pumps

As the condensate from the Poihipi Rd Power Plant is available at approximately 7.8 kPa, pumping will need to be performed in order for this condensate to be used as boiler feed water. In order to facilitate deaeration, the condensate must first be increased in pressure to 1.15 bara for oxygen desorption. The condensate will then be increased in pressure to 4.5 bara for the boiler feed water. Two stages of pumping are therefore required to be performed on the Poihipi Rd condensate in order for it to be used as boiler feed water

#### **Costing the condensate pumps**

The costs for the condensate pumps were estimated using the FACT method [71], using the cost estimates displayed in Table 19. The costs for the pumps displayed in Table 19 are for heavy duty hydrocarbon pumps, as carbon steel pumps will likely be used, price of the pump will be approximately 70% of that for the hydrocarbon pumps.

**Table 19. The cost of pumps and motors for single stage pumps [71].**

<b>Pump power</b> <i>HP</i>	<b>Cost</b> <i>2006USD</i>
0 - 10	10000
10 - 50	10000+150/HP
50 - 500	15000 + 175/HP
500 - 1000	25000 + 200/HP
> 1000	40000 + 225/HP

The power requirement of the pumps was taken from the UniSim model for the boiling of the Poihipi Rd condensate, which assumes a 75% adiabatic efficiency for the condensate pumps.

#### 5.3.6.2 Condensate Preheating

In order to maximize the amount of steam that may be generated in the boiler, preheating on the steam turbine condensate is designed to be performed using heat from high temperature SGW. The Karapiti SGW reinjection system was used as the basis for SGW resources available for preheating the condensate, due to the proximity of this reinjection system to the source of condensate at

Poihipi Rd. This SGW is available at approximately 105°C, and as there is an average flow of approximately 3000 t/h, this will be sufficient to adequately preheat the condensate as there is only 54 t/h of condensate available for use from Poihipi Rd. As the preheater will be similar in essence to the preheaters and vaporizers used in the Wairakei Binary Plant which uses SGW to heat pentane for an organic Rankine cycle, the design of the condensate preheater is based on the binary plant heat exchangers. A shell and tube heat exchanger with carbon steel tubes will be used to preheat the condensate. A shell and tube heat exchanger will be used to increase the temperature of the condensate from approximately 40°C to 100°C. The flowrate of SGW to the preheater was designed to ensure the exit temperature of SGW from the preheater was greater than 90°C, based on the design of the Wairakei Binary Plant heat exchangers.

### Costing the tubular preheater

The FACT method was used in order to estimate the cost for the preheater heat exchanger [71]. The operating pressure of the heat exchanger, the heat duty of the heat exchanger, and the type of heat exchange occurring were used to estimate the heat exchange area.

The heat flux typical of different types of heat exchange is displayed in Table 20.

**Table 20. Heat flux typical for different types of heat exchange in tubular heat exchangers [71]**

Type of heat exchange	Flux (Btu/h/ft <sup>2</sup> )
Gas to Gas	3000
Liquid to Liquid	8000
Phase Change	10000
Steam Condensing	12000

By then using the heat duty of the preheater, which is calculated by the UniSim model, the heat exchange area could be calculated.

The cost of the heat exchanger in 2006 USD could then be estimated using the different prices displayed in Table 21. The Karapiti reinjection pumps, which would likely provide the SGW used to preheat the Poihipi Rd Condensate, had an average outlet pressure of approximately 19.7 bara (285 psi) and a maximum outlet pressure of 27.2 bara (394 psi) the operating pressure of 300-600 psi was used for the preheater.

**Table 21. The prices for heat exchangers based on their design pressures [71].**

Design pressure <i>Psi</i>	Cost of heat exchanger <i>2006 USD</i>
0-300	10000+35/ft <sup>2</sup>
300-600	10000+40/ft <sup>2</sup>
>600	10000+45/ft <sup>2</sup>

#### 5.3.6.3 Boiler and Feed Water Cleaning

As described in Section 4.6, the cleaning of the Poihipi Rd condensate will likely consist of deaeration, and pH dosing of the condensate in order to ensure it is suitable for use as boiler feed water.

### Costing of the Boiler and Feed water Cleaning Equipment

The cost of the boiler was estimated using the FACT technique for a package boiler, which includes: forced draft fans, instruments, controls, burners, soot-blowers, feed water deaerator, chemical injections system, steam drum, mud drum and stack, and is shop assembled. This costing was performed using the FACT method for packaged boilers at 17.2 barg and 38°C superheat to include the associated equipment. It is therefore expected that the actual cost of the boiler will be lower than that estimated using this method, as the actual pressure is approximately 4.5 bara, and there is no superheating performed. The boiler is designed to be constructed from A285C carbon steel.

The method for estimating the capital costs of package boilers was taken from a report performed for the National Energy Technology Laboratory (NETL) by Loh, Lyons and White [90]. The cost of the boiler in 1<sup>st</sup> Quarter 1998 USD can be found using the boiler capacity in Figure 55.

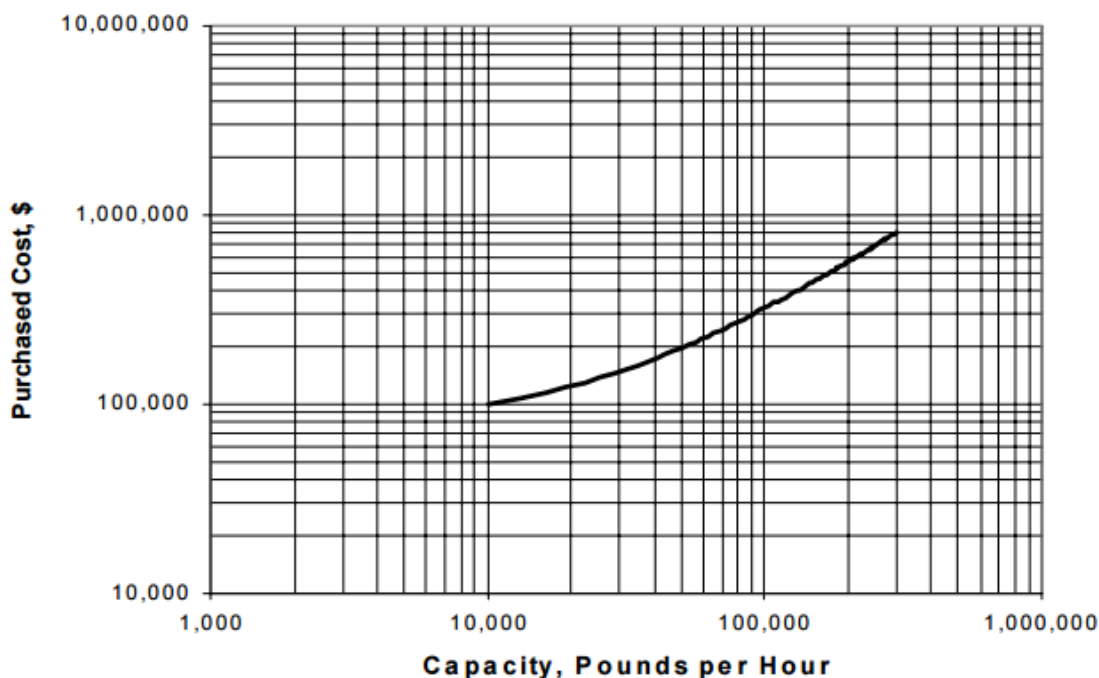


**Figure 55. The estimated cost (1<sup>st</sup> Quarter 1998 USD) for packaged steam boilers based on the steam production capacity [90]**

The price of caustic soda was found by contacting New Zealand vendors, and given at 2.50 2016 NZD/kg[92] tax exclusive. Therefore using a GST of 15%, the cost of NaOH was estimated as \$2.88 2016NZD/kg. The cost of the pH dosing could then be calculated using this value, and the method for calculating the mass flowrate of NaOH required in Section 4.6.1.



### 5.3.7 Boiling IP SGW

Due to the large blowdown required in order to prevent mineral scaling in the boiler when using SGW as the feed water, it is believed that the design of the boiler will be significantly different from conventional boiler design. However, it was assumed that the cost of the boiler could be estimated as if it were a conventional boiler, due to a lack of available information on the expected cost of a boiler with an exceptionally large blowdown.

#### Costing the SGW Boiler

As there is no deaerator, or chemical dosing required, it was determined that the method of costing the SGW boiler in the same manner as for the Poihipi Rd condensate boiler would likely overestimate the cost of the boiler. The FACT method was used to estimate the costs for the steam boiler [71], which uses the heating duty required of the boiler to estimate the cost of the boiler. However, it is noted that this method assumes a 2MPag boiler, which is significantly higher pressure than the 350 kPag boiler required for this configuration. The cost of the boiler in December 2004 NZD can be estimated using Figure 56.

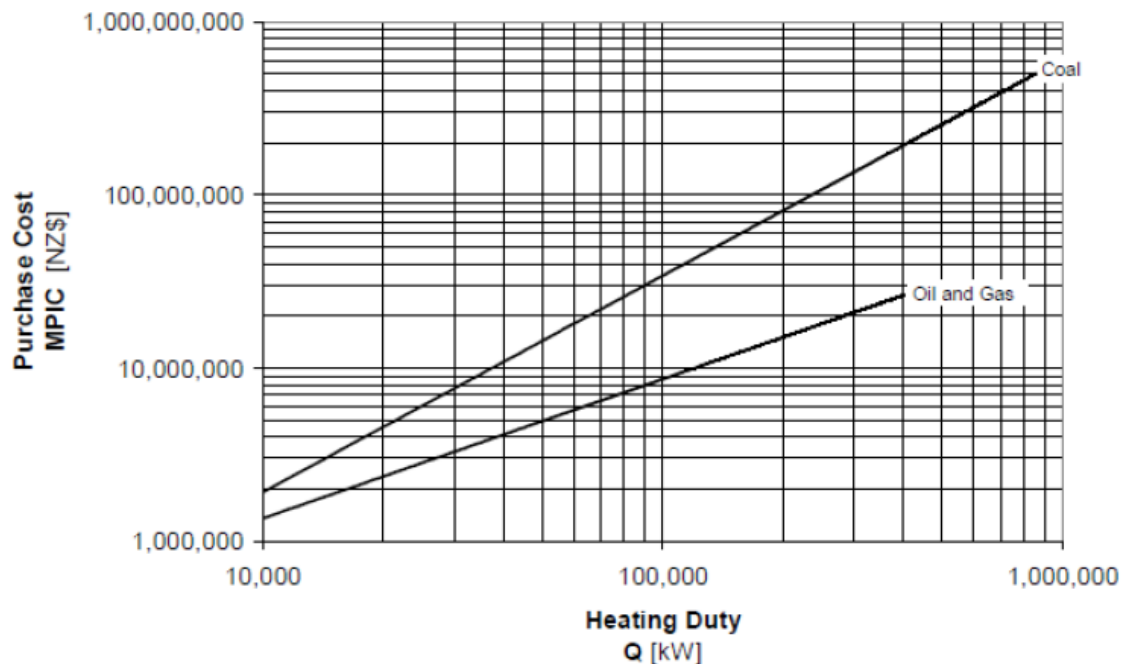


Figure 56. The estimated cost (December 2004 NZD) for steam boilers based on the heating duty [71].

It was observed that the price generated for the standalone boiler was much larger than for the packaged boiler for the same heating requirement. This was attributed to the much larger design pressure of the standalone boiler compared to the package boiler. It was considered unlikely that the exclusion of the deaerator, dosing equipment, and forced draft fans and other equipment included in the price of the package boiler would result in an increase in the cost of the boiler. Therefore, the lower price of the package boiler was used as the estimate for the cost of the boiler, generated using the method described in Section 5.3.6.3.

### 5.3.8 Total Installed Costs

The cost of the process equipment alone does not accurately estimate the cost associated with purchasing and installing the process equipment. The cost associated with minor equipment such as piping, electrical, and instrumentation, and the costs of engineering and construction must be accounted for. The Society of Chemical Engineers New Zealand has developed a relationship to estimate the magnitude of these associated costs based on the cost of the major equipment, as displayed in Table 22.

**Table 22. Costs associated with purchasing and installing process equipment based on the equipment cost [71]**

	Item	Value	Subtotals
A	Major Equipment Costs	100	100
B	Instrumentation and Control Systems	15% of A	15
C	<b>Major Equipment including I&amp;C</b>		<b>115</b>
D	Minor Material (piping, electrical, etc)	60% of C	69
E	<b>Total Equipment Cost</b>		<b>184</b>
F	Freight Insurance and Handling	15% of E	28
G	Engineering	20% of E	37
H	Construction Labour	60% of E	110
I	Construction Equipment	10% of E	18
J	Construction Supervision	10% of E	18
K	<b>Total Installation Costs</b>		<b>211</b>
L	Total Capital Costs	E + K	<b>395</b>
M	Owners Costs	8% of L	32
N	<b>Total Installed costs inside battery limits</b>	L + M	<b>427</b>

It is noted that not all of the major equipment costs will incur the entirety of the associated costs displayed in Table 22:

- It was considered unlikely that the refurbishment and recertification of the steam turbines would incur any costs over and above those already stated.
- The wood chip storage was not expected to require instrumentation and controls
- The cost estimated for the package boiler includes the instrumentation and controls, therefore this would not be accounted for again using the value in Table 22
- The chipper was not expected to have any minor material, freight costs, or engineering costs, as these were included in the quoted cost
- The dryer would not have any of the associated costs, as the price generated was for the installed cost of the dryer
- It was assumed that none of the additional process equipment would incur the associated owners' costs.

## 5.4 Operating costs

The continuous costs from implementing the configurations are predominantly the cost of the delivered landing residues. However there are also other factors, such as for chemical additives.

### 5.4.1 Ongoing Costs from Bringing Turbines Back into Service

The steam turbines at Wairakei generally incur ongoing costs, both planned and corrective in order to ensure continued operation of these turbines. The total planned and corrective costs for the turbines in the Wairakei A and B Stations is approximately \$500,000/year, which includes both mechanical and electrical costs. As analysis for the operating costs for each machine, or by the type of turbine is not performed, it was assumed that the operating cost were spread evenly between the seven turbines at the Wairakei A and B Stations. Therefore, ongoing cost for bringing turbines back into service was set at approximately \$71,400 for each machine brought back into service. It is assumed that G7 would be removed from service if no additional steam is generated, once its certification expires in 2021. Therefore the operational costs of G7 will also be added to the operating costs after this point.

As the recertification of the turbines occurs every five years, if any turbines are returned to service this will incur additional costs from this recertification. Again, it was assumed that unless additional steam was supplied to the Wairakei Power Stations G7 likely would not be recertified once its certification runs out.

### 5.4.2 Parasitic Load

As power is produced at Wairakei, the power used on site is viewed less as an operating cost, and more as a reduction in the net power generation, this power use is called the parasitic load. Some of the additional process equipment required for the implementation of the hybrid configurations requires electricity to operate. The motors for the biomass dryer, the chipper, conveyors, and fans have an associated power requirement, which must be taken into account when calculating the net power generation from the hybrid configurations.

#### 5.4.2.1 Fan and Blower Motors

The power requirements for the air blower to the gasifier was calculated in the UniSim model, with an assumed adiabatic efficiency of 75%. The power use of the blower is approximately 23.5 kW/m<sup>3</sup>/s of air inlet to the blower.

The power requirements for the fans for the boilers and furnaces was estimated using Equation 52 [40].

$$P_{fan} = \frac{kVH}{\eta} \quad (52)$$

Where:

- $P_{fan}$  = the power use of the fan (kW)
- $k$  = the compressibility factor
- $V$  = the inlet volume (m<sup>3</sup>/s)
- $H$  = the pressure rise across the fan (kPa)
- $\eta$  = the static efficiency of the fan

The static efficiency of the fan was assumed to be 70%.

The compressibility factor for the air could be determined using Table 23 based on the pressure ratio of the inlet and outlet pressure from the fan. A pressure ratio of 0.95 was assumed for the fans for the syngas burners.

**Table 23. Pressure ratios and associated compressibility factors for centrifugal air fans [40].**

Pressure ratio	1	0.98	0.97	0.95
Compressibility factor	1	1.05	1.1	1.15

Using the pressure ratio of 0.95, a pressure difference of approximately 5.3 kPa was found, if air at atmospheric pressure is used. The power requirement of the fans was thus found as 8.7 kW/m<sup>3</sup>/s for the boiler and furnace fans.

#### 5.4.2.2 Dryer Motor

By investigating the power requirements for rotary drum dryers at different wood chip loads, the estimate power consumption of the dryer could be estimated using Equation 53 [93].

$$P_{Dryer} = 0.0013\dot{m}_{wood} + 4.0256 \quad (53)$$

Where:

- $P_{dryer}$  = the power consumption of the dryer (kW)
- $\dot{m}_{wood}$  = the mass flowrate of 50% wet (WB) wood chips (kg/hr)

#### 5.4.2.3 Conveyor Motors

The power consumption from the conveyor motors was calculated using that manufacturer's data shown in Table 15 for the appropriate capacity conveyor. However, it is noted this method assumes that the motor operates continuously at full load during the operation.

#### 5.4.2.4 Condensate Pumps

There is an associated power requirement with pumping the Poihipi Rd condensate before the deaerator and the boiler. The power requirements for the condensate pumps were estimated using the UniSim simulation, with an assumed adiabatic efficiency of 75% for the pumps.

#### 5.4.2.5 Chipper

The full load power requirements for the chipper are 300 kW. In order to calculate the power requirements for the chipper, it was assumed that the power use of the chipper would be proportional to the landing residue flowrate supplied to the chipper. As the maximum capacity of the chipper is 50 t/h of wet wood, the power use of the chipper was estimated using Equation 54.

$$P_{chipper} = 300 \frac{\dot{m}_{wood}}{50} \quad (54)$$

Where:

$P_{chipper}$  = the power consumption of the chipper (kW)

$\dot{m}_{wood}$  = the mass flowrate of wet wood to the chipper (t/h)

### 5.4.3 Silica Scale Removal

Hydrofluoric acid cleaning is expected to be required to be performed on the heat exchangers in some of the proposed hybrid configurations in order to maintain heat exchanger performance and reduce pressure losses. It is expected that hydrofluoric acid cleaning will be required for the following configurations:

- Heating additional SGW for use in the Binary Plant
- Operating a boiler using condensate as boiler feed water

It is also possible that silica scaling may occur if the IP SGW from Flash Plant 14 is heated to produce additional steam due to the relatively high concentrations of silica in the SGW. However, significant silica scaling has not been observed in the separation stages at FP14, and boiling of some of the IP SGW after the first separation stage is not expected to significantly increase the mineral concentration in the LP SGW, due to the high flows (approximately 1500 t/h) of LP SGW to the second separation stage. However, it is possible that silica scaling may occur on the heat exchanger surfaces, and this will have an associated cost for silica scale removal if experienced.

#### 5.4.3.1 Heating additional SGW for use in the Binary Plant

Currently, hydrofluoric acid cleaning is performed twice yearly on the heat exchangers at the Wairakei Binary Plant to remove silica build up. As discussed in Section 3.3.4, more frequent silica removal would likely be required in order to utilize the additional SGW. The current costs for silica scale removal were used as a basis for estimating the cleaning costs.

The cost of the biannual HF cleaning on all eight of the heat exchangers in the binary plant is \$360000/year. The annual generation that is lost as a result of the binary plant closure is also approximately 1.1 GWh, corresponding to an estimated \$77000/year of lost revenue. In order to perform plant cleaning twice as often, the cleaning cost was assumed to double for a total additional cost of \$437000/year.

#### 5.4.3.2 Operating a Boiler Using Condensate as the Boiler Feed water

As SGW from FP16 is designed to be used in order to preheat the Poihipi Rd condensate, it is expected that silica scaling will likely occur in the preheater. This is due to the fact that silica scaling is observed to occur uniformly throughout the Binary Plant, and does not observed to increase as the temperature of the SGW decreases. In order to estimate the costs associated with the HF cleaning of the preheater, the cost of the Binary Plant cleaning was used as a basis. The costs of HF cleaning were then scaled based on the relative amount of SGW that will be passed through the condensate preheater compared to the Binary Plant heat exchangers. As the cost of cleaning the binary plant heat exchangers is \$360,000/year for both units. It was assumed that the cleaning of the condensate preheater would be performed over 24 hours, as currently the Binary Plant cleaning takes two days to clean four heat exchangers, and the condensate preheater is expected to be significantly smaller than these heat exchangers. The costs for the hydrofluoric acid cleaning of the condensate preheater were estimated using Equation 55.

$$C_{HF} = 360000 \frac{\dot{m}_{SGW,CP}}{\dot{m}_{SGW,BP}} \quad (55)$$

Where:

- $C_{HF}$  = the annual cost of hydrofluoric acid cleaning (NZD/year)
- $\dot{m}_{SGW,BP}$  = The average mass flowrate of SGW to the binary plant (2440 t/h)
- $\dot{m}_{SGW,CP}$  = the average mass flowrate of SGW to the condensate preheater (t/h)

This cost generated in Equation 55 may be an overestimation, due to the fact that each unit in the Binary Plant has four heat exchangers, and the condensate preheating will likely occur in one heat exchanger. However, as the entrance temperature of the SGW to the preheater will be lower than that for the Binary Plant, increased silica scaling may occur, due to the decreased solubility of silica in the SGW. There is therefore significant uncertainty associated with estimating the regularity and associated total cost for silica scaling in the condensate preheater. It may be the case that a higher flowrate of SGW and a consequently larger heat exchanger would be preferable, due to the increased exit temperature of the SGW from the heat exchanger. A trial of silica scaling would likely need to be performed in order for more accurate estimation of silica scaling rates that may occur in the condensate preheater.

#### **5.4.4 Silica Inhibition at the Binary Plant**

Currently there is an ongoing trial of silica inhibition chemicals being performed on the Wairakei Binary Plant, in order to reduce silica deposition. While it is unclear at this stage if the silica inhibition will be continued, the additional flowrate of SGW to the Binary Plant would increase the amount of inhibition chemicals required. The designed dosing rate of the inhibition chemicals is 18 mg/kg, with an associated price of \$3.1/kg. The average flow to the binary plant will be increased from approximately 2440 t/h to 2690 t/h if the additional SGW is used in the binary plant. The additional flow will cause an associated additional cost of \$123417/year if the inhibition chemicals are continued.

#### **5.4.5 Wages**

New operators will likely need to be hired in order to ensure there is adequate staff to operate the new process equipment. In general there are 4.8 operators are required for each shift position in process plants [94]. As there are already many operators at the Power Stations on the Wairakei Geothermal Field, it is unclear how many new staff would be required, as it may be possible to operate additional process equipment with the existing staff. Therefore the costs associated with the wages of the additional workers has been excluded from this analysis.

### **5.5 Economic Evaluation**

In order to estimate any economic benefits from implementing any of the hybrid configurations, the expected useful life of the plant had to be determined. A life cycle assessment of a biomass gasification combined cycle plant was performed by Mann and Spath for the National Renewable Energy Laboratory (NREL) [95]. A useful life of 30 years was assumed for the combined cycle plant. The combined cycle plant has many of the same elements as the hybrid configurations, including a dual fluidized bed gasifier being used to produce syngas. Due to this, it was assumed that the same useful life of 30 years could be used for the hybrid configurations as was used for the combined cycle plant.

Straight line depreciation was performed on the plant to calculate the yearly income tax, and it was assumed that there would be no scrap value from any of the additional process equipment. The depreciation was calculated using values from the United States IRS on a 30 year recovery period for straight line depreciation [96].

It was assumed that the additions to the plant would take one year to complete, and the hybrid configurations may begin operation after this period. The engineering costs were expected to be paid before construction began, and the remainder of the installed costs to be paid during the construction. When the capital cost estimates included the engineering costs, such as for the wood chip dryer, the engineering costs were estimated as a proportion of the total installed costs based on the values displayed in Table 22.

The income tax rate was used as that for Contact Energy at 28%. As Contact Energy is a large and profitable company, any losses sustained in the implementation of the hybrid configurations would reduce the taxable income for Contact Energy. Therefore any yearly losses incurred from the implementation of the hybrid configurations will offset the total income of Contact Energy.

It was assumed that all of the operating costs would increase with inflation at approximately 3% annually.

The hybrid configurations were evaluated based on their net present value (NPV) for the 30 year operation period. The net present value of a project was calculated using Equation 56.

$$NPV = -C_0 + \sum_{t=1}^T \frac{C_t}{(1+i)^t} \quad (56)$$

Where:

$C_0$  = the initial investment (\$)

$C_t$  = the free cash flow at year  $t$  (\$)

$i$  = the discount rate

The discount rate was assumed to be 7%, taken from the NZ treasury [97]. The free cash flow was calculated by subtracting the income tax from the gross profit for each year throughout the expected life of the hybrid plants.

## 5.6 Economic Optimization

The price of the landing residues used to create the syngas is seen to increase as the required amount of these residues increases, due to the increasing transportation distance. Therefore, the larger the gasifier for the proposed hybrid plants, the relatively more expensive the landing residue feed will become. However, the capital investment for the process equipment required generally becomes relatively cheaper as the size of the hybrid plant increases, due to the economies of scale for new process equipment. The hybrid configurations will also generally become relatively more efficient the more additional steam they can provide to the Wairakei A and B Stations. This is due to the no load flow of steam required for the steam turbines, as the larger the amount of steam generated, the smaller the relative amount of steam to provide this no load flow becomes. Therefore, there is a balance between these three factors, where the flowrate of landing residues may be optimized in order to provide the most economical sized plant.

There are however, limits on the scaling that may be performed on the hybrid configurations. As the MP turbines must be modified to operate using superheated steam, this configuration has been discretized into the amount of turbines that are converted, and the optimization was set to alter this number of modified turbines. The boiler using geothermal condensate is limited by the amount of the Poihipi Rd condensate that is available for use, effectively setting a maximum size for the boiler. Similarly, there is a maximum size for the boiler using IP SGW as the feed water, as the larger the amount of steam generated, the more concentrated the minerals in the SGW will become. This limit is set by the precipitation of the minerals, but further research would need to be



performed in order to quantify this limit. The amount of SGW which may be heated for use in the Binary Plant is limited by the maximum flowrate of SGW to the plant, of 2800 t/h, and the amount of SGW available to heat in T-line.

The costs of the landing residue input, the additional process equipment required, the expected additional power generation, operating costs, and the resultant value of the additional power were calculated with reference to the flowrate of landing residues. Therefore, the flowrate of landing residues could be changed, in order to maximize the profits from hybridization. In order to optimize the amount of MP turbines to modify to utilize superheated steam, the expected flowrate of landing residues required for each turbine modified was used to perform the economic analysis.

In the case of heating SGW for use in the Binary Plant, maximum flowrate of SGW that may be heated is set by the maximum allowable flowrate to the Binary Plant and the SGW flowrate in the T-line. Therefore there is no benefit in increasing the plant size to larger than is necessitated by this flowrate of SGW. However, the amount of SGW to be heated can be limited, in order to reduce the size of the process equipment required, and to utilize relatively cheaper landing residues. As the process equipment is sized in order to provide the maximum flowrate of syngas required to heat the SGW, outliers of large SGW flowrates to heat can result in oversized process equipment. Therefore the size of the equipment required can be optimized by setting a maximum flowrate of SGW to perform heating on. Optimization was performed on the maximum allowable SGW flowrate to heat in order to augment the SGW in X-line.

## **5.7 Different Scenarios for the Steam Flow to Wairakei**

As discussed in Section 3.2.4, each configuration was evaluated in three different scenarios reflecting the different possibilities for the future operation of the plant, depending on the steam input to the Wairakei A and B Stations:

- **Scenario 1**

IP steam bypasses sporadically, the amount of bypassing is the same rate as for the period from January 2015-July 2016. All IP turbines and MP turbines are fully loaded, and additional IP steam and bypassing IP steam requires recertification of G1 to be utilized. G7 is assumed to be completely unloaded, and therefore the no load flow requirements for G1 and G7 must be met before any additional power generation can be performed from additional IP and LP steam respectively.

- **Scenario 2**

The average enthalpy of the extracted two-phase fluid has decreased to the point that effectively no bypassing of IP steam occurs. However all of the IP turbines are fully loaded, and all of the LP turbines with the exception of G7 are fully loaded. Recertification of G1 is required in order to generate additional power from IP steam. The no load flow requirements for the IP and LP turbines must be met in order to generate power from the IP and LP steam.

- **Scenario 3**

The average enthalpy of the extracted two-phase fluid has decreased to the point that not bypassing occurs, and the IP steam turbine G4 is not fully loaded. As the LP turbines are

currently all fully loaded with the exception of G7, reduction in the IP steam flow will likely cause a LP turbine to become partially loaded. It is therefore assumed that some additional IP and LP steam may be utilized without having to meet the no load flow requirements, as an IP and an LP turbine are not fully loaded. It is also assumed that the costs associated with the recertification and operation of the steam turbines may not need to be paid in this configurations, as the turbines were already in operation.

These configurations greatly impact the economics of the hybrid plants, and the net present value (NPV) of each hybrid plant configuration was therefore found for each configuration.

## 6.0 Results

The results of the process modelling, capital cost estimation, and economic evaluation are displayed in the following sections for the four hybrid configurations and for each steam flow scenario. More detailed cash flow analyses and capital cost breakdowns are present in the Appendices than in the following sections.

### 6.1 Gasification Model

The modified UniSim gasification model calculated that for each ton of wet wood input to the gasifier, there would be a requirement of 735 kg of IP steam input to the gasifier, and 1.32 tons of syngas created in the BFB reactor of the gasifier. However, a portion of the produced syngas was required to be returned to the gasifier in order to provide the additional heat for gasification. The proportion of recycled syngas is dependent on the temperature of the produced flue gas from syngas combustion. As the superheating of geothermal steam produced flue gas at 200°C, which was subsequently used in conjunction with the gasifier flue gas as the drying medium for the rotary drum dryer, there was consequently a smaller proportion of the produced syngas that was recycled. This configuration required 15% of the syngas to be returned to the CFB reactor in the gasifier, whereas all the other hybrid configurations required a 20% recycle ratio. The molar composition of the produced syngas was approximately 29% H<sub>2</sub>, 10% CO, 13% CO<sub>2</sub>, 42% H<sub>2</sub>O, 5% CH<sub>4</sub>, and 1% other, which corresponds to a syngas with a lower heating value of 7.15 MJ/kg.

The effectiveness of gasifiers can be expressed by the cold gas efficiency of the gasifier, which is a ratio of the combustion energy of the syngas and the energy inputs to the gasifier, as displayed in Equation 57.

$$\text{Cold gas efficiency} = \frac{\text{combustion energy of syngas}}{\text{Combustion energy of biomass} + \text{external energy}} \quad (57)$$

The combustion energy of the syngas was calculated using the lower heating values for the combustible components of the syngas, namely H<sub>2</sub>, CO, and CH<sub>4</sub>, and the amount of each of these components produced in the gasifier. Generally the cold gas efficiency is relatively low in similar gasifiers, in the range of 60-70% [98]. However, it was found that the cold gas efficiency was 84% for the superheating of geothermal steam, and 79% for all other configurations. This large efficiency is attributed to the use of geothermal steam as the gasification agent, removing the necessity for additional energy input to generate steam.

### 6.2 Superheating Geothermal Steam

After optimization had been performed on the amount of MP turbines to modify to utilize superheated steam instead of IP steam for the first stage input, it was found that it was most economical for the 30 year plant life was achieved when two of the three MP turbines were modified.

### 6.2.1 Scenario 1

The results from the process modelling, energy analysis, and economic evaluation for modifying two MP turbines to use superheated steam at the Wairakei Power Plant is displayed in Table 24. As can be seen the net present value of the project is -\$67 million for the 30 year life of the project, with a \$49 million capital investment required.

**Table 24. Results for modifying two MP turbines to utilize superheated steam in Scenario 1**

<b>Biomass input</b>	<i>t/h</i>	15.0
	<i>MW</i>	40.1
<b>Gasifier IP steam requirement</b>	<i>t/h</i>	11.1
<b>IP steam saving from using superheated steam</b>	<i>t/h</i>	148.6
<b>Net IP steam generation</b>	<i>t/h</i>	137.5
<b>Average amount of bypassing steam</b>	<i>t/h</i>	88
<b>Average power generation from additional and bypassing steam</b>	<i>MW</i>	11.8
<b>Parasitic load from additional equipment</b>	<i>MW</i>	0.3
<b>Reduction in power generation from MP turbines</b>	<i>MW</i>	5.2
<b>Net average power generation</b>	<i>MW</i>	6.3
<b>Energy efficiency</b>	%	15.7
<b>Installed capital costs</b>	\$	49,204,933
<b>Net present value for 30 year plant life</b>	\$	-67,435,840

A breakdown of the estimated installed capital costs for the project is displayed in Figure 57, it was seen that the capital costs of this configuration were the same for Scenario 2 as for Scenario 1. The cost of modifying the existing MP steam turbines to utilize superheated steam was seen to account for the majority of the capital costs.

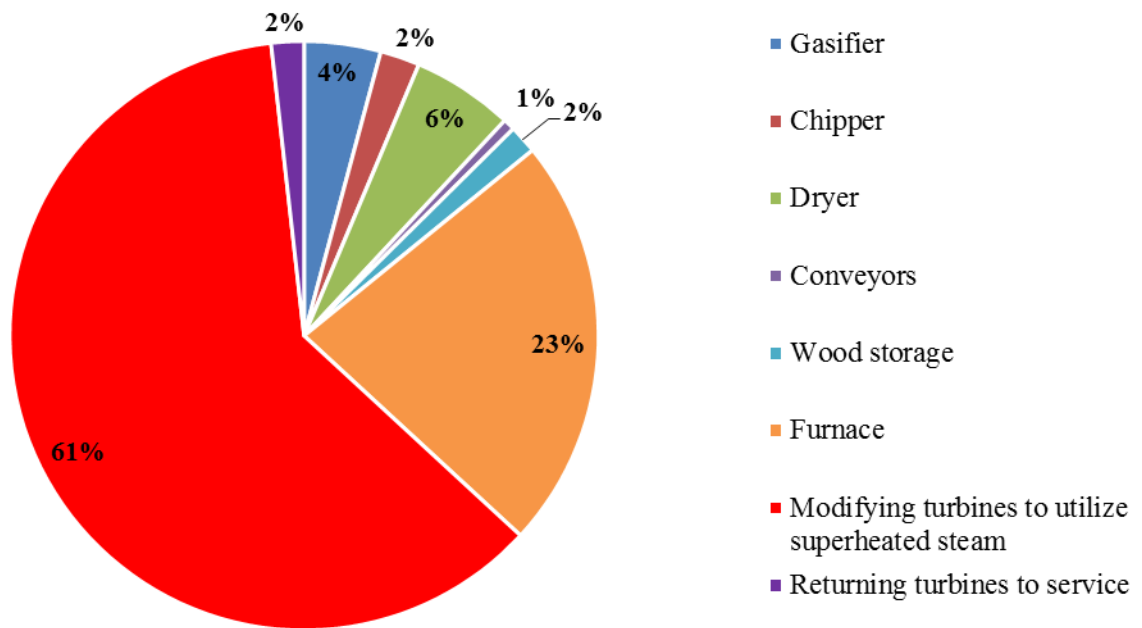


**Figure 57. The installed capital cost breakdown for modifying two MP turbines to utilize superheated steam in Scenario 1 and Scenario 2**

The cumulative discounted cash flow for the project is displayed in Figure 58. The cost of the biomass input outweighs the value of the additional power generated by installing this hybrid configuration, as evidenced by the decreasing cumulative discounted cash flow throughout the 30 year operating life of the project.

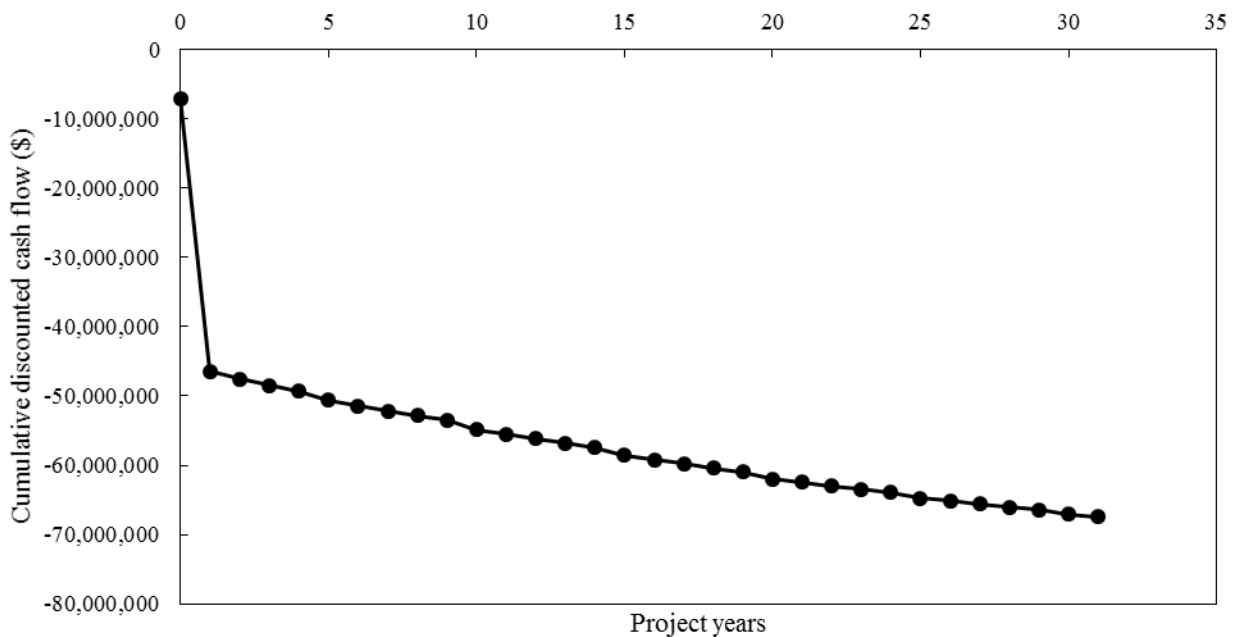


**Figure 58. The cumulative discounted cash flow for modifying two MP turbines to utilize superheated steam in Scenario 1**

A summary of the cash flows for the implantation of this project is displayed in Table 25.

**Table 25. The cash flow summary for superheating geothermal steam in Scenario 1, all values given in \$1000's**

Year	Capital Cost	Revenue	Operating costs	Cost of biomass	Income tax	Free Cash flow
0	-7116	0	0	0	0	-7116
1	-42089	0	0	0	0	-42089
2	0	3970	-76	-5908	726	-1287
3	0	4090	-78	-6019	887	-1121
4	0	4239	-80	-6133	878	-1097
5	0	4342	-1047	-6249	1152	-1801
6	0	4451	-171	-6367	909	-1177
7	0	4566	-176	-6487	912	-1185
8	0	4688	-181	-6610	914	-1190
9	0	4770	-186	-6735	927	-1224
10	0	4721	-1912	-6863	1460	-2594
20	0	5144	-2570	-8293	1926	-3793
30	0	5831	-3454	-10043	2471	-5194

It is clear from Table 25 that this option is not viable due to the fact that the delivered cost of landing residues is always greater than the additional Revenue generated. Moreover, the costs of landing residues increase at a greater rate than the value of the electricity generated. This is due to forecasts of wholesale power prices increasing at considerably less than inflation whereas the cost of landing residues increases at around inflation.

The sensitivity analysis for this project is displayed in Figure 59. As can be seen, the sale price of power, cost of the landing residues, and capital costs have a relatively large influence on the NPV of the project. However, none of the altered factors investigated resulted in a positive NPV for the 30 year plant life.

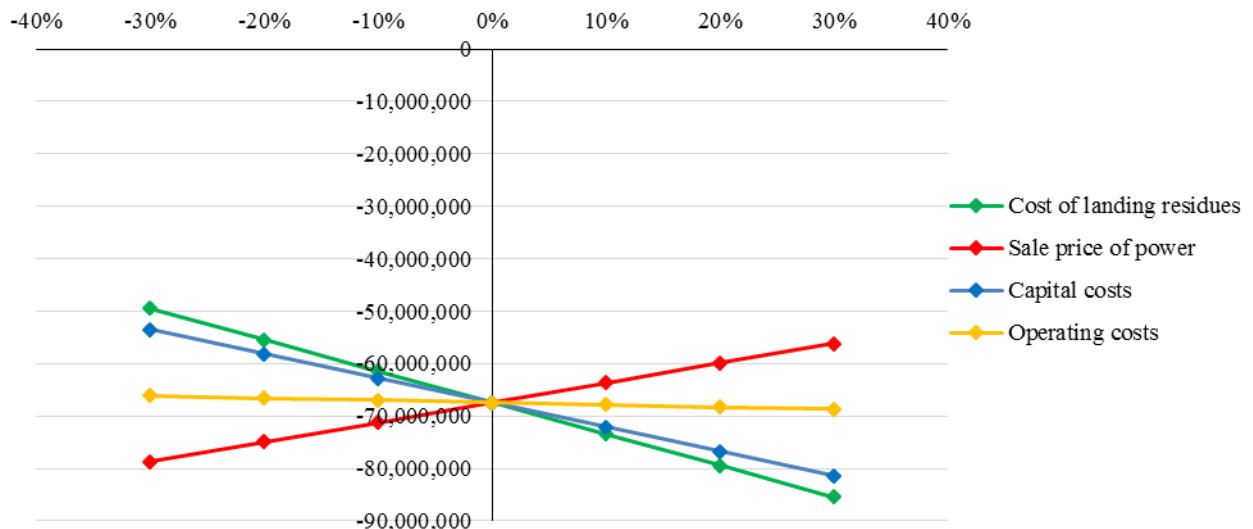


**Figure 59. Sensitivity analysis for modifying two MP turbines to utilize superheated steam in Scenario 1**

### 6.2.2 Scenario 2

The results from the process modelling, energy analysis, and economic evaluation for modifying two MP turbines to use superheated steam at the Wairakei Power Plant is displayed in for Scenario 2 in Table 26. The net present value for the project is -\$90 million dollars for the 30 year plant life.

**Table 26. Results for modifying two MP turbines to utilize superheated steam in Scenario 2**

<b>Biomass input</b>	<i>t/h</i>	15.0
	<i>MW</i>	40.1
<b>Gasifier IP steam requirement</b>	<i>t/h</i>	11.1
<b>IP steam saving from using superheated steam</b>	<i>t/h</i>	148.6
<b>Net IP steam generation</b>	<i>t/h</i>	137.5
<b>Average power generation from additional steam</b>	<i>MW</i>	8.2
<b>Parasitic load from additional equipment</b>	<i>MW</i>	0.3
<b>Reduction in power generation from MP turbines</b>	<i>MW</i>	5.2
<b>Net average power generation</b>	<i>MW</i>	2.7
<b>Energy efficiency</b>	%	6.6
<b>Installed capital costs</b>	\$	49,204,933
<b>Net present value for 30 year plant life</b>	\$	-90,075,032

This configuration requires the same process equipment for Scenario 1. The breakdown of the installed capital costs can therefore be seen in Figure 57.

The cumulative discounted cash flow for the project is displayed in Figure 60, as can be seen this project does not become revenue positive at any point.

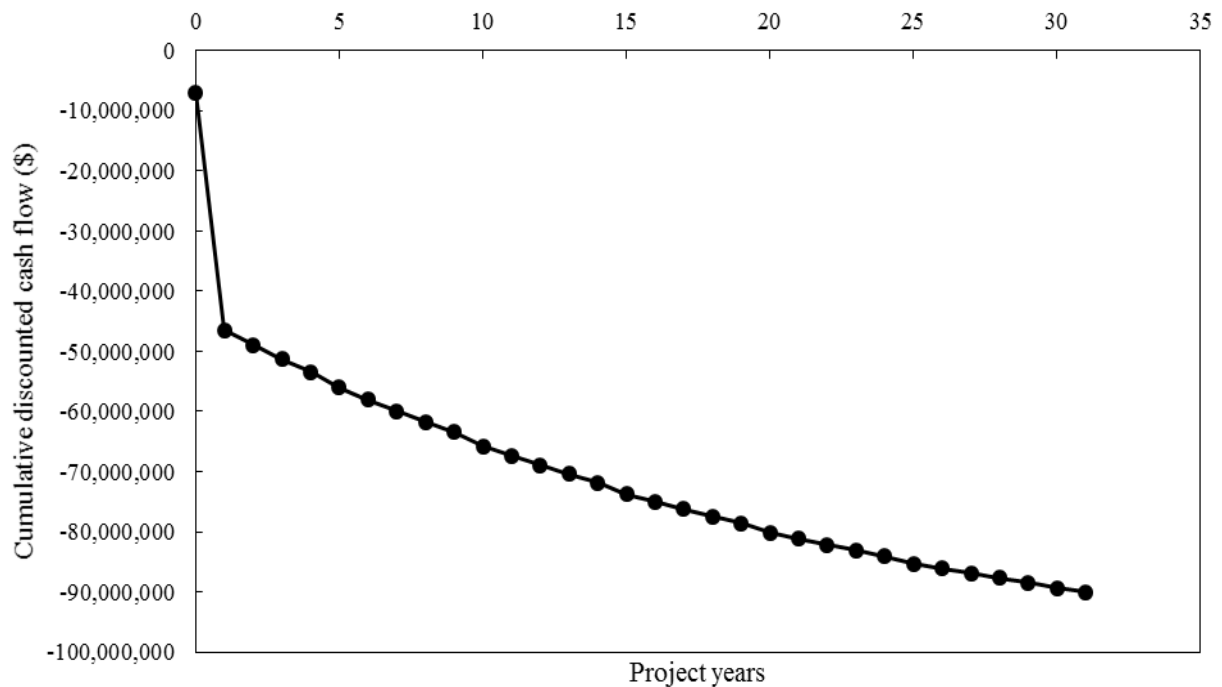


**Figure 60. The cumulative discounted cash flow for modifying two MP turbines to utilize superheated steam in Scenario 2**

A summary of the cash flows for the implantation of this project is displayed in Table 27.

**Table 27. The cash flow summary for superheating geothermal steam in Scenario 2, all values given in \$1000's**

Year	Capital Cost	Revenue	Operating costs	Cost of biomass	Income tax	Free Cash flow
0	-7116	0	0	0	0	-7116
1	-42089	0	0	0	0	-42089
2	0	1662	-76	-5871	1362	-2922
3	0	1712	-78	-5981	1542	-2805
4	0	1775	-80	-6094	1557	-2843
5	0	1818	-1047	-6209	1847	-3590
6	0	1864	-171	-6327	1622	-3011
7	0	1912	-176	-6446	1644	-3066
8	0	1963	-181	-6568	1665	-3121
9	0	1997	-186	-6693	1692	-3190
10	0	1977	-1912	-6820	2216	-4539
20	0	2154	-2570	-8241	2749	-5908
30	0	2442	-3454	-9979	3403	-7589

The sensitivity analysis for this project is displayed in Figure 61. The reduction in power generation associated with the loss of bypassing IP steam in this scenario resulted in a decrease in the sensitivity of the NPV of the project to the wholesale price of power.



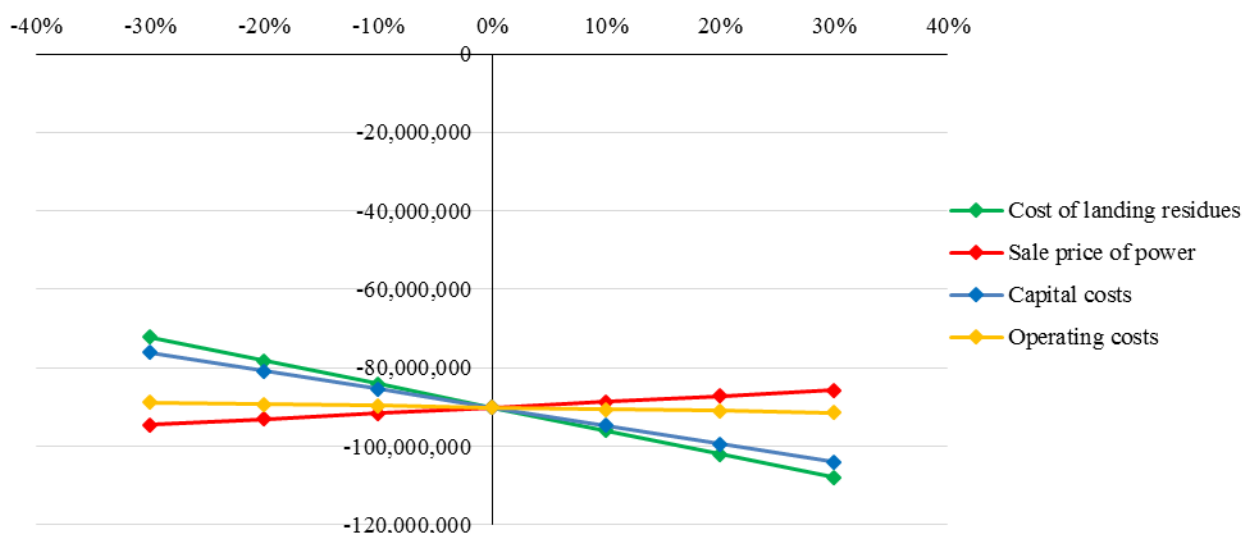


Figure 61. Sensitivity analysis for modifying two MP turbines to utilize superheated steam in Scenario 2

### 6.2.3 Scenario 3

The results from the process modelling, energy analysis, and economic evaluation for modifying two MP turbines to use superheated steam at the Wairakei Power Plant is displayed in for Scenario 3 in Table 28. The net present value for the project is -\$27 million dollars for the 30 year plant life, with a \$48 million capital investment required.

Table 28. Results for modifying two MP turbines to utilize superheated steam in Scenario 23

<b>Biomass input</b>	<i>t/h</i>	15.0
	<i>MW</i>	40.1
<b>Gasifier IP steam requirement</b>	<i>t/h</i>	11.1
<b>IP steam saving from using superheated steam</b>	<i>t/h</i>	148.6
<b>Net IP steam generation</b>	<i>t/h</i>	137.5
<b>Average power generation from additional steam</b>	<i>MW</i>	17.5
<b>Parasitic load from additional equipment</b>	<i>MW</i>	0.3
<b>Reduction in power generation from MP turbines</b>	<i>MW</i>	5.3
<b>Net average power generation</b>	<i>MW</i>	12.0
<b>Energy efficiency</b>	%	29.7
<b>Installed capital costs</b>	\$	48,444,933
<b>Net present value for 30 year plant life</b>	\$	-27,081,730

As this configuration did not require the return of the IP steam turbine, G1, to service there was consequently a slightly reduced installed capital cost for the project compared to Scenario 1 and Scenario 2, the breakdown of the installed capital costs is displayed in Figure 62.

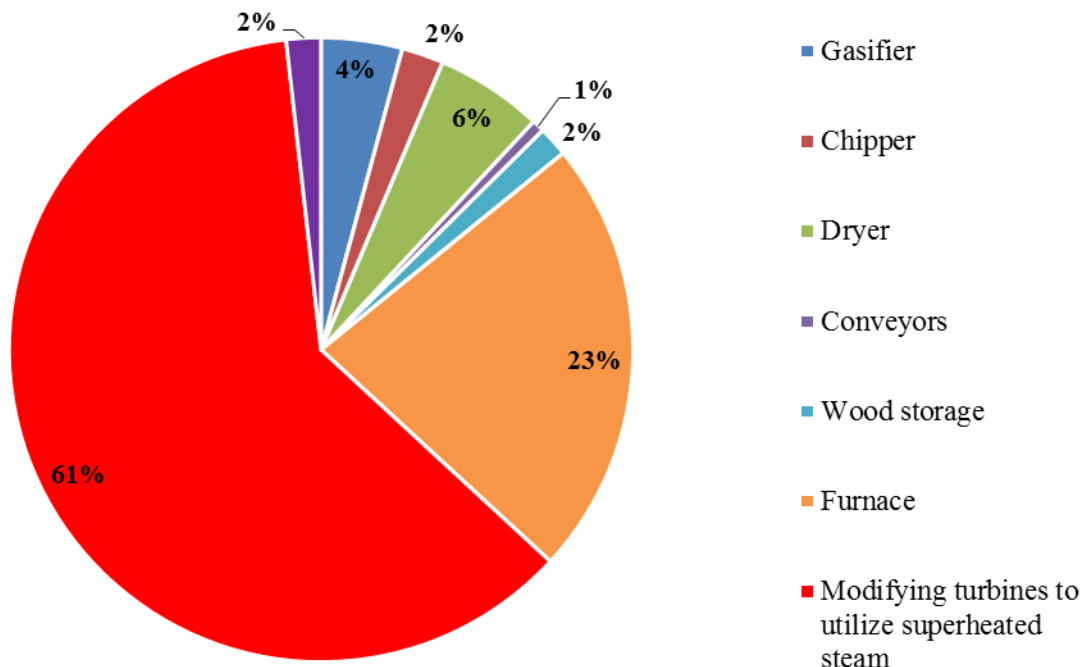


**Figure 62. The installed cost breakdown for modifying two MP turbines to utilize superheated steam in Scenario 3**

The cumulative discounted cash flow for this project is displayed in Figure 63. As can be seen, Scenario 3 would result in a project which is revenue positive, but does not generate returns large enough to recover the large capital investment.

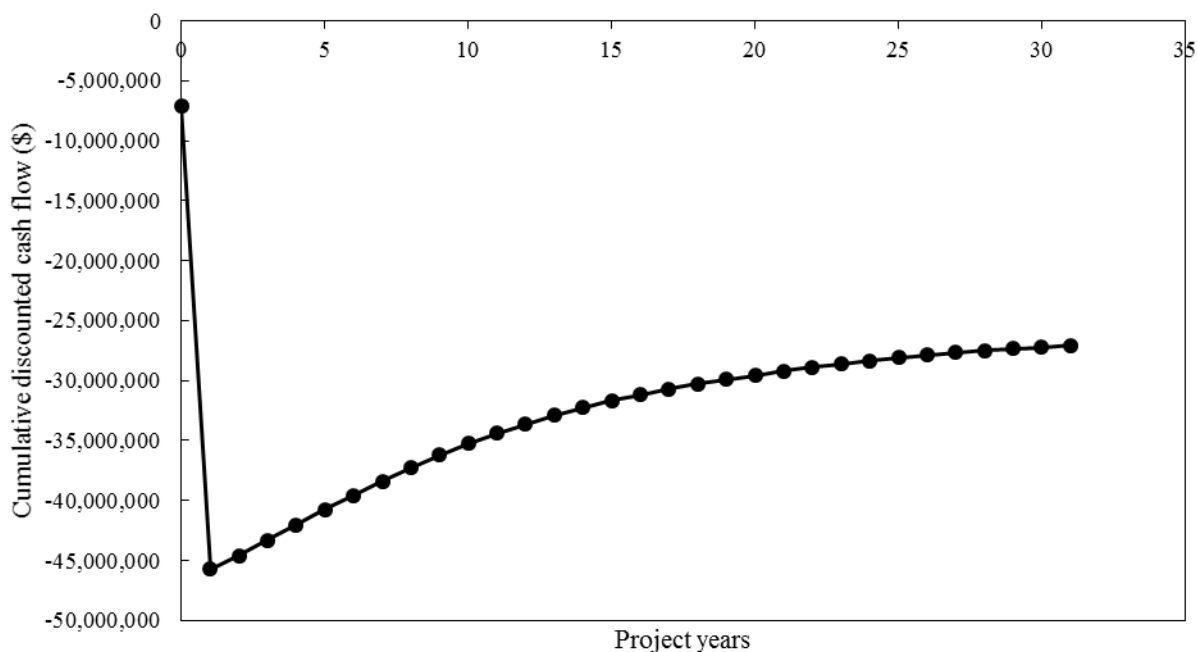


**Figure 63. The cumulative discounted cash flow for modifying two MP turbines to utilize superheated steam in Scenario 3**

A summary of the cash flows for the implantation of this project is displayed in Table 29.

**Table 29. The cash flow summary for superheating geothermal steam in Scenario 1, all values given in \$1000's**

Year	Capital Cost	Revenue	Operating costs	Cost of biomass	Income tax	Free Cash flow
0	-7116	0	0	0	0	-7116
1	-41329	0	0	0	0	-41329
2	0	7486	0	-5871	-293	1322
3	0	7711	0	-5981	-167	1563
4	0	7993	0	-6094	-214	1685
5	0	8188	0	-6209	-236	1742
6	0	8392	0	-6327	-261	1805
7	0	8610	0	-6446	-288	1876
8	0	8839	0	-6568	-318	1952
9	0	8995	0	-6693	-327	1975
10	0	8902	0	-6820	-265	1817
20	0	9699	0	-8241	-90	1368
30	0	10995	0	-9979	34	1049

In this case the revenue exceeds the cost of the landing residues, however the income is not large enough to offset the large capital investment required.

The sensitivity analysis of this project is displayed in Figure 64. Due to the fact that there was no turbine recertification required for this configuration in Scenario 3, there were no additional operating costs associated with implementing the configuration. As can be seen, the sale price of power would need to be larger than 130% of that estimated in order for this project to recover the initial investment. There would need to be significant changes to several factors in order to recover the initial investment of this project.

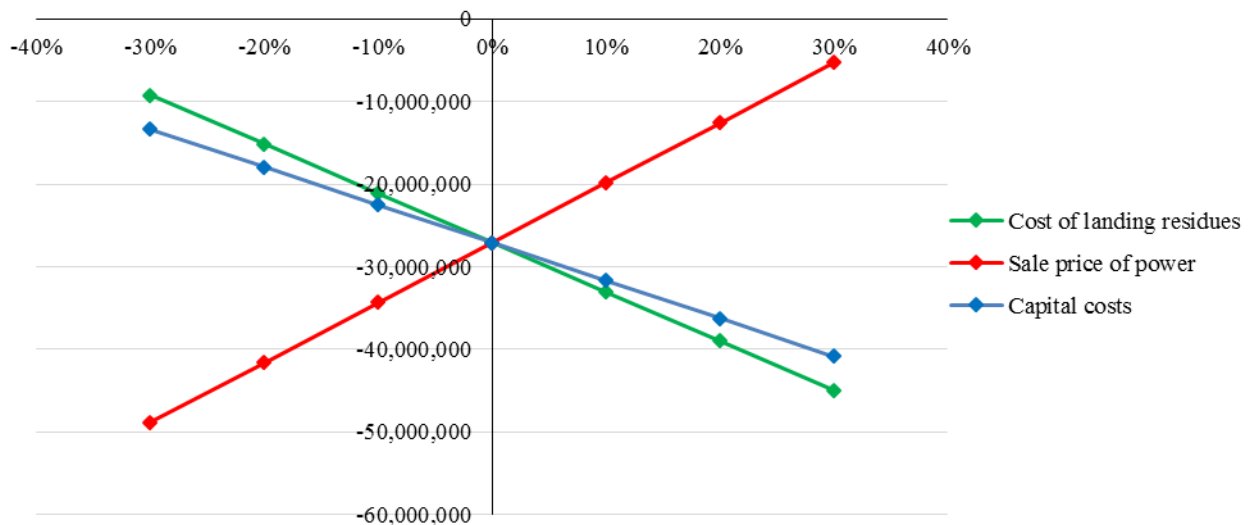


**Figure 64. Sensitivity analysis for modifying two MP turbines to utilize superheated steam in Scenario 2**

### 6.3 Creating Additional IP Steam by Boiling Poihipi Rd Condensate

Optimization was performed on the size of the gasification plant in order to maximize the NPV of this configuration. It was found that the NPV of this project after 30 years was expected to decrease as the size of the hybrid plant increased. Optimization on the size of the hybrid plant did not result in a size of plant which would result in the project recovering its initial investment. Therefore, the gasification plant was sized in order to utilize the average amount of Poihipi Rd condensate available for use, as to compare the power generation and project economics to the other hybrid configurations. This resulted in a 42MW gasification plant based on the thermal input of the biomass.

The installed capital costs are slightly higher for Scenario 1 than in Scenario 2 or Scenario 3. This is due to the fact that the additional steam estimated to be bypassing the IP manifold in Scenario 1 necessitates the return of the IP turbine G1 to service. Whereas, the net steam generation from the boiler is not large enough to meet the no load flow for the IP turbine, and therefore G1 would not be returned to service for either Scenario 2 or Scenario 3.

#### 6.3.1 Scenario 1

The results from the process modelling, energy analysis, and economic evaluation for using Poihipi Rd condensate as boiler feed water to generate additional IP steam for the Wairakei Power Plant in Scenario 1 is displayed in Table 30. The NPV of the project was found to be -\$50 million, requiring a capital investment of \$10.3 million.

**Table 30. Results for generating steam from Poihipi Rd condensate in Scenario 1**

<b>Biomass input</b>	<i>t/h</i>	15.6
	<i>MW</i>	41.7
<b>Gasifier IP steam requirement</b>	<i>t/h</i>	11.5
<b>IP steam generated in boiler</b>	<i>t/h</i>	52.6
<b>Net IP steam generation</b>	<i>t/h</i>	41.2
<b>Average amount of bypassing steam</b>	<i>t/h</i>	88
<b>Average power generation from generated and bypassing steam</b>	<i>MW</i>	4.5
<b>Parasitic load from additional equipment</b>	<i>MW</i>	0.3
<b>Net average power generation</b>	<i>MW</i>	4.2
<b>Energy efficiency</b>	%	10.1
<b>Installed capital costs</b>	\$	10,306,633
<b>Net present value for 30 year plant life</b>	\$	-49,519,081

The breakdown of the installed capital costs associated with boiling Poihipi Rd condensate are displayed in Figure 65. The process equipment that were seen to contribute most heavily to the installed capital costs were the package boiler, gasifier, and the rotary drum dryer.

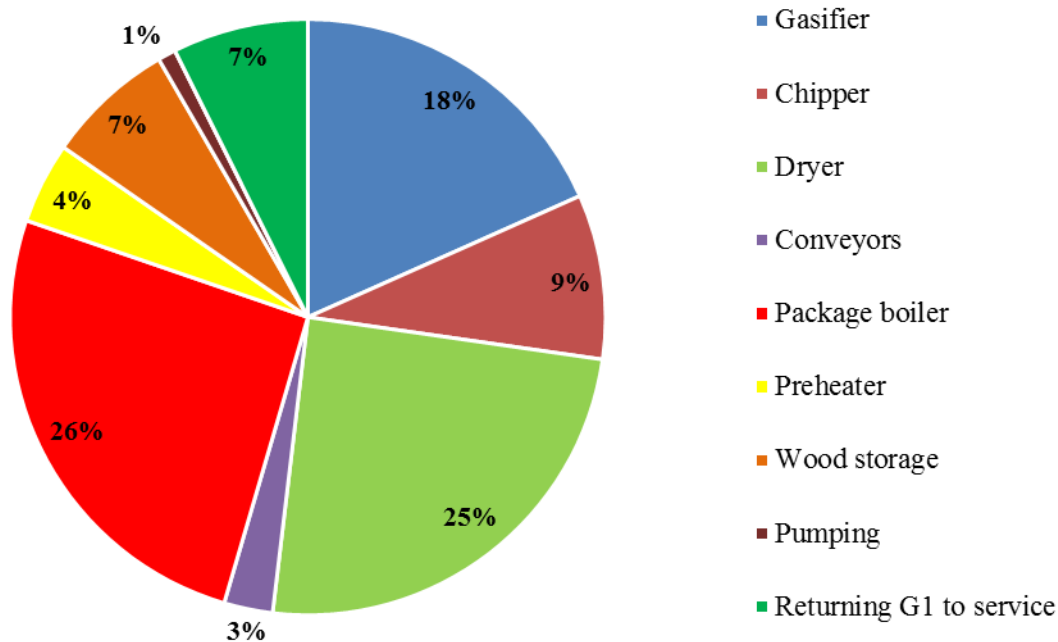


**Figure 65. The installed cost breakdown for using Poihipi Rd condensate as boiler feed water in Scenario 1**

The cumulative discounted cash flows for this project is displayed in Figure 66. It can be seen that the implementation of the hybrid configuration does not generate yearly profit, with the estimated cost for the landing residues being greater than the estimated value of the additional power generated.

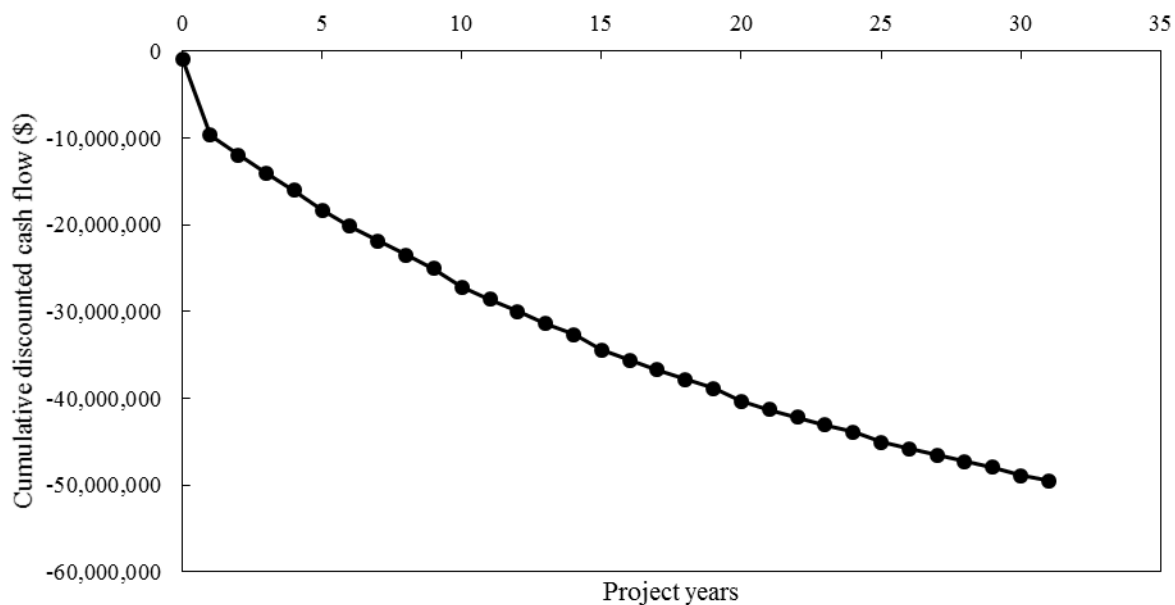


**Figure 66. The cumulative discounted cash flow for using Poihipi Rd condensate as boiler feed water in Scenario 1**

A summary of the cash flows for the implantation of this project is displayed in Table 31.

**Table 31. The cash flow summary for using Poihipi Rd condensate as boiler feed water in Scenario 1, all values given in \$1000's**

Year	Capital Cost	Revenue	Operating costs	Cost of biomass	Income tax	Free Cash flow
0	-888	0	0	0	0	-888
1	-9419	0	0	0	0	-9419
2	0	2649	-108	-6135	1031	-2563
3	0	2728	-111	-6250	1066	-2567
4	0	2828	-114	-6368	1072	-2582
5	0	2897	-1053	-6488	1349	-3295
6	0	2969	-204	-6611	1126	-2720
7	0	3046	-210	-6736	1141	-2759
8	0	3127	-216	-6864	1156	-2797
9	0	3182	-223	-6994	1179	-2856
10	0	3149	-1900	-7127	1694	-4182
20	0	3432	-2553	-8612	2214	-5519
30	0	3890	-3431	-10428	2840	-7129

The sensitivity analysis for this project is displayed in Figure 67. The sale price of power and the cost of the landing residues were seen to have the greatest influence on the NPV of the project. However, within the  $\pm 30\%$  sensitivity range chosen for this analysis, none of the manipulated factors resulted in the project recovering its initial investment.

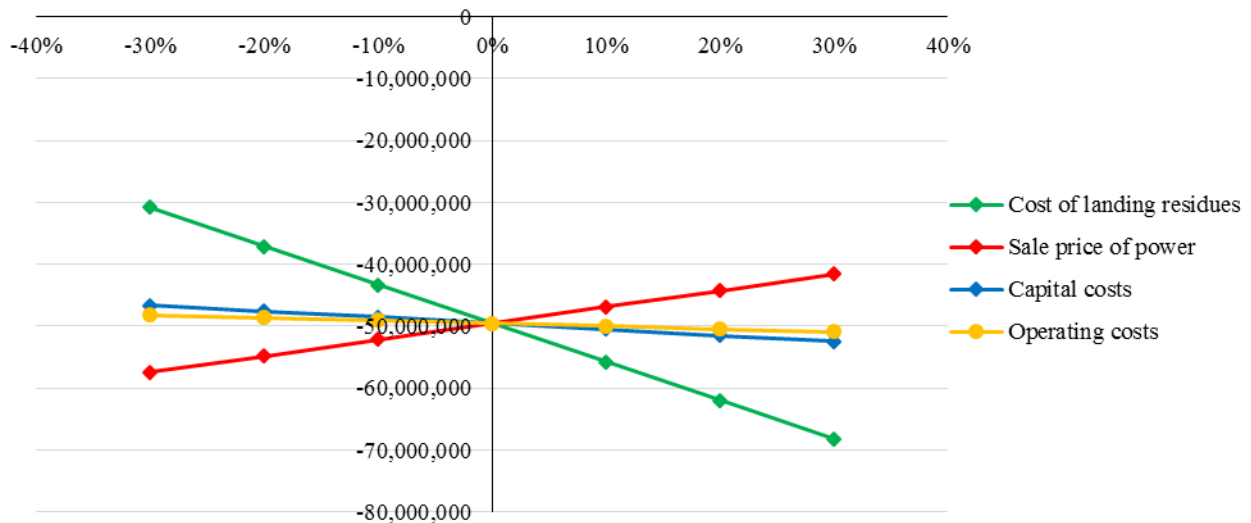


**Figure 67. Sensitivity analysis for using Poihipi Rd condensate as boiler feed water in Scenario 1**

### 6.3.2 Scenario 2

The results from the process modelling, energy analysis, and economic evaluation for using Poihipi Rd condensate as boiler feed water to generate additional IP steam for the Wairakei Power Plant

in Scenario 2 is displayed in Table 32. The NPV for the 30 year plant life of the hybrid configuration was calculated as -\$62 million, and requires a \$9.6 million capital investment.

**Table 32. Results for generating steam from Poihipi Rd condensate in Scenario 2**

<b>Biomass input</b>	<i>t/h</i>	15.6
	<i>MW</i>	41.7
<b>Gasifier IP steam requirement</b>	<i>t/h</i>	11.5
<b>IP steam generated in boiler</b>	<i>t/h</i>	52.7
<b>Net IP steam generation</b>	<i>t/h</i>	41.2
<b>Average power generation from generated steam</b>	<i>MW</i>	2.0
<b>Parasitic load from additional equipment</b>	<i>MW</i>	0.3
<b>Net average power generation</b>	<i>MW</i>	1.7
<b>Energy efficiency</b>	%	4.1
<b>Installed capital costs</b>	\$	9,546,633
<b>Net present value for 30 year plant life</b>	\$	-62,138,611

The breakdown of the installed capital costs is displayed in Figure 68. There is no cost associated with returning steam turbines to service, as all of the steam generated in the boiler is only used in the LP turbine G7, which is already in service.

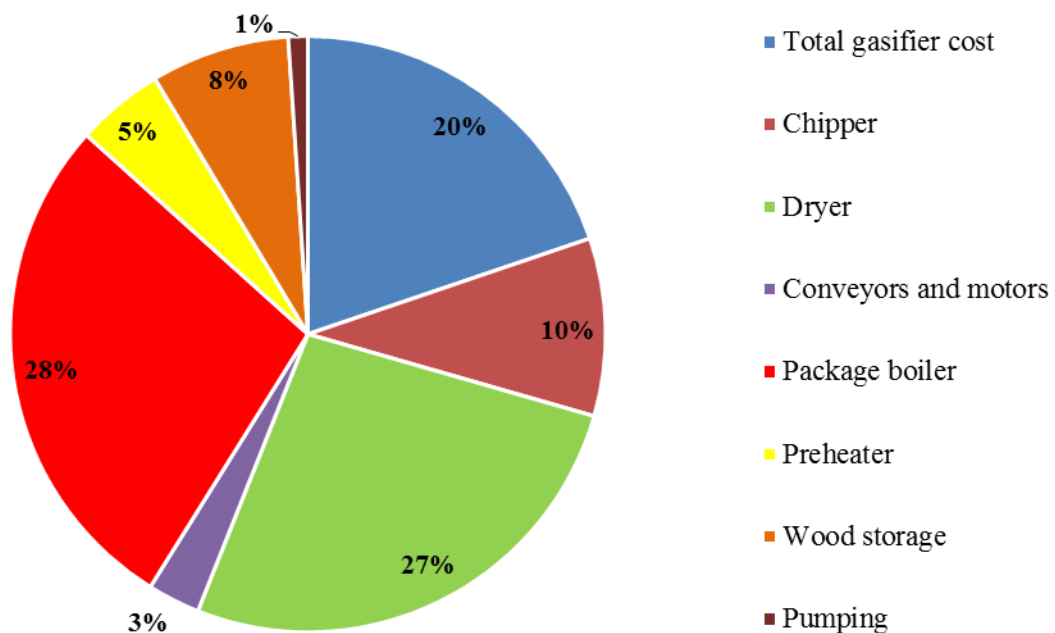


**Figure 68. The installed capital cost breakdown for using Poihipi Rd condensate as boiler feed water in Scenario 2**

The cumulative discounted cash flows for this project are displayed in Figure 69. Similar to in Scenario 1, the project is not expected to become revenue positive at any point in the life of the hybrid plant.

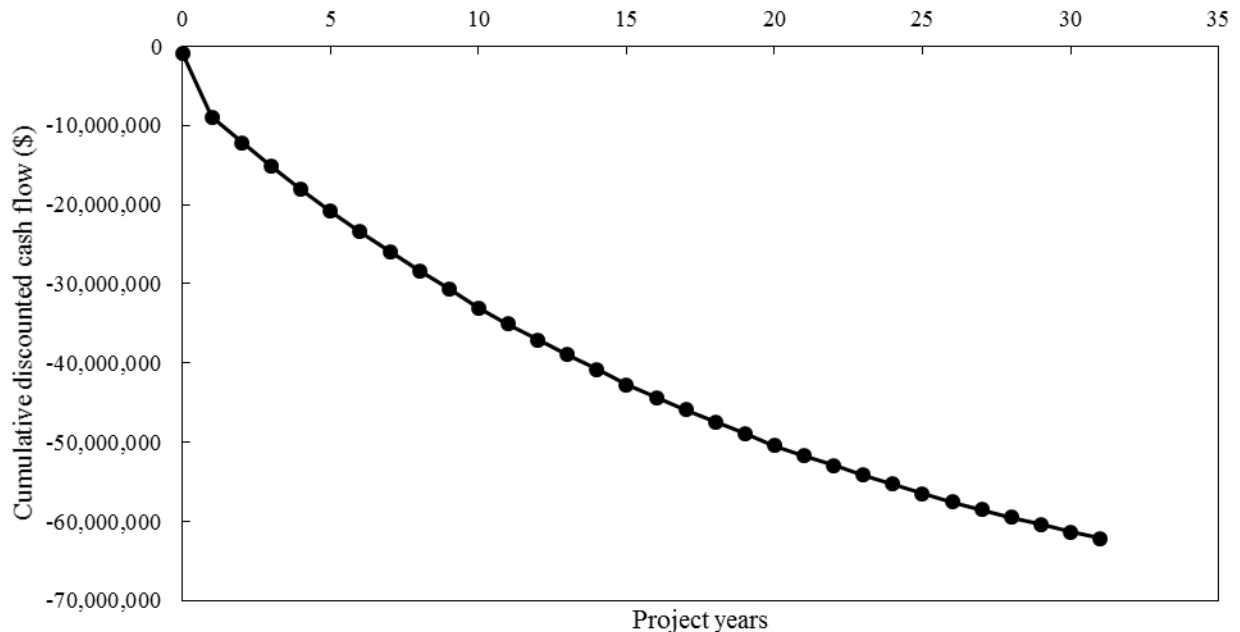


**Figure 69. The cumulative discounted cash flow for using Poihipi Rd condensate as boiler feed water in Scenario 2**

A summary of the cash flows for the implantation of this project is displayed in Table 33.

**Table 33. The cash flow summary for using Poihipi Rd condensate as boiler feed water in Scenario 2, all values given in \$1000's**

Year	Capital Cost	Revenue	Operating costs	Cost of biomass	Income tax	Free Cash flow
0	-888	0	0	0	0	-888
1	-8659	0	0	0	0	-8659
2	0	1063	-34	-6135	1451	-3656
3	0	1095	-35	-6250	1495	-3696
4	0	1135	-36	-6368	1517	-3752
5	0	1162	-118	-6488	1566	-3878
6	0	1191	-121	-6611	1593	-3948
7	0	1222	-125	-6736	1621	-4018
8	0	1255	-128	-6864	1648	-4089
9	0	1277	-132	-6994	1680	-4170
10	0	1264	-815	-7127	1912	-4766
20	0	1377	-1095	-8612	2374	-5956
30	0	1561	-1472	-10428	2937	-7402

The sensitivity analysis from Scenario 2 is displayed in Figure 70. The reduced power generation for this configuration in Scenario 2 causes the value for the price of power to have a smaller impact on the NPV of the project than in the other scenarios.



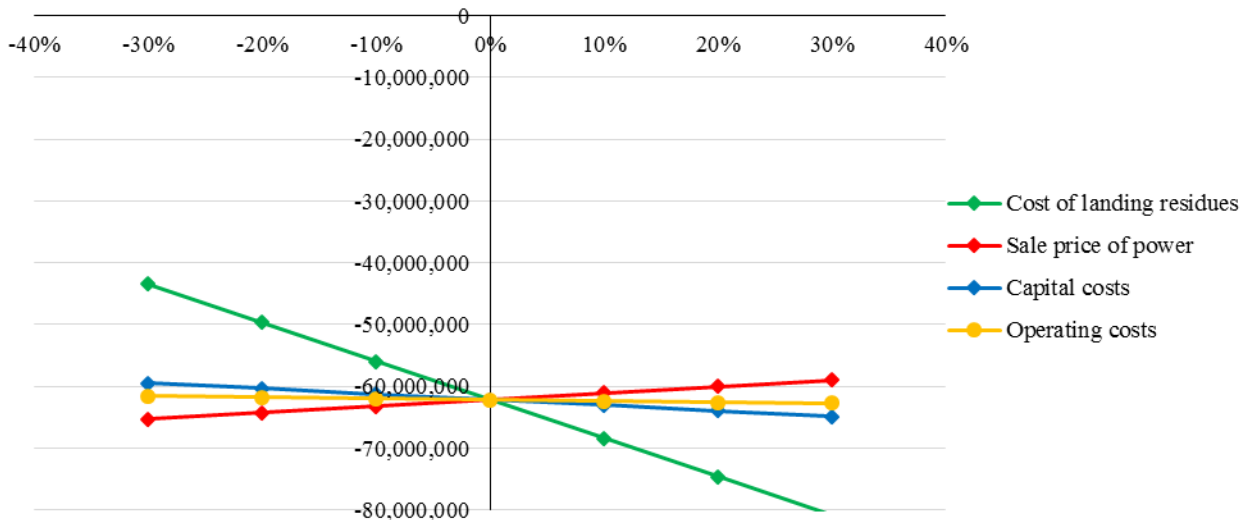


Figure 70. Sensitivity analysis for using Poihipi Rd condensate as boiler feed water in Scenario 2

### 6.3.3 Scenario 3

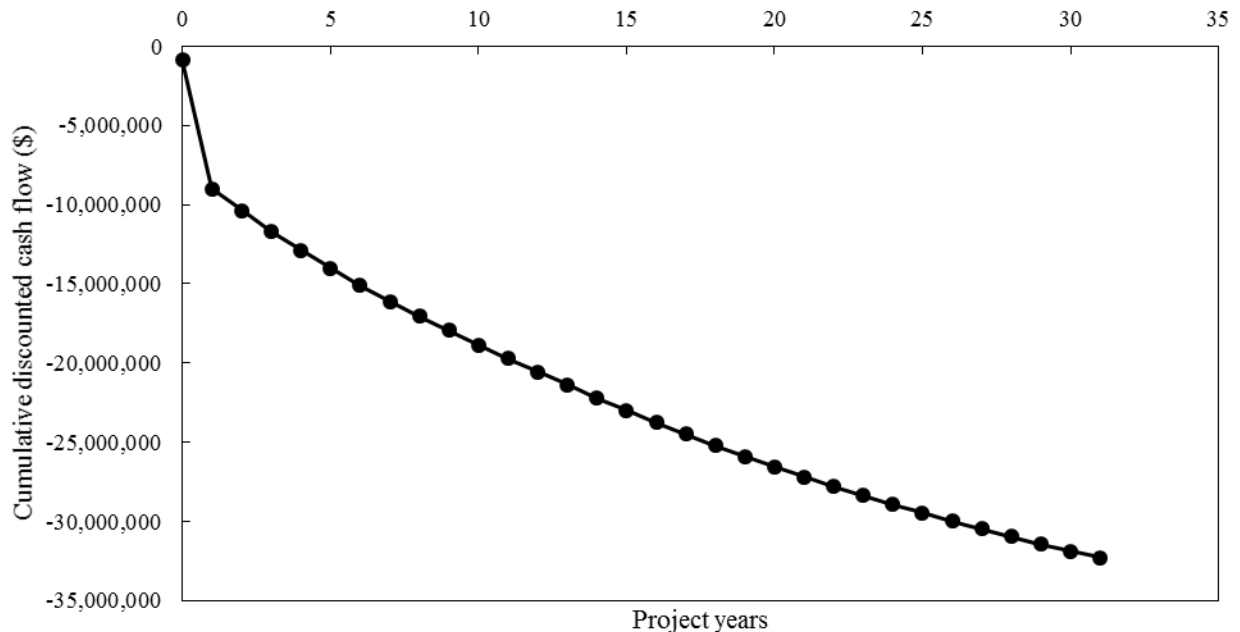
The results from the process modelling, energy analysis, and economic evaluation for using Poihipi Rd condensate as boiler feed water to generate additional IP steam for the Wairakei Power Plant in Scenario 3 is displayed in Table 34. The NPV of this project was found to be -\$32 million for the 30 year plant life, and required a \$9.6 million investment.

Table 34. Results for generating steam from Poihipi Rd condensate in Scenario 1

<b>Biomass input</b>	<i>t/h</i>	15.6
	<i>MW</i>	41.7
<b>Gasifier IP steam requirement</b>	<i>t/h</i>	11.5
<b>IP steam generated in boiler</b>	<i>t/h</i>	52.7
<b>Net IP steam generation</b>	<i>t/h</i>	41.2
<b>Average power generation from generated steam</b>	<i>MW</i>	6.5
<b>Parasitic load from additional equipment</b>	<i>MW</i>	0.3
<b>Net average power generation</b>	<i>MW</i>	6.2
<b>Energy efficiency</b>	%	14.8
<b>Installed capital costs</b>	\$	9,546,633
<b>Net present value for 30 year plant life</b>	\$	-32,281,561

The installed capital costs and the distribution of the installed costs is the same in Scenario 3 as in Scenario 2, and therefore, the capital cost breakdown can be seen in Figure 68.

The cumulative discounted cash flows for this project can be seen in Figure 71. Though Scenario 3 resulted in the highest NPV of the three scenarios for this configuration, the additional power generation was not sufficient to result in the project becoming revenue positive at any point in the hybrid plants operation.



**Figure 71. The cumulative discounted cash flow for using Poihipi Rd condensate as boiler feed water in Scenario 3**

A summary of the cash flows for the implantation of this project is displayed in Table 35.

**Table 35. The cash flow summary for using Poihipi Rd condensate as boiler feed water in Scenario 3, all values given in \$1000's**

Year	Capital Cost	Revenue	Operating costs	Cost of biomass	Income tax	Free Cash flow
0	-888	0	0	0	0	-888
1	-8659	0	0	0	0	-8659
2	0	3895	-34	-6135	658	-1616
3	0	4012	-35	-6250	678	-1595
4	0	4159	-36	-6368	671	-1575
5	0	4260	-37	-6488	676	-1589
6	0	4367	-38	-6611	681	-1602
7	0	4480	-39	-6736	685	-1611
8	0	4599	-41	-6864	687	-1618
9	0	4680	-42	-6994	701	-1654
10	0	4632	-43	-7127	753	-1786
20	0	5047	-58	-8612	1056	-2567
30	0	5721	-78	-10428	1382	-3404

The sensitivity analysis for this project is displayed in Figure 72. The relatively large amount of power generated for this configuration in Scenario 3 served to increase the sensitivity of the NPV of the project to the price of power.

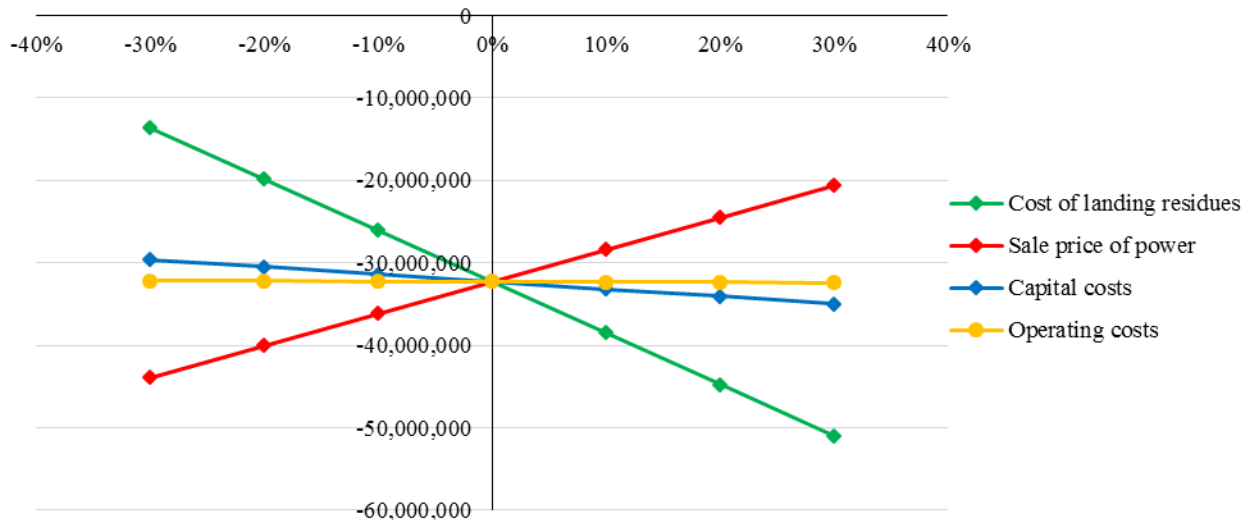


Figure 72. Sensitivity analysis for using Poihipi Rd condensate as boiler feed water in Scenario 1

## 6.4 Creating Additional IP Steam by Boiling IP SGW

Even after optimization was performed on the size of the gasifier in order to find the most economical sized plant, no size of the hybrid plant resulted in a recovery of the initial investment. Due to this, the same flowrate of biomass was selected as for the configuration using the Poihipi Rd condensate as boiler feed water for a direct comparison between these two configurations. This resulted in a 42MW gasification plant based on the thermal input of the biomass.

### 6.4.1 Scenario 1

The results of the process modelling, energy analysis, and economic evaluation for boiling the IP SGW from FP14 is displayed in Table 36 for Scenario 1. The project had a NPV of -\$44 million for the 30 year hybrid plant life, and required a capital investment of \$9 million.

Table 36. Results for generating steam using IP SGW from FP14 in Scenario 1

<b>Biomass input</b>	<i>t/h</i>	15.6
	<i>MW</i>	41.7
<b>Gasifier IP steam requirement</b>	<i>t/h</i>	11.5
<b>IP steam generated in boiler</b>	<i>t/h</i>	56.1
<b>Net IP steam generation</b>	<i>t/h</i>	44.6
<b>Average amount of bypassing steam</b>	<i>t/h</i>	88
<b>Average power generation from generated and bypassing steam</b>	<i>MW</i>	4.9
<b>Parasitic load from additional equipment</b>	<i>MW</i>	0.3
<b>Net average power generation</b>	<i>MW</i>	4.6
<b>Energy efficiency</b>	%	11.0
<b>Installed capital costs</b>	\$	9,019,905
<b>Net present value for 30 year plant life</b>	\$	-44,310,228

The breakdown of the installed capital costs for this project is displayed in Figure 73. The boiler, dryer, and gasifier were seen to be the most expensive pieces of equipment.

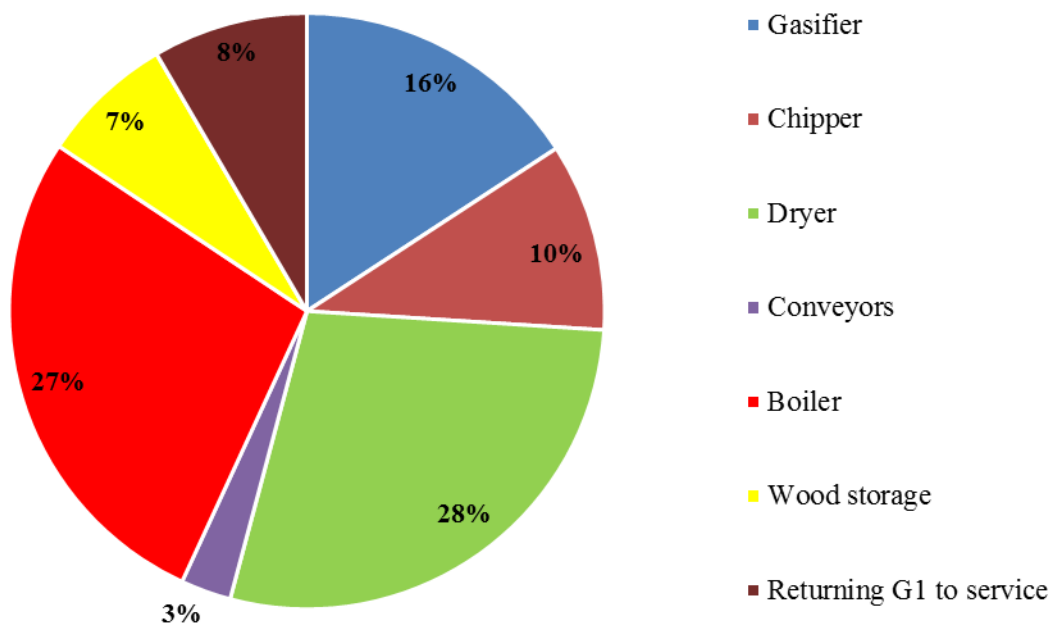


**Figure 73. The breakdown of the installed capital costs for using IP SGW from FP14 to generate additional steam in Scenario 1**

The cumulative discounted cash flow for generating additional steam from FP14 IP SGW is displayed in Figure 74. As can be seen, this configuration does not become revenue positive over the 30 year life of the hybrid plant.

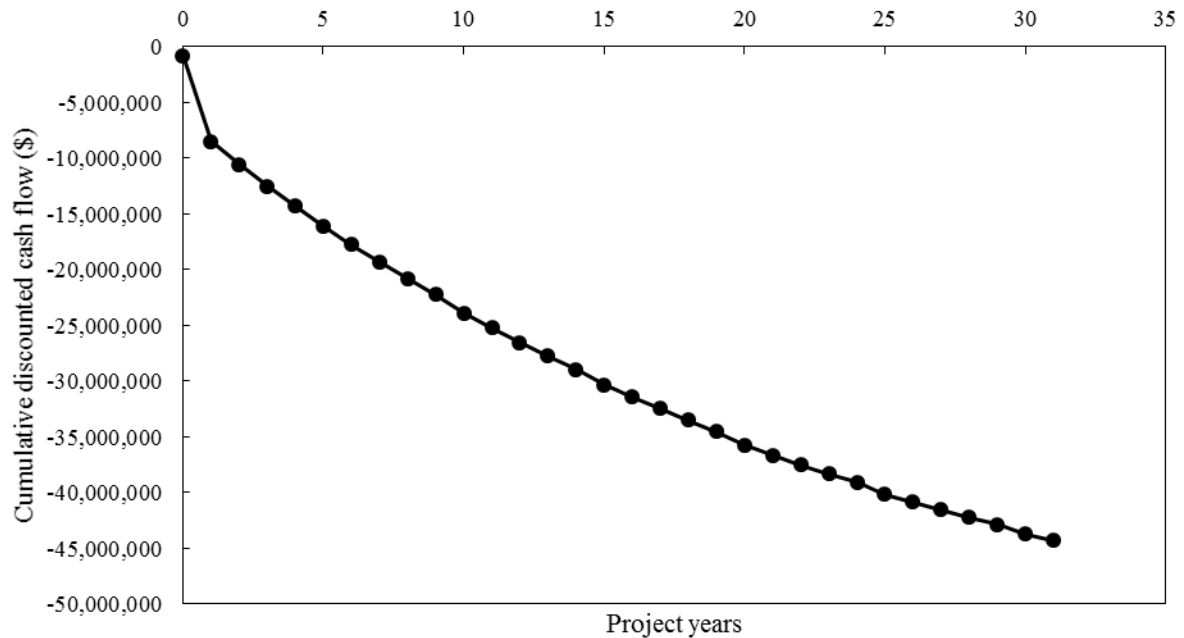


**Figure 74. The cumulative discounted cash flows for generating additional steam by boiling IP SGW from FP14 in Scenario 1**

A summary of the cash flows for the implantation of this project is displayed in Table 37.

**Table 37. The cash flow summary for boiling IP SGW from FP14 in Scenario 1, all values given in \$1000's**

Year	Capital Cost	Income	Operating costs	Cost of biomass	Income tax	Free Cash flow
0	-814	0	0	0	0	-814
1	-8206	0	0	0	0	-8206
2	0	2883	-74	-6135	955	-2371
3	0	2970	-76	-6250	987	-2370
4	0	3078	-78	-6368	990	-2378
5	0	3153	-161	-6488	1026	-2470
6	0	3232	-166	-6611	1040	-2505
7	0	3316	-171	-6736	1053	-2538
8	0	3404	-176	-6864	1065	-2571
9	0	3464	-181	-6994	1086	-2625
10	0	3428	-865	-7127	1325	-3239
20	0	3735	-1849	-8612	1930	-4795
30	0	4234	-3224	-10428	2684	-6734

The sensitivity analysis for this project is displayed in Figure 75. This project was seen to be relatively insensitive to manipulations of the capital and operating costs, as these were relatively small compared to the cost of landing residues, and the value of the additional power generated.

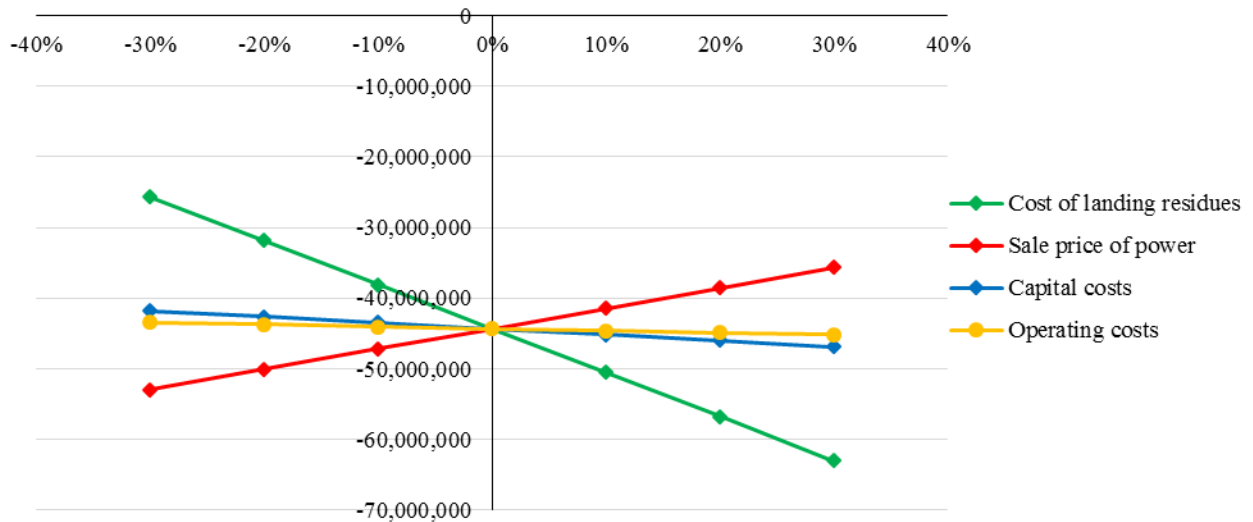


Figure 75. Sensitivity analysis for generating additional steam fusing IP SGW from FP14 as feed water in Scenario 1

#### 6.4.2 Scenario 2

The results of the process modelling, energy analysis, and economic evaluation for boiling the IP SGW from FP14 is displayed in Table 38 for Scenario 2. The NPV of the project was found to be -\$58 million for the 30 year hybrid plant life, and required a capital investment of \$8.3 million.

Table 38. Results for generating steam using IP SGW from FP14 in Scenario 2

<b>Biomass input</b>	<i>t/h</i>	15.6
	<i>MW</i>	41.7
<b>Gasifier IP steam requirement</b>	<i>t/h</i>	11.5
<b>IP steam generated in boiler</b>	<i>t/h</i>	56.1
<b>Net IP steam generation</b>	<i>t/h</i>	44.6
<b>Average power generation from generated steam</b>	<i>MW</i>	2.3
<b>Parasitic load from additional equipment</b>	<i>MW</i>	0.3
<b>Net average power generation</b>	<i>MW</i>	2.0
<b>Energy efficiency</b>	%	4.8
<b>Installed capital costs</b>	\$	8,259,905
<b>Net present value for 30 year plant life</b>	\$	-58,950,702

The breakdown of the installed capital costs is displayed in Figure 76. There was a reduction in the capital costs for this configuration in Scenario 2 compared to Scenario 1, as the boiler did not generated additional IP steam sufficient to justify the return of the IP turbine G1 to service.

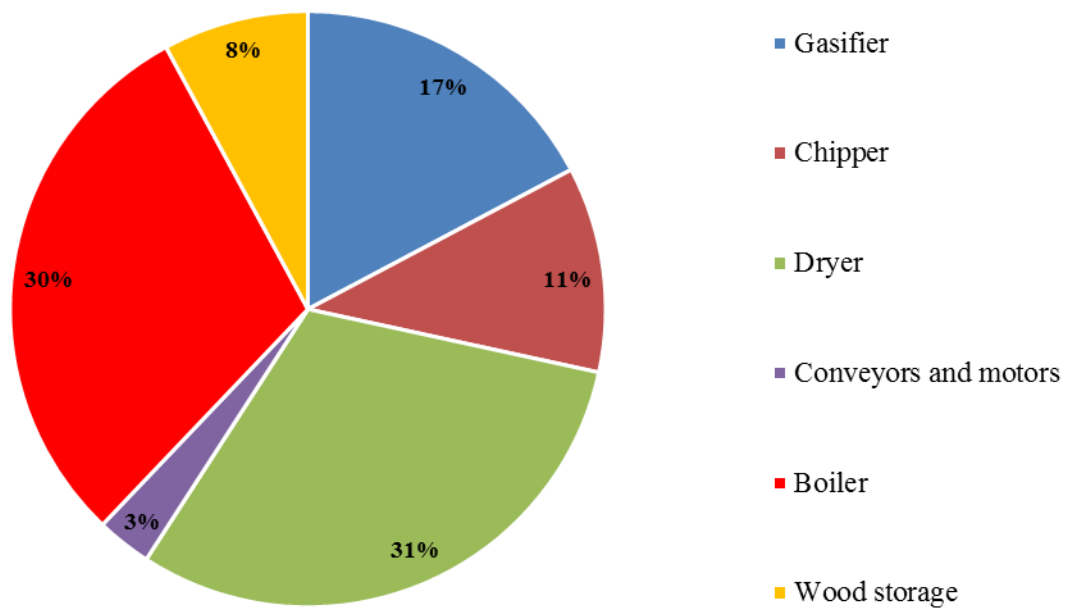


**Figure 76. The breakdown of the installed capital costs for using IP SGW from FP14 to generate additional steam in Scenario 2 and Scenario 3**

The cumulative discounted cash flows are displayed in Figure 77. This project is not expected to become revenue positive at any point.

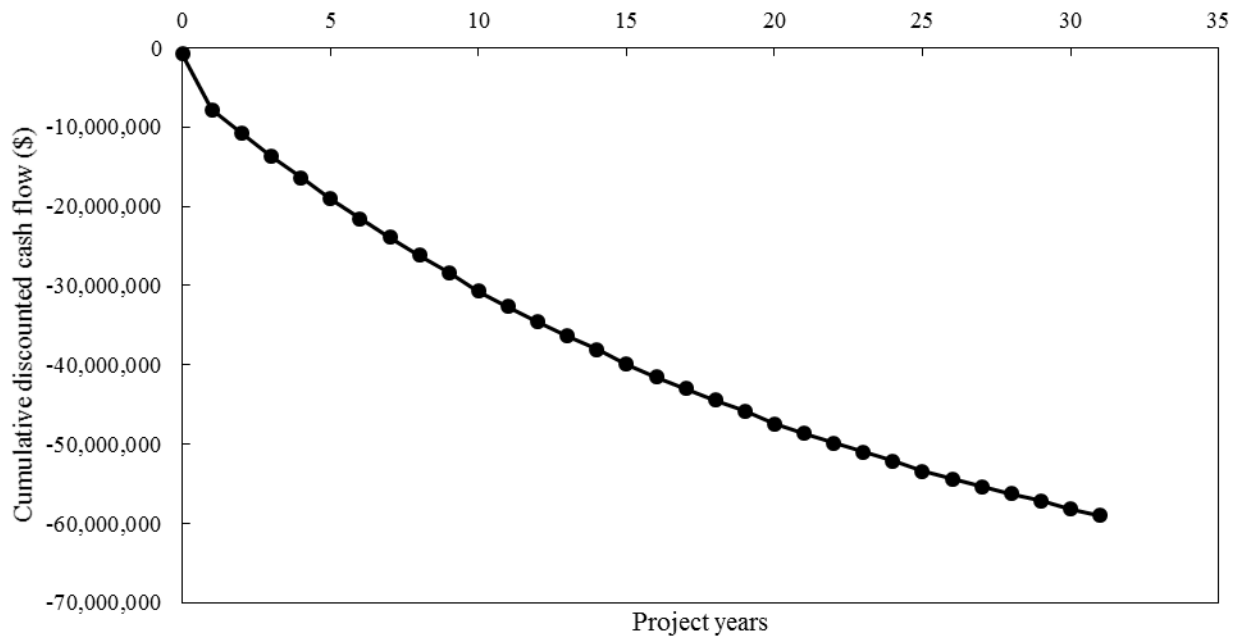


**Figure 77. The cumulative discounted cash flows for generating additional steam by boiling IP SGW from FP14 in Scenario 2**

A summary of the cash flows for the implantation of this project is displayed in Table 39.

**Table 39. The cash flow summary for boiling IP SGW from FP14 in Scenario 2, all cash values given in \$1000's**

Year	Capital Cost (\$)	Income (\$/year)	Operating costs (\$/year)	Cost of biomass (\$/year)	Income tax \$/year	Income after tax \$/year	Free Cash flow \$/year
0	-814	0	0	0	0	0	-814
1	-7446	0	0	0	0	0	-7446
2	0	1265	0	-6135	1383	-3557	-3486
3	0	1303	0	-6250	1425	-3665	-3522
4	0	1351	0	-6368	1445	-3715	-3572
5	0	1384	-80	-6488	1492	-3836	-3693
6	0	1419	-83	-6611	1517	-3901	-3758
7	0	1455	-85	-6736	1542	-3966	-3824
8	0	1494	-88	-6864	1568	-4032	-3889
9	0	1520	-90	-6994	1598	-4109	-3966
10	0	1505	-772	-7127	1830	-4706	-4564
20	0	1639	-1724	-8612	2475	-6364	-6221
30	0	1859	-3056	-10428	3295	-8473	-8330

The sensitivity analysis for this project is displayed in Figure 78. The reduction of power generation in this scenario from Scenario 1 served to decrease the sensitivity of the NPV of this project to changes in the wholesale price of power.

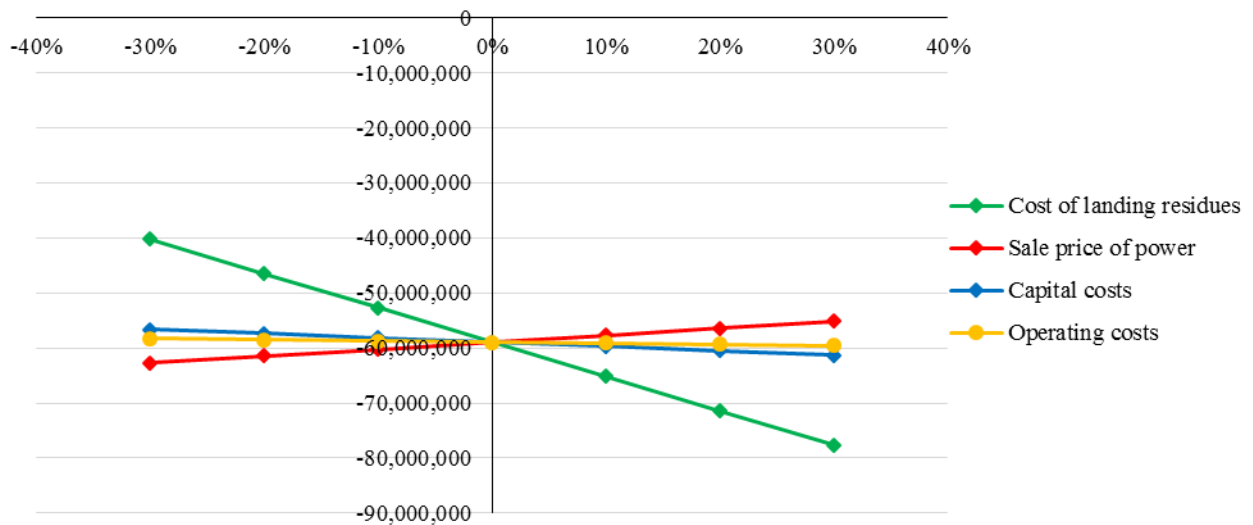


**Figure 78. Sensitivity analysis for using Poihipi Rd condensate as boiler feed water in Scenario 2**



### 6.4.3 Scenario 3

The results of the process modelling, energy analysis, and economic evaluation for boiling the IP SGW from FP14 is displayed in Table 40 for Scenario 3. This project was found to have a NPV of -\$27 million, and requires a capital investment of \$8.3 million.

**Table 40. Results for generating steam using IP SGW from FP14 in Scenario 3**

<b>Biomass input</b>	<i>t/h</i>	15.6
	<i>MW</i>	41.7
<b>Gasifier IP steam requirement</b>	<i>t/h</i>	11.5
<b>IP steam generated in boiler</b>	<i>t/h</i>	56.1
<b>Net IP steam generation</b>	<i>t/h</i>	44.6
<b>Average power generation from generated steam</b>	<i>MW</i>	7.1
<b>Parasitic load from additional equipment</b>	<i>MW</i>	0.3
<b>Net average power generation</b>	<i>MW</i>	6.8
<b>Energy efficiency</b>	%	16.2
<b>Installed capital costs</b>	\$	8,259,905
<b>Net present value for 30 year plant life</b>	\$	-27,232,629

The same process equipment is required in this scenario as in Scenario 2, the cost breakdown is therefore displayed in Figure 76.

The cumulative discounted cash flows are displayed in Figure 79. Similar to the other steam flow scenarios, this configuration is not expected to become revenue positive at any point in the hybrid plants operation.

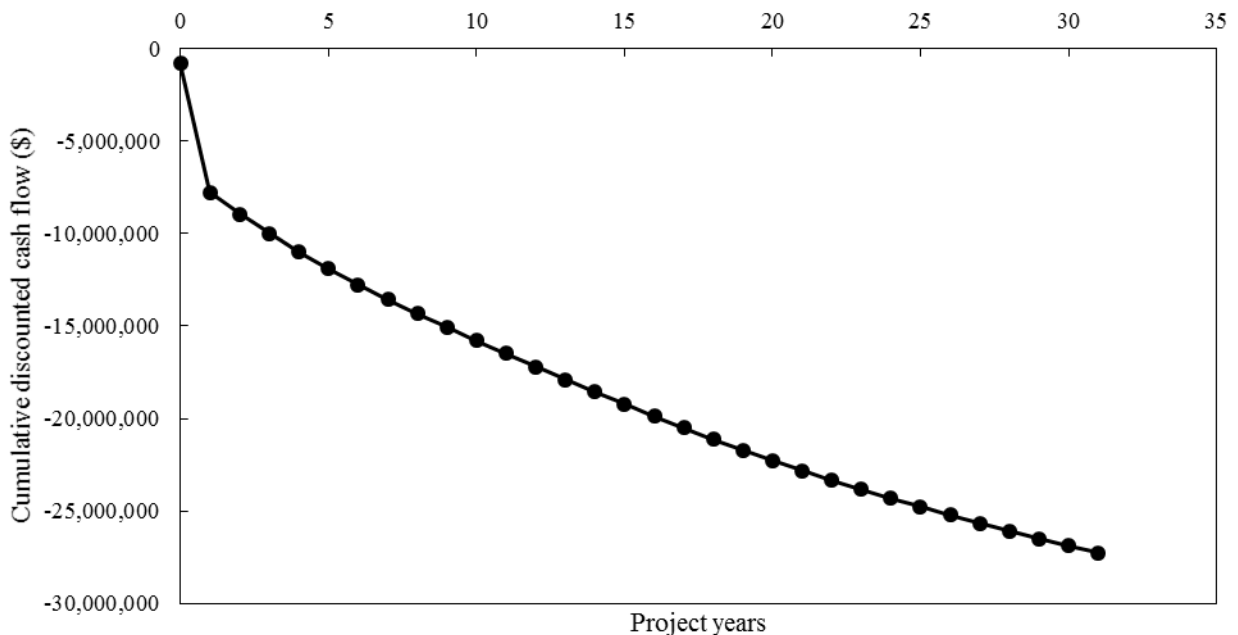


**Figure 79. The cumulative discounted cash flows for generating additional steam by boiling IP SGW from FP14 in Scenario 3**

A summary of the cash flows for the implantation of this project is displayed in Table 41.

**Table 41. The cash flow summary for boiling IP SGW from FP14 in Scenario 3, all values given in \$1000's**

Year	Capital Cost	Income	Operating costs	Cost of biomass	Income tax	Free Cash flow
0	-814	0	0	0	0	-814
1	-7446	0	0	0	0	-7446
2	0	4243	0	-6135	550	-1342
3	0	4371	0	-6250	566	-1313
4	0	4531	0	-6368	555	-1283
5	0	4641	0	-6488	557	-1290
6	0	4757	0	-6611	559	-1295
7	0	4880	0	-6736	560	-1296
8	0	5010	0	-6864	559	-1295
9	0	5098	0	-6994	571	-1325
10	0	5046	0	-7127	623	-1458
20	0	5498	0	-8612	912	-2202
30	0	6232	0	-10428	1215	-2981

The sensitivity analysis is displayed in Figure 80. The increase in the power generation in this scenario results in a higher sensitivity of the NPV of the project to changes in the wholesale price of power.

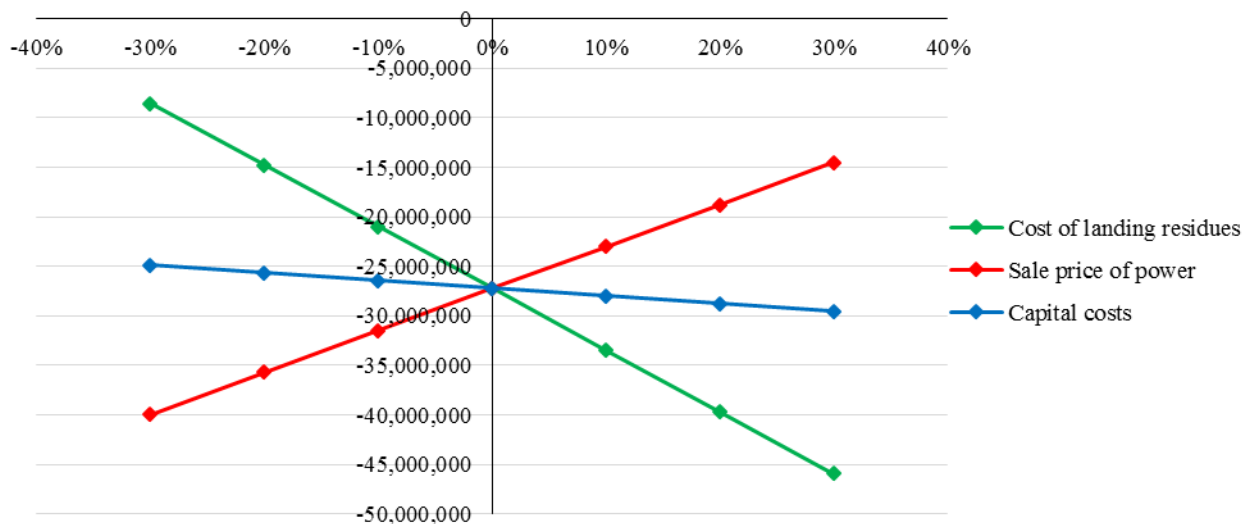


**Figure 80. Sensitivity analysis for using Poihipi Rd condensate as boiler feed water in Scenario 3**

## 6.5 Heating Additional SGW to Utilize in the Binary Plant

Optimization was performed to find the most economic sized gasification plant to heat and supply additional SGW to the Wairakei Binary Plant. However, as for the other configurations, it was found that there was no limit on the SGW that would result in a recovery of the capital investment for the hybrid configuration after 30 years. Therefore, in order to compare the two applicable scenarios for this configuration, it was assumed that there would be no limit on the amount of SGW to be heated other than those associated with the amount available for use in T-line, and the maximum of 2800 t/h for the total SGW flow to the Wairakei Binary Plant. This configuration was only evaluated for Scenario 1 and Scenario 2, as this configuration does not produce additional steam, and therefore the unused capacity of the Wairakei steam turbines has no effect on the power generation or plant economics of this configuration.

### 6.5.1 Scenario 1

The results of the process modelling, energy analysis, and economic evaluation for heating SGW to generate additional power from the Binary Plant is displayed in Table 42 for Scenario 1. This project resulted in an NPV of -\$17 million for the 30 year life of the hybrid plant, and required a \$7.8 million capital investment.

**Table 42. Results for generating additional power by heating makeup SGW for the Binary Plant for Scenario 1**

<b>Average biomass input</b>	<i>t/h</i>	3.4
	<i>MW</i>	9.3
<b>Maximum biomass input</b>	<i>t/h</i>	6.2
	<i>MW</i>	16.2
<b>Average IP steam requirement for the gasifier</b>	<i>t/h</i>	2.5
<b>Power loss from gasifier steam use</b>	<i>MW</i>	0.22
<b>Average SGW added to the Binary Plant</b>	<i>t/h</i>	267
<b>Average additional power generation from the Binary Plant</b>	<i>MW</i>	1.75
<b>Parasitic load from additional equipment</b>	<i>MW</i>	0.3
<b>Net average power generation</b>	<i>MW</i>	1.43
<b>Average energy efficiency</b>	%	15.5
<b>Installed capital costs</b>	\$	7,767,617
<b>Net present value for 30 year plant life</b>	\$	-17,133,272

The breakdown of the installed capital costs is displayed in Figure 81. As can be seen, the furnace is expected to be the most expensive piece of process equipment.

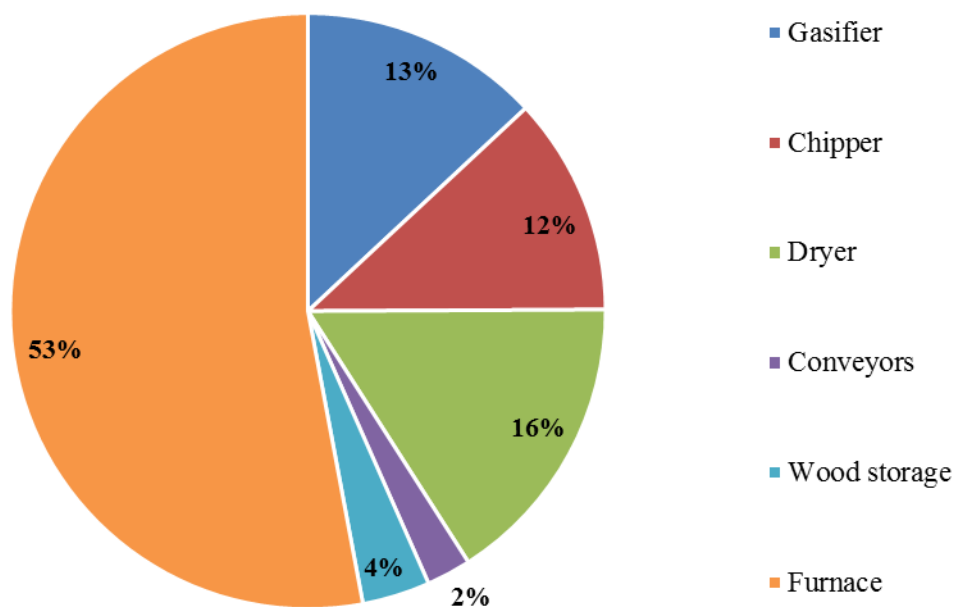


**Figure 81. The breakdown of the installed capital costs for generating additional power by heating makeup SGW for the Binary Plant**

The cumulative discounted cash flows are displayed in Figure 82. This project is seen to never become revenue positive.

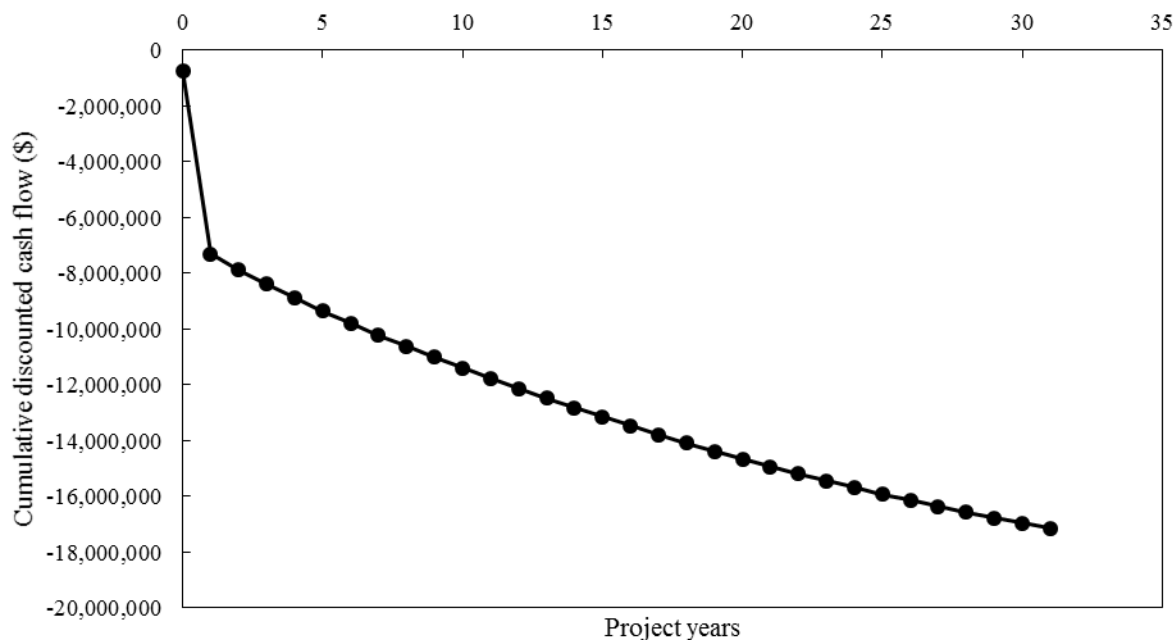


**Figure 82. The cumulative discounted cash flows for generating additional power by heating makeup SGW for the Binary Plant for Scenario 1**

A summary of the cash flows for the implantation of this project is displayed in Table 43.

**Table 43. Cash flow analysis for generating additional power by heating makeup SGW for the Binary Plant in Scenario 1, all values given in \$1000's**

Year	Capital Cost	Income	Operating costs	Cost of biomass	Income tax	Free Cash flow
0	-723	0	0	0	0	-723
1	-7045	0	0	0	0	-7045
2	0	904	-595	-1219	269	-640
3	0	931	-612	-1242	287	-636
4	0	965	-631	-1265	290	-641
5	0	988	-650	-1289	295	-655
6	0	1013	-669	-1313	300	-669
7	0	1039	-689	-1338	306	-682
8	0	1067	-710	-1363	311	-696
9	0	1086	-731	-1389	319	-716
10	0	1075	-753	-1416	335	-759
20	0	1171	-1012	-1711	464	-1089
30	0	1327	-1360	-2072	618	-1487

The sensitivity analysis is displayed in Figure 83. As can be seen, the NPV of the project is relatively insensitive to changes in the cost of landing residues, value of power, capital costs, and operating costs.

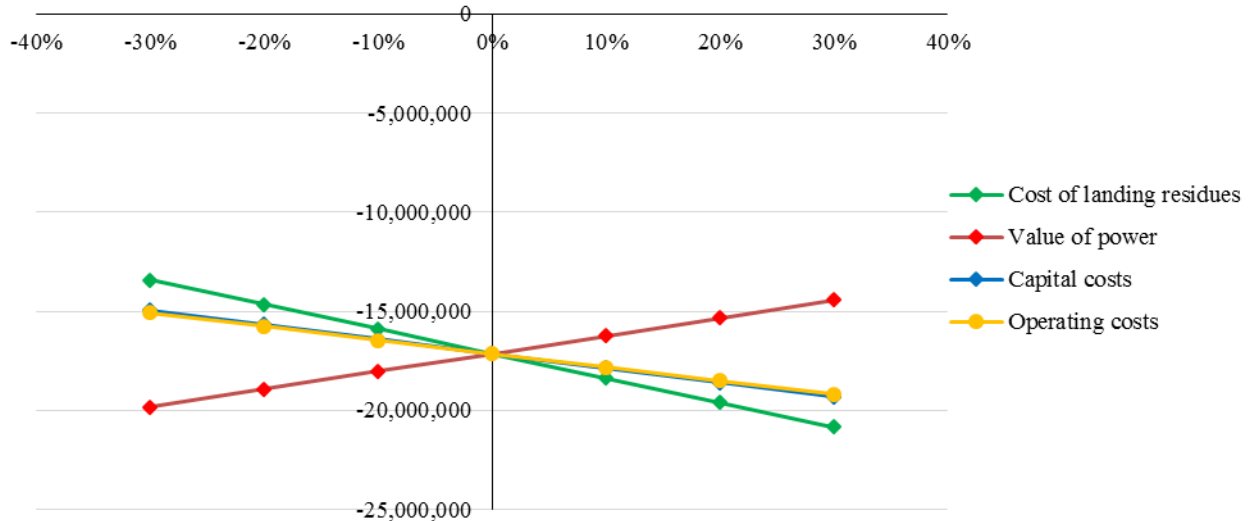


**Figure 83. Sensitivity analysis for generating additional power by heating makeup SGW for the Binary Plant for Scenario 1**

### 6.5.2 Scenario 2 & Scenario 3

The results of the process modelling, energy analysis, and economic evaluation for heating SGW to generate additional power from the Binary Plant is displayed in Table 44 for Scenario 2. This

project resulted in a NPV of -\$18 million for the 30 year life of the hybrid configuration, and required a capital investment of \$7.8 million.

The steam flow scenario was not seen affect the NPV of the project as strongly as in the other hybrid configurations. This is due to the additional power generation coming from the binary plant and not by increasing the steam supply to Wairakei. Therefore only the power losses from steam used in the biomass gasifier are affected by changes in the steam flow to Wairakei.

**Table 44. Results for generating additional power by heating makeup SGW for the Binary Plant for Scenario 2**

<b>Average biomass input</b>	<i>t/h</i>	3.4
	<i>MW</i>	9.3
<b>Average biomass input</b>	<i>t/h</i>	6.2
	<i>MW</i>	16.2
<b>Average IP steam use by the gasifier</b>	<i>t/h</i>	2.5
<b>Power loss from gasifier steam use</b>	<i>MW</i>	0.38
<b>Average SGW added to the Binary Plant</b>	<i>t/h</i>	267
<b>Average additional power generation from the Binary Plant</b>	<i>MW</i>	1.75
<b>Parasitic load from additional equipment</b>	<i>MW</i>	0.09
<b>Net average power generation</b>	<i>MW</i>	1.28
<b>Average energy efficiency</b>	%	13.8
<b>Installed capital costs</b>	\$	7,769,678
<b>Net present value for 30 year plant life</b>	\$	-18,119,856

The breakdown of the installed capital costs is the same for Scenario 2 as it is for Scenario 1, and is displayed in Figure 81. The cumulative discounted cash flows are displayed in Figure 84.

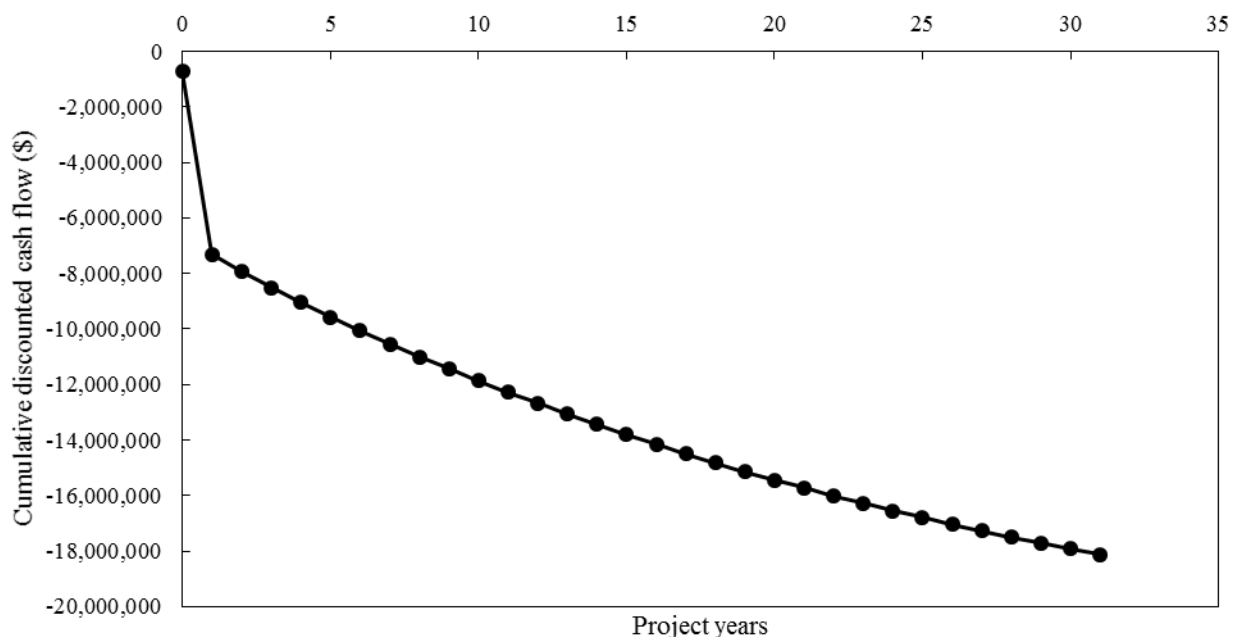


**Figure 84. The cumulative discounted cash flows for generating additional power by heating makeup SGW for the Binary Plant for Scenario 2**

A summary of the cash flows for the implantation of this project is displayed in Table 45.

**Table 45. Cash flow analysis for generating additional power by heating makeup SGW for the Binary Plant in Scenario 2 and Scenario 3, all cash values given in \$1000's**

Year	Capital Cost	Income	Operating costs	Cost of biomass	Income tax	Free Cash flow
0	-723	0	0	0	0	-723
1	-7045	0	0	0	0	-7045
2	0	806	-595	-1219	296	-711
3	0	830	-612	-1242	316	-708
4	0	861	-631	-1265	319	-716
5	0	882	-650	-1289	325	-732
6	0	904	-669	-1313	331	-748
7	0	927	-689	-1338	337	-763
8	0	952	-710	-1363	343	-779
9	0	969	-731	-1389	352	-800
10	0	959	-753	-1416	368	-842
20	0	1045	-1012	-1711	499	-1180
30	0	1184	-1360	-2072	658	-1590

The sensitivity analysis is displayed in Figure 85, as in Scenario 1, this project is relatively insensitive to manipulations performed in the sensitivity analysis compared to the other hybrid configurations.

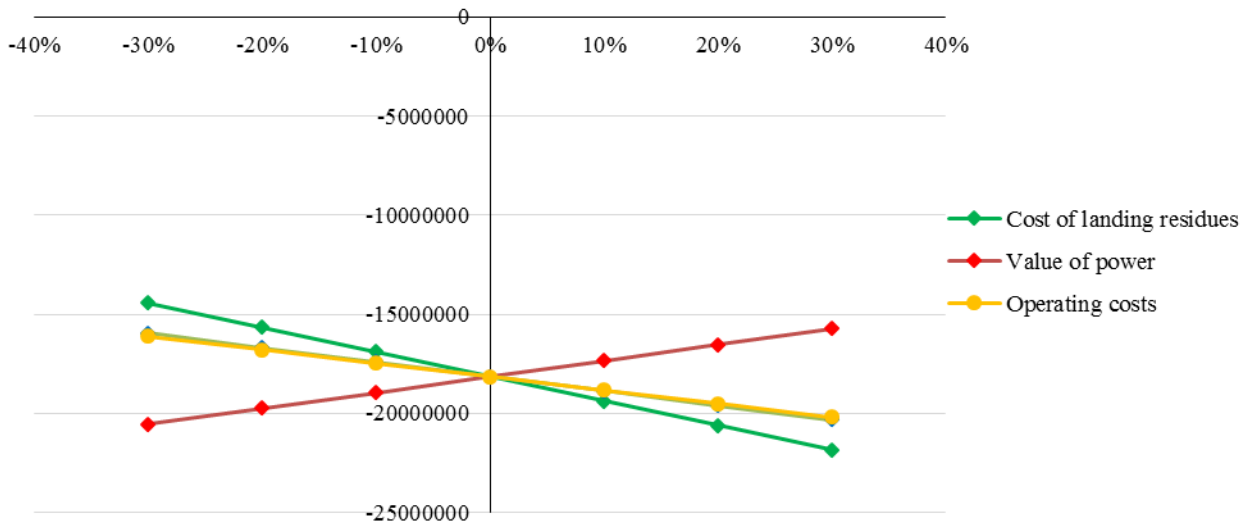


**Figure 85. Sensitivity analysis for generating additional power by heating makeup SGW for the Binary Plant for Scenario 2**

## **6.6 Discussion**

### **6.6.1 Biomass Gasification**

The cold gas efficiency of the dual fluidized bed gasifier is seen to be relatively high compared to other gasifiers of the same type, due to the use of geothermal IP steam in the DFB gasifier. This high efficiency indicates that the integration of geothermal and gasification technologies may be a viable method to increase the efficiency of biomass gasifiers using steam as the gasification agent. However, this cold gas efficiency does not take into account the loss of power generation caused by the reduction of steam input to the steam turbines. While this is taken into account in the overall biomass-electricity efficiencies for the plant configurations, the cold gas efficiencies of 79-84% do not accurately represent all of the inputs for gasification. By using the enthalpy of the IP steam, at 2.744 MJ/kg, the cold gas efficiency of the gasifier drops to 69% in the superheating geothermal steam configuration, and 65% in all other configurations. This is a more accurate representation of the actual performance of the gasifier, and is within the expected range for cold gas efficiencies given by Devi, Ptasiński, and Janssen, of 60-70% [98].

The dual fluidized bed (DFB) gasifier was selected for this project, due in part to the experience that the Department of Chemical and Process Engineering at the University of Canterbury has with using this type of gasifier. This allowed use of sophisticated heat and material models for biomass gasification, which would have been outside the scope of this project to create. However, as a major advantage of the DFB gasifier is the ability to create energy dense syngas which may be used to synthesize liquid fuels, it may be more favourable to use a different type of gasifier. An air blown gasifier produces less energy dense syngas, but would remove the need to utilize geothermal IP steam in the gasifier. However, the subsequent energy requirement for blowers or compressors for the air input to the gasifier, and the lower flame temperature from the dilute syngas may limit any benefits from using an air blown gasifier.

### **6.6.2 Hybrid Power Plant Energy Efficiency**

The energy efficiency of the hybrid plants was seen to be highly dependent on the amount of steam input to the Wairakei Power Plant. The presence of the bypassing IP steam in Scenario 1 served to increase the efficiency of every configuration. However, the configurations creating additional IP steam supply to Wairakei were seen to be the most efficient when the steam could be used in partially loaded turbines as in Scenario 3. The uncertainty associated with estimating the amount of steam input to Wairakei therefore has a corresponding uncertainty in the potential energy efficiency of the different hybrid configurations.

The net steam production in the hybrid configurations is also seen to greatly impact the plant efficiency. The no load flow of the steam turbines is seen to greatly impact the power generation capacity of the produced steam, as more steam is produced, the proportion required to satisfy the no load flow requirement decreases. This is of specific importance for the configuration boiling Poihipi Rd condensate, as there is a maximum of 54 t/h of condensate available, the resultant IP steam generation would not be large enough to satisfy the no load flow requirement for an unloaded



IP turbines. Therefore, there is an associated decrease of the power generation ability of the steam as it is throttled down to LP.

Due to the availability of bypassing steam in Scenario 1, additional power generation is possible without the implementation of a biomass gasifier if the IP steam turbine G1 is returned to service. Due to this, the energy efficiency of configurations that return the IP turbine G1 to service is seen to decrease as the size of the gasification plant increases. However, the method used to estimate the bypassing steam has a relatively large uncertainty associated with it, due to the accuracy of the steam flow measurements to Wairakei. Also, the elimination of the negative results for the expected bypassing steam may serve to overestimate the bypassing steam, as it reduced the effect of negatively deviated estimates but did not remove positively deviated estimates.

The superheating of the geothermal steam was found to have largest energy efficiency of the hybrid configurations. This configuration in Scenario 3 attained a comparable power generation efficiency to those for gasification gas engine and syngas combustion and steam generation power plants at similar plant sizes [99] However, the relatively high energy efficiency that was attained by this configuration in Scenario 3, at 29%, however requires very specific steam flows to Wairakei. Scenario 3 assumes that the steam flow to Wairakei has decreased to the point where the IP turbine G4 is partially loaded. There is a saving of 138 t/h of IP steam by modifying two of the MP turbines and the full load capacity of G4 is 241 t/h, 100 t/h of which is the no load flow requirement. Therefore there would need to be a geothermal steam flow to G4 within 100 – 103 t/h in order for the all additional IP steam to be utilized in G4 without contributing to the no load flow of the turbine. This range is broader for the configurations implementing a boiler, as they generate significantly less steam than is saved in the superheated geothermal steam configuration.

While each steam flow scenario was created to estimate the efficiencies of the hybrid plant configurations, they also show how the performance of these plants is expected to change throughout their life. As the steam flow to Wairakei is expected to decrease in coming years, there could be a continuous progression of the performance of the hybrid plants from Scenario 1 through Scenario 2 to Scenario 3, and potentially further into steam flow cases that were not investigated. However, with decreasing steam flow to Wairakei, steam turbines will be removed from service essentially reverting the case to one similar to Scenario 1, where the remaining turbines are fully loaded, and there is sporadic bypassing of additional steam.

The decreasing enthalpy of the geothermal reservoir may also serve to increase the SGW loading of the Wairakei Binary Plant without hybridization. As more SGW will be produced from the lower enthalpy two-phase fluid extracted from the reservoir, flow of SGW to the binary plant is likely to increase.

Typical power generation efficiencies for a gasification combustion and steam cycle plants are approximately 20% for a 10 MWe plant size [100]. This is seen to be higher than almost all of the hybrid configurations. It would be expected that a hybrid geothermal/gasification plant would have a higher efficiency than a gasification power plant [25]. As the gasifier cold gas efficiency is relatively high; the relatively low power generation efficiencies are therefore attributed to the design constraints associated with retrofitting the gasifier to an existing power plant.

### 6.6.3 Hybrid Power Plant Economic Assessment

The results from the economic assessment do not appear to be promising for the financial viability of any of the hybrid configurations. None of the hybrid configurations are seen to recover the initial capital investment from the hybridization of the Wairakei Geothermal System with a biomass gasifier. Only one configuration, the superheating of geothermal steam, is seen to be cash flow positive in any of the 30 years lives of the proposed hybrid plants, and this only occurs in Scenario 3, where the steam may be used in partially loaded IP and LP turbines, and this required specific steam flows to Wairakei.

There is significant uncertainty associated with some of the estimates for the capital costs for the implementation of the hybrid configurations, this is most apparent in the rough estimates for the cost of modifying the MP turbines to utilize superheated steam. The associated costs estimated from the FACT method may also be an overestimation for some of the process equipment, as these are estimated purely based on the major equipment costs. These associated costs may unrealistically inflate the installed cost of process equipment that has a large equipment cost, such as if expensive materials were used in the construction. The cost estimates for the minor materials, such as piping and electrical, at 60% of the major equipment cost, while potentially valid for the construction of new process plants, is likely an overestimation in this case; as the majority of the piping and electrical infrastructure required for the hybrid configurations is already present on the Wairakei site. However, as only the superheating of geothermal steam was seen to be cash flow positive, and this only in specific circumstances; the capital costs of the hybrid configurations is not seen to be the main factor which causes the retrofitting of the Wairakei Geothermal System with biomass gasification to be financially impractical.

The factors which were seen to consistently have the greatest impact on the NPV of the hybrid configurations were the price of electricity, and the cost of the landing residues. As estimates for the price of electricity were based on those used by Contact Energy, it is unlikely that, barring large disruption of the electricity market, these would have an associated uncertainty large enough to cause the hybrid configurations to become prudent investments. However, there is significant uncertainty attached to the estimation of the prices for the landing residues. As landing residues are not a commonly sold good, there is very little information for the expected cost of the landing residues. The price estimates were entirely based on those reported by Scion in their report on bioenergy options in New Zealand [66]. The method for inflating the cost of the landing residues based on the historical costs for pulp logs, while imperfect, will likely not misrepresent the inflation of the landing residues to the degree that would be required for any of the hybrid configurations to be economically viable. Similarly, it is unlikely that the wiggle factor used to increase the straight line distance to a more accurate travel distance would have an associated uncertainty large enough to cause any of the configurations to be economically viable. Therefore the cost of landing residues reported by Scion would need to significantly overestimate the true costs for delivered landing residues in order for retrofitting a biomass gasifier to become a prudent investment. The analysis performed into the expected cost of landing residues and the wholesale price of power also forecasted the price of the landing residues to increase at a greater rate than the value of power. This served to decrease the free cash flow of the hybrid configurations throughout the operational life of the hybrid plants.

As the performance of the biomass gasifier using geothermal IP steam as the gasification agent was seen to be relatively good, the inefficiencies associated with retrofitting syngas use into an existing geothermal power plant served to limit the power production, and therefore the economics of the hybrid plants. It may be possible, instead of using the syngas on site, to sell the syngas directly as a synthetic natural gas, or to further refine into liquid fuels using Fischer-Tropsch synthesis for the sale of biofuels. Alternatively, if the hybridization of a biomass gasification and geothermal steam production could be planned from the design stages of the plant production, it is likely that higher power generation efficiencies would be attained by removing the design constraints present when retrofitting an existing geothermal plant with biomass gasification.

#### 6.6.3.1 Breakeven Price of Landing Residues

As the estimated price of landing residues is based on a single report performed by Hall and Gilford of Scion [66], there is some uncertainty associated with the price of landing residues. The cost of landing residues that yields a NPV for the hybrid configurations of zero for the 30 year plant life may be in order to estimate the landing residue costs that would cause the hybrid configurations to become economically viable. Therefore, if new estimates for the delivered costs of landing residues become available, the feasibility of the hybrid configuration may be re-evaluated. The estimated rate of inflation based on the inflation of pulp logs, at approximately 2%, was again used in order to calculate the initial cost of landing residues which caused the hybrid configurations to break even. The calculated breakeven prices of landing residues are displayed in Table 46.

**Table 46. The breakeven prices of landing residues for the hybrid configurations**

Configuration	Breakeven Cost of Landing Residues in 2016 (\$/GJ)		
	Scenario 1	Scenario 2	Scenario 3
Superheating Geothermal Steam	-0.583	-2.39	2.54
Boiling Poihipi Rd Condensate	0.96	0.01	2.25
Boiling IP SGW from FP14	1.35	0.25	2.63
Heating Additional SGW for Use in the Binary Plant	-1.61	-1.94	-1.94

As can be seen, if landing residues can be obtained for less than approximately \$2.50/GJ, some of the hybrid configurations may recuperate their capital investment over the 30 years of plant operation. However, as this is only expected to occur in Scenario 3, the uncertainty associated with the geothermal steam flow to Wairakei is seen to greatly impact the breakeven costs of landing residues. As the estimated initial costs of landing residues for the hybrid configurations was within the range of \$4-5/GJ, the price of landing residues would have to have been significantly lower than those estimated in this study in order for the hybrid configurations to become economically viable.

It is noted that due to the capital investments required, some of the hybrid configurations yielded negative values for the breakeven costs of landing residues. These configurations would require payment to receive the landing residues. This is considered to be an unlikely occurrence, as there is no obvious reason for forestry plantations to pay for landing residues to be removed. However, it may be possible to identify other types of feedstock, which are waste products, where it may be possible to receive payment to dispose of the feedstock. Possibilities for this could include

municipal waste, and wastewater solids, which would otherwise be disposed of in landfills or by incineration. Therefore, if another source of feedstock is identified which may be obtained for significantly less the estimated costs of forest residues, it may cause the hybridization of gasification and geothermal power generation to become more economically appealing.

#### 6.6.4 Using Natural Gas Instead of Biomass Gasification

It is possible to use natural gas to provide the additional heat to the hybrid configurations instead of installing a biomass gasifier to create syngas. This would reduce the capital costs of the hybrid configurations, as it would remove the requirement for the biomass gasifier, and the biomass pre-treatment and handling equipment. As the costs of the landing residues increase with the delivery distance, this effectively limited the size of the gasification plant. However, the price of natural gas will likely not increase with increasing natural gas requirement for the hybrid configurations. The average industrial price of natural gas in New Zealand has historically been relatively variable, and therefore forecasting prices for the hybrid configurations would prove difficult, as seen in Figure 86.

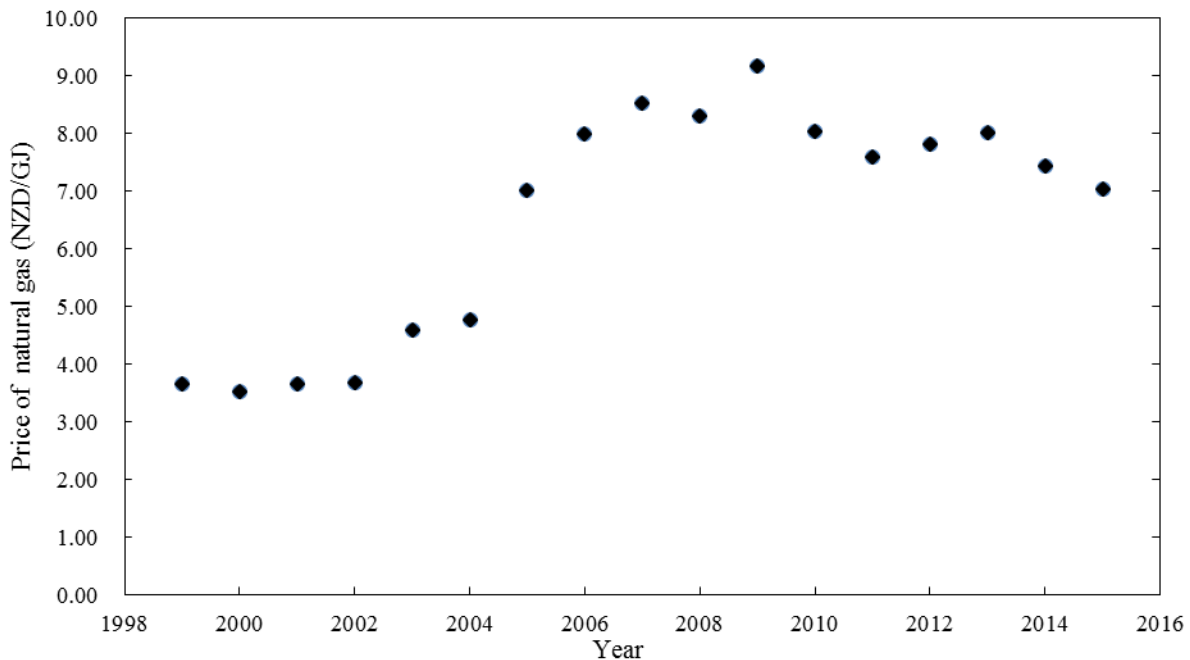


Figure 86. The industrial natural gas prices in New Zealand from 1999-2015 [101]

The average price for landing residues for a 40 MW gasification plant in 2015 was calculated at \$4.26/GJ, so even using a cold gas efficiency of the 65% which includes the enthalpy of the input IP steam to the gasifier, the resultant price of the syngas is \$6.55/GJ. As the average industrial price for natural gas in 2015 of \$7.04/GJ, there is a higher operating cost associated with using natural gas in the hybrid configurations instead of operating a biomass gasifier. As only the superheating of geothermal steam was seen to be cash flow positive throughout the life of the hybrid plant, and this only under specific geothermal steam flow circumstances, the reduction of capital costs associated with eliminating the need for biomass gasification would not recuperate

the capital initial investment for all other configurations. In the superheating geothermal steam configuration, the biomass gasifier and associated equipment only accounted for \$6.2 million, with the majority of the capital costs coming from the modifications performed on the MP turbines, and the furnace to superheat the geothermal steam. Comparing this with the cumulative discounted cash flow displayed in Figure 63, it is clear that this reduction in capital costs would likely not cause the project to recover its initial investment, especially with the added costs associated with an increased relative cost of fuel from buying natural gas instead of generating syngas. It is therefore very unlikely that the use of natural gas as a substitute for biomass gasification without a significant reduction in the cost of natural gas.

#### **6.6.5 Remaining Life of the Wairakei A and B Stations**

The remaining life of the Wairakei A and B Stations may be shorter than the estimated life of the additional process equipment required for hybridization. Currently, the resource content for the Wairakei A and B Stations ends in 2026, though this does not necessarily mean that these Power Stations will be removed from service. There is the possibility of renewing the resource consents if it is determined that the Wairakei A and B Stations still have remaining useful life. Alternatively, new power stations could be constructed in order to utilize the geothermal steam which will be unused in the absence of the Wairakei A and B Stations.

Even if it is decided that the Wairakei A and B Stations should be removed from service, this will not necessarily remove the possibility of implementing the hybrid configurations. It may be the case that the modifications performed to the MP turbine(s) in order for it to utilize superheated steam will increase the useful life of the modified turbines. In both of the configurations utilizing boilers, it may be that the geothermal steam generated in the boiler can still be utilized at the other Power Stations on the Wairakei Geothermal Field. However, as these stations are already fully loaded, the removal of the Wairakei A and B Stations would likely not provide a situation where there is unused capacity at the Poihipi Rd or Te Mihi Power Stations. Therefore, unless there are much more strict steam extraction limits put in place on the Wairakei Geothermal Field, which creates unused capacity at either of these power plants, there would likely be no reason to implement the hybrid configurations.

As the Wairakei Binary Plant is a relatively recent addition to the Wairakei Geothermal Field, it is not expected that it would require to be removed from service in the near future. In fact, if the Wairakei A and B Stations are removed from service, it may be the case that the geothermal steam used in the biomass gasifier as the gasification agent no longer results in diminished power generation at these Stations. Currently, this steam use is factored into the net power generation from the addition of the hybrid configuration to the binary plant. However, if the steam was no longer to be utilized in steam turbines, then there would be no power losses from using the steam in the gasifier. This would result in an increase in the net power generation of the Binary Plant.

## 7.0 Conclusions and Recommendations

While investigations have been performed into the possibility of hybridizing geothermal power plants with additional sources of heating, to this Author's knowledge this is the first in depth investigation into retrofitting an existing geothermal steam power plant with additional heating. Furthermore, using a biomass gasifier to supply the heat to the geothermal power plant is a desirable first step for the implementation of commercial biomass gasification in New Zealand, as it would serve to reduce the relative costs of a gasification plant, due to shared equipment.

Four hybrid configurations were designed to produce syngas from biomass combustion in order to increase the power generation from the geothermal power plants on the Wairakei Geothermal Field. The water sampling performed showed that the condensate from the Poihipi Rd Power Plant would likely be suitable as a source of boiler feed water, but would require pH dosing and deaeration. Three different scenarios were created in order to represent the potential future steam flows to Wairakei. The process modelling performed on the biomass gasification, Wairakei Power Station, and the hybrid configurations were created in order to estimate the impact that the different hybrid configurations would have on the power generation at Wairakei. Plant design and capital cost estimation was performed in order to determine the investment required in order to implement the hybrid configurations. An economic evaluation was then performed in order to evaluate the financial implications of implementing the hybrid configurations.

As the geothermal steam is expected to be used in the biomass gasifier to produce the syngas, and as the majority of the hybrid configurations provide additional steam to the turbines at Wairakei; the existing geothermal steam supply to Wairakei has a very large impact on the additional power that may be generated. The presence of IP steam bypassing the IP and MP turbines to the LP steam manifold serves to increase the power generation from returning an IP turbine to service, or mitigate the power losses from using steam in the gasifier. The loading of the steam turbines is also seen to greatly impact the power generation from the additional steam supply to Wairakei, as the no load flow requirement for the steam turbines can greatly detract from the amount of steam that directly contributes to the power generation.

While the superheating of geothermal steam is observed to be the configuration with the highest energy efficiency, it also is the least flexible of the hybrid configurations. As turbines are required to be modified, in the event of the closure of the gasifier, there will be a significant impact on the power generation of the Wairakei A and B Stations. However, this is not the case with the other configurations, as the existing geothermal power generation is not modified to incorporate the hybridization.

There is also some uncertainty associated with the practicality of the hybrid configurations. The superheating of the geothermal steam could cause great damage to the MP turbines, if there are liquid droplets present in the IP steam feed to the superheater. While it is believed that the operation of a boiler using the IP SGW and a large blowdown would not result in scaling within the boiler, the fact remains that the mineral content of the SGW is far greater than would be acceptable in a conventional boiler. Similarly, as increased mineral scaling has been observed with the mixing of two sources of SGW, the addition of the heated SGW to the Binary Plant could exacerbate mineral scaling. Due to the wealth of experience in operating steam boilers, the utilization of the Poihipi

Rd condensate as boiler feed water is likely the most practical hybrid configuration. Unfortunately it also has a relatively low energy efficiency, and requires the addition of several pieces of process equipment.

It was determined that in all scenarios of future steam flow to Wairakei, none of the hybrid configurations are expected to recuperate their initial capital investment. Only one configuration was seen to be cash flow positive during the plant life, and this only in the case of very specific steam flows to Wairakei. The efficiency losses associated with implementing retrofitted additional heating in a plant that was only designed to utilize geothermal resources served to significantly reduce the power generation that may be possible from the hybridization of geothermal and biomass resources. It was believed that the reduction in capital costs for hybrid geothermal biomass gasification power plant may cause the implementation of biomass gasification to become economically feasible. However, it is clear from the yearly losses expected with the implementation of the hybrid configurations, that the capital costs are not the main barrier to retrofitting the Wairakei Power Plant with a biomass gasifier.

Overall, and in spite of reasonable solutions to most engineering factors, the limiting factor is the cost of fuel in the form of the landing residues. It was initially thought that the close proximity and availability of forestry landing residues would result in viable options for boosting geothermal power generation via gasification. This is clearly not the case based on the input costs for the landing residues. The economics would be much more positive if there was a large, reliable and cheap source of biomass available. Possible situations where this might occur are:

- There is a large sawmill adjacent to the geothermal plant and the “waste” from the saw mill has no other market.
- Large quantities of sludge from sewage treatment is readily available. Assuming the sludge can be delivered with low water content. There is also the possibility of being paid to dispose of this waste.
- Large volumes of biomass from food processing plants have no alternate use.

## **7.1 Recommendations**

### **7.1.1 Power and Fuel Cogeneration**

Due to the limitations imposed by retrofitting an existing geothermal power plant with biomass gasification in order to generate power, it may be possible to generate syngas to sell as a synthetic natural gas or further refined into liquid biofuels by Fischer-Tropsch synthesis. As the utilization of the syngas at Wairakei for power generation was seen to be greatly impacted by the design constraints of the existing plant, direct sale of the syngas or liquid biofuels may be profitable, as it would still utilize relatively cheap geothermal steam for the biomass gasification. However, this would require a significant changes to the gasification design, as impurities in the syngas, such as tars, would become problematic with the change in use of the syngas. The combustion of syngas was designed to be used while still at high temperatures in the hybrid configurations, which avoided the necessity for tar removal, as it would not condense at the elevated temperatures.

However, this would not be the case if the syngas was to be sold as a natural gas substitute or used as an input to Fischer-Tropsch synthesis. It may also be necessary to remove other contaminants such as chlorides and ammonia from the syngas in order to sell as a natural gas substitute, and these would certainly be required for liquid synthesis, as there are strict tolerances on the contaminants in syngas for Fischer-Tropsch synthesis.

The wholesale price of natural gas has been highly variable in New Zealand, which causes uncertainties in the economic evaluation of a hybrid geothermal/gasification plant which produces both power and syngas. The average wholesale price of natural gas in 2015 of \$5.29/GJ [101] does not compare particularly favourably with the delivered costs of landing residues as the price of landing residues for a 40 MW gasification plant was estimated at \$4.69/GJ for 2016. Therefore a gasification plant with a cold gas efficiency of 70%, the cost of biomass to produce 1 GJ of syngas would be \$6.70. Therefore price forecasting for the expected sale price of synthetic natural gas would be required, in order to evaluate the viability of a hybrid geothermal/gasification power and syngas cogeneration plant.

The price of liquid fuels is seen to be more stable than that of natural gas in New Zealand, and therefore the price forecasting for liquid biofuels should prove to be simpler than for natural gas. The smallest cost for liquid fuels reported by the Ministry of Business Innovation and Employment for heavy fuel oil was seen to have an average price of \$12.40/GJ in 2015[101]. Integration of liquid biofuel synthesis to a geothermal power plant may therefore prove to be profitable.

It is recommended that a study into the plant design and market considerations for a geothermal/gasification power and liquid biofuel cogeneration plant be performed in order to determine if sale of the syngas will cause hybridization to be economically feasible. It is however unlikely that a geothermal/gasification power and synthetic natural gas cogeneration plant would prove to be profitable without a drastic increase in the wholesale price of natural gas.

### **7.1.2 Further Research into Gasification Feedstocks Prices**

Due to the relatively large costs associated with the landing residues estimated in this study, the economics associated with the hybrid configurations designed in this study were rather pessimistic. However, due to the fact that only one basis for the cost estimates for landing residues in New Zealand could be found, it is difficult to verify the validity of these cost estimates. Therefore if new information is discovered, which suggests that the landing residue costs estimated in this study are significantly higher than would be expected, it re-evaluation of the feasibility of the hybrid configurations could be performed. Similarly, if an alternate source of feedstock is identified, it may cause the economics surrounding biomass gasification retrofitting to a geothermal power plant to become more promising. This is especially true if a waste product is identified that may be used as a feedstock to a gasifier, as revenue may be generated by disposing of the feedstock, instead of paying for it. Possible waste product which may be used as gasification feedstocks are municipal waste and wastewater solids.

### **7.1.3 Designing a New Geothermal/Gasification Power Plant**



By designing a new geothermal/gasification power plant, the limitations associated with retrofitting an existing geothermal plant with biomass gasification would be removed. More efficient power generation would be possible in the hybridization occurred from the design stage, as higher quality steam produced in a boiler or by superheating geothermal steam. This steam could then be used in new efficient steam turbines designed for the higher quality steam. Conventional steam power plants create much higher quality steam than the geothermal steam generated on the Wairakei Geothermal System to generate power, due to the greater efficiency that is possible by using superheated steam. The desired reduction in the relative costs of the biomass gasifier and associated equipment would still be achieved through shared equipment with the geothermal portion of the plant. Due to this, it is suggested that hybridization of geothermal and gasification power generation be researched for a new hybrid power plant. As Contact Energy has resource consents to construct a new geothermal power station on the Wairakei Geothermal field, the Tauhara II Power Station, it may be possible to integrate biomass gasification into the design of this power plant.

## 8.0 References

1. REN21, *Renewables 2014 Global Status Report*. 2014.
2. U.S., *CHINA RATIFY PARIS CLIMATE AGREEMENT*. 2016 7 Sep 2016]; Available from: <http://www.reuters.com/article/us-china-climatechange-idUSKCN11901W?il=0>.
3. *Modelling Electricity Demand in New Zealand - overview guide*. 2014, New Zealand Electricity Authority.
4. Gray, J., *Mighty River Battles Flat Demand*, in *NZ Herald*. 2014.
5. New Zealand Ministry of Business Innovation & Employment, *Energy in New Zealand*. 2015.
6. DiPippo, R., *Part 1 - Resource Identification and Development*, in *Geothermal Power Plants (Second Edition)*, R. DiPippo, Editor. 2008, Butterworth-Heinemann: Oxford. p. 1-2.
7. DiPippo, R., *Chapter 7 - Dry-Steam Power Plants*, in *Geothermal Power Plants (Second Edition)*, R. DiPippo, Editor. 2008, Butterworth-Heinemann: Oxford. p. 135-156.
8. *Appendix A - Worldwide State of Geothermal Power Plant Development as of May 2007*, in *Geothermal Power Plants (Second Edition)*, R. DiPippo, Editor. 2008, Butterworth-Heinemann: Oxford. p. 413-432.
9. Thain, I.A. and B. Carey, *Fifty years of geothermal power generation at Wairakei*. *Geothermics*, 2009. **38**(1): p. 48-63.
10. DiPippo, R., *Chapter 5 - Single-Flash Steam Power Plants*, in *Geothermal Power Plants (Second Edition)*, R. DiPippo, Editor. 2008, Butterworth-Heinemann: Oxford. p. 81-112.
11. E.W. Lemmon, M.O.M.a.D.G.F., *Thermophysical Properties of Fluid Systems*, in *NIST Chemistry WebBook*. National Institute of Standards and Technology.
12. Schlömer S., T.B., L. Fulton, E. Hertwich, A. McKinnon, D. Perczyk, J. Roy, R. Schaeffer, R. Sims, P. Smith, and R. Wiser, *Annex III: Technology-specific cost and performance parameters*. In: *Climate Change 2014: Mitigation of Climate Change. Contribution of Working Group III to the Fifth Assessment Report of the Intergovernmental Panel on Climate Change*. 2014, Cambridge University Press, Cambridge, United Kingdom and New York, NY, USA.
13. DiPippo, R., *Chapter 8 - Binary Cycle Power Plants*, in *Geothermal Power Plants (Second Edition)*, R. DiPippo, Editor. 2008, Butterworth-Heinemann: Oxford. p. 157-189.
14. New Zealand Geothermal Association. *Price* 7/5/2016]; Available from: <http://www.nzgeothermal.org.nz/price.html>.
15. Higman, C. and M. van der Burgt, *Chapter 1 - Introduction*, in *Gasification (Second Edition)*, C. Higman and M.v.d. Burgt, Editors. 2008, Gulf Professional Publishing: Burlington. p. 1-9.
16. Higman, C. and M. van der Burgt, *Chapter 4 - Feedstocks and Feedstock Characteristics*, in *Gasification (Second Edition)*, C. Higman and M.v.d. Burgt, Editors. 2008, Gulf Professional Publishing: Burlington. p. 47-90.
17. Basu, P., *Chapter 8 - Biomass Handling*, in *Biomass Gasification and Pyrolysis*, P. Basu, Editor. 2010, Academic Press: Boston. p. 269-299.
18. Gopalakrishnan, P., *Modelling of Biomass Steam Gasification in a Bubbling Fluidized Bed Gasifier*, in *Chemical and Process Engineering*. 2013, University of Canterbury.
19. Basu, P., *Chapter 6 - Design of Biomass Gasifiers*, in *Biomass Gasification and Pyrolysis*, P. Basu, Editor. 2010, Academic Press: Boston. p. 167-228.
20. Williamson, C., *Liquid Fuel from Biomass Derived Synthesis Gas via Fischer-Tropsch [PowerPoint slides]*. Department of Chemical & Process Engineering, University of Canterbury.
21. Roberts, K., *Diagrams of the Wairakei Geothermal Field*. 2015, Contact Energy.
22. White, B., *Wairakei Energy and Efficiency Audit*. 2000, PARSONS BRINCKERHOFF.

23. Dowell, M. *Te Mihi Geothermal Power Station*. 10/05/2016]; An overview of the work that the McConnell Dowell Contruction Company performed constructing the Te Mihi Power Station]. Available from: [www.mccinnelldowell.com/markets/power/100-te-mihi-geothermal-power-station](http://www.mccinnelldowell.com/markets/power/100-te-mihi-geothermal-power-station).
24. Zarrouk, S.J., B.C. Woodhurst, and C. Morris, *Silica scaling in geothermal heat exchangers and its impact on pressure drop and performance: Wairakei binary plant, New Zealand*. Geothermics, 2014. **51**(0): p. 445-459.
25. DiPippo, R., *Chapter 9 - Advanced Geothermal Energy Conversion Systems*, in *Geothermal Power Plants (Third Edition)*, R. DiPippo, Editor. 2012, Butterworth-Heinemann: Boston. p. 183-221.
26. DiPippo, R. *Geothermal electric power production in the United States: a survey and update for 1990–1994*. in *Proceedings of the World Geothermal Congress*. 1995.
27. Tanaka, Y., et al., *Performance of a Hybrid Power Generation System Using Biomass Gasification and Concentrated Solar Thermal Processes*. Energy Procedia, 2014. **61**(0): p. 2149-2153.
28. Horlock, J.H., *Combined Power Plants : Including Combined Cycle Gas Turbine (CCGT) Plants*. Thermodynamics and fluid mechanics series. 1992, Oxford [England] ; New York Pergamon Press.
29. Bixley, P.F., A.W. Clotworthy, and W.I. Mannington, *Evolution of the Wairakei geothermal reservoir during 50 years of production*. Geothermics, 2009. **38**(1): p. 145-154.
30. Kristmannsdóttir, H. and H. Ármannsson, *Environmental aspects of geothermal energy utilization*. Geothermics, 2003. **32**(4–6): p. 451-461.
31. Kingston Reynolds Thom and Allardice Ltd, *An Investigation into Hybrid Geothermal/Gas Power Plants*. 1980, New Zealand Energy Research and Development Committee.
32. Ian Thain, R.D., *Hybrid Geothermal-Biomass Power Plants: Applications, Designs and Performance Analysis*, in *World Geothermal Congress 2015*. 2015: Melbourne, Australia.
33. Rosalind Julian, K.L., *Geothermal Materials Selection in Old Lessons, New Directions*, N.Z.G. Association, Editor. 2014, Quest Integrity Group.
34. Woolcock, P.J. and R.C. Brown, *A review of cleaning technologies for biomass-derived syngas*. Biomass and Bioenergy, 2013. **52**(0): p. 54-84.
35. Baratieri, M., et al., *The use of biomass syngas in IC engines and CCGT plants: A comparative analysis*. Applied Thermal Engineering, 2009. **29**(16): p. 3309-3318.
36. Brown, R.C. and T.R. Brown, *Biorenewable resources: engineering new products from agriculture*. 2013: John Wiley & Sons.
37. Ronald DiPippo, H.E.K., Robert J. Correia and Joseph Kestin, *Fossil Superheating in Geothermal Steam Power Plants*. 1978, Brown University: Providence, Rhode island.
38. Morris, C., *Superheating Steam for a Geothermal Turbine*. 2014.
39. Kennedy, G.C., *A portion of the system silica-water*. Economic Geology and the Bulletin of the Society of Economic Geologists, 1950: p. 629-653.
40. Rayaprolu, K., *Boilers: A Practical Reference*, C. Press, Editor. 2012.
41. Gallup, D.L., J.L. Featherstone, and C.E. Flint, *Use of steam condensate to dilute brine stream additives*. 1995, Google Patents.
42. Chris Morris, A.R., *Geothermal Turbines - A Maintainer's Perspective*, in *World Geothermal Congress*. 2015: Melbourne, Australia.
43. Puladian, N., *Development of an integrated system model for production of fischer-tropsch liquid fuels from woody biomass*, in *Department of Chemical and Process Engineering*. 2015, University of Canterbury: Christchurch, New Zealand.
44. Iguaz, A., et al., *Mathematical modelling and simulation for the drying process of vegetable wholesale by-products in a rotary dryer*. Journal of food engineering, 2003. **59**(2): p. 151-160.
45. Xu, Q. and S. Pang, *Mathematical modeling of rotary drying of woody biomass*. Drying Technology, 2008. **26**(11): p. 1344-1350.
46. Amos, W.A., *Report on Biomass Drying Technology*. 1998, National Renewable Energy Laboratory: Colorado, U.S.A.

47. Fagbemi, L., L. Khezami, and R. Capart, *Pyrolysis products from different biomasses: Application to the thermal cracking of tar*. Applied Energy, 2001. **69**(4): p. 293-306.
48. Koppatz, S., C. Pfeifer, and H. Hofbauer, *Comparison of the performance behaviour of silica sand and olivine in a dual fluidised bed reactor system for steam gasification of biomass at pilot plant scale*. Chemical Engineering Journal, 2011. **175**: p. 468-483.
49. Nguyen, T.D.B., et al., *Three-stage steady-state model for biomass gasification in a dual circulating fluidized-bed*. Energy Conversion and Management, 2012. **54**(1): p. 100-112.
50. The Engineering Toolbox. *Butterfly Valves - Typical Flow Coefficients*. [cited 2016 11/7].
51. Sarco, S., *Steam Sizing Chart*. Spirax Sarco.
52. Brooks, C., *Boiler Efficiency Guide*, C. Brooks, Editor. 2010: USA.
53. Saidur, R., J.U. Ahamed, and H.H. Masjuki, *Energy, exergy and economic analysis of industrial boilers*. Energy Policy, 2010. **38**(5): p. 2188-2197.
54. Davis, J.R., *ASM specialty handbook: heat-resistant materials*. 1997: Asm International.
55. Gary Eng, I.B., Charles Hendtlass, *New Zealand Energy Information Handbook*. 2008, New Zealand Centre for Advanced Engineering: Christchurch.
56. Muller, L., *Water Analysis at Wairakei*, S. Chester, Editor. 2015.
57. Electric, G., *Handbook of Industrial Water Treatment*. GE Water
58. Fegley Jr, B., et al., *Solubility of Rock in Steam Atmospheres of Planets*. arXiv preprint arXiv:1602.00658, 2016.
59. Millero, F.J., *The effect of pressure on the solubility of minerals in water and seawater*. Geochimica et Cosmochimica Acta, 1982. **46**(1): p. 11-22.
60. Federation, W.E. and A.P.H. Association, *Standard methods for the examination of water and wastewater*. American Public Health Association (APHA): Washington, DC, USA, 2005.
61. Heselton, K.E., *Boiler operator's handbook*. 2005: The Fairmont Press, Inc.
62. American Boiler Manufacturers Association, *Deaerator White Paper for use with Industrial/Commercial and Institutional Boilers*. 2011.
63. Branam, C.R., *Rules of thumb for chemical engineers*. 2012: Butterworth-Heinemann.
64. North Carolina Department of Environment and Natural Resources, *Boiler Blowdown Fact Sheet*. 2004.
65. Reserve Bank of New Zealand. *Inflation Calculator*. 2016; Available from: <http://www.rbnz.govt.nz/monetary-policy/inflation-calculator>.
66. Peter Hall, J.G., *Bioenergy Options for New Zealand, A Situation Analysis of Biomass Resources and Conversion Technologies*, M. Richardson, Editor. 2007, Scion, Energy Group.
67. New Zealand Ministry of Primary Industries. *Indicative New Zealand Radiata Pine Log Prices by Quarter*. 2016 [cited 2016 25/7/2016]; Available from: <http://www.mpi.govt.nz/news-and-resources/open-data-and-forecasting/forestry/indicative-new-zealand-radiata-pine-log-prices-by-quarter/>.
68. New Zealand Ministry of Primary Industries, *Indicative New Zealand Radiata Pine Log Prices by Quarter*. 2016.
69. Sherwin, A., *National Exotic Forest Description*. 2014, Ministry for Primary Industries: Wellington, New Zealand.
70. Domínguez-Caamaño, P., J.A.C. Benavides, and J.C.P. Prado, *AN IMPROVED METHODOLOGY TO DETERMINE THE WIGGLE FACTOR: AN APPLICATION FOR SPANISH ROAD TRANSPORT*. Brazilian Journal of Operations & Production Management, 2016. **1**(1): p. 52-56.
71. Society of Chemical Engineers New Zealand, *Cost Estimating by the FACT Method*. 2004.
72. van der Drift, A., J. van Doorn, and J.W. Vermeulen, *Ten residual biomass fuels for circulating fluidized-bed gasification*. Biomass and Bioenergy, 2001. **20**(1): p. 45-56.
73. Hakkila, P., *Utilization of residual forest biomass*. 1989: Springer.
74. Naimi, L.J., et al. *Cost and performance of woody biomass size reduction for energy production*. in 2006 ASAE Annual Meeting. 2006. American Society of Agricultural and Biological Engineers.

75. Goho, C.D., *A study of logging residue at woods landings in Appalachia*. Vol. 219. 1976: US Dept. of Agriculture, Forest Service, Northeastern Forest Experiment Station.
76. Merat, M.S., *Contact Energy, Wairakei, NZ- Disc Chipper for Chipping Residues and Logs up to 500mm dia, up to m metres long*, S. Chester, Editor. 2016: Southern Cross Engineering.
77. Holmberg, H. and P. Ahtila, *Evaluation of energy efficiency in biofuel drying by means of energy and exergy analyses*. Applied Thermal Engineering, 2005. **25**(17–18): p. 3115-3128.
78. Ruiz, J.A., et al., *Biomass gasification for electricity generation: Review of current technology barriers*. Renewable and Sustainable Energy Reviews, 2013. **18**: p. 174-183.
79. Brammer, J.G. and A.V. Bridgwater, *Drying technologies for an integrated gasification bio-energy plant*. Renewable and Sustainable Energy Reviews, 1999. **3**(4): p. 243-289.
80. Penniall, C.L. and C.J. Williamson, *Feasibility study into the potential for gasification plant in the New Zealand wood processing industry*. Energy Policy, 2009. **37**(9): p. 3377-3386.
81. Brammer, J.G. and A.V. Bridgwater, *The influence of feedstock drying on the performance and economics of a biomass gasifier-engine CHP system*. Biomass and Bioenergy, 2002. **22**(4): p. 271-281.
82. Worley, M. and J. Yale, *Biomass Gasification Technology Assessment: Consolidated Report*. 2012, National Renewable Energy Laboratory (NREL), Golden, CO.
83. Woodenergy *Wood Fuel Characteristics*.
84. K.C. Dhuyvetter, J.P.H., III, G. Boomer, J.F. Smith, R. Rodriguez, *Bunkers, piles, or bags: Which is most economical?* Western Dairy News, 2006. **6**(1).
85. University of Georgia, C.o.A.E.S., *Extension Engineering Handbook*. University of Georgia.
86. Henan Province Yingda Machinery Manufacturing Co., L. *Wood chips auger conveyor with capacity 18t/h*. [cited 2016 17/05]; Details on wood chip transfer augers ]. Available from: [https://www.alibaba.com/product-detail/Wood-chips-auger-conveyor-with-capacity\\_60242259797.html?spm=a2700.7724857.29.84.QwY13y](https://www.alibaba.com/product-detail/Wood-chips-auger-conveyor-with-capacity_60242259797.html?spm=a2700.7724857.29.84.QwY13y).
87. Henan Wantai Machinery Co., L. *Wood Chip Conveyor*. [cited 2016 19/05].
88. Rutherford, J.P., *Heat and Power Applications of Advanced Biomass Gasifiers in New Zealand's Wood Industry A Chemical Equilibrium Model and Economic Feasibility Assessment*, in *Chemical and Process Engineering*. 2006, University of Canterbury.
89. Bhatia, A., *Overview of Refractory materials*. 2012, PDH Center.
90. Loh, H., J. Lyons, and C. White, *Process equipment cost estimation. Final Report, National Energy Technology Center*. 2002, DOE/NETL-2002/1169.
91. Angus, H.T., *Cast iron: physical and engineering properties*. 2013: Elsevier.
92. Galu, N., *Cost of caustic soda*, S. Chester, Editor. 2016, recochem.com.
93. Wei, S., *Quotation of Rotary Dryer*, S. Chester, Editor. 2016, ShangHai Tongli Heavy Machinery Co.: China.
94. Towler, G.P. and R.K. Sinnott, *Chemical engineering design: principles, practice and economics of plant and process design*. 2008, Amsterdam;Boston;: Elsevier/Butterworth-Heinemann.
95. Mann, M.K. and P.L. Spath, *Life cycle assessment of a biomass gasification combined-cycle power system*. 1997, National Renewable Energy Lab., Golden, CO (US).
96. United States Department of the Treasury Inland Revenue Service, *How to Depreciate Properly*. 2016.
97. Treasury, N.Z., *Public Sector Discount Rates for Cost Benefit Analysis*. 2008.
98. Devi, L., K.J. Ptasinski, and F.J.J.G. Janssen, *A review of the primary measures for tar elimination in biomass gasification processes*. Biomass and Bioenergy, 2003. **24**(2): p. 125-140.
99. Bridgwater, A.V., *The technical and economic feasibility of biomass gasification for power generation*. Fuel, 1995. **74**(5): p. 631-653.
100. Bridgwater, A., A. Toft, and J. Brammer, *A techno-economic comparison of power production by biomass fast pyrolysis with gasification and combustion*. Renewable and Sustainable Energy Reviews, 2002. **6**(3): p. 181-246.

101. Ministry of Buisness Innovation & Employment, *Energy Prices*, in *Energy & Building Trends*. 2016.

## **9.0 Appendices**

### **9.1 Water testing results**

#### **9.1.1 Boiler water testing**





## ANALYSIS REPORT

Page 1 of 2

<b>Client:</b>	Contact Energy Limited	<b>Lab No:</b>	1590936	SPv1
<b>Contact:</b>	Contact Energy Limited C/- Wairakei Power Station Private Bag 2001 Taupo 3352	<b>Date Registered:</b>	27-May-2016	
		<b>Date Reported:</b>	14-Jun-2016	
		<b>Quote No:</b>	77223	
		<b>Order No:</b>	4500117891	
		<b>Client Reference:</b>		
		<b>Submitted By:</b>	Farrah Hiramis	

Sample Type: Aqueous						
Sample Name:		Poihipi Rd Condensate 25-May-2016 10:18 am	Te Mihi Blowdown 25-May-2016 2:47 pm	Ohaaki Blowdown 25-May-2016 11:00 am		
Lab Number:		1590936.1	1590936.2	1590936.3		
Individual Tests						
Total Alkalinity	g/m <sup>3</sup> as CaCO <sub>3</sub>	11.0	1.5	69	-	-
Free Carbon Dioxide	g/m <sup>3</sup> at 25°C	1.2	81	2.0	-	-
Total Dissolved Solids (TDS)	g/m <sup>3</sup>	< 10	26	53	-	-
Total Calcium	g/m <sup>3</sup>	< 0.053	0.060	1.00	-	-
Total Copper	g/m <sup>3</sup>	< 0.00053	< 0.00053	< 0.00053	-	-
Total Iron	g/m <sup>3</sup>	< 0.021	< 0.021	0.041	-	-
Total Magnesium	g/m <sup>3</sup>	< 0.021	< 0.021	0.037	-	-
Total Dissolved Silica	g/m <sup>3</sup> as SiO <sub>2</sub>	< 0.011	0.05	0.64	-	-
Total Sodium	g/m <sup>3</sup>	0.061	0.22	0.27	-	-
Chloride	g/m <sup>3</sup>	0.8	< 0.5	< 0.5	-	-
Total Ammoniacal-N	g/m <sup>3</sup>	2.5	6.8	42	-	-
Silicon	g/m <sup>3</sup>	< 0.005	0.021	0.30	-	-
Sulphate	g/m <sup>3</sup>	< 0.5	27	72	-	-
Hydrogen sulphide profile						
pH	pH Units	7.3	4.6	7.8	-	-
Electrical Conductivity (EC)	mS/m	2.2	8.3	37.1	-	-
Sample Temperature*	°C	20.0	20.0	20.0	-	-
Un-ionised hydrogen sulphide	g/m <sup>3</sup>	0.34	< 0.002	0.003	-	-
Total Sulphide	g/m <sup>3</sup>	0.90	< 0.002	0.022	-	-

## SUMMARY OF METHODS

The following table(s) gives a brief description of the methods used to conduct the analyses for this job. The detection limits given below are those attainable in a relatively clean matrix. Detection limits may be higher for individual samples should insufficient sample be available, or if the matrix requires that dilutions be performed during analysis.

Sample Type: Aqueous			
Test	Method Description	Default Detection Limit	Sample No
Filtration, Unpreserved	Sample filtration through 0.45µm membrane filter.	-	1-3
Total Digestion	Boiling nitric acid digestion. APHA 3030 E 22 <sup>nd</sup> ed. 2012 (modified).	-	1-3
pH	pH meter. APHA 4500-H <sup>+</sup> B 22 <sup>nd</sup> ed. 2012. Note: It is not possible to achieve the APHA Maximum Storage Recommendation for this test (15 min) when samples are analysed upon receipt at the laboratory, and not in the field.	0.1 pH Units	1-3
Total Alkalinity	Titration to pH 4.5 (M-alkalinity), autotitrator. APHA 2320 B (Modified for alk <20) 22 <sup>nd</sup> ed. 2012.	1.0 g/m <sup>3</sup> as CaCO <sub>3</sub>	1-3
Free Carbon Dioxide	Calculation: from alkalinity and pH, valid where TDS is not >500 mg/L and alkalinity is almost entirely due to hydroxides, carbonates or bicarbonates. APHA 4500-CO <sub>2</sub> D 22 <sup>nd</sup> ed. 2012.	1.0 g/m <sup>3</sup> at 25°C	1-3
Electrical Conductivity (EC)	Conductivity meter, 25°C. APHA 2510 B 22 <sup>nd</sup> ed. 2012.	0.1 mS/m	1-3



This Laboratory is accredited by International Accreditation New Zealand (IANZ), which represents New Zealand in the International Laboratory Accreditation Cooperation (ILAC). Through the ILAC Mutual Recognition Arrangement (ILAC-MRA) this accreditation is internationally recognised.  
The tests reported herein have been performed in accordance with the terms of accreditation, with the exception of tests marked \*, which are not accredited.



Sample Type: Aqueous			
Test	Method Description	Default Detection Limit	Sample No
Total Dissolved Solids (TDS)	Filtration through GF/C (1.2 µm), gravimetric. APHA 2540 C (modified; drying temperature of 103 - 105°C used rather than 180 ± 2°C) 22 <sup>nd</sup> ed. 2012.	10 g/m <sup>3</sup>	1-3
Sample Temperature*	Supplied by customer, otherwise 20°C.	0.1 °C	1-3
Total Calcium	Nitric acid digestion, ICP-MS, trace level. APHA 3125 B 22 <sup>nd</sup> ed. 2012.	0.053 g/m <sup>3</sup>	1-3
Total Copper	Nitric acid digestion, ICP-MS, trace level. APHA 3125 B 22 <sup>nd</sup> ed. 2012 / US EPA 200.8.	0.00053 g/m <sup>3</sup>	1-3
Total Iron	Nitric acid digestion, ICP-MS, trace level. APHA 3125 B 22 <sup>nd</sup> ed. 2012.	0.021 g/m <sup>3</sup>	1-3
Total Magnesium	Nitric acid digestion, ICP-MS, trace level. APHA 3125 B 22 <sup>nd</sup> ed. 2012.	0.021 g/m <sup>3</sup>	1-3
Total Dissolved Silica	Calculation: Silicon x 2.14.	0.005 g/m <sup>3</sup> as SiO <sub>2</sub>	1-3
Total Sodium	Nitric acid digestion, ICP-MS, trace level. APHA 3125 B 22 <sup>nd</sup> ed. 2012.	0.021 g/m <sup>3</sup>	1-3
Chloride	Filtered sample. Ferric thiocyanate colorimetry. Discrete Analyser. APHA 4500 Cl <sup>-</sup> E (modified from continuous flow analysis) 22 <sup>nd</sup> ed. 2012.	0.5 g/m <sup>3</sup>	1-3
Total Ammoniacal-N	Filtered sample. Phenol/hypochlorite colorimetry. Discrete Analyser. (NH <sub>4</sub> -N = NH <sub>4</sub> <sup>+</sup> -N + NH <sub>3</sub> -N). APHA 4500-NH <sub>3</sub> F (modified from manual analysis) 22 <sup>nd</sup> ed. 2012.	0.010 g/m <sup>3</sup>	1-3
Silicon	Analysed as received (filtration, if required), ICP-MS, trace level. APHA 3125 B 22 <sup>nd</sup> ed. 2012.	0.005 g/m <sup>3</sup>	1-3
Un-ionised hydrogen sulphide	Calculation from Total Sulphide, Electrical Conductivity, pH and Temperature*.  *Note: For accurate calculation of the un-ionised Hydrogen Sulphide the sample temperature should be taken using a calibrated thermometer at the time of sampling and recorded on the paperwork submitted with the sample. If a sample temperature is not supplied, a nominal temperature of 20°C will show in the results table above and be used in the calculation. In this case, please interpret the un-ionised Hydrogen Sulphide result with caution.  APHA 4500-S <sup>2-</sup> H (modified) 22 <sup>nd</sup> ed. 2012.	0.002 g/m <sup>3</sup>	1-3
Sulphide Distillation	Acid distillation of sample into alkaline trapping solution using Simple Distillation system. APHA 4500-S <sup>2-</sup> I 22 <sup>nd</sup> ed. 2012.	-	1-3
Total Sulphide	Sulphide distillation. Automated methylene blue colorimetry, discrete analyser. APHA 4500-S <sup>2-</sup> I (modified) 22 <sup>nd</sup> ed. 2012.	0.002 g/m <sup>3</sup>	1-3
Sulphate	Filtered sample. Ion Chromatography. APHA 4110 B 22 <sup>nd</sup> ed. 2012.	0.5 g/m <sup>3</sup>	1-3

These samples were collected by yourselves (or your agent) and analysed as received at the laboratory.

Samples are held at the laboratory after reporting for a length of time depending on the preservation used and the stability of the analytes being tested. Once the storage period is completed the samples are discarded unless otherwise advised by the client.

This report must not be reproduced, except in full, without the written consent of the signatory.



Peter Robinson MSc (Hons), PhD, FNZIC  
Client Services Manager - Environmental

### 9.1.2 Previous Testing Performed on the Poihipi Rd Condensate

Sample Name:		Cooling Pond 14-May-2008 10:30 am	Poihipi Cooling Pond 30-Apr-2008 9:00 am	Condenser 14-May-2008 10:30 am	Poihipi Condensate 30-Apr-2008 10:15 am
Lab Number:		642352.1	640546.2	642352.2	640546.1
Individual Tests					
Dissolved Mercury	g/m <sup>3</sup>	< 0.000080	< 0.000080	< 0.000080	< 0.000080
Total Mercury	g/m <sup>3</sup>	0.00022	0.00070	0.0023	0.00067
Total Nitrogen	g/m <sup>3</sup>	6.4	7.0	2.6	2.7
Nitrate-N + Nitrite-N	g/m <sup>3</sup>	3.0	3.1	0.15	0.16
Total Kjeldahl Nitrogen (TKN)	g/m <sup>3</sup>	3.4	3.9	2.4	2.6
ICP-MS Extended Total Metals, trace level					
Total Aluminium	g/m <sup>3</sup>	< 0.0032	< 0.0032	< 0.0032	< 0.0032
Total Antimony	g/m <sup>3</sup>	< 0.00021	0.00028	< 0.00021	< 0.00021
Total Arsenic	g/m <sup>3</sup>	0.019	0.023	0.0017	0.0016
Total Barium	g/m <sup>3</sup>	0.0010	0.00023	< 0.00021	< 0.00021
Total Boron	g/m <sup>3</sup>	0.83	0.64	0.34	0.24
Total Bromine	g/m <sup>3</sup>	1.0	0.75	0.066	0.038
Total Cadmium	g/m <sup>3</sup>	< 0.000053	< 0.000053	< 0.000053	< 0.000053
Total Caesium	g/m <sup>3</sup>	< 0.00011	< 0.00011	< 0.00011	< 0.00011
Total Calcium	g/m <sup>3</sup>	0.47	0.057	< 0.053	< 0.053
Total Chromium	g/m <sup>3</sup>	0.0017	0.0016	0.00071	< 0.00053
Total Cobalt	g/m <sup>3</sup>	< 0.00021	< 0.00021	< 0.00021	< 0.00021
Total Copper	g/m <sup>3</sup>	0.012	0.012	0.00059	0.00057
Total Iron	g/m <sup>3</sup>	0.052	< 0.021	0.032	< 0.021
Total Lanthanum	g/m <sup>3</sup>	< 0.00021	< 0.00021	< 0.00021	< 0.00021
Total Lead	g/m <sup>3</sup>	0.00011	< 0.00011	< 0.00011	< 0.00011
Total Lithium	g/m <sup>3</sup>	0.00060	< 0.00042	< 0.00042	< 0.00042
Total Magnesium	g/m <sup>3</sup>	< 0.021	< 0.021	< 0.021	< 0.021
Total Manganese	g/m <sup>3</sup>	0.0018	0.0011	< 0.00053	< 0.00053
Total Molybdenum	g/m <sup>3</sup>	< 0.00021	< 0.00021	< 0.00021	< 0.00021
Total Nickel	g/m <sup>3</sup>	0.0014	< 0.00053	< 0.00053	< 0.00053
Total Potassium	g/m <sup>3</sup>	< 0.053	< 0.053	< 0.053	< 0.053
Total Rubidium	g/m <sup>3</sup>	0.00013	< 0.00011	< 0.00011	< 0.00011
Total Selenium	g/m <sup>3</sup>	< 0.0011	< 0.0011	< 0.0011	< 0.0011
Total Silver	g/m <sup>3</sup>	< 0.00011	< 0.00011	< 0.00011	< 0.00011
Total Sodium	g/m <sup>3</sup>	0.99	0.72	0.057	0.034
Total Strontium	g/m <sup>3</sup>	< 0.00053	< 0.00053	< 0.00053	< 0.00053
Total Thallium	g/m <sup>3</sup>	< 0.000053	< 0.000053	< 0.000053	< 0.000053
Total Tin	g/m <sup>3</sup>	< 0.00053	< 0.00053	< 0.00053	< 0.00053
Total Uranium	g/m <sup>3</sup>	< 0.000021	< 0.000021	< 0.000021	< 0.000021
Total Vanadium	g/m <sup>3</sup>	< 0.0011	< 0.0011	< 0.0011	< 0.0011
Total Zinc	g/m <sup>3</sup>	0.0047	< 0.0011	< 0.0011	< 0.0011



WAIRAKEI ANALYTICAL LABORATORY

Private Bag 2000, Taupo

Phone: (07) 374 8211

Fax: (07) 374 8199

e.mail: w.labmanager@gns.cri.nz

To:  
Ruth Smith  
Contact Energy  
Private Bag 2001  
TAUPO

### ANALYTICAL REPORT: Poihipi Waters

		2701294 12/07/2007 WK680	2701295 12/07/2007 CT POND	2701296 12/07/2007 CONDENSER COND	2701297 12/07/2007 WK 305
Bicarbonate (total)	mg/L	21	22	29	27
pH		6.68	6.16	6.67	6.77
Analysis temperature	° C	18	17	16	16
HCO <sub>3</sub> /Date Analysed		12/07/2007	13/07/2007	13/07/2007	13/07/2007
Aluminium	mg/L	<0.15	<0.15	<0.15	<0.15
Ammonia (total as NH <sub>3</sub> )	mg/L	5.1	4.9	2.7	2.8
Arsenic	mg/L	0.10	0.11	<0.015	<0.015
Boron	mg/L	1.5	1.5	0.45	0.39
Cadmium	mg/L	<0.00005	<0.00005	<0.00005	<0.00005
Calcium	mg/L	<0.05	<0.05	<0.05	0.08
Chloride	mg/L	3.2	3.5	0.27	0.14
Conductivity	µS/cm	60	61	24	23
Copper	mg/L	0.021	0.024	0.002	0.0022
Fluoride	mg/L	<0.1	<0.1	<0.1	<0.1
Lead	mg/L	0.0002	0.0002	0.0002	0.0001
Lithium	mg/L	<0.01	<0.01	<0.01	<0.01
Magnesium	mg/L	<0.01	<0.01	<0.01	<0.01
Mercury by AA	µg/L	5.4	4.8	0.73	0.50
Mercury by AA	µg/L	5.4	4.7	0.90	0.58
Potassium	mg/L	<0.9	<0.9	<0.9	<0.9
Silica (as SiO <sub>2</sub> )	mg/L	<0.6	<0.6	<0.6	<0.6
Sodium	mg/L	2.5	2.5	<0.8	<0.8
Sulphate	mg/L	5.3	5.4	1.2	1.1
Sulphide (total as H <sub>2</sub> S)	mg/L	<0.01	<0.01	0.33	0.093
H <sub>2</sub> S/Date Analysed		12/07/2007	12/07/2007	12/07/2007	12/07/2007
Zinc	mg/L	0.007	0.013	0.013	0.006
Nitrate (as N)	mg/L	1.6	1.5	0.11	0.04
Total Kjeldahl Nitrogen	mg/L	4.8	5.0	2.6	2.6
Total N	mg/L	6.4	6.5	2.7	2.6
	Br (July 08) mg/L	2.9	2.9	0.20	0.12

**Analyst Comments:** The results pertain to samples as received. This document shall not be reproduced, except in full. Samples are held in storage for a period of twelve (12) months after the reporting of results.

Report Date:  
Report No.  
Customer Ref.  
Page

8/08/2007  
WAL070712002  
WK903  
1 of 2

*A Noddings*  
Ann Noddings  
Analyst

*B Mountain*  
Bruce Mountain, Ph.D.  
Geochemist



This laboratory is accredited by International Accreditation New Zealand. The tests reported herein have been performed in accordance with its terms of accreditation, with the exception of the tests marked with a †

## 9.2 Process Equipment Capital Costs

The following tables display to total installed costs for the process equipment required for the hybrid configurations.

### Superheating Geothermal Steam, Scenario 1 & Scenario 2

Process Equipment	Total Installed Costs of Process Equipment
Total gasifier cost	\$ 1,841,853
Chipper	\$ 920,968
Dryer	\$ 2,454,390
Conveyors and motors	\$ 272,479
Wood storage	\$ 691,855
Furnace	\$ 9,938,882
Furnace Fan	\$ 61,244
Cost of modifying MP turbines	\$ 32,263,262
Cost of bringing IP turbine to service	\$ 760,000
<b>Total</b>	<b>\$ 49,204,933</b>

### Superheating Geothermal Steam, Scenario 3

Process Equipment	Total Installed Costs of Process Equipment
Total gasifier cost	\$ 1,841,853
Chipper	\$ 920,968
Dryer	\$ 2,454,390
Conveyors and motors	\$ 272,479
Wood storage	\$ 691,855
Furnace	\$ 9,938,882
Furnace Fan	\$ 61,244
Cost of modifying MP turbines	\$ 32,263,262
<b>Total</b>	<b>\$ 48,444,933</b>

### Boiling Poihipi Rd Condensate, Scenario 1

Process Equipment	Total Installed Costs of Process Equipment
Total gasifier cost	\$ 1,889,544.06
Chipper	\$ 920,967.84
Dryer	\$ 2,538,220.38
Conveyors and motors	\$ 272,478.95
Package boiler	\$ 2,650,829.32
Condensate preheater	\$ 453,901.46
Wood storage	\$ 719,976.86
Pumps	\$ 100,714.86
Cost of Returning IP turbine to Service	\$ 760,000.00
<b>Total</b>	<b>\$ 10,306,633.74</b>

### Boiling Poihipi Rd Condensate, Scenario 2 & 3

Process Equipment	Total Installed Costs of Process Equipment
Total gasifier cost	\$ 1,889,544
Chipper	\$ 920,968
Dryer	\$ 2,538,220
Conveyors and motors	\$ 272,479
Package boiler	\$ 2,650,829
Condensate preheater	\$ 453,901
Wood storage	\$ 719,977
Pumps	\$ 100,715
<b>Total</b>	<b>\$ 9,546,633.74</b>

### Boiling IP SGW, Scenario 1

Process Equipment	Total Installed Costs of Process Equipment
Total gasifier cost	\$ 1,425,290
Chipper	\$ 920,968
Dryer	\$ 2,538,220
Conveyors and motors	\$ 247,132
Boiler	\$ 2,475,293
Wood storage	\$ 653,002
Returning IP turbine to service	\$ 760,000
<b>Total</b>	<b>\$ 9,019,906</b>

### Boiling IP SGW, Scenario 2 & Scenario 3

Process Equipment	Total Installed Costs of Process Equipment
Total gasifier cost	\$ 1,425,290
Chipper	\$ 920,968
Dryer	\$ 2,538,220
Conveyors and motors	\$ 247,132
Boiler	\$ 2,475,293
Wood storage	\$ 653,002
<b>Total</b>	<b>\$ 8,259,906</b>

### Heating Additional SGW for use in the Wairakei Binary Plant

Process Equipment	Total Installed Costs of Process Equipment
Total gasifier cost	\$ 1,014,437.78
Chipper	\$ 920,967.84
Dryer	\$ 1,243,969.62
Conveyors and motors	\$ 187,693.74
Wood storage	\$ 285,804.02
Furnace	\$ 4,081,075.90
Furnace Fan	\$ 33,668.96
<b>Total</b>	<b>\$ 7,767,617.87</b>

## 9.3 Cash Flow Analysis for the Implementation of the Hybrid Configurations

Superheating Geothermal Steam, Scenario 1

Year	Capital Cost (\$)	Wholesale cost of power (\$/MWh)	Average Cost of wood (\$/GJ)	Sales Revenue (\$/year)	Operating costs (\$/year)	Cost of wood (\$/year)	Depreciation \$/year	Income tax \$/year	Free Cash flow \$/year	Discounted Cash Flow (DCF) \$/year	Cumulative DCF \$/year
0	7116274	68.0	4.69	0	0	0	0	0	-7116274	-7116274	-7116274
1	42088659	72.9	4.78	0	0	0	0	0	-42088659	-39335196	-46451469
2	0	75.1	4.87	3970244	75779	5908074	580336	-726305	-1287304	-1124381	-47575851
3	0	77.3	4.96	4089616	78052	6019353	1160324	-887072	-1120717	-914839	-48490689
4	0	80.2	5.05	4239094	80393	6132857	1160324	-877655	-1096502	-836516	-49327206
5	0	82.1	5.15	4342482	1046659	6248634	1160324	-1151678	-1801133	-1284183	-50611389
6	0	84.2	5.25	4450859	170579	6366731	1160324	-909097	-1177354	-784521	-51395909
7	0	86.4	5.35	4566336	175696	6487198	1160324	-911927	-1184631	-737729	-52133638
8	0	88.6	5.45	4687518	180967	6610084	1160324	-913880	-1189653	-692389	-52826027
9	0	90.2	5.55	4770366	186396	6735441	1160324	-927303	-1224169	-665867	-53491893
10	0	89.3	5.66	4720983	1912201	6863321	1160324	-1460162	-2594378	-1318850	-54810743
11	0	91.6	5.76	4841394	197748	6993778	1160324	-982928	-1367204	-649549	-55460292
12	0	90.2	5.87	4771473	203680	7126867	1160324	-1041432	-1517642	-673851	-56134144
13	0	92.3	5.98	4881177	209791	7262643	1160324	-1050443	-1540814	-639383	-56773527
14	0	91.9	6.10	4858860	216084	7401163	1160673	-1097337	-1661051	-644184	-57417711
15	0	93.2	6.22	4929679	2216765	7542486	1160324	-1677171	-3152402	-1142575	-58560286
16	0	93.7	6.33	4953436	229244	7686672	1160673	-1154483	-1807997	-612431	-59172717
17	0	94.1	6.46	4974629	236121	7833782	1160324	-1191568	-1903707	-602665	-59775382
18	0	95.1	6.58	5027059	243205	7983878	1160673	-1220995	-1979029	-585523	-60360905
19	0	94.9	6.71	5019104	250501	8137024	1160324	-1268049	-2100372	-580770	-60941676
20	0	97.3	6.83	5143999	2569838	8293285	1160673	-1926343	-3792782	-980127	-61921803
21	0	100.0	6.97	5289286	265756	8452728	1160324	-1285066	-2144132	-517836	-62439639
22	0	101.2	7.10	5349493	273729	8615421	1160673	-1316092	-2223565	-501888	-62941526
23	0	102.3	7.24	5409700	281941	8781434	1160324	-1347920	-2305755	-486392	-63427918
24	0	103.4	7.38	5469907	290399	8950838	1160673	-1380961	-2390369	-471253	-63899172
25	0	104.6	7.52	5530114	2979147	9123705	1160324	-2165258	-4407481	-812075	-64711246
26	0	105.7	7.66	5590320	308084	9300110	1160673	-1449993	-2567881	-442178	-65153424
27	0	106.9	7.81	5650527	317327	9480130	1160324	-1486031	-2660899	-428219	-65581643
28	0	108.0	7.96	5710734	326847	9663842	1160673	-1523376	-2756579	-414596	-65996239
29	0	109.1	8.12	5770941	336652	9851325	1160324	-1561661	-2855376	-401360	-66397598
30	0	110.3	8.28	5831148	3453648	10042662	1160673	-2471234	-5193928	-682311	-67079910
31	0	111.4	8.44	5891355	357154	10237934	1160324	-1641936	-3061798	-375906	-67455816
32							621764	-174094	174094	19976	-67435840



Superheating Geothermal Steam, Scenario 2

Year	Capital Cost (\$)	Wholesale cost of power (\$/MWh)	Average Cost of wood (\$/GJ)	Sales Revenue (\$/year)	Operating costs (\$/year)	Cost of wood (\$/year)	Depreciation \$/year	Income tax \$/year	Free Cash flow \$/year	Discounted Cash Flow (DCF) \$/year	Cumulative DCF \$/year
0	7116274	68.0	4.69	0	0	0	0	0	-7116274	-7116274	-7116274
1	42088659	72.9	4.78	0	0	0	0	0	-42088659	-39335196	-46451469
2	0	75.1	4.87	1662464	75779	5870887	580336	-1362071	-2922131	-2552302	-49003772
3	0	77.3	4.96	1712449	78052	5981465	1160324	-1542070	-2804998	-2289714	-51293486
4	0	80.2	5.05	1775040	80393	6094256	1160324	-1556781	-2842828	-2168780	-53462266
5	0	82.1	5.15	1818331	1046659	6209304	1160324	-1847428	-3590204	-2559766	-56022031
6	0	84.2	5.25	1863712	170579	6326658	1160324	-1622278	-3011247	-2006521	-58028552
7	0	86.4	5.35	1912066	175696	6446367	1160324	-1643690	-3066307	-1909542	-59938094
8	0	88.6	5.45	1962809	180967	6568480	1160324	-1665150	-3121489	-1816735	-61754829
9	0	90.2	5.55	1997500	186396	6693048	1160324	-1691835	-3190109	-1735208	-63490037
10	0	89.3	5.66	1976822	1912201	6820124	1160324	-2216432	-4539072	-2307434	-65797471
11	0	91.6	5.76	2027241	197748	6949760	1160324	-1758565	-3361701	-1597120	-67394591
12	0	90.2	5.87	1997963	203680	7082011	1160324	-1805455	-3482273	-1546171	-68940762
13	0	92.3	5.98	2043900	209791	7216933	1160324	-1832082	-3550742	-1473432	-70414194
14	0	91.9	6.10	2034555	216084	7354582	1160673	-1875099	-3661012	-1419803	-71833997
15	0	93.2	6.22	2064209	2216765	7495016	1160324	-2466211	-5181361	-1877964	-73711961
16	0	93.7	6.33	2074157	229244	7638295	1160673	-1947135	-3846247	-1302857	-75014818
17	0	94.1	6.46	2083031	236121	7784479	1160324	-1987410	-3950159	-1250519	-76265337
18	0	95.1	6.58	2104985	243205	7933631	1160673	-2025107	-4046744	-1197286	-77462623
19	0	94.9	6.71	2101654	250501	8085814	1160324	-2070596	-4164065	-1151399	-78614021
20	0	97.3	6.83	2153951	2569838	8241092	1160673	-2748942	-5908036	-1526749	-80140770
21	0	100.0	6.97	2214788	265756	8399532	1160324	-2131031	-4319469	-1043208	-81183979
22	0	101.2	7.10	2239998	273729	8561201	1160673	-2171569	-4423363	-998411	-82182390
23	0	102.3	7.24	2265209	281941	8726169	1160324	-2212903	-4529998	-955589	-83137979
24	0	103.4	7.38	2290419	290399	8894507	1160673	-2255445	-4639043	-914572	-84052551
25	0	104.6	7.52	2315630	2979147	9066287	1160324	-3049236	-6680568	-1230889	-85283440
26	0	105.7	7.66	2340840	308084	9241583	1160673	-2343460	-4865367	-837794	-86121234
27	0	106.9	7.81	2366050	317327	9420470	1160324	-2388980	-4982767	-801878	-86923113
28	0	108.0	7.96	2391261	326847	9603026	1160673	-2435800	-5102813	-767474	-87690587
29	0	109.1	8.12	2416471	336652	9789330	1160324	-2483554	-5225957	-734575	-88425162
30	0	110.3	8.28	2441682	3453648	9979463	1160673	-3402588	-7588841	-996924	-89422086
31	0	111.4	8.44	2466892	357154	10173507	1160324	-2582746	-5481023	-672922	-90095008
32	0	0	0	0	0	0	621764	-174094	174094	19976	-90075032



Superheating Geothermal Steam, Scenario 3

Year	Capital Cost (\$)	Wholesale cost of power (\$/MWh)	Average Cost of wood (\$/GJ)	Sales Revenue (\$/year)	Operating costs (\$/year)	Cost of wood (\$/year)	Depreciation \$/year	Income tax \$/year	Free Cash flow \$/year	Discounted Cash Flow (DCF) \$/year	Cumulative DCF \$/year
0	7116274	68.0	4.69	0	0	0	0	0	-7116274	-7116274	-7116274
1	41328659	72.9	4.78	0	0	0	0	0	-41328659	-38624915	-45741189
2	0	75.1	4.87	7486122	0	5870887	567667	293319	1321917	1154613	-44586576
3	0	77.3	4.96	7711206	0	5981465	1134994	166529	1563211	1276046	-43310530
4	0	80.2	5.05	7993055	0	6094256	1134994	213866	1684934	1285428	-42025102
5	0	82.1	5.15	8187999	0	6209304	1134994	236236	1742458	1242349	-40782753
6	0	84.2	5.25	8392350	0	6326658	1134994	260595	1805096	1202812	-39579941
7	0	86.4	5.35	8610088	0	6446367	1134994	288044	1875678	1168078	-38411864
8	0	88.6	5.45	8838584	0	6568480	1134994	317831	1952273	1136241	-37275623
9	0	90.2	5.55	8994798	0	6693048	1134994	326692	1975058	1074301	-36201322
10	0	89.3	5.66	8901684	0	6820124	1134994	265039	1816521	923427	-35277895
11	0	91.6	5.76	9128726	0	6949760	1134994	292312	1886653	896335	-34381559
12	0	90.2	5.87	8996886	0	7082011	1134994	218367	1696508	753270	-33628290
13	0	92.3	5.98	9203738	0	7216933	1134994	238507	1748298	725481	-32902808
14	0	91.9	6.10	9161659	0	7354582	1135334	188088	1618989	627872	-32274936
15	0	93.2	6.22	9295191	0	7495016	1134994	186251	1613924	584960	-31689976
16	0	93.7	6.33	9339988	0	7638295	1135334	158580	1543112	522706	-31167270
17	0	94.1	6.46	9379948	0	7784479	1134994	128933	1466535	464268	-30703003
18	0	95.1	6.58	9478808	0	7933631	1135334	114756	1430421	423210	-30279793
19	0	94.9	6.71	9463808	0	8085814	1134994	68040	1309954	362213	-29917580
20	0	97.3	6.83	9699304	0	8241092	1135334	90406	1367806	353467	-29564112
21	0	100.0	6.97	9973252	0	8399532	1134994	122844	1450877	350406	-29213707
22	0	101.2	7.10	10086776	0	8561201	1135334	109267	1416307	319679	-28894027
23	0	102.3	7.24	10200299	0	8726169	1134994	94958	1379172	290932	-28603096
24	0	103.4	7.38	10313823	0	8894507	1135334	79515	1339800	264137	-28338958
25	0	104.6	7.52	10427346	0	9066287	1134994	63298	1297761	239111	-28099847
26	0	105.7	7.66	10540869	0	9241583	1135334	45907	1253380	215826	-27884021
27	0	106.9	7.81	10654393	0	9420470	1134994	27700	1206222	194118	-27689903
28	0	108.0	7.96	10767916	0	9603026	1135334	8276	1156614	173957	-27515946
29	0	109.1	8.12	10881440	0	9789330	1134994	-12008	1104117	155198	-27360748
30	0	110.3	8.28	10994963	0	9979463	1135334	-33554	1049054	137811	-27222937
31	0	111.4	8.44	11108487	0	10173507	1134994	-56004	990983	121666	-27101271
32	0	0	0	0	0	0	608190	-170293	170293	19540	-27081731

Boiling Poihipi Rd Condensate, Scenario 1

Year	Capital Cost (\$)	Wholesale cost of power (\$/MWh)	Average Cost of wood (\$/GJ)	Sales Revenue (\$/year)	Operating costs (\$/year)	Cost of wood (\$/year)	Depreciation \$/year	Income tax \$/year	Free Cash flow \$/year	Discounted Cash Flow (DCF) \$/year	Cumulative DCF \$/year
0	888059	68.0	4.71	0	0	0	0	0	-888059	-888059	-888059
1	9418575	72.9	4.80	0	0	0	0	0	-9418575	-8802406	-9690465
2	0	75.1	4.89	2648622	107614	6134838	87399	-1030744	-2563086	-2238699	-11929164
3	0	77.3	4.98	2728257	110843	6250386	174746	-1066161	-2566811	-2095282	-14024446
4	0	80.2	5.07	2827977	114168	6368245	174746	-1072171	-2582265	-1969998	-15994444
5	0	82.1	5.17	2896949	1053373	6488464	174746	-1349497	-3295391	-2349568	-18344012
6	0	84.2	5.26	2969249	203926	6611092	174746	-1125744	-2720025	-1812467	-20156480
7	0	86.4	5.36	3046286	210044	6736180	174746	-1140911	-2759027	-1718183	-21874663
8	0	88.6	5.47	3127129	216345	6863781	174746	-1155768	-2797229	-1628013	-23502676
9	0	90.2	5.57	3182398	222836	6993947	174746	-1178557	-2855828	-1553381	-25056057
10	0	89.3	5.68	3149454	1899630	7126733	174746	-1694464	-4182447	-2126144	-27182201
11	0	91.6	5.78	3229782	236406	7262195	174746	-1244198	-3024621	-1436976	-28619177
12	0	90.2	5.89	3183136	243498	7400389	174746	-1297939	-3162812	-1404326	-30023503
13	0	92.3	6.01	3256322	250803	7541374	174746	-1318968	-3216887	-1334894	-31358397
14	0	91.9	6.12	3241434	258327	7685209	174798	-1365532	-3336570	-1293979	-32652377
15	0	93.2	6.24	3288678	2202192	7831953	174746	-1937660	-4807808	-1742571	-34394947
16	0	93.7	6.36	3304527	274060	7981671	174798	-1435280	-3515923	-1190965	-35585912
17	0	94.1	6.48	3318665	282281	8134424	174746	-1476380	-3621660	-1146525	-36732437
18	0	95.1	6.60	3353643	290750	8290278	174798	-1512611	-3714774	-1099068	-37831504
19	0	94.9	6.73	3348335	299472	8449299	174746	-1561051	-3839385	-1061622	-38893126
20	0	97.3	6.86	3431655	2552944	8611554	174798	-2214140	-5518704	-1426138	-40319264
21	0	100.0	6.99	3528579	317710	8777114	174746	-1607477	-3958768	-956094	-41275359
22	0	101.2	7.12	3568744	327242	8946048	174798	-1646216	-4058329	-916018	-42191377
23	0	102.3	7.26	3608909	337059	9118429	174746	-1685971	-4160608	-877667	-43069044
24	0	103.4	7.40	3649074	347171	9294331	174798	-1726823	-4265604	-840949	-43909994
25	0	104.6	7.54	3689239	2959562	9473829	174746	-2497291	-6246861	-1150979	-45060973
26	0	105.7	7.69	3729404	368313	9657002	174798	-1811798	-4484112	-772144	-45833116
27	0	106.9	7.84	3769570	379363	9843927	174746	-1855970	-4597750	-739918	-46573034
28	0	108.0	7.99	3809735	390743	10034686	174798	-1901338	-4714357	-709050	-47282084
29	0	109.1	8.15	3849900	402466	10229361	174746	-1947868	-4834058	-679489	-47961572
30	0	110.3	8.30	3890065	3430944	10428036	174798	-2840240	-7128675	-936474	-48898046
31	0	111.4	8.47	3930230	426976	10630799	174746	-2044641	-5082904	-624043	-49522089
32	0	0	0	0	0	0	93638	-26219	26219	3008	-49519081

Boiling Poihipi Rd Condensate, Scenario 2

Year	Capital Cost (\$)	Wholesale cost of power (\$/MWh)	Average Cost of wood (\$/GJ)	Sales Revenue (\$/year)	Operating costs (\$/year)	Cost of wood (\$/year)	Depreciation \$/year	Income tax \$/year	Free Cash flow \$/year	Discounted Cash Flow (DCF) \$/year	Cumulative DCF \$/year
0	888059	68.0	4.71	0	0	0	0	0	-888059	-888059	-888059
1	8658575	72.9	4.80	0	0	0	0	0	-8658575	-8092126	-8980185
2	0	75.1	4.89	1062637	34043	6134838	74751	-1450679	-3655565	-3192912	-12173097
3	0	77.3	4.98	1094587	35064	6250386	149457	-1495290	-3695574	-3016689	-15189786
4	0	80.2	5.07	1134595	36116	6368245	149457	-1517383	-3752384	-2862676	-18052462
5	0	82.1	5.17	1162267	117593	6488464	149457	-1566109	-3877681	-2764733	-20817195
6	0	84.2	5.26	1191274	121121	6611092	149457	-1593311	-3947628	-2630471	-23447666
7	0	86.4	5.36	1222181	124754	6736180	149457	-1620699	-4018055	-2502242	-25949909
8	0	88.6	5.47	1254616	128497	6863781	149457	-1648393	-4089269	-2379992	-28329901
9	0	90.2	5.57	1276790	132352	6993947	149457	-1679711	-4169799	-2268094	-30597995
10	0	89.3	5.68	1263572	814805	7126733	149457	-1911678	-4766287	-2422939	-33020934
11	0	91.6	5.78	1295800	140412	7262195	149457	-1751754	-4355053	-2069054	-35089988
12	0	90.2	5.89	1277086	144625	7400389	149457	-1796868	-4471060	-1985204	-37075192
13	0	92.3	6.01	1306448	148963	7541374	149457	-1829337	-4554552	-1889977	-38965170
14	0	91.9	6.12	1300475	153432	7685209	149502	-1872547	-4665619	-1809407	-40774577
15	0	93.2	6.24	1319430	944582	7831953	149457	-2129837	-5327268	-1930847	-42705424
16	0	93.7	6.36	1325789	162776	7981671	149502	-1951085	-4867574	-1648816	-44354240
17	0	94.1	6.48	1331461	167660	8134424	149457	-1993622	-4977001	-1575591	-45929831
18	0	95.1	6.60	1345494	172689	8290278	149502	-2034753	-5082721	-1503794	-47433624
19	0	94.9	6.73	1343365	177870	8449299	149457	-2081313	-5202491	-1438532	-48872157
20	0	97.3	6.86	1376793	1095029	8611554	149502	-2374202	-5955589	-1539037	-50411194
21	0	100.0	6.99	1415679	188702	8777114	149457	-2155886	-5394251	-1302782	-51713976
22	0	101.2	7.12	1431793	194363	8946048	149502	-2200273	-5508344	-1243306	-52957282
23	0	102.3	7.26	1447908	200194	9118429	149457	-2245648	-5625067	-1186590	-54143872
24	0	103.4	7.40	1464022	206200	9294331	149502	-2292083	-5744426	-1132494	-55276366
25	0	104.6	7.54	1480136	1269439	9473829	149457	-2635525	-6627607	-1221131	-56497498
26	0	105.7	7.69	1496251	218758	9657002	149502	-2388123	-5991386	-1031690	-57529187
27	0	106.9	7.84	1512365	225320	9843927	149457	-2437775	-6119107	-984750	-58513937
28	0	108.0	7.99	1528480	232080	10034686	149502	-2488581	-6249705	-939970	-59453907
29	0	109.1	8.15	1544594	239042	10229361	149457	-2540514	-6383295	-897254	-60351161
30	0	110.3	8.30	1560708	1471628	10428036	149502	-2936768	-7402188	-972404	-61323565
31	0	111.4	8.47	1576823	253600	10630799	149457	-2647969	-6659607	-817620	-62141185
32	0	0	0	0	0	0	80087	-22424	22424	2573	-62138612

Boiling Poihipi Rd Condensate, Scenario 3

Year	Capital Cost (\$)	Wholesale cost of power (\$/MWh)	Average Cost of wood (\$/GJ)	Sales Revenue (\$/year)	Operating costs (\$/year)	Cost of wood (\$/year)	Depreciation \$/year	Income tax \$/year	Free Cash flow \$/year	Discounted Cash Flow (DCF) \$/year	Cumulative DCF \$/year
0	888059	68.0	4.71	0	0	0	0	0	-888059	-888059	-888059
1	8658575	72.9	4.80	0	0	0	0	0	-8658575	-8092126	-8980185
2	0	75.1	4.89	3895025	34043	6134838	74730	-657604	-1616252	-1411697	-10391882
3	0	77.3	4.98	4012136	35064	6250386	149415	-678364	-1594950	-1301955	-11693837
4	0	80.2	5.07	4158781	36116	6368245	149415	-670598	-1574981	-1201546	-12895382
5	0	82.1	5.17	4260210	37200	6488464	149415	-676163	-1589290	-1133142	-14028524
6	0	84.2	5.26	4366534	38316	6611092	149415	-681041	-1601832	-1067369	-15095893
7	0	86.4	5.36	4479823	39465	6736180	149415	-684666	-1611155	-1003347	-16099239
8	0	88.6	5.47	4598710	40649	6863781	149415	-687438	-1618282	-941855	-17041095
9	0	90.2	5.57	4679988	41868	6993947	149415	-701468	-1654360	-899862	-17940957
10	0	89.3	5.68	4631540	43124	7126733	149415	-752565	-1785752	-907786	-18848743
11	0	91.6	5.78	4749670	44418	7262195	149415	-757780	-1799163	-854769	-19703512
12	0	90.2	5.89	4681074	45751	7400389	149415	-816055	-1949012	-865384	-20568897
13	0	92.3	6.01	4788699	47123	7541374	149415	-825780	-1974019	-819148	-21388044
14	0	91.9	6.12	4766805	48537	7685209	149460	-872592	-2094348	-812224	-22200269
15	0	93.2	6.24	4836282	49993	7831953	149415	-894622	-2151042	-779637	-22979905
16	0	93.7	6.36	4859590	51493	7981671	149460	-930449	-2243125	-759824	-23739729
17	0	94.1	6.48	4880381	53038	8134424	149415	-967819	-2339262	-740550	-24480280
18	0	95.1	6.60	4931818	54629	8290278	149460	-997514	-2415575	-714682	-25194961
19	0	94.9	6.73	4924013	56268	8449299	149415	-1044671	-2536882	-701469	-25896430
20	0	97.3	6.86	5046542	57956	8611554	149460	-1056280	-2566689	-663281	-26559711
21	0	100.0	6.99	5189077	59694	8777114	149415	-1063201	-2584530	-624198	-27183909
22	0	101.2	7.12	5248143	61485	8946048	149460	-1094478	-2664912	-601506	-27785415
23	0	102.3	7.26	5307209	63330	9118429	149415	-1126710	-2747839	-579648	-28365063
24	0	103.4	7.40	5366275	65230	9294331	149460	-1159968	-2833317	-558579	-28923642
25	0	104.6	7.54	5425342	67186	9473829	149415	-1194225	-2921449	-538275	-29461917
26	0	105.7	7.69	5484408	69202	9657002	149460	-1229552	-3012244	-518695	-29980611
27	0	106.9	7.84	5543474	71278	9843927	149415	-1265921	-3105810	-499819	-30480431
28	0	108.0	7.99	5602540	73416	10034686	149460	-1303406	-3202156	-481611	-30962042
29	0	109.1	8.15	5661606	75619	10229361	149415	-1341981	-3301393	-464053	-31426095
30	0	110.3	8.30	5720672	77888	10428036	149460	-1381719	-3403532	-447112	-31873207
31	0	111.4	8.47	5779739	80224	10630799	149415	-1422596	-3508689	-430772	-32303980
32	0	0	0	0	0	0	80064	-22418	22418	22418	-32281562

Boiling IPSGW, Scenario 1

Year	Capital Cost (\$)	Wholesale cost of power (\$/MWh)	Average Cost of wood (\$/GJ)	Sales Revenue (\$/year)	Operating costs (\$/year)	Cost of wood (\$/year)	Depreciation \$/year	Income tax \$/year	Free Cash flow \$/year	Discounted Cash Flow (DCF) \$/year	Cumulative DCF \$/year
0	814166	68.0	4.71	0	0	0	0	0	-814166	-814166	-814166
1	8205740	72.9	4.80	0	0	0	0	0	-8205740	-7668915	-8483082
2	0	75.1	4.89	2883010	73571	6134838	84101	-954660	-2370739	-2070695	-10553777
3	0	77.3	4.98	2969693	75779	6250386	168152	-986895	-2369577	-1934281	-12488057
4	0	80.2	5.07	3078237	78052	6368245	168152	-990139	-2377921	-1814104	-14302162
5	0	82.1	5.17	3153313	160787	6488464	168152	-1025945	-2469993	-1761071	-16063232
6	0	84.2	5.26	3232011	165611	6611092	168152	-1039596	-2505095	-1669251	-17732483
7	0	86.4	5.36	3315865	170579	6736180	168152	-1052533	-2538361	-1580764	-19313246
8	0	88.6	5.47	3403862	175696	6863781	168152	-1065055	-2570560	-1496089	-20809336
9	0	90.2	5.57	3464023	180967	6993947	168152	-1086132	-2624760	-1427695	-22237031
10	0	89.3	5.68	3428163	864878	7126733	168152	-1324848	-3238600	-1646340	-23883371
11	0	91.6	5.78	3515600	191988	7262195	168152	-1149886	-2788697	-1324890	-25208261
12	0	90.2	5.89	3464827	197748	7400389	168152	-1204410	-2928901	-1300467	-26508729
13	0	92.3	6.01	3544488	203680	7541374	168152	-1223241	-2977325	-1235484	-27744213
14	0	91.9	6.12	3528283	209791	7685209	168202	-1269777	-3096939	-1201046	-28945259
15	0	93.2	6.24	3579708	1002631	7831953	168152	-1518448	-3736428	-1354254	-30299512
16	0	93.7	6.36	3596960	222567	7981671	168202	-1337134	-3270143	-1107711	-31407223
17	0	94.1	6.48	3612349	229244	8134424	168152	-1377452	-3373867	-1068080	-32475303
18	0	95.1	6.60	3650421	236121	8290278	168202	-1412370	-3463607	-1024756	-33500059
19	0	94.9	6.73	3644645	243205	8449299	168152	-1460483	-3587376	-991939	-34491999
20	0	97.3	6.86	3735338	1849388	8611554	168202	-1930266	-4795339	-1239207	-35731205
21	0	100.0	6.99	3840839	258016	8777114	168152	-1501484	-3692807	-891861	-36623066
22	0	101.2	7.12	3884558	265756	8946048	168202	-1538726	-3788520	-855119	-37478185
23	0	102.3	7.26	3928278	273729	9118429	168152	-1576969	-3886911	-819932	-38298117
24	0	103.4	7.40	3971997	281941	9294331	168202	-1616294	-3987981	-786217	-39084334
25	0	104.6	7.54	4015717	2439170	9473829	168152	-2258322	-5638961	-1038974	-40123308
26	0	105.7	7.69	4059436	299111	9657002	168202	-1698166	-4198510	-722965	-40846273
27	0	106.9	7.84	4103156	308084	9843927	168152	-1740762	-4308093	-693303	-41539576
28	0	108.0	7.99	4146875	317327	10034686	168202	-1784535	-4420602	-664868	-42204444
29	0	109.1	8.15	4190595	326847	10229361	168152	-1829454	-4536159	-637615	-42842059
30	0	110.3	8.30	4234314	3224421	10428036	168202	-2684177	-6733966	-884622	-43726681
31	0	111.4	8.47	4278034	346752	10630799	168152	-1922947	-4776570	-586434	-44313115
32	0	0	0	0	0	0	90105	-25229	25229	2895	-44310220

Boiling IPSGW, Scenario 2

Year	Capital Cost (\$)	Wholesale cost of power (\$/MWh)	Average Cost of wood (\$/GJ)	Sales Revenue (\$/year)	Operating costs (\$/year)	Cost of wood (\$/year)	Depreciation \$/year	Income tax \$/year	Free Cash flow \$/year	Discounted Cash Flow (DCF) \$/year	Cumulative DCF \$/year
0	814166	68.0	4.71	0	0	0	0	0	-814166	-814166	-814166
1	8205740	72.9	4.80	0	0	0	0	0	-7445740	-6958635	-7772801
2	0	75.1	4.89	1265398	0	6134838	71432	-1383444	-3485996	-3044804	-10817605
3	0	77.3	4.98	1303445	0	6250386	142821	-1425134	-3521808	-2874844	-13692449
4	0	80.2	5.07	1351086	0	6368245	142821	-1444794	-3572364	-2725340	-16417789
5	0	82.1	5.17	1384038	80393	6488464	142821	-1491739	-3693080	-2633115	-19050904
6	0	84.2	5.26	1418580	82805	6611092	142821	-1517079	-3758238	-2504273	-21555177
7	0	86.4	5.36	1455385	85289	6736180	142821	-1542494	-3823591	-2381140	-23936317
8	0	88.6	5.47	1494008	87848	6863781	142821	-1568124	-3889497	-2263723	-26200039
9	0	90.2	5.57	1520414	90484	6993947	142821	-1597915	-3966102	-2157297	-28357336
10	0	89.3	5.68	1504674	771680	7126733	142821	-1830237	-4563502	-2319853	-30677190
11	0	91.6	5.78	1543052	95994	7262195	142821	-1668228	-4146909	-1970167	-32647356
12	0	90.2	5.89	1520766	98874	7400389	142821	-1713969	-4264528	-1893501	-34540858
13	0	92.3	6.01	1555731	101840	7541374	142821	-1744485	-4342998	-1802190	-36343047
14	0	91.9	6.12	1548618	104895	7685209	142864	-1787618	-4453868	-1727287	-38070334
15	0	93.2	6.24	1571190	894589	7831953	142821	-2043489	-5111864	-1852775	-39923109
16	0	93.7	6.36	1578762	111283	7981671	142864	-1863976	-4650217	-1575189	-41498298
17	0	94.1	6.48	1585516	114622	8134424	142821	-1905778	-4757751	-1506182	-43004480
18	0	95.1	6.60	1602227	118061	8290278	142864	-1945713	-4860398	-1438017	-44442497
19	0	94.9	6.73	1599691	121602	8449299	142821	-1991929	-4979281	-1376813	-45819309
20	0	97.3	6.86	1639498	1724138	8611554	142864	-2474936	-6221258	-1607691	-47427001
21	0	100.0	6.99	1685804	129008	8777114	142821	-2061679	-5158639	-1245879	-48672879
22	0	101.2	7.12	1704993	132878	8946048	142864	-2104703	-5269230	-1189334	-49862214
23	0	102.3	7.26	1724182	136865	9118429	142821	-2148701	-5382410	-1135403	-50997617
24	0	103.4	7.40	1743372	140970	9294331	142864	-2193742	-5498187	-1083949	-52081566
25	0	104.6	7.54	1762561	2293971	9473829	142821	-2841457	-7163782	-1319921	-53401487
26	0	105.7	7.69	1781750	149556	9657002	142864	-2286948	-5737859	-988034	-54389520
27	0	106.9	7.84	1800939	154042	9843927	142821	-2335158	-5861872	-943353	-55332873
28	0	108.0	7.99	1820128	158664	10034686	142864	-2384504	-5988717	-900716	-56233589
29	0	109.1	8.15	1839317	163423	10229361	142821	-2434961	-6118506	-860034	-57093624
30	0	110.3	8.30	1858507	3056095	10428036	142864	-3295177	-8330448	-1094347	-58187971
31	0	111.4	8.47	1877696	173376	10630799	142821	-2539404	-6387075	-784160	-58972131
32	0	0	0	0	0	0	76531	-21429	21429	21429	-58950702

Boiling IPSGW, Scenario 3

Year	Capital Cost (\$)	Wholesale cost of power (\$/MWh)	Average Cost of wood (\$/GJ)	Sales Revenue (\$/year)	Operating costs (\$/year)	Cost of wood (\$/year)	Depreciation \$/year	Income tax \$/year	Free Cash flow \$/year	Discounted Cash Flow (DCF) \$/year	Cumulative DCF \$/year
0	814166	68.0	4.71	0	0	0	0	0	-814166	-814166	-814166
1	7445740	72.9	4.80	0	0	0	0	0	-7445740	-6958635	-7772801
2	0	75.1	4.89	4243257	0	6134838	71432	-549644	-1341938	-1172100	-8944902
3	0	77.3	4.98	4370838	0	6250386	142821	-566263	-1313285	-1072032	-10016933
4	0	80.2	5.07	4530594	0	6368245	142821	-554532	-1283119	-978885	-10995818
5	0	82.1	5.17	4641092	0	6488464	142821	-557254	-1290118	-919836	-11915655
6	0	84.2	5.26	4756921	0	6611092	142821	-559158	-1295013	-862922	-12778577
7	0	86.4	5.36	4880339	0	6736180	142821	-559625	-1296216	-807218	-13585795
8	0	88.6	5.47	5009854	0	6863781	142821	-559089	-1294837	-753607	-14339402
9	0	90.2	5.57	5098399	0	6993947	142821	-570744	-1324805	-720606	-15060008
10	0	89.3	5.68	5045620	0	7126733	142821	-622702	-1458412	-741383	-15801390
11	0	91.6	5.78	5174311	0	7262195	142821	-624598	-1463287	-695197	-16496587
12	0	90.2	5.89	5099582	0	7400389	142821	-684216	-1616591	-717786	-17214373
13	0	92.3	6.01	5216829	0	7541374	142821	-690862	-1633682	-677920	-17892293
14	0	91.9	6.12	5192978	0	7685209	142864	-737826	-1754404	-680388	-18572682
15	0	93.2	6.24	5268667	0	7831953	142821	-757710	-1805577	-654424	-19227106
16	0	93.7	6.36	5294058	0	7981671	142864	-792534	-1895079	-641929	-19869035
17	0	94.1	6.48	5316708	0	8134424	142821	-828950	-1988766	-629592	-20498627
18	0	95.1	6.60	5372743	0	8290278	142864	-856912	-2060623	-609664	-21108291
19	0	94.9	6.73	5364241	0	8449299	142821	-903806	-2181252	-603134	-21711425
20	0	97.3	6.86	5497724	0	8611554	142864	-911874	-2201956	-569027	-22280452
21	0	100.0	6.99	5653003	0	8777114	142821	-914741	-2209370	-533592	-22814044
22	0	101.2	7.12	5717350	0	8946048	142864	-944037	-2284661	-515678	-23329722
23	0	102.3	7.26	5781696	0	9118429	142821	-974275	-2362457	-498353	-23828075
24	0	103.4	7.40	5846043	0	9294331	142864	-1005522	-2442765	-481583	-24309658
25	0	104.6	7.54	5910390	0	9473829	142821	-1037753	-2525686	-465356	-24775014
26	0	105.7	7.69	5974737	0	9657002	142864	-1071036	-2611228	-449642	-25224655
27	0	106.9	7.84	6039084	0	9843927	142821	-1105346	-2699497	-434431	-25659086
28	0	108.0	7.99	6103431	0	10034686	142864	-1140753	-2790501	-419698	-26078784
29	0	109.1	8.15	6167778	0	10229361	142821	-1177233	-2884349	-405432	-26484216
30	0	110.3	8.30	6232125	0	10428036	142864	-1214857	-2981054	-391612	-26875829
31	0	111.4	8.47	6296472	0	10630799	142821	-1253601	-3080725	-378230	-27254059
32	0	0	0	0	0	0	76531	-21429	21429	21429	-27232630

Heating additional SGW for use in the Wairakei Binary Plant, Scenario 1.

Year	Capital Cost (\$)	Wholesale cost of power (\$/MWh)	Average Cost of wood (\$/GJ)	Sales Revenue (\$/year)	Operating costs (\$/year)	Cost of wood (\$/year)	Depreciation \$/year	Income tax \$/year	Free Cash flow \$/year	Discounted Cash Flow (DCF) \$/year	Cumulative DCF \$/year
0	722569	68.0	4.2	0	0	0			-722569	-722569	-722569
1	7045048	72.9	4.3	0	0	0			-7045049	-6584158	-7306727
2	0	75.1	4.3	903710	594547	1218612	51763	-269139	-640310	-559271	-7865998
3	0	77.3	4.4	930882	612384	1241577	103494	-287440	-635638	-518870	-8384868
4	0	80.2	4.5	964906	630755	1265000	103494	-289616	-641233	-489194	-8874061
5	0	82.1	4.6	988440	649678	1288894	103494	-295015	-655117	-467089	-9341151
6	0	84.2	4.7	1013109	669168	1313266	103494	-300390	-668936	-445740	-9786891
7	0	86.4	4.8	1039394	689243	1338127	103494	-305612	-682365	-424943	-10211834
8	0	88.6	4.9	1066977	709921	1363489	103494	-310779	-695653	-404876	-10616710
9	0	90.2	5.0	1085835	731218	1389360	103494	-318707	-716037	-389476	-11006186
10	0	89.3	5.0	1074594	753155	1415752	103494	-335386	-758927	-385800	-11391986
11	0	91.6	5.1	1102002	775749	1442676	103494	-341577	-774846	-368124	-11760110
12	0	90.2	5.2	1086087	799022	1470144	103494	-360241	-822838	-365350	-12125460
13	0	92.3	5.3	1111058	822993	1498167	103494	-367807	-842295	-349522	-12474982
14	0	91.9	5.4	1105978	847682	1526756	103526	-384156	-884304	-342948	-12817931
15	0	93.2	5.5	1122098	873113	1555924	103494	-394921	-912018	-330557	-13148488
16	0	93.7	5.7	1127506	899306	1585683	103526	-409083	-948401	-321256	-13469744
17	0	94.1	5.8	1132329	926285	1616046	103494	-423779	-986223	-312213	-13781957
18	0	95.1	5.9	1144264	954074	1647026	103526	-436901	-1019935	-301762	-14083719
19	0	94.9	6.0	1142453	982696	1678635	103494	-454264	-1064614	-294375	-14378094
20	0	97.3	6.1	1170882	1012177	1710888	103526	-463598	-1088585	-281311	-14659405
21	0	100.0	6.2	1203952	1042542	1743797	103494	-472047	-1110341	-268162	-14927566
22	0	101.2	6.3	1217656	1073819	1777378	103526	-486378	-1147162	-258930	-15186496
23	0	102.3	6.5	1231361	1106033	1811645	103494	-501147	-1185170	-250008	-15436504
24	0	103.4	6.6	1245065	1139214	1846611	103526	-516400	-1224360	-241378	-15677882
25	0	104.6	6.7	1258769	1173391	1882293	103494	-532114	-1264800	-233038	-15910921
26	0	105.7	6.8	1272474	1208592	1918705	103526	-548338	-1306486	-224971	-16135892
27	0	106.9	7.0	1286178	1244850	1955864	103494	-565049	-1349488	-217174	-16353065
28	0	108.0	7.1	1299882	1282196	1993786	103526	-582295	-1393804	-209631	-16562696
29	0	109.1	7.2	1313587	1320661	2032486	103494	-600055	-1439505	-202341	-16765037
30	0	110.3	7.4	1327291	1360281	2071982	103526	-618379	-1486593	-195289	-16960327
31	0	111.4	7.5	1340995	1401090	2112291	103494	-637246	-1535139	-188474	-17148800
32	0	-	-	-	-	-	55458	-15528	15528	15528	-17133272



Heating additional SGW for use in the Wairakei Binary Plant, Scenarios 2&3

Year	Capital Cost (\$)	Wholesale cost of power (\$/MWh)	Average Cost of wood (\$/GJ)	Sales Revenue (\$/year)	Operating costs (\$/year)	Cost of wood (\$/year)	Depreciation \$/year	Income tax \$/year	Free Cash flow \$/year	Discounted Cash Flow (DCF) \$/year	Cumulative DCF \$/year
0	722569	68.0	4.19	0	0	0	0	0	-722569	-722569	-722569
1	7045049	72.9	4.27	0	0	0	0	0	-7045049	-6584158	-7306727
2	0	75.1	4.35	806168	594547	1218612	51763	-296451	-710541	-620614	-7927340
3	0	77.3	4.43	830406	612384	1241577	103494	-315574	-707980	-577923	-8505263
4	0	80.2	4.51	860758	630755	1265000	103494	-318778	-716220	-546401	-9051664
5	0	82.1	4.60	881751	649678	1288894	103494	-324888	-731932	-521857	-9573521
6	0	84.2	4.68	903758	669168	1313266	103494	-331008	-747669	-498203	-10071725
7	0	86.4	4.77	927206	689243	1338127	103494	-337025	-763141	-475246	-10546970
8	0	88.6	4.86	951812	709921	1363489	103494	-343026	-778572	-453136	-11000106
9	0	90.2	4.96	968634	731218	1389360	103494	-351523	-800421	-435376	-11435482
10	0	89.3	5.05	958607	753155	1415752	103494	-367862	-842437	-428253	-11863734
11	0	91.6	5.15	983057	775749	1442676	103494	-374882	-860487	-408811	-12272546
12	0	90.2	5.24	968859	799022	1470144	103494	-393064	-907243	-402827	-12675372
13	0	92.3	5.34	991135	822993	1498167	103494	-401385	-928639	-385352	-13060725
14	0	91.9	5.45	986603	847682	1526756	103526	-417581	-970254	-376281	-13437006
15	0	93.2	5.55	1000983	873113	1555924	103494	-428833	-999220	-362163	-13799169
16	0	93.7	5.66	1005807	899306	1585683	103526	-443158	-1036024	-350937	-14150106
17	0	94.1	5.76	1010110	926285	1616046	103494	-458000	-1074221	-340071	-14490177
18	0	95.1	5.87	1020756	954074	1647026	103526	-471483	-1108860	-328072	-14818249
19	0	94.9	5.99	1019141	982696	1678635	103494	-488792	-1153398	-318924	-15137173
20	0	97.3	6.10	1044501	1012177	1710888	103526	-498985	-1179579	-304826	-15441999
21	0	100.0	6.22	1074002	1042542	1743797	103494	-508433	-1203904	-290759	-15732757
22	0	101.2	6.34	1086227	1073819	1777378	103526	-523179	-1241791	-280289	-16013046
23	0	102.3	6.46	1098453	1106033	1811645	103494	-538361	-1280864	-270194	-16283240
24	0	103.4	6.59	1110678	1139214	1846611	103526	-554028	-1321119	-260454	-16543694
25	0	104.6	6.71	1122903	1173391	1882293	103494	-570157	-1362624	-251062	-16794756
26	0	105.7	6.84	1135128	1208592	1918705	103526	-586795	-1405375	-241999	-17036756
27	0	106.9	6.98	1147353	1244850	1955864	103494	-603920	-1449442	-233259	-17270015
28	0	108.0	7.11	1159578	1282196	1993786	103526	-621580	-1494823	-224825	-17494840
29	0	109.1	7.25	1171803	1320661	2032486	103494	-639755	-1541589	-216690	-17711530
30	0	110.3	7.39	1184029	1360281	2071982	103526	-658493	-1589742	-208840	-17920370
31	0	111.4	7.53	1196254	1401090	2112291	103494	-677774	-1639353	-201268	-18121638
32	0	0	0	0	0	0	55458	-15528	15528	1782	-18119856

